Identification and Characterization of Sex-specific Transcripts in the Blood Brain Barrier of *Drosophila melanogaster*

A Dissertation

Presented to

the Faculty of the Department of Biology and Biochemistry

University of Houston

In Partial Fulfillment of the

Requirements for the Degree

Doctor of Philosophy

By

Chamala Lama

December 2013

Identification and Characterization of Sex-specific Transcripts in the Blood Brain Barrier of *Drosophila melanogaster*

Chamala Lama

Approved by:

Dr. Brigitte Dauwalder,
Committee Chair

Dr. Gregg Roman

Dr. Preethi Gunaratne

Dr. Kathleen M. Beckingham

Dr. Dan Wells
Dean, College of Natural Sciences and Mathematics

Acknowledgements

First of all, I would like to thank from the bottom of my heart my mentor, Dr. Brigitte Dauwalder. Her continuous support has helped and encouraged me during all these years. I appreciate her willingness to be there for me anytime for any scientific or any other kind of problems. Without her, this dissertation would not have been possible. I thank her for providing all the resources for the completion of my projects in the lab. It has been a pleasant and memorable experience to be part of her lab and learn from her. I will always be grateful to Brigitte for her mentoring, guidance, and for being a wonderful human being. Thank you!!!

I would also like to express my deepest gratitude to my committee members: Dr. Gregg Roman, Dr. Preethi Gunaratne, and Dr. Kathleen M Beckingham. They were always there to guide me through my PhD years with their comments, support, and kindness. They are wonderful mentors, scientists, and people.

I would like to thank Biology of Behavior Institute (BOBI) and National Science Foundations (NSF) for providing the funding for the projects.

I would like to thank Ashley Benham for her generous help and constructive comments in my microRNA projects. I would also like to thank Weimen Xiao for helping me in the analysis of my data. Special thank goes to Peter Chang from University of Southern California for helping in the analysis of my data.

Besides, there are a lot of other friends that in one way or another made the completion of this dissertation possible. I would like to thank all the current and former members of the Dauwalder lab, who in one way or another made working and learning fun. Valbona Hoxha, Thilini Wijesekara, Sumit Saurav, Yuanli Li, and Nancy Vanaphan,

thank you for being great friends and lab members. I am very grateful to Mike de la Flor for his generous help. Many thanks go to my friends Adrian, Emiliano, Ana, Yier, Ruth, and Vrutant for their continuous and unconditional friendship.

I would also like to thank graduate Advisors Amanda Paul and Rosezelia Jackson for always listening to me and my problems and for being such a wonderful and helpful people. Many thanks to Kathleen for helping me with confocal microscopy.

I would like to thank my parents: Tirtha Bahadur Tamang and Mai Tamang for being the most wonderful parents one could wish for. I thank them for their unconditional love, support and for always believing in me. I would also like to thank my sisters Bimala Lama and Kamala Lama; and my brothers Uttar Singh Lama and Pema Kumar Lama for their continuous love, encouragement and support. I would also like to extend my thanks to my sister in law Deepa Lama and my little niece Sehana for their love and support.

A special thanks goes to my husband Prajjwal Tamrakar for his constant support and making it possible for me to finish this dissertation. Without whom I could not have made it. He has helped me in every possible way to complete this chapter of my life. I will always be grateful to him for being a part of my life.

Thank you to all of you!!!

Identification and Characterization of Sex-specific Transcripts in the Blood Brain Barrier of *Drosophila melanogaster*

An Abstract of a Dissertation

Presented to the

Faculty of the Department of Biology and Biochemistry

University of Houston

In Partial Fulfillment of the

Requirements for the Degree

Doctor of Philosophy

By

Chamala lama

December 2013

Abstract

In *Drosophila*, a male displays a series of complex stereotypic acts in courting a female. This behavior is mainly controlled by male specific transcription factors that define male neuronal circuits inside the brain. In our lab, we have shown that male factors which are secreted outside of the CNS are also required for normal mating behavior. How these endocrine factors interact with the CNS is unknown. We have evidence that the Blood brain barrier (bbb) plays an important role in this communication. Specific feminization of the bbb in otherwise normal males severely reduces their courtship. This suggests that male specific factors in the bbb play an important role in mating behavior. To identify these factors, I have used several genomic screens on dissected brains and isolated bbb cells. Studies that include mRNA sequencing and microarray hybridizations have identified several male-specific candidate genes with possible novel roles in courtship. I examined and found an adult role for one of the male preferentially expressed bbb-specific candidate genes, *Hr46* in the regulation of male courtship behavior in the bbb. In addition, I have identified bbb-expressed microRNAs and their possible targets. I explored a role for *miR-184*, the most abundant miRNA in the bbb of *Drosophila* in male courtship. Alterations of the *miR-184* levels in the adult bbb resulted in significant reduction in courtship suggesting its importance for normal male courtship in the bbb. Conditional RNAi knockdown of *sinu*, a *miR-184* target in the adult bbb showed significant reduction in courtship indicating a physiological requirement in the bbb. Dye injection analysis shows that the the bbb permeability of *miR-184* and *sinu* mutants is intact. *quiver*, another putative *miR-184* target and a gene down-regulated in the mRNA sequencing experiment, was also found to affect male courtship behavior.

Taken together, these data are the first to identify sex-specific transcripts in the bbb and bbb-specific miRNAs; and to reveal a novel role for *miR-184* in the bbb for male courtship behavior of *Drosophila melanogaster*.

Table of Contents

List of Figures

List of Tables

Chapter I

Introduction

All animals are born with a set of instincts or innate behaviors. These innate behaviors manifest themselves without prior experience. These behaviors are hardwired into the nervous systems through genetic programs so that animals react instinctively to environmental stimuli in a way that enhances their prospects for survival and reproduction. Therefore to understand the molecular basis of such complex animal behavior, one must identify the relevant cells and understand the molecules that mediate their function. In this context, *Drosophila* serves as an excellent model organism by providing the ideal combination of instinctive behaviors, powerful methods of genetic manipulation, and electrical and optical recoding of neuronal activity (Stockinger et al., 2005). Among many different innate behaviors, *Drosophila* sexual instincts are the most attractive model for such purposes.

1.1 Courtship behavior

The mating behavior of *Drosophila melanogaster* is a complex and robust behavior. This behavior is composed of a series of consecutive stereotyped steps that the courting male performs and that can easily be observed and quantified (Greenspan and Ferveur, 2000). Courtship behavior of *Drosophila melanogaster* involves multimodal sensory integration such as vision stimuli, auditory stimuli, and chemosensory stimuli exchanged between the two partner flies (Greenspan and Ferveur, 2000).

When a male fly finds a female using the visual and acoustic cues (Ejima and Griffith, 2008), he orients himself towards the female by positioning his body axis toward the female (orientation) and starts to chase her (following). Then the male touches the back of the abdomen of female with his forelegs (tapping) to investigate the non-volatile

pheromones present on her body. While following a female, the male starts to extend and vibrate one of the two wings, one at a time, to sing a courtship song (Singing). This courtship song is generated by unilateral extension and vibration of a wing and is crucial for the female flies to identify their conspecific males. This unilateral wing vibration produces a species-specific courtship song that consists of sine song (a humming sound) and a pulse song with rhythmic elements, which stimulate the female to mate (Von Schilcher, 1976). Upon exposure to a conspecific song, the female usually slows down, a sign of willingness to accept the male courtship (receptivity) (Ferveur, 2010). The male fly then licks the female's genitalia (licking) to perceive female sex-specific pheromones. To date, only three gustatory receptors (Gr) have been implicated in the reception of pheromones – *Gr39a* is thought to detect female-enriched cuticular hydrocarbons CHCs (Watanabe et al., 2011), while *Gr32a* and *Gr33a* may serve detect male-enriched CHCs (Lacaille et al., 2007; Miyamoto and Amrein, 2008). The licking is usually immediately followed by attempted copulation, which involves curling of the male's abdomen towards the female's genitalia. If the female is receptive, she raises her wings and opens her vaginal plates and the copulation takes place and persists for 15-20 minutes (Figure 1.1). All of these elementary actions (except for copulation) occur repeatedly during courtship although in some cases tapping is not obvious (Yamamoto and Koganezawa, 2013). Interestingly, mating behavior shows plasticity despite its stereotyped pattern. For example, a male copulates for longer period of time after the sight of a rival male. Similarly, when a male perceives rejection from a fertilized female, he fails to vigorously court females for several hours (Kim et al., 2012; Siegel and Hall, 1979).

In general, mosaic analysis studies have shown that the different step of courtship are regulated by different regions of the central nervous system (CNS) and that they are stereotypically displayed in this order (Ferveur and Greenspan, 1998; Spieth, 1974; Stockinger et al., 2005). The recognition of a mate is controlled mainly by the FruM protein-expressing specific antennal glomeruli in the anterior brain, while the lateral and dorsal posterior brain is involved in the early steps of male courtship behavior such as orientation, tapping, and wing extension (Ferveur and Greenspan, 1998; Hall, 1977, 1979; Kohatsu et al., 2011; Rideout et al., 2010). The role of the thoracic ganglion has been shown mainly in the control of courtship song (Clyne and Miesenbock, 2008; Pan et al., 2011; Rideout et al., 2007; von Philipsborn et al., 2011). The thoracic and abdominal ganglion regions are mainly responsible for attempted copulation and copulation (Billeter et al., 2006; Hall, 1977).

Although the female seems to have a mainly passive role in courtship to the observer, she is the one that ultimately decides acceptance by slowing down and allowing copulation. The neuronal basis of female sexual behaviors has only recently been explored with studies primarily focusing on sensory elements that modulate post-mating responses (Rezaval et al., 2012). Besides sensory input from the courting male (his courtship song), major factors that influence female receptivity are her age (very young females are not sexually mature), and whether or not she has previously mated (Dauwalder, 2011). Sexually mature females elicit mild rejection behaviors. A receptive female will slow down her general locomotion activity and opens her vaginal plate for copulation to take place (Hall, 1994). Once the copulation takes place; the male transfers his sperm together with the seminal fluid to the female. The seminal fluid contains male

sex peptides (peptides synthesized in the male accessory glands), which mediate various post-mating responses in the female. The best studied is the sex-peptide (SP). The post-mating responses include the changes in the quality and quantity of anti-male aphrodisiac pheromones; the extrusion of the ovipositor to refuse the male and active rejection in response to a male trying to copulate (Kubli, 2003; Rezaval et al., 2012).

1.2 Sex determination pathway

Sexual behavior in flies is regulated by the same master regulator genes that control general somatic sexual development and are part of a cascade of alternative splicing. In *Drosophila melanogaster*, sex is determined by a series of splicing events on a cell–by-cell basis such that each cell makes the decision to be either a male or a female or by signals between adjacent tissues but without the involvement of sex hormones as in mammals (Christiansen et al., 2002; Cline and Meyer, 1996).

The primary signal lies in the ratio of X chromosomes to the autosomes (X:A). The Y chromosome does not play a role in the determination of the sex of the fly. This X:A ratio determines whether a functional form of the master regulator protein Sex-lethal (Sxl) is produced (in females) or not (in males) (Fig. 1.2). When the ratio of X and A is 1, the sex of the fly is female. In females, functional *Sxl* protein is expressed which acts as a splicing regulator to control female-specific expression of the transformer (TraF) protein, itself a splicing regulator (Baker, 1989). The activity of Sxl is maintained by a positive auto-regulatory feedback loop. TraF interacts with the ubiquitously expressed Tra-2, another splicing regulator. Together they control the female-specific splicing of *doublesex* (*dsx*) and *fruitless* (*fru*) pre-mRNAs resulting in the production of the female–

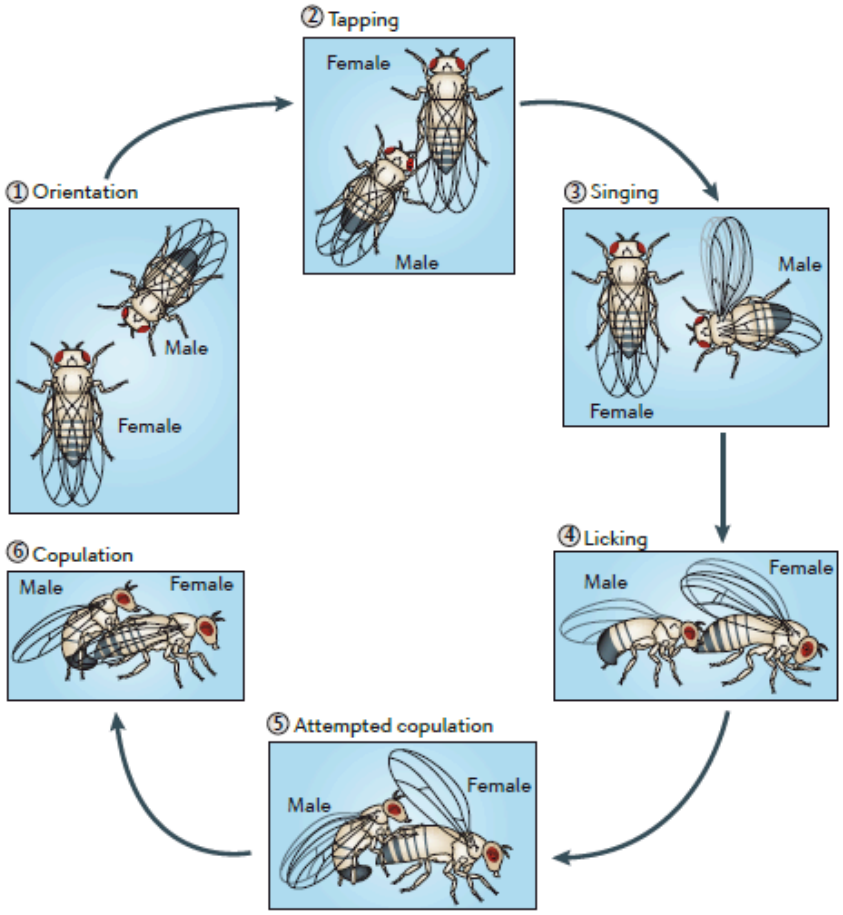

Figure 1.1: Male courtship in *Drosophila melanogaster*: The male courting behavior consists of discrete steps: Orientation towards and immediate following of the female (Step 1); touching her back with his forelegs (tapping) (Step 2); unilateral wing vibration and extension (singing) (step 3); licking the female's genitalia (step 4); attempted copulation (step 5); and finally copulation (step 6) (Yamamoto and Koganezawa, 2013).

specific *dsx* protein (DsxF). The female specific form of the *fruitless* mRNA is not expressed due to translational control (Lee et al., 2000 and Usui-Aoki et al., 2000). The role of DsxF is very important in the somatic sex-specific differentiation of the body (Baker 1989, Ryner and Backer, 1991). In addition to its role in somatic sex-determination outside the nervous system, recent studies have demonstrated that *dsx* plays an important role in the regulation of sexual behavior. For example, DsxF promotes the cell death of certain male specific neurons in the female brain to prevent females from exhibiting male-specific behavior (Kimura et al., 2011).

In contrast to females, the X to A ratio in males is 0.5 and there is no Sxl activity. As a result *tra* transcripts are produced by the default splicing pathway and contain a premature stop codons. This absence of the Tra protein in males leads to the default splicing of *dsx* and *fruitless* to produce male-specific mRNAs, which in turn produce male specific *dsx* (DsxM) and FruM proteins. The main role of *tra* in the control of sexual differentiation and sex-specific behavior was demonstrated by the fact that females with a chromosomal mutation in the *tra* gene are transformed into males with male courtship behavior (Boggs et al., 1987; McRobert and Tompkins, 1985).

Since *dsx* and *fru* are downstream of *tra*, further studies have examined the role of these two genes in controlling the male courtship behavior and a large body of evidence points to the fact that the sex-specific products of *fruitless* (the FruM) and *dsx* (DsxM) are the main players in the regulation of male courtship behavior in *Drosophila* (Arbeitman et al., 2010; Baker et al., 2001; Dauwalder, 2008; Demir and Dickson, 2005; Kimura et al., 2008; Pan et al., 2011; Rideout et al., 2007; Rideout et al., 2010). Based on the many earlier studies, it was proposed that there are two independent pathways

downstream of *tra*, one through *dsx* and another through *fru* in the nervous system that controls the male courtship behavior (Baker et al., 2001). However, it has become evident in recent years that the two pathways are both significantly contributing and interacting with each other in regulating male courtship behavior both in the CNS and the other tissues (Kimura et al., 2008).

1.2.1 *Fruitless* and *doublesex* neural circuitry defining the neural sex

Among mutants with defective aspects of courtship behavior, *fru* has caught special attention due to its unique and robust phenotypes (Yamamoto and Koganezawa, 2013). It is well established that *fru* is central to male courtship behavior. The *fru* gene is a large gene with four promoters (P1-P4) encoding putative transcription factors with a BTB domain. The most distal promoter, P1 generates the *fru* primary transcript that is regulated by *tra*-dependent, sex-specific splicing (Hall, 1977). The sex-specific splicing of this gene produces mRNAs that differ at their 5' end between the sexes (Heinrichs et al., 1998). The P1 promoter is active in ~ 2000 *fru* expressing neurons where sex-specific splicing occurs (Lee et al., 2000; Usui-Aoki et al., 2000). The male P1 promoter-derived transcripts encode proteins, whereas their female counterparts do not. The proteins encoded by P1 promoter transcripts have a 101 amino acid amino terminal stretch called M sequence (M for male specific) and this feature is absent in the non sex-specific *fru* proteins called FruCOM (COM for common) (Ryner et al., 1996; Usui-Aoki et al., 2000). Therefore, male–specific Fru proteins are referred to as FruM to distinguish them from the non-sex-specific FruCOM proteins. FruM belongs to the BTB-Zn-finger family of transcriptional regulators (Ito et al., 1996).

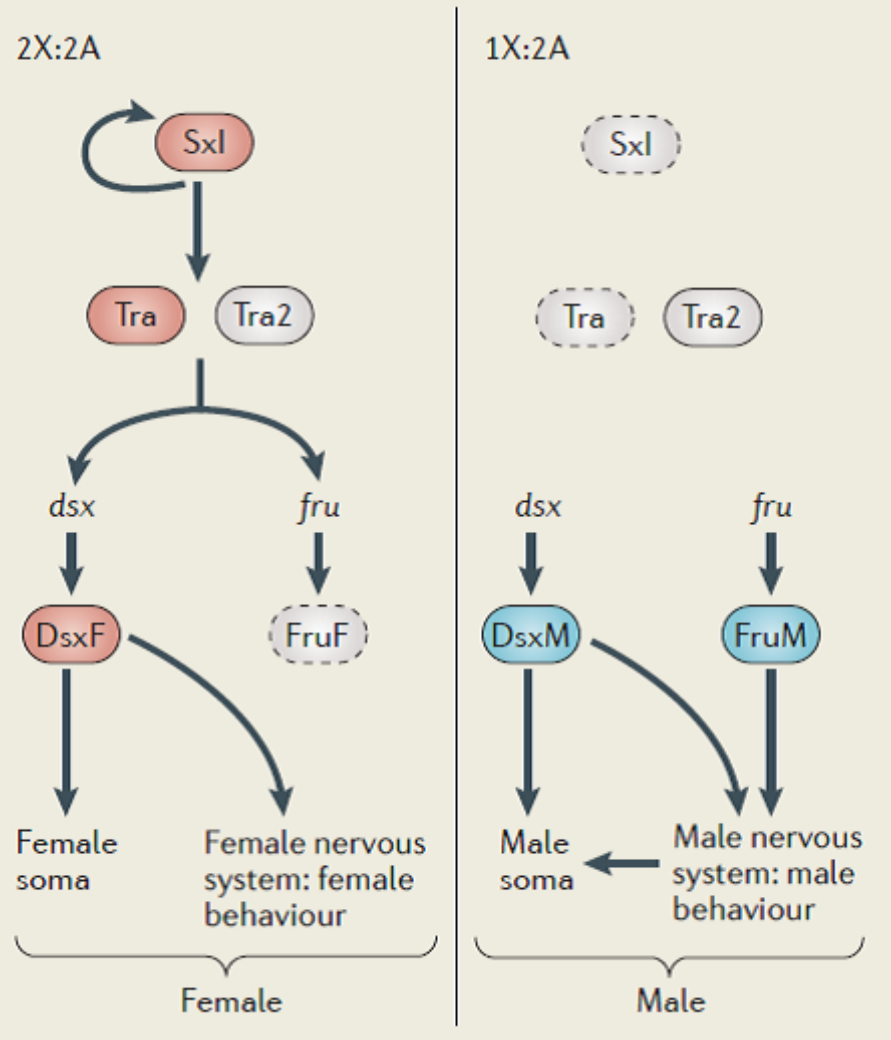

Figure1.2: Regulators of the *Drosophila* sex-determination pathway (Yamamoto and Koganezawa, 2013)

Interestingly, the circuitry of *fru* neurons is largely the same in male and females; indicating that it is the expression of FruM that gives the competence for the execution of sexual behavior to those neurons (Billeter and Goodwin, 2004; Manoli et al., 2005; Stockinger et al., 2005). FruM neurons are mainly organized in 48 distinct clusters in largely uncharacterized circuits involving sensory, olfactory, and motor components of the male courting behavior (Kimura et al., 2008; Manoli et al., 2005; Meissner et al., 2011; Pan et al., 2011; Stockinger et al., 2005; Yu et al., 2010). Moreover, Demir and Dickson, 2005, and Manoli and Baker, 2005 have observed that the expression of male specific FruM isoforms in otherwise normal females leads to the females displaying male courtship behavior and courting other females albeit at lower levels compared to normal males (Demir and Dickson, 2005; Manoli et al., 2005). This indicates that other sex-specific factors are also necessary for the execution of normal male courtship behavior (Dauwalder, 2008; Lazareva et al., 2007; Pan et al., 2011).

A number of studies have now shown that Fru expressing neurons in conjunction with *doublesex* are sufficient for almost all the steps performed in male sexual behavior (Manoli et al., 2006; Pan et al., 2011; Ryner et al., 1996; Yamamoto et al., 1998). Since Fru belongs to the BTB-zinc finger family of proteins and Dsx has been shown to act as transcription factor, these proteins regulate gene expression. This generates differential transcriptional states in cells depending on whether they do, or do not have these factors. Consistent with the expected role of a transcriptional regulator, FruM proteins were found to co-precipitate with chromatin regulators such as Histone Deacetylase (HDAC1) and with the heterochromatin protein HP1a as well as with the transcriptional cofactor Bonus (Bon). This indicates that FruM proteins form complexes with these proteins *in*

vivo (Ito et al., 2012). In fact by over-expressing individual FruM isoforms in *fru*-expressing neurons in either males or females and assaying the global transcriptional response by RNA-sequencing Dalton et al. (2013) have identified several sets of genes regulated downstream of FruM isoforms, including many annotated with neuronal functions. They found that the three FruM isoforms have different regulatory activities that depend on the sex of the fly. By determining the binding sites of individual FruM isoforms using Systematic Evolution of Ligands by Exponential enrichment (SELEX) they demonstrated that the distinct zinc finger domain of each FruM isoforms confers different DNA binding specificities (Dalton et al., 2013).

Doublesex (dsx) is the other branch of *tra* in the sex-determination hierarchy. The *dsx* gene is translated in both the sexes, with different carboxyl termini (Lee et al., 2000). In contrast to *fru, dsx* is required for somatic sex determination of various tissues both neuronal and non-neuronal (Rideout et al., 2010; Robinett et al., 2010; Sanders and Arbeitman, 2008). DsxF has been shown to play an important role in specifying female neuronal circuitry by inducing cell death in certain male specific neuronal clusters such as P1 neurons of the CNS (Kimura et al., 2008) and TN1 neurons of the thoracic ganglion (Sanders and Arbeitman, 2008). DsxM is expressed widely in somatic and neuronal systems. The role of *dsx* has been implicated in the regulation of neuronal cell numbers, axonal projections and synaptic density in a sex-specific manner (Kimura et al., 2008; Rideout et al., 2010; Sanders and Arbeitman, 2008). Male *dsx* mutants, which appear intersexual in appearance, perform lower level of courtship with females and display defective courtship song (Villella and Hall, 1996), indicating the importance of *dsx* in male courtship. The importance of DsxM and FruM co-expression in different neuronal

clusters for the regulation of courtship behavior shows an emerging picture of neuronal circuits that are characterized and specified by the presence or absence of *fru* and/or *dsx* (Rideout et al., 2007; Sanders and Arbeitman, 2008). In many cases, it has been shown that *dsx* is required for the development of specific *fru*-positive male specific neurons (Rideout et al., 2010) and that DsxM is required in the abdominal ganglia for the differentiation of male specific serotonergic neurons (Billeter et al., 2006) as well as for an increased number of neurons in the abdominal ganglia of males (Taylor and Truman, 1992). Therefore, in addition to its role in the development of external sexual morphology (Burtis and Baker, 1989), *dsx* cooperates with *fru* in directing the development of male–specific neuronal circuits that define male courtship behavior.

1.2.2 Downstream target genes and the blood brain barrier

Both Fru and Dsx are transcriptional regulators controlling the expression of downstream targets. However, we have limited knowledge about the sex-specific genes they regulate and what role they might play in courtship and other behaviors. Several genomic screening studies have been performed to identify sex-specific transcripts and transcripts that change in *fru* and *dsx* mutants (Dauwalder et al., 2002; Fujii and Amrein, 2002; Goldman and Arbeitman, 2007) but, the biological role of only a few of these transcripts has been characterized so far. Interestingly, many identified potential downstream targets of *dsx* and *fru* were found to be express in the head outside of the CNS in tissues such as fat body and glial cells as well as in the PNS (Dauwalder, 2008; Goldman and Arbeitman, 2007). The role of fat body cells surrounding the brain has received considerable attention recently (Dauwalder, 2008; Fujii and Amrein, 2002;

Goldman and Arbeitman, 2007) due to the fact that many of the sex-differentially expressed genes are present in this tissue.

The *takeout* (*to*) gene, with its male preferential expression in male fat body (in heads); is one of the downstream targets of *fru* and *dsx*. It was identified in a subtractive screen (Dauwalder et al., 2002). A mutation in *takeout* affects male courtship behavior, and genetic interaction studies showed that *takeout* interacts genetically with *fru*, indicating that they act in the same overall pathway in regulation of mating behavior. *takeout* is a part of a large family of secreted factors that are predicted to bind small lipophiles (Sarov-Blat et al., 2000; So et al., 2000). The fat body is a major secretory tissue, and Takeout has been found in the circulating hemolymph of the fly (Lazareva et al., 2007). How *takeout* interacts with the neuronal circuits in the brain to regulate courtship behavior is still an open question. When the adult fat body was feminized in otherwise normal males, the courtship index dropped more than observed in *takeout* mutants alone, suggesting that there are additional sex-specific factors that are secreted into the hemolymph and affect the courtship behavior (Lazareza et al., 2007). This poses the question about the exact mechanism by which such secreted factors from the hemolymph and the other non-neuronal tissues would interact with the neuronal circuits in the brain to regulate courtship behavior. The hemolymph does not have unrestricted access to the brain, since flies possess a **blood brain barrier (bbb)** that forms a tight barrier to restrict access to the brain and nervous system. How hemolymph factors negotiate the blood brain barrier to interact with the brain is unknown. Interaction of hemolymph components with the brain will likely involve specific receptors, transporters

and signaling events that are largely unidentified at present. For these reasons, we have become very interested in the bbb and the role it might play in courtship.

1.3 The blood brain barrier (bbb)

The complex nervous systems of mammals are comprised of two different cell types; one comprising of different types of neurons to perceive and integrate information and the other comprising of glial cells which provide essential functions that can directly modulate behavior, neurotransmitter metabolism and CNS immune-competency (Dong and Benveniste, 2001). The CNS (central nervous system) physiology requires special chemical, metabolic and cellular conditions for normal function, and evolution has established an elaborate barrier protection system known as the blood brain barrier (bbb) for this purpose. One of the initial indications that such a barrier existed was the inability of water-soluble dyes to penetrate the brain tissue (As reviewed in DeSalvo et al., 2011). The bbb structures are the anatomic and physiologic constructs that mediate the communication between the brain and the body (DeSalvo et al., 2011). The direct role of the bbb in CNS diseases such as multiple sclerosis, stroke and cancer, has been indicated. In addition, its role as a pharmacologic obstacle to the brain for drug delivery in neuronal diseases has been a long-standing challenge.

1.3.1 The blood brain barrier in *Drosophila*

Drosophila has an open circulatory system comprising of hemolymph, the blood of the fly which bathes all the cell and tissues (except for the retina, central brain, and

peripheral nerves). The CNS is protected from the harmful assaults of the hemolymph (such as its very high potassium content) by the presence of a thin layer of glially derived epithelial cells (Schwabe et al., 2005; Stork et al., 2008; Treherne, 1962), the ***Drosophila* bbb**. The bbb prevents unregulated passage of circulating molecules into the brain, maintaining a controlled and stable environment. This cellular layer uses two properties to promote neuroprotection: a tight diffusion barrier and a complex array of transcellular transporters (Mayer et al., 2009). Initially, the existence of a blood brain barrier in *Drosophila* was observed as septate junctions with a regular smooth ladder-like appearance (Tepass and Hartenstein, 1994). The barrier is established at the end of embryonic development by a thin layer of epithelial cells, which are thought to be glia derived from the neural ectoderm, named surface glia. This glial epithelium ensheathes the entire nerve cord and generates an ionic seal by forming intercellular septate junctions (SJs) (Carlson et al., 2000; Edwards et al., 1993).

Many studies have used the dye penetration assays to establish the barrier integrity/function of the *Drosophila* blood brain barrier. In these assays, the dyes cannot penetrate the nervous system if the bbb is intact; indicating that the nervous system is insulated. Moreover, the use of differently sized dextrans allow for addressing a possible size selectivity of the different barrier layers (Bainton et al., 2005; Schwabe et al., 2005; Stork et al., 2008). The *Drosophila* septate junctions (SJ) have been suggested to be the functional homologues of vertebrate tight junctions (Baumgartner et al., 1996). SJs contain regularly spaced, electron-dense septa that give them a ladder-like appearance. The septa are thought to serve as a series of filters that impede the penetration of small molecules through the intercellular cleft; the more septa, the tighter the seal (Abbott,

1991). The surface glia which form the functional blood brain barrier in *Drosophila* is composed of two types of specialized glial cells: the perineurial glial cells (PG cells) and the subperineurial glial cells (SPG cells) (Auld et al., 1995).

Perineurial glial (PG) cells form the apical glial layer and are located just below the neural lamella, the extracellular matrix that surrounds both the central and the peripheral nervous system. They are small and slender oblong cells with many thin cell protrusions within the perineurial layer itself, which never invade into the neural tissue (Awasaki et al., 2008; Stork et al., 2008). Post embryonically, the PG develops from the dorsal ectoderm (Schmidt et al., 1997)where they proliferate significantly and enlarge as the brain surface itself grows (Awasaki et al., 2008). Except for its suggested role in supporting the peripheral nerves (Yager et al., 2001) and as an internal diffusion barrier for the larger macromolecules, the function of perineurial glia is largely unknown and there are only few genetic markers available (Stork et al., 2008).

Underneath the perineurium is a thin layer (~1μm) of ensheathing large sheet-like cells (40-80 μm in width), the basal glial layer on the brain surface known as the subperineurial glial (SPG) layer (Bainton et al., 2005; Schwabe et al., 2005; Stork et al., 2008). The SPG cells are generated during embryonic development from the ventrolateral neuroectoderm and subsequently migrate to the surface of the developing CNS, once in place, they do not divide further. At the nerve cord surface, the SPG spread out until they form a continuous sheet of cells that completely ensheath the nerve cord forming the blood nerve barrier via the formation of septate junctions (Awasaki et al., 2008; Stork et al., 2008; Schwabe et al., 2005).

1.3.2 Homology between the *Drosophila* and the vertebrate blood brain barrier

With recent identification of homologous proteins at the epithelial junctions of the bbb in both flies and mammals (Wu et al., 2004), *Drosophila* is becoming a popular model in the field due to its relatively simpler nervous system, smaller population of glial cells and growing number of genetic tools (Awasaki et al., 2008). In vertebrates, the two primary cells, the polarized vascular endothelium (VE) and a tightly associated single layer of astrocytic glia (AG) forms the basis of the bbb and the tight junction between the VE cells is central to its barrier function (Zlokovic, 2008). The VE/AG interface in vertebrates is comparable to the PG/SPG interface in the *Drosophila*.

The tight junctions in vertebrate bbb are seen as focal contacts between the membranes of the nearby epithelial cells conferring a high electrical resistance that limits the paracellular flow of molecules from the blood to the brain (Ballabh et al., 2004). In *Drosophila*, the septate junctions (SJ) formed by SPG cells have long been considered to be the structural basis of the blood brain barrier (Carlson et al., 2000). The SJs appear as electron–dense septa that form a ladder-like continuous band around the cells (Daneman and Barres, 2005, figure 1.4). These *Drosophila* septate junctions are a functional and molecular equivalent to the vertebrate tight junctions, though they differ morphologically. Interestingly, it has been found that the *Drosophila* SJ bears a striking resemblance to the mammalian paranodal myelin loops and axon junctions. Paranodal junctions contain Caspr, Contactin, Protein 4.1, and Nf155 (Bhat et al., 2001; Poliak and Peles, 2003; Sherman and Brophy, 2005), and *Drosophila* glial cells contain their respective homologs

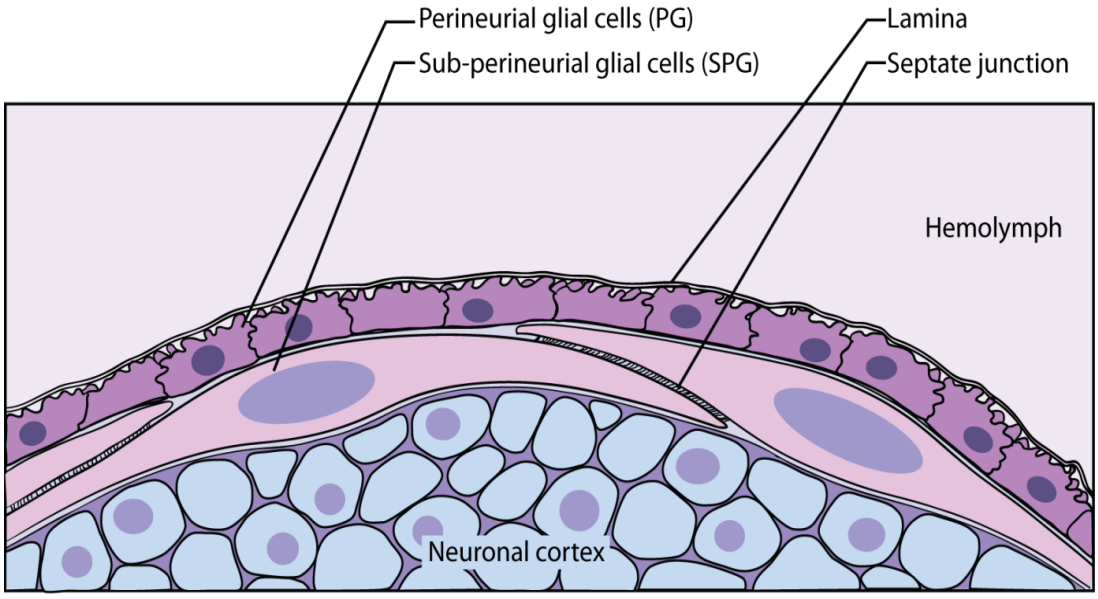

Figure 1.3: A schematic of the blood brain barrier in *Drosophila melanogaster*, modified from (Daneman and Barres, 2005). The bbb is mainly composed of two glial cell layers: the outer perineurial and the inner sub-perineurial layer. These layers are responsible for the insulation of the CNS from the harmful components of the surrounding hemolymph.

Neurexin IV, Contactin, Coracle, and Neuroglian (Banerjee et al., 2006; Faivre-Sarrailh et al., 2004).

In mammals, the endothelial cell tight junctions between the cells are formed through the binding of claudin proteins (Furuse and Tsukita, 2006), on opposing membranes to form a tight but selective porous seal. Similarly, the *Drosophila* claudin-like proteins such as si*nuous* (sinu) and megatracheal are required for the establishment of normal blood brain barrier formation (Wu et al., 2004; Stork et al., 2008). Moreover, the mammalian homologue of the xenobiotic ABC transporter *Mdr1/P*-glycoproteins, *Mdr65* is also found in the *Drosophila* bbb (Mayer et al., 2009). Therefore, taken together, these findings indicate that the *Drosophila* blood brain barrier is functionally and structurally similar to the vertebrate blood brain barrier.

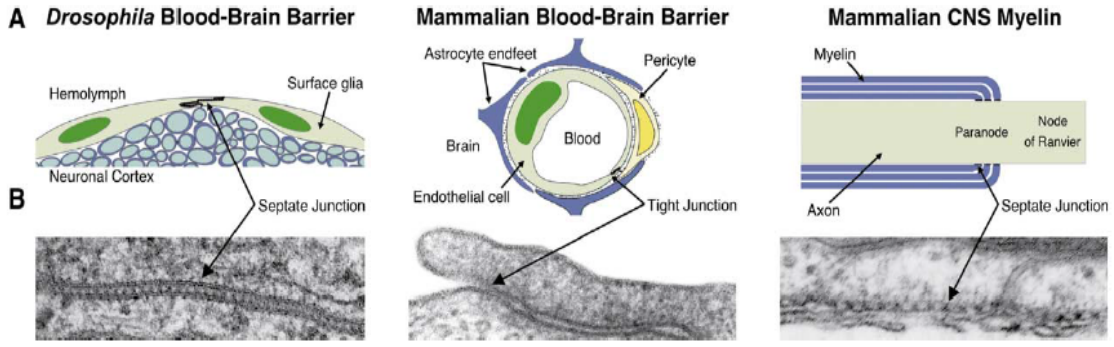

Figure 1.4: A comparison of *Drosophila* bbb, mammalian bbb and mammalian CNS myelin (Daneman and Barres, 2005). A) Cross-sectional schematic representation. B) Electron micrographs displaying the morphology of the *Drosophila* septate junctions, mammalian tight junctions, and mammalian CNS myelin septate junctions.

1.3.3 Role of the adult bbb function

Several studies have identified important proteins that are required for the development of a tight and functional barrier. Neurexin IV, Contactin, and Neuroglian, Sinu, and Moody are important components of the bbb (Baumgartner et al., 1996; Faivre-Sarrailh et al., 2004; Schwabe et al., 2005; Bainton et al., 2005; Stork et al., 2008; Blauth et al., 2010). While insight into the development of the *Drosophila* bbb has been gained, very little is known about the adult bbb and the mechanisms that underlie its function beyond the exclusion function that is based on its tight junctions. Interaction of hemolymph components with the brain will likely involve specific receptors, transporters and signaling events that are largely unidentified at present. A *Drosophila* ABC transporter, *Mdr65*, has been described (Mayer et al., 2009). Furthermore, the putative G protein coupled receptor (GPCR) *moody* which is specifically expressed in the SPG barrier cells has been shown to mediate the behavioral response to ethanol and cocaine independent of its developmental function in barrier set-up (Bainton et al., 2005).

Very recent work from our lab has shown that *moody* is also required for male courtship behavior and that the sexual identity of the bbb is important for male courtship behavior (Hoxha et al., 2013). To test the role of the bbb in male courtship behavior, the bbb was feminized by targeted expression of the female–specific Tra protein in otherwise normal males. Feminization of the adult bbb significantly reduced male competence to perform courtship behavior compared to the males with normal bbb. This indicates that the bbb is sexually dimorphic and that sex-specific factors in the bbb are physiologically important for the regulation of male courtship (Hoxha et al., 2013). Thus, two established behaviors (ethanol response and courtship) depend on the proper adult function of the

bbb. This allows us to experimentally test candidate genes and processes. We believe that other behavioral processes are likely to depend on bbb functions as well. Based on the feminization results described above, I hypothesized that there are many factors/molecules that are present sex-specif ically in the bbb which are required for the regulation of male courtship behavior in *Drosophila*.

In order to identify the bbb factors and their sex-specific roles in the regulation of *Drosophila* male courtship behavior, I identified sex-specific transcripts in the bbb using high-throughput microarray technology. As a complementary approach, changes in transcripts (mRNAs) upon feminization of bbb cells in males were determined by Next Generation Sequencing (NGS) using the Illumina sequencing platform. Many sex-specific genes were identified in the bbb and the role of several candidate genes in courtship behavior of *Drosophila* was characterized. Since miRNAS are important regulators of gene expression, I profiled miRNAs expressed in the bbb by using the Illumina sequencing platform. As an integration of the two approaches (mRNA sequencing and microRNA sequencing), in chapter IV of this dissertation, a novel role for a microRNA and its predicted target in the bbb for the regulation of male courtship behavior was established, thus demonstrating a functional significance of microRNA-mRNA pairs in regulating bbb-mediated courtship behavior.

1.4 Role of microRNAs in gene regulation

1.4.1 Introduction

Small non-coding RNAs have been linked with an increasing variety of important functions in many biological processes in a living cell. MicroRNAs (miRNAs) are one of

the classes of small non-coding RNAs that are involved in post-transcriptional regulation of gene expression in multi-cellular organisms largely by interacting with the 3'UTR of their targets, affecting both the stability and translation of mRNAs (Hutvagner and Zamore, 2002). miRNAs are 20-24 nucleotides (nt) long and are well conserved in eukaryotic organisms and are thought to be an evolutionary component of genetic regulation. Since the identification of first microRNA *lin-4* in *C. elegans* in 1993 (Lee et al., 1993), 1872 precursors, 2578 mature miRNAs in humans; 223 precursors, 368 mature miRNAs *C. elegans*; 1186 precursors, 1908 mature miRNAs in mouse and 238 precursors, 426 mature miRNAs in *Drosophila* have been identified (http://www.mirbase.org/cgi-bin/browse.pl).

1.4.2 Biogenesis

In the genome, miRNAs are found largely within the introns of protein coding genes or within intergenic regions (Hammond et al., 2000). miRNA genes are first transcribed into primary miRNAs (pri-miRNAs). Pri-miRNAs are either transcribed from independent miRNA genes or are portions of introns of protein-coding RNA polymerase II transcripts. Pri-miRNAs fold into hairpin structures containing imperfectly base-paired stems and are processed in two steps, catalysed by the RNase III-type endonucleases Drosha (also known as RN3) and Dicer. Both Drosha and Dicer function in complexes with proteins containing dsRNA-binding domains (dsRBDs). The Drosha partners are the *pasha* protein in *Drosophila* or DiGeorge syndrome critical region gene 8 (DGCR8) in mammals. This process leads to the production of ~70-nucleotide hairpins known as pre-miRNAs (Figure 1.5). A single pri-miRNA sometimes contains sequences for several different pre-miRNAs.

In animals, pre-miRNAs are transported to the cytoplasm by exportin5, where they are cleaved by another RNAse III enzyme, Dicer, in a complex with TAR RNA-binding protein (TRBP) in mammals and the *loquacious* gene product in *Drosophila* to yield ~20-bp miRNA duplexes with 2 nt overhangs. One strand is then selected to function as a mature miRNA, while the other strand is degraded. Occasionally, both arms of the pre-miRNA hairpin give rise to mature miRNAs (Bushati and Cohen, 2007; Du and Zamore, 2005; Peters and Meister, 2007; Rana, 2007).

Vertebrates and *C. elegans* contain a single *dicer* gene, but *Drosophila* and plants express two or more Dicer proteins that function as heterodimers with different dsRBD proteins and have specialized functions (Bushati and Cohen, 2007; Du and Zamore, 2005; Peters and Meister, 2007; Rana, 2007). Although either strand of the duplex could potentially act as a functional miRNA, with few exceptions, only one strand (the mature miRNA) is incorporated into a ribonucleoportein complex (RISC) or miRNA-induced silencing complexes (miRISCs). The assembly is a dynamic process, usually coupled with pre-miRNA processing by Dicer, but its details are not well understood (Bushati and Cohen, 2007; Du and Zamore, 2005; Peters and Meister, 2007; Rana, 2007). Strand selection for the mature miRNA (miR) into RISC is based on the thermodynamic stability of the two ends of the dsRNA. The strand with less stable 5'-end is taken up by RISC and the remaining strand is the passenger or miR* is subsequently degraded (Murchison and Hannon, 2004). The PAZ and PIWI domain (PPD) containing Argonaute family protein, Argonaute 2 is the major component of the RISC complex whereby the PAZ domain of Ago 2 specifically recognizes the miRNAs duplexes by their characteristic 2-nt 3' overhangs (Lingel et al., 2003, 2004; Yan et al., 2003). In the active RISC complex, the

5’ end of the guiding miRNA strand is anchored to the PAZ domain of Ago 2. One miRNA can regulate multiple rounds of mRNA regulation from an active RISC complex (Hutvagner and Zamore, 2002).

1.4.3 Target recognition and regulation

In plants, microRNAs generally base pair to mRNAs with perfect or near perfect complementarity and trigger endonucleolytic mRNA cleavage by an RNAi-like mechanism (Jones-Rhoades et al., 2006). However in animals, the predominant gene silencing occurs by imperfect complementarity leading to translational repression. The miRNAs accomplish this process by base pairing of the miRNA with the target RNA sequence via an antisense mechanism forming a miRNA: mRNA duplex. The mature miRNA stringently requires two main regions: 1) a highly conserved “seed region” between the nucleotides 2 and 8 responsible for nucleation of the interaction and the specificity of target recognition, and 2) a conserved “anchor region” residing in position 13 through 16 which increases the duplex stability (Brennecke et al., 2005; Doench and Sharp, 2004; Grimson et al., 2007; Lewis et al., 2005; Lytle et al., 2007). Specifically, when the mRNA is unpaired at the adjacent positions 10 and 11 of miRNA, the mRNA is prevented from entering the catalytic site of Ago 2, thus inhibiting cleavage.

For the most part, the mature miRNAs mediate gene silencing by binding to the 3’UTR of the target mRNAs where they inhibit translation and/or induce mRNA degradation by RISC. However, in some instances, the 5’-UTRs or even Open Reading

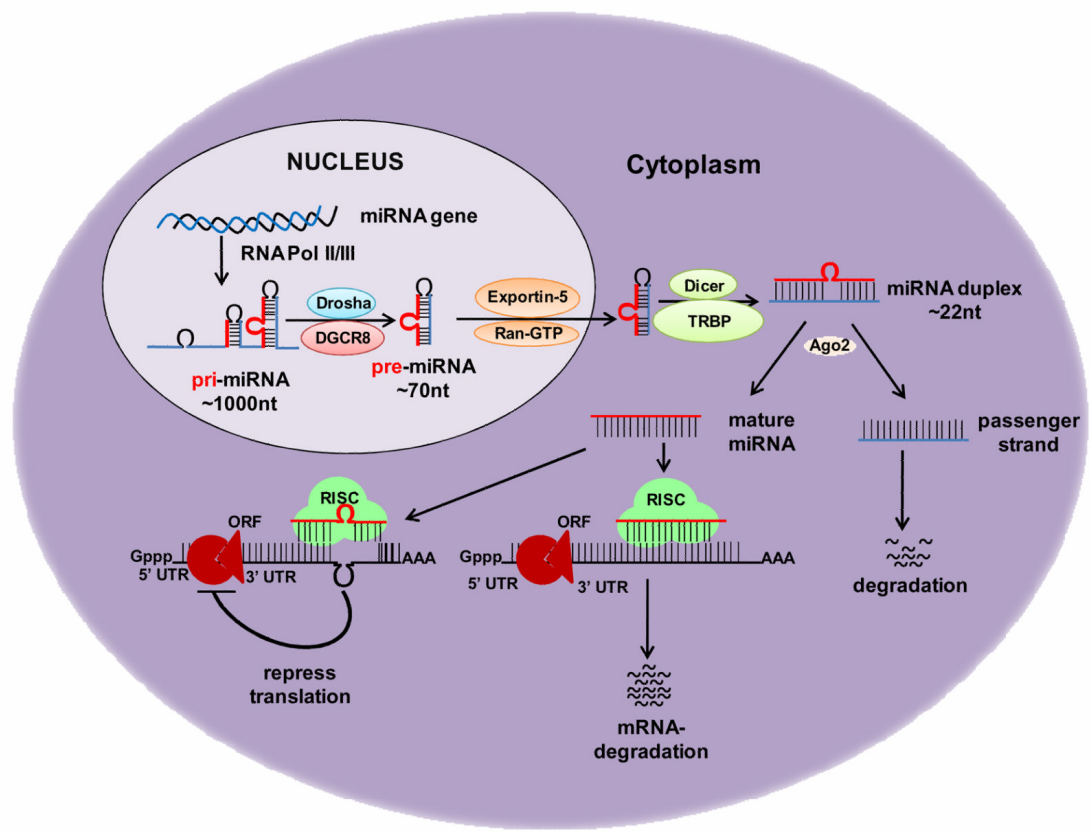

Figure 1.5: MicroRNA biogenesis: MicroRNA (miRNA) genes are generally transcribed by RNA polymerase II/III in the nucleus to form large primary transcript (pri-miRNA). These pri-miRNA transcripts are processed to release the ~70-nucleotide hairpin RNA known as precursor-miRNA (pre-miRNA), which is transported to the cytoplasm and undergoes another processing to yield a transient ~22- nucleotide RNA duplex. The RNA duplex is unwound into a mature single-stranded miRNA, and loaded into RNA-induced silencing complex (RISC). miRNA then binds to complementary sites in the 3'-untranslated region (3'-UTR) of target mRNA and regulate its expression either by causing degradation of mRNA or repression of their translation, depending on the degree of complementarity between the miRNA and its target (Bhardwaj et al., 2010).

Frames (ORFs) have been shown to participate in the binding (Kloosterman et al., 2004; Lytle et al., 2007).

Over 1000 miRNAs identified to date have predicted target sites on 60% of the genes in the mammalian genome showing the widespread impact miRNAs could have on the transcriptomes (Friedman et al., 2009). Moreover, one miRNA can regulate the activity of many mRNAs and many mRNAs possess multiple miRNA binding sites within the 3'-UTR, giving rise to complex regulatory network.

1.4.4 Target prediction

To date, more than 1000 human miRNAs and 426 *Drosophila* miRNAs are recorded in miRbase (miRbase.org) each potentially targeting thousands of mRNAs. Different miRNA target prediction algorithms use different methods to assess the relative strength of interaction between the miRNAs and their potential targets. The common leading programs for miRNA target prediction are PicTar, MiRanda, and Targetscan.

1.4.5 Role of miRNAs in *Drosophila*

Since the identification of the first miRNA *lin-4* in *Caenorhabditis elegans* in 1993 (Lee et al., 1993), about 426 miRNAs in *Drosophila* have been identified (http://www.mirbase.org). As we know, miRNAs play an important role in the development, proliferation, differentiation, immunity, apoptosis, behavior, and diseases of organisms; *Drosophila* has been used extensively as a model organism to study the role of miRNAs in these processes.

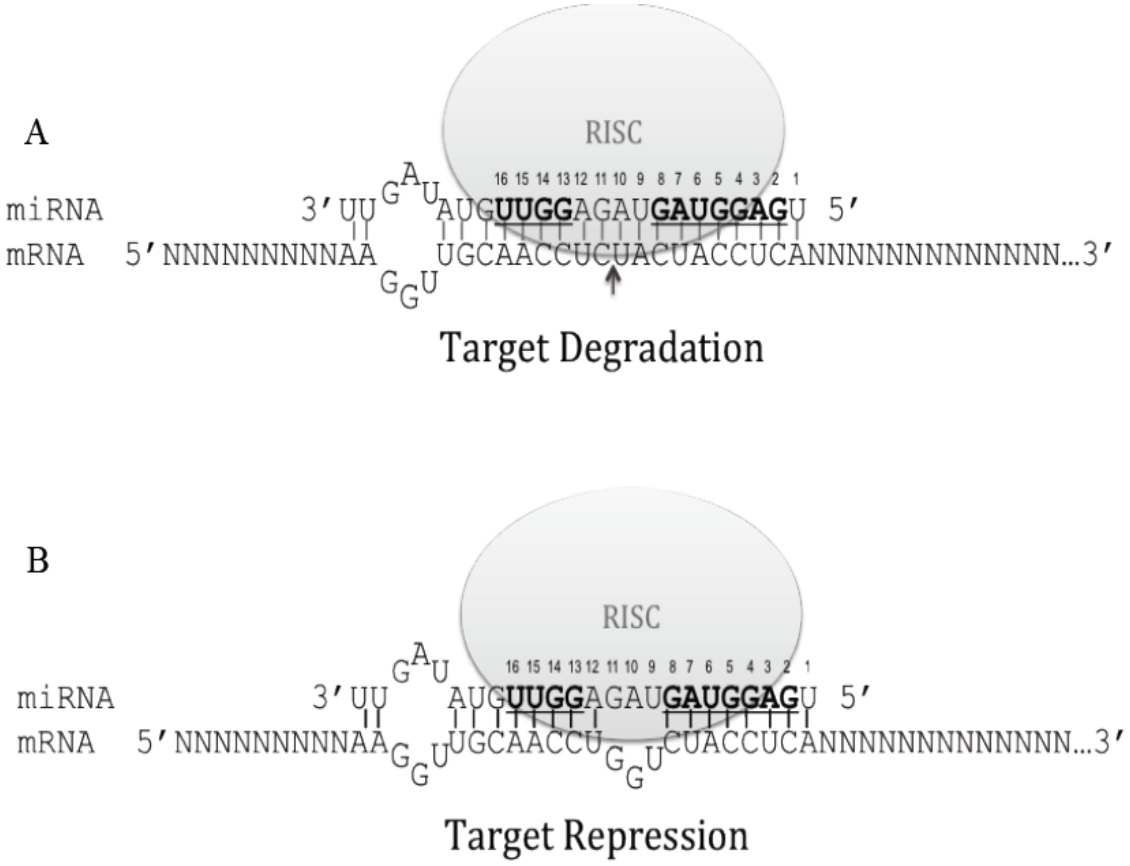

Figure 1.6: miRNA target regulation: A miRNA: mRNA duplex can undergo two possible fates. A) When the miRNA is complementary to the target mRNA at positions 10 and 11, the mRNA is subjected to cleavage by Argonaute 2 (arrow). B) When the miRNA: mRNA duplex is not paired at the 10^{th} and 11^{th} positions, it is not cleaved by Argonaute 2 resulting in translational repression (Benham, 2011).

Most miRNAs display a tissue- and/or developmental- specific expression pattern, which suggests highly specific and diverse roles for miRNAs. For example, *miR-1* is found exclusively in muscles, where it regulates cardiac differentiation in *Drosophila* (Kwon et al., 2005). *miR-9a* is specifically expressed in epithelial cells and has been shown to control the generation of sensory organs (Li et al., 2006). *miR-9a* ensures the precise specification of sensory organ precursors in *Drosophila*. *miR-278* is predominantly expressed in larval fat body cells, where it regulates genes involved in insulin secretion. *Drosophila* lacking *miR-278* are defective in energy homeostasis (Teleman et al., 2006).

A number of studies have shown that different morphogenetic processes of *Drosophila* are affected by *let-7* and/or *miR-125* depletion, such as the terminal cell-cycle exit in wing formation and the maturation of neuromuscular junctions (Caygill and Johnston, 2008). *let-7* also plays an important role in abdominal neuromusculature remodeling (Sokol et al., 2008) and in innate immunity (Garbuzov and Tatar, 2010), as well as in steroid (ecdysone) hormone mediated neuronal differentiation (Kucherenko and Shcherbata, 2013). Neuronal misexpression of three miRNAs (*miR-8, miR-289*, and *miR-958*) led to suppressed activity-dependent synaptic growth at *Drosophila* neuromuscular junction (Nesler et al., 2013).

bantam plays a positive role in the regulation of tissue growth control by regulating its target (Zhang and Lai, 2013). For example, *bantam* acts as the proliferation –promoting microRNA in the regulation of *Drosophila* wing disc development (Zhang et al., 2013). A recent study has implicated an unexpected role of *bantam* microRNA in controlling body size in *Drosophila*. The data suggest that, in addition to its well-

characterized function in autonomously inducing tissue growth, *bantam* activity in ecdysone-producing cells promotes systemic growth by repressing ecdysone release. Further, it was also found that the regulation of ecdysone production by insulin signaling relies on the repression of *bantam* activity (Boulan et al., 2013). In addition, *bantam* is critical for optic lobe development and for the proliferation of glial cells during development (Li and Padgett, 2012). Constitutive *miR-277* expression shortens lifespan through branched-chain amino acid catabolism and as a result it can modulate the activity of the TOR kinase, a central growth regulator, in cultured cells (Esslinger et al., 2013)

A role of *mir-282* has been described in the regulation of the nervous system-specific adenylate cyclase (rutabaga) affecting the viability, longevity, and egg production in *Drosophila* (Vilmos et al., 2013). Similarly, the functions of *Drosophila miR-989* (Kugler et al., 2013) and *miR-7* (Huang et al., 2013) have been described in oogenesis. In addition, a role of *miR-7* in photoreceptor differentiation of *Drosophila* eye has been shown previously (Li and Carthew, 2005).

Hedgehog (Hh) proteins act as morphogens in a variety of developmental contexts to control cell fate and growth in a concentration-dependent manner. In this context, various miRNAs such as *miR-932*, *miR-960,* and *miR-5* were found to play important roles in the regulation of the *Hh* signaling pathways (Gao et al., 2013a; Gao et al., 2013b; Wu et al., 2012a).

Drosophila miR-275 and *miR-306* have been implicated in the regulation of proper spermatid terminal differentiation (Eun et al., 2013) whereas the *miR-310/13*-deficient flies exhibit abnormal germ and somatic cell differentiation in the male gonads (Pancratov et al., 2013).

So far, most of the studies on microRNAs in flies have focused on developmental processes although a few studies have examined the functional role of miRNAs in adults. An adult behavioral role of *miR-276a* has been shown to be required in memory formation and in ellipsoid body for naïve response to odors (Li et al., 2013). A role for *bantam* has been shown in the regulation of the master circadian gene *clk* for its *in vivo* rhythmicity (Kadener et al., 2009). Similarly, a cluster of oscillating *miRNAs 959-964* has been shown to impact the feeding time and other circadian outputs in *Drosophila* (Vodala et al., 2012). A CNS-specific miRNA, *miR-124* plays an important role in neuroblast differentiation (Weng and Cohen, 2012) during development. An adult role of this miRNA has been shown to be in the control of male sexual differentiation and behavior by limiting inappropriate expression of the female form of the transformer protein, TraF. *miR-124* is required for appropriate sex-specific pheromones production in males (Weng et al., 2013).

1.4.6 Role of *miR-184* in *Drosophila melanogaster*

miR-184 is a single copy gene and evolutionarily conserved from flies to humans. It lies within a 50 kb region on the right arm of the second chromosome (see figure 2.6). In *Zebrafish*, it is expressed in lens, hatching gland and epidermis (Wienholds et al., 2005). In vertebrates, overexpression of *miR-184* has been attributed an oncogenic role in the anti-apoptotic and proliferative processes of tongue squamous cell carcinoma (SCC) (Wong et al., 2008). Many studies have shown the important role of *miR-184* in neuroblastoma pathogenesis (Chen and Stallings, 2007; Foley et al., 2010; Tivnan et al., 2010).

In *Drosophila*, *miR-184* was originally identified by expression cloning from the small RNA fraction of embryos (Aravin et al., 2003). It is expressed in the mesoderm as seen by *in situ* hybridization (Aboobaker et al., 2005). A study done by Li et al. (2011) has examined the temporal and spatial expression pattern of *miR-184* by *in situ* hybridization and a modified ribonuclease protection assay (RPA) method. The expression of *miR-184* was generally seen in all tissues, and was relatively high in head disc and eye discs. The expression is highly dynamic during development with a peak level expression at embryonic stage 12-13. In larvae and adults, *miR-184* remained expressed with strong expression at larval stage 3 (Li et al., 2011).

Multiple roles of *miR-184* in the female germline development of *Drosophila* have been shown indicating the importance of this miRNA during development (Iovino et al., 2009). In this study, loss of *miR-184* led to multiple severe defects during oogenesis and early embryogenesis, resulting in the complete loss of egg production. *In vivo miR-184* targets were identified and characterized for three phenotypes: *saxophone* for stem cell differentiation, *gurken* transport factor *K10* for dorso-ventral patterning of the egg shell and anteroposterior patterning of the blastoderm. Additionally, predicted *miR-184* targets were verified in an in vitro system. A role for *miR-184** has been implicated in Parkinson's disease (PD) as a critical mediator of the PD pathogenesis (Gehrke et al., 2010).

Despite the extensive characterization of its expression during development and in adults, roles for this miRNA has not been characterized in any adult fly behaviors or signaling pathways.

1.5 Statement of the problem

The bbb is under intense study in vertebrates for its role in health and diseases (Khan, 2005) and its role as a pharmacologic obstacle for the delivery of drugs to the brain has been a long-standing challenge. However, due to its complexity, it is hard to examine its morphology and functional aspects. *Drosophila,* a simpler organism, is an excellent model for understanding the function of the bbb due to the availability of a great number of genetic, molecular and electrophysiological tools. While insight into the development of the *Drosophila* bbb has been gained, very little is known about the adult bbb and the mechanisms that underlie its function beyond the exclusion function that is based on its tight junctions. It is particularly unknown how hemolymph components communicate with the brain through the bbb. Very recent work from our lab has shown that the sexual identity of the bbb is important for the male courtship behavior (Hoxha et al., 2013). Based on this work I hypothesized that there are many factors/molecules that are sex-specifically present in the bbb which are required for the regulation of male courtship behavior in *Drosophila*.

In chapter III of this dissertation, this hypothesis was tested by examining the transcriptome of the bbb and identifying sex-specific transcripts. As a complementary approach, changes in transcripts were examined upon feminization of bbb cells in males. Many sex-specific genes were found to be expressed in the bbb and the role for several candidate genes in courtship behavior of male *Drosophila* was characterized. In addition, since miRNAs are important regulators of gene expression, I examined and identified miRNAs expressed in the bbb. These experiments are described in chapter IV of this study. To examine whether miRNAs have a sex-specific role in the bbb, a possible role

for the most abundant miRNA, *miR-184* was assessed in the regulation of male courtship behavior by altering the levels of *miR-184* by overexpression and/or silencing of this miRNA in the bbb. In addition, a role of the *miR-184* target *sinu* in the regulation of courtship behavior was examined.

1.6 Gene expression systems used in this study

1.6.1 Gal4-UAS binary system

One of the most frequently used approaches in fly genetics is the use of the Gal4-UAS system. By using this method, spatially restricted expression of genes of interest can be achieved (Brand and Perrimon, 1993). The system expresses the yeast transcriptional activator Gal4 downstream of a cell/tissue-specific enhancer sequence or defined promoter (Genomic enhancer-Gal4) in one transgenic line. In the second line, an Upstream Activating Sequence (UAS) is placed upstream of a gene of interest. The UAS target transgene is silent in the absence of a Gal4 transcriptional activator. However, when these two elements are brought together by crossing the two lines, the gene of interest (located downstream of UAS) will be expressed in the specific tissues/organ of the progeny due to the activity of the promoter Gal4 (Fig 1.7).

This Gal4 binary system is a powerful tool allowing us to express a gene of interest only in the desired places (cells/tissues/organs). Yet, it does not allow the temporal control of the expression of gene of interest. To solve this problem, The TARGET (Temporal and Regional Gene Expression Targeting) system was developed (McGuire et al., 2003; McGuire et al., 2004a). A temperature sensitive $Gal80^{ts}$ protein, another yeast protein, is used to control the timing of the expression of the gene of interest. The $Gal80^{ts}$ coding sequence is driven ubiquitously by placing it downstream of

a universal promoter such as tubulin-1α. At the permissive temperature (19°C), the Gal80^{ts} prevents the Gal4 transcriptional activator from activating the expression of the gene of interest. Therefore, at this temperature, Gal80^{ts} represses Gal4 activity. At restrictive temperature (29-32°C), the conformation of Gal80^{ts} protein changes and it no longer is able to suppress Gal4 and hence Gal4 now can activate the expression of the gene of interest. The rate of induction is intermediate at 29°C and maximal at 32°C (Roman, 2004). Additionally, by introducing multiple copies of Gal80^{ts}, TARGET offers dose dependent repression of Gal4 activation of a gene of interest (McGuire et al., 2003; Roman, 2004). The TARGET system is advantageous in that it is induced by temperature and is therefore rapid and easily controlled.

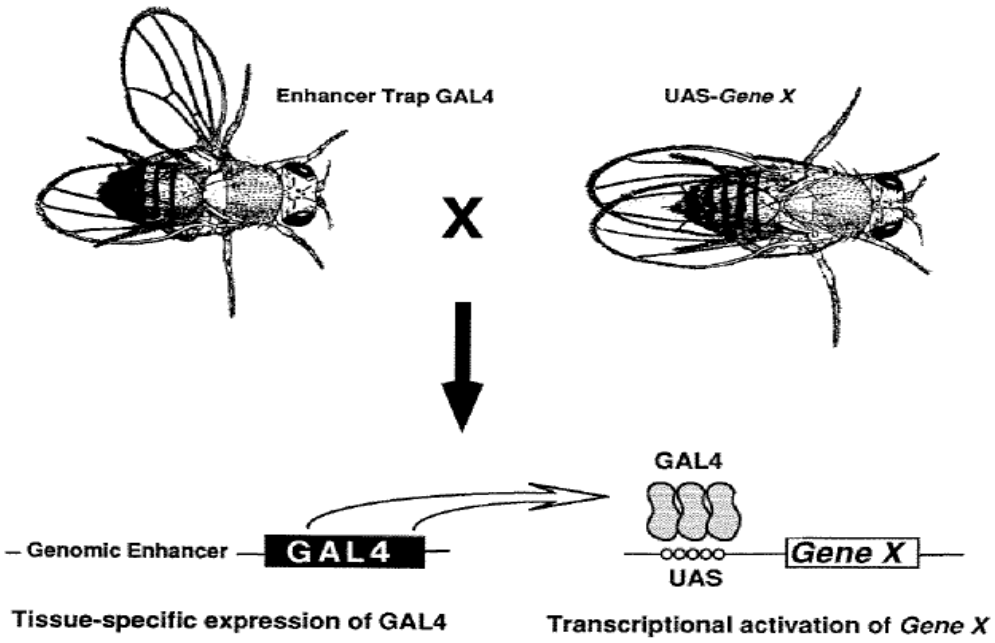

Figure 1.7: Gal4 binary system in *Drosophila* (Brand and Perrimon, 1993). The genomic enhancer-Gal4 and UAS-target X are brought together by crossing two transgenic lines. In the progeny, the gene of interest X is activated only in the specific tissues that express Gal4.

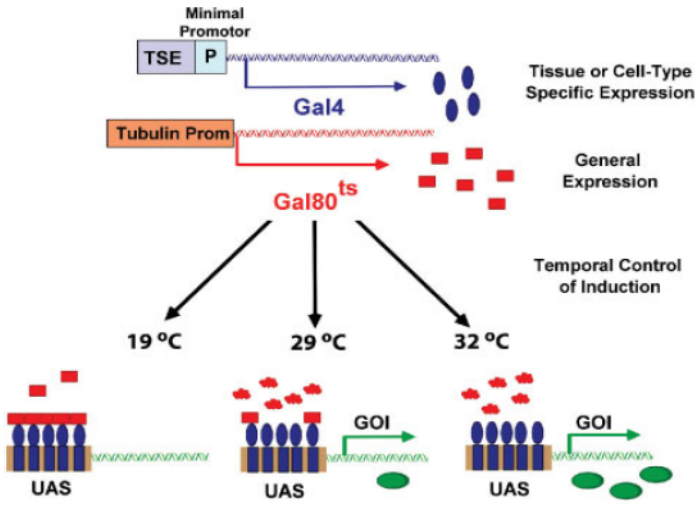

Figure 1.8: The principles of the TARGET system (Roman, 2004). At 19°C, the expression of GAL4 prevented and consequently the GOI is suppressed by an active universally expressed Gal80^{ts} protein. The expression is permitted at 30°C or higher.

1.6.2 Inducible heat shock system for temporal control of gene expression

The use of heat shock promoters is another way of temporally controlling the expression of a gene in *Drosophila*. The expression from heat shock promoters significantly increases at high temperature. The highly conserved *hsp70 promoter* is used in many model organisms including flies (Lindquist, 1986). Heat shock proteins are induced in the cells when the flies are exposed to a high temperature of 29-37°C. In this system, the *hsp70* heat shock promoter is cloned upstream of a gene of interest which can this way be induced by heat shock to control the temporal expression of the gene of interest (Figure 1.9).

Although this system is temporally controlled, it is not spatially restricted and hence may not be useful for certain cell/tissue-specific purposes. However, the method is flexible in

terms of regulating the level and strength of the transgene expression by changing the intensity and length of the heat shock (McGuire et al., 2004b).

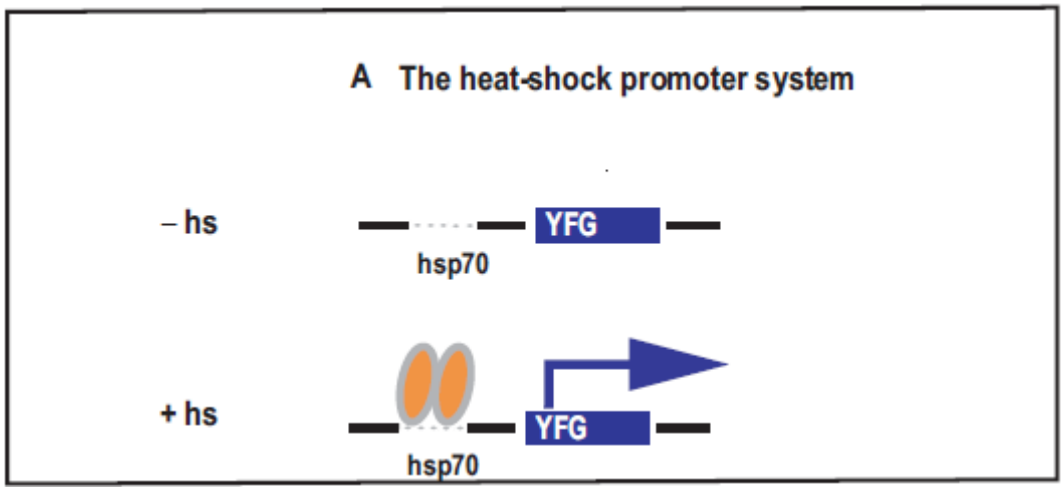

Figure 1.9: The heat-shock promoter system (McGuire et al., 2004a). In this system, a copy of gene of interest (GOI) is cloned downstream of the heat shock promoter. The fly is subjected to heat shock regimen to induce the expression of the GOI ubiquitously.

Chapter II

Materials and Methods

2.1 Drosophila stocks

Flies were kept on standard cornmeal/sugar-based food at 25°C under uncontrolled light conditions. *Canton S (CS)* flies were used as a wild-type control. The resources for the flies used in this study are summarized in Table 1. The rest of the flies were from the stock collection in our lab.

Table 2.1: List of fly stocks

Genotype name	Annotation in the text	Mutagen	Fly stock source
w (CS10); Gal80^{ts10}	*Gal80^{ts10}*	P-element	Courtesy of Dr.Gregg Roman
w(CS10); Gal80^{ts20}	*Gal80^{ts20}*	P-element	Courtesy of Dr.Gregg Roman
moody-Gal4/TM3,SB	*SPG-Gal4 III*	P-element	Courtesy of Dr.Roland Bainton
moody-Gal4/CYO	*SPG-Gal4 II*	P-element	Courtesy of Dr.Roland Bainton
w ; UAS-traF (stock number 4590)	*UAS-TraF*	P-element	Bloomington Drosophila Stock Center
w^{1118}; P {UAS-RedStinger}4/CyO (stock number 8546	*UAS- DS Red Stinger*	P-element	Bloomington Drosophila Stock Center
w(CS10); Sco/CyO; Gal80^{ts2}	*Gal8^{ts2}*	P-element	Courtesy of Dr.Gregg Roman
w^{1118}; P{UAS-miR-184 (Stock number 27.2)	*UAS-miR-184 27.2*	In Vitro Construct	I generated these flies in the lab
w^{1118}; P{UAS-miR-184 SPONGE (Stock number 7.1 Sp)	*UAS miR-184 Sponge 7.1 Sp*	In vitro construct	I generated these flies
yv;{TRiP. JF02542} att P2 UAS-Hr46 RNAi (BL27253)	*UAS-Hr46 RNAi 27253*	P-element	Bloomington Drosophila Stock Center
yv;{TRiP. JF02542} att P2 UAS-Hr46 RNAi (BL27254)	*UAS-Hr46 RNAi 27254*	P-element	Bloomington Drosophila Stock Center
VDRC v16792 *w[1118]; P{GD5741}v16792*	*UAS-qvr RNAi 16792/GD*	P-element	Vienna Drosophila RNAi Center

Table 2.1: List of fly stocks (Cont.)

Genotype name	Annotation in the text	Mutagen	Fly stock source
VCRC v104533 P{KK109915}VIE-260B	*UAS-qvr RNAi 103=4533/KK*	P-element	Vienna Drosophila RNAi Center
quiver /sleepless mutant P1	*qvr mutant P1*	P-element	Courtesy of Dr. Amita Sehgal lab
quiver/sleepless mutant P2	*qvr mutant P2*	P-element	Courtesy of Dr. Amita Sehgal lab
quiver/sleepless mutant Ex40	*Ex40*	Imprecise excision of P1	Courtesy of Dr. Amita Sehgal lab
VCRC v8353 w[1118]; P{GD2436}	*UAS- Neurexin RNAi 8353*	P-element	Vienna Drosophila RNAi Center
VDRC v9039 w[1118]; P{GD2436}	*UAS- Neurexin RNAi 9039*	P-element	Vienna Drosophila RNAi Center
VCRC v108128 P{KK102207}VIE-260B	*UAS-Neurexin RNAi 108128*	P-element	Vienna Drosophila RNAi Center
f05119 (PBac{WH}f05119	*Line f05119*	Piggy Bac Transposase	Exelexis at Harvard Medical School
d08710 (P{XP}d08710)	*Line d08710*	P-element	Exelexis at Harvard Medical School
9 P{ry[+t7.2]=hsFLP}1, w[1118]; Adv[1]/CyO	*hsp FLP*	P-element	Bloomington Drosophila Stock Center
X/Y; +/+; hsp70-GAL4/+	*hsp-Gal4*	P-element	Courtesy of Dr Roman

2.2 Whole brain dissection for RNA sequencing

For the feminization of the bbb, the SPG-Gal4 driver was used to express the female specific form of protein TraF in the bbb by crossing the *SPG-Gal4* transgenic flies with the *UAS-TraF* transgenic flies. Similarly, control crosses were set by crossing the wild type w^{1118} flies with the SPG-Gal4 line and the UAS-TraF lines separately. The crosses were raised and reared at 25°C. The young male progenies were isolated on day one in a group of 10-20 in a fresh food vial and entrained in a 12 hour Light/Dark cycle

incubator for 4-5 days. These male flies 4-5 days of age were anaesthetized on ice about 10-15 minutes before dissection. The dissecting petri-dish (60 x 15 mm) half filled with 1.2% RNAse free agarose was placed at the center of a big (90mm diameter) empty petri-dish. Then the dissecting dish was filled with about 1-2 ml of dissecting buffer, the 1 X Phosphate Buffered Saline (PBS). Ice was filled around the dissecting dish to keep the buffer cold all the time during the dissection procedure. The ice was replaced frequently to make sure that the buffer remained cold all the time.

The fly brains were always dissected between Zeitgeber time ZT5 and ZT7 to minimize the circadian influence on gene expression. The brains were dissected by using straight Dumont # 5 fine forceps (Fine Science Tools, Inc). Once dissected, the brains were thoroughly cleaned off of fat body, cuticle debris and trachea. The cleaned brains were immediately transferred to a small droplet of Trizol reagent (~ 20µl, Invitrogen) frozen on a sterile weigh boat sitting on dry ice. Once the dissection was done for the day, the Trizol droplets with the brains were stored at -80°C in a pre-cooled 1.5 ml eppendorff's tube until processed for total RNA extraction. It was always made sure that the amount of dry ice was sufficient to maintain the temperature of the Trizol droplet cold~ -70°C. At least 450 brains were dissected for each genotype. For every dissection session, an equal number of brains were dissected for each genotype as far as possible. The forceps were cleaned with RNAZap wipes before moving from one genotype to the other to prevent cross-contamination of the samples.

2.3 Isolation of individual blood brain barrier cells for microarray and microRNA sequencing

To isolate blood brain barrier cells, flies bearing the bbb-specific transgenic, the SPG-Gal4 driver were crossed to flies carrying the fluorescent reporter transgene, UAS-DS Red Stinger (DS Red). This resulted in the expression of the visible fluorescent marker DS-Red to mark the nuclei of bbb cells (Figure 2.1). The progenies (males and females) were collected on day one and aged for 4-5 days in a 12 hour Light/Dark cycle incubator. After 4-5 days, their brains were dissected in ice-cold 1 X PBS between ZT5 and ZT7 as described in section 2.1. The dissected brains were then transferred to a new petri dish containing ice-cold 1X PBS (within half an hour). Carefully, under the fluorescent microscope, the individual and/or group of blood brain barrier cells marked with DS Red reporter were isolated manually by using Dumont # 5 SF superfine forceps (Fine Science Tools, Inc). The cells were then immediately transferred to the frozen droplet of Trizol reagent on dry ice as described in section 2.5 and stored in -80°C until processed further. Cells were isolated from at least 50 brains for each genotype. The approximate total number of cells isolated per brain varied from ~60-120. The forceps were cleaned with RNAZaps while moving from one genotype to the other.

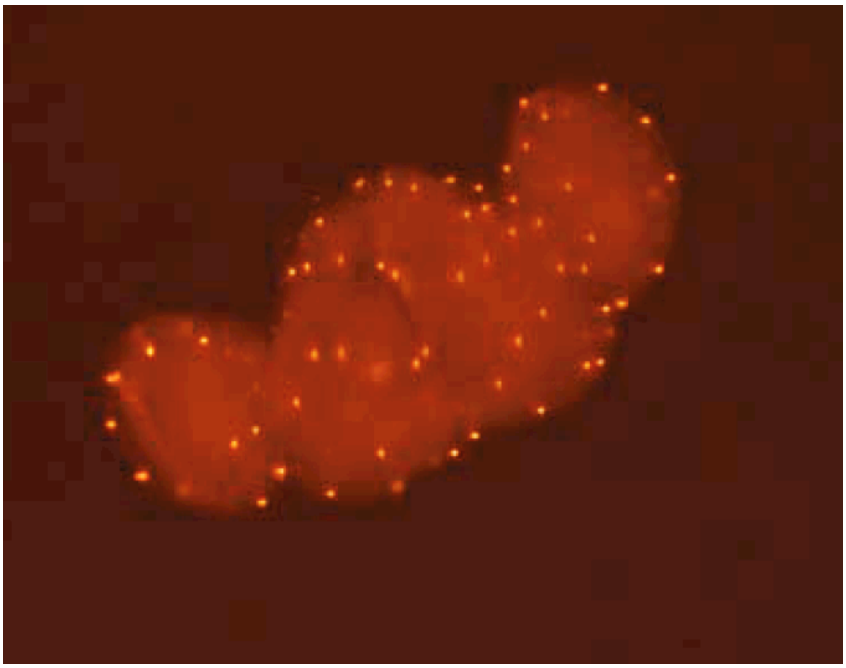

Figure 2.1 SPG-Gal4 driving the expression of DS Red Stinger.

2.4 Procedure for the microarray experiment

The isolated bbb cells of male and female flies were provided to the company, GenUs Biosystems for microarray for analysis. A total of 3 biological replicates for each males and females were submitted. Before running the actual experiment, samples from male and female bbb cells were provided to the company for a pilot experiment to determine the method and starting quantity of the bbb cells. As shown in the figure below, the amount of RNA recovered is similar in both procedures. Interestingly, the procedure using RLT buffer recovers small RNA as well.

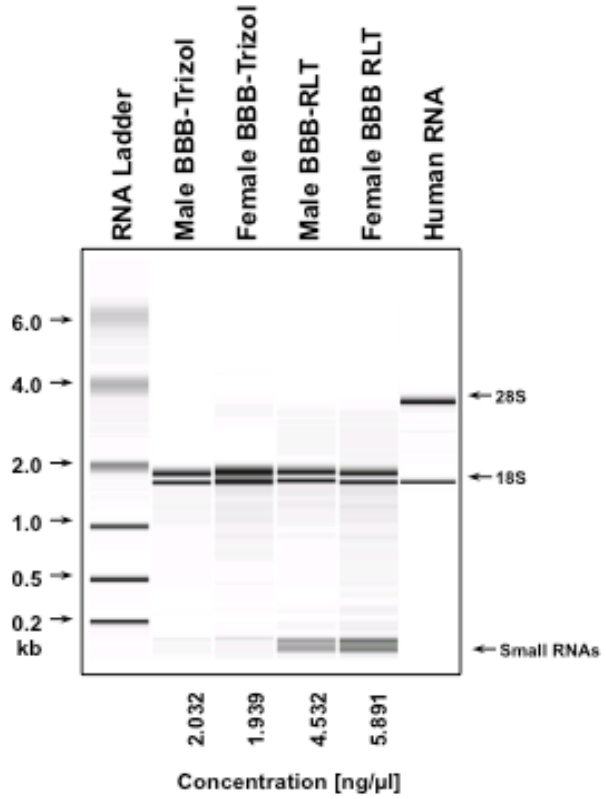

Figure 2.2: The first two samples (~10 µl droplets of trizol) were diluted in TRI reagent and processed. The second two samples (~300 µl of aqueous PBS+Trizol) were diluted in RLT buffer and processed. All samples were eluted in 24 µl of water and 1 µl of aliquot was run on an Agilent Bioanalyzer picogel. The concentrations are as noted.

After confirming that the total cells obtained from ~50 male and ~50 female brains were sufficient for RNA preparation, the following materials and methods as described by the company protocol were used.

Cells were lysed in TRI reagent (Ambion) and Total RNA was isolated using phenol/chloroform extraction followed by purification over RNeasy spin columns (Qiagen). The concentration and purity of Total RNA was measured by

spectrophotometry at OD260/280 and the quality of the Total RNA sample was assessed using an Agilent Bioanalyzer with the RNA6000 Nano Lab Chip (Agilent Technologies). Labeled cRNA was prepared by linear amplification of the Poly (A)+ RNA population within the Total RNA sample. Briefly, 1 μg of Total RNA was reverse transcribed after priming with a DNA oligonucleotide containing the T7 RNA polymerase promoter 5' to a d (T)24 sequence. After second-strand cDNA synthesis and purification of double-stranded cDNA, in vitro transcription was performed using T7 RNA polymerase. The quantity and quality of the cRNA was assayed by spectrophotometry and on the Agilent Bioanalyzer as indicated for Total RNA analysis.

One microgram of purified cRNA was fragmented to uniform size and applied to *Drosophila* (V2) Gene Expression microarray (Agilent Technologies, Design ID 021791) in hybridization buffer. Arrays were hybridized at 37° C for 18 hrs in a rotating incubator, washed, and scanned with a G2565 Microarray Scanner (Agilent Technologies).

Arrays were processed with Agilent Feature Extraction software and data was analyzed with GeneSpring GX software (both Agilent Technologies). To compare individual expression values across arrays, raw intensity data from each gene was normalized to the 75^{th} percentile intensity of each array. Genes with values greater than background intensity in all female or all male replicates were filtered for further analysis. Differentially expressed genes were identified with fold change > 1.5 fold and Welch T-test p-value < 0.05.

2.5 Material and methods for mRNA sequencing

mRNA seq was performed on whole fly brains. The whole brain was isolated as described in section 2.2 both from the experimental as well as the respective control flies. The experimental flies were the flies expressing the female specific form of the Tra protein, TraF in their bbb in otherwise normal males. The control flies expressed only the SPG-Gal4 driver in white eyed CS flies (w^{1118}) or the UAS-TraF reporter line in white eyed- CS flies (w^{1118}). All strains were outcrossed to cantonized w^{1118} *{(CS* (w^{1118})*}* for 10 generations to minimize the effect of genetic background. Control and the experimental brains samples were subjected to whole RNA extraction by using the RNeasy mini kit (Qiagen) following the company protocol. After isolation of RNA, the sample was sent to the Baylor College of Medicine Microarray Core Facility. In order to determine integrity, concentration, and overall quality of the sample, I submitted the samples for quality check or SAQC at a concentration of 50ng/µl in DEPC treated water. Once the QC was passed, the actual samples of total 2 biological replicates were submitted to the facility at a total amount of 5µg or more. The protocol described below was used by the BCM Core Facility:

The Genomic and RNA Profiling Core first conducted sample quality checks using the NanoDrop spectrophotometer and Agilent Bioanalyzer 2100. Then Illumina TruSeq RNA v1 library preparation protocol was used. The process was as follows:

2.5.1 Illumina truSeq RNA sample preparation protocol

A double-stranded DNA library was created using 2 ug of total RNA, preparing the fragments for hybridization onto a flowcell. First, cDNA was created using the fragmented 3' poly (A) selected portion of total RNA and random primers. Libraries were created from the cDNA by first blunt ending the fragments, attaching an adenosine to the 3' end and finally ligating unique adapters to the ends (For more information on this process, see below). The ligated products were then amplified using 15 cycles of PCR. The resulting libraries were quantitated using the NanoDrop spectrophotometer and fragment size assessed with the Agilent Bioanalyzer. A qPCR quantitation was performed on the libraries to determine the concentration of adapter ligated fragments using a Bio-Rad iCycler iQ Real-Time PCR Detection System and a KAPA Library Quant Kit.

2.5.2 Cluster generation by bridge amplification

Using the concentration from the Bio-Rad qPCR machine above, 6pM of library was loaded onto a flowcell and amplified by bridge amplification using the Illumina Cluster Station instrument. A paired-end 75-cycle run was used to sequence the flowcell on a Illumina Genome Analyzer (GAII) Sequencing System.

Terminology used: End Repair: converts the overhangs caused by fragmentation into blunt or polished ends. The 3' to 5' exonuclease activity of the End Repair mix will remove the 3' overhangs and polymerase activity fills in the 5' overhangs.

Adenylation: a single 'A' nucleotide is added to the 3' ends of the blunt fragments.

Adapter Ligation: an adapter is ligated to the 3' end of the DNA fragment with a corresponding 'T' nucleotide.

2.6 MicroRNA next generation sequencing

Isolated bbb cells were collected from 50 males and 50 female brains as described in section 2.3. microRNA sequencing was done in collaboration with Dr. Ashley Benham from Dr. Preethi Gunaratne's lab. Briefly, total RNA isolation from the bbb cells was done by using the miRNAeasy mini kit from Qiagen. We followed the manufacturer's recommended procedure and suggestions for determining the starting amount of samples and choosing the appropriate disruption method. Cells were homogenized using a syringe and needle. The lysate was passed through a 20-gauge (0.9mm) needle attached to a sterile plastic syringe at least 5-10 times or until a homogenous lysate was achieved. Then the sample was briefly vortexed. The protocol for purification of total RNA including small RNAs from animal cells was followed as described in the manual with some changes in the protocol. 350µl QIAzol lysis reagent was added instead of 700 µl at step 2. And after step 7, we adopted the protocol explained in Appendix A of the manual to enrich miRNA and other smaller RNAs and separate them from other larger RNAs species (>200nt). The miRNA fraction was eluted in 10µl of nuclease free water. The reason for following this procedure was to use the smRNAs for sequencing and keep the larger RNAs for another uses. Because of the very low concentration of RNA, we used the entire miRNA sample in the downstream steps.

2.6.1 Protocol optimized for extremely low starting RNA material.

The following protocols for microRNA sequencing were adopted from the method developed by Benham A, (2011). However, the protocols were optimized for

extremely low starting RNA material because we wanted to use every bit of RNA we extracted.

The library prep protocol was adapted to accommodate the larger starting volume of the isolated RNA. So reactions had to be scaled up so the final reaction conditions were at the correct condition and concentration.

1. First ligation reaction changed from 10.0µl to 15.0 µl reaction volume.
2. Second ligation reaction changed from 12.5 µl to 18.13 µl reaction volume.
3. The RT reaction usually used only 4.0 µl from the 12.5 µl ligation reaction. Again, to maximize our potential output we used all 18.13 µl of the ligation reaction. We scaled the RT reaction volume from 10.0 µl to a 30.0 µl reaction to accommodate the higher volume of ligation reaction used.
4. The PCR reaction is normally 50.0 µl and we were able to keep the reaction at 50.0 µl even using all 30.0 µl of the RT reaction as the cDNA sample. 15 cycles of PCR were used to enrich the library without introducing bias into the sample due to over and /or underrepresentation of amplicons.

The method was a success. The entire procedure was risky and not forgiving since there were no backups to be allotted during preparation.

2.6.2 Preparation of small RNA library for illumina platform sequencing

For ligation of the 3'adapter, 1 µl of 10X v1.5 sRNA adapter (Illumina part # 15000263) was diluted by mixing in 4.0 µl of nuclease-free water to make a 2X working solution. Then, in a nuclease-free 200 µl PCR tube, 0.5 µl of the diluted 3' adapter (2X) was added to 8.0 µl of the RNA sample (which corresponds to approximately 50ng of RNA). This mixture was incubated at 70°C for two minutes and then transferred

immediately on ice. In the next step, 1.5 µl of the 10X T4 RNL2 truncated reaction buffer, 2.4 µl of 50mM MgCl2, 2.25 µl of T4RNA Ligase 2 truncated (from New England Biolabs, 200,000units/ml) and 0.5 µl of RNAaseOUT were added to the sample mix. Therefore, the final volume of the ligation reaction was 15.0 µl. The reaction was then incubated in the thermocycler at 22°C for 1 hour. Before the incubation was complete, the SRA 5'adapter was prepared. The ligation sample was removed from the thermocycler and kept at room temperature during preparation of the SRA 5' adapter. In a new clean nuclease-free 200 µl PCR tube, the SRA 5' adapter was aliquoted and heated to 70°C for two minutes then transferred to ice. 0.63 µl of the 5' adapter was directly added to the ligation mixture above along with 1.25 µl of 10mM ATP, and 1.25 µl of the T4 RNA ligase making the total reaction volume 18.13 µl per sample. The reaction mixture was then incubated for 1 hour at 20°C in the thermocycler and ligated RNA products were stored at -20°C until further processed.

2.6.3 Reverse transcription of adapted RNA

In a sterile nuclease-free 200 µl PCR tube, 0.895 µl of the stock 5X SRA RT primer (Illumina; part 10000597) was combined with all the ligated RNA (18.13 µl) making the total volume of the reaction 19.025 µl. The entire mixture was incubated in the thermocycler at 65°C for 10 minutes, then immediately placed on ice. In a separate 200 µl PCR tube, the RT master mix was prepared by combining 6.0 µl of the 5X first stand buffer (Invitrogen, part 18064-014), 1.5 µl of the 10mM dNTP mix, 3 µl of the 100mM DTT (Invitrogen part 1864-014) and 0.5 µl of RNaseOUT (part 1000560) making the total master mix volume 11 µl. The total RT volume was scaled up to 30 µl. So, to the 19.03 µl of cooled RNA template with SRA RT primer, 11 µl of the RT-PCR

master mix are added. The mixture was incubated at 48°C in a thermocycler for 3 minutes then immediately, 1 µl of the Superscript II reverse transcriptase (RT) (Invitrogen, part #18064-014) was added making the final volume of RT reaction to 30 µl and incubated for 1 hour in a thermocycler at 44°C. The 30 µl RT reaction was stored at -20°C until needed.

2.6.4 PCR amplification of cDNA library

For each 50 µl PCR reaction, the master mix was prepared for 2 samples and with additional 10% extra for pipetting error. Briefly, 14.3 µl of Ultra-pure water, 22.0 µl 5X Phusion HF buffer (NEB), 2.2 µl Primer GX1 (Illumina), 2.2 µl Primer GX2 (Illumina), 2.2 µl 10mM DNTP mix and 1.1 µl Phusion DNA Polymerase were mixed . The 20 µl of the master mix was directly added to the 30 µl of the reverse-transcribed cDNA reaction from previous reaction making the final PCR volume of 50 µl. The samples were amplified in the thermocycler with the following settings: Step 1: 30 seconds at 98°C, Step 2: 15 cycles of 10 seconds at 98°C, 30 seconds at 60°C and 15 seconds at 72°C followed by Step 3: 10 minutes at 72°C and Step 4: Hold at 4°C. PCR products were stored at -20°C until needed.

2.6.5 Gel Purification of smRNA library constructs

A precast 6% TBE (polyacrylamide) gel from Invitrogen (EC2652BOX) was used for sample separation and isolation in the Xcell lock electrophoresis unit (Invitrogen EEI0001). TBE (1X) was prepared by diluting 100ml of 10X TBE buffer (Ambion AM 9865) with 900ml deionized water and mixed. The gel cast was inserted into Xcell surelock electrophoresis unit following invitrogen's instructions. The 1X TBE buffer was

added into the middle and surrounding chambers. The gel was checked for any leaks. The combs were removed and the wells were rinsed 3 times with 1X TBE. We used 19 gauge needle and a 10 ml syringe. A map of the gel with the lane/well assignments was made before loading the sample. Each sample was loaded in two wells (25 µl each) with a lane gap between the two different samples. The ladder used was 10 bp ladder from Invitrogen. Briefly, 2 µl of 10bp ladder was mixed with 1 µl of 6X gel loading dye from Promega. 11 µl of the 6X loading dye was directly added to each 50 µl PCR reaction and mixed well. Into 2 consecutive wells, 25 µl of this mixture was loaded accordingly as specified in the map. The gel was run at constant 200V for 32-33 minutes (Figure 2.3). The gel was removed from the cast and stained with 1XTBE with ethidium bromide for 3 minutes by gentle shaking. The gel bands were visualized using an UV illuminator and a picture was taken. The gel band from 90-100bp was cut with a clean razor blade by making the horizontal cut at first and then the vertical to excise the target band. The gel piece was transferred to 0.5µl tube whose bottom was punctured 5 times by a 21 gauge needle. The tube was placed into a 2 ml RNAse-free round bottom tube and centrifuged at 13K rpm for 2 minutes at room temperature. One milliliter of 1X elution buffer was made by mixing 100 µl of 10X in 900 µl of nuclease-free water. From this, 300 µl of elution buffer was added to each of 2ml tube containing the gel fragments of the samples and incubated at 4°C overnight on a rotating orbitron.

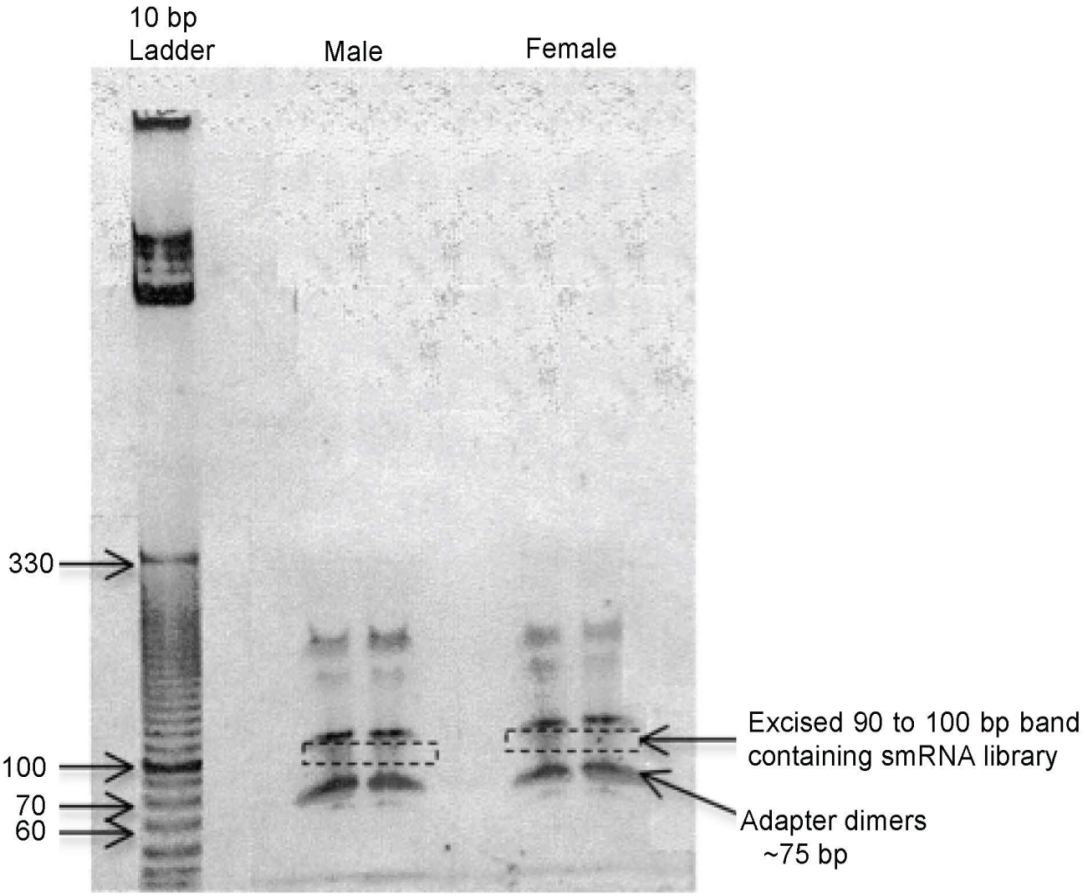

Figure 2.3: Gel purification of smRNA library: The smRNA population is gel purified after PCR amplification of the adapted RNA sample. 6% TBE pre-cast gel from Invitrogen is used by gel electrophoresis at a constant 220 V for 33 minutes.

2.6.6 Precipitating cDNA

The 1X TBE eluted sample with the gel debris was transferred on to of a Xspin-X cellulose acetate filter and spun at 13K rpm for two minutes. To this eluted sample (~300 µl), 2 µl of glycogen, 30.0 µl of 3M NaOH, pH 5.2, and 975 µl of 100% ethanol (pre-chilled at -20°C) was added and vortexed for 15-30 seconds at the maximum speed and centrifuged at 14,000 rpm for 20-25 minutes at 10°C. The supernatant was decanted without disturbing the pellet and washed with RT 70% ethyl alcohol and air dried. The pellet was resuspended in 10 µl of nuclease-free water and stored at -20°C until processed.

2.6.7 Quantification of the eluted smRNA library by picogreen assay

To determine the smRNA concentration, the XX Model fluorometer was used and the sample dilution was made by adding 1 µl of stock sample to 29 µl of TE buffer pH 8 in a 0.5mL tube making the total volume of 30µl. 5µl Stock picogreen (provided by the sequencing center, light sensitive) was added to 1mL of TE pH 8 (protect from light) to make 2X picogreen working solution. The total diluted sample (30 µl), and 30 µl of 2x picogreen working solution were mixed gently into the provided cuvettes (next to fluorometer in sequencing room). The samples were always protected from light with aluminum foil. Then they were incubated at room temp for 3 minutes. The cuvette is then placed into the blue light cassette and measurement could be recorded. Using the concentration regression formula provided on the computer next to fluorometer, the concentrations were measured from the reading. Illumina/Solexa calculator (file located in folder on desktop next to fluorometer) was used to find out the proper dilution to make

2.5nM, 5nM or 10nM for sequencing and set aside for submission. At least 5µl sample volume at a concentration of 8pM was submitted.

2.6.8 QC gel

1 or 2 µl of the remaining sample was run on 6% TBE gel for verification of correct band isolation. A smear from 90 to 100bp was used as a mark as confirmation (according to 10bp ladder). After the final QC confirmation, the sample was submitted to the sequencing center.

2.6.9 Small RNA mapping

For analysis of the resulting data, those reads containing insert sequence along with the adapter sequence (the read length being 36nt) for miRNA mapping (the same adapter being used for sequencing run) was filtered. Each sequence read which did not pass the Illumina and no-calls filter was removed. Reads with copy number less than 4, insert less than 10nt or more than consecutive, repetitive nucleotides were removed. The remaining validated reads were aligned to the miRNA reference database (miR base version 17). Reads with exact match or loose match were observed. Up to three mismatches were allowed for loose matches in a single alignment.

2.7 Phusion Polymerase PCR

The PCR for the amplifying *miR-184* sequence from genomic DNA was performed using a high-fidelity DNA polymerase called Phusion (Bio Labs, Ipswich, MA) and was set up by combining 10µl 5X Phusion HF buffer, 1µl genomic DNA, 1µl 10mM dNTP, 1µl of each primer (100ng/µl), 35.5 µl of ddH2o and 0.5µl Phusion DNA

Polymerase into a PCR tube for a total volume of 50µl, and mixed by pipetting. The PCR condition was: 98°C for 30 seconds initial denaturation; 98°C for 10 seconds denaturation, then 72°C for 3 minutes annealing, 35 cycles; 72°C for 10 minutes for final extension.

2.8 Generation of transgenic flies

The transgenic lines for overexpression and inhibition of microRNA 184 were established by Rainbow Transgenic Flies, Inc., CA in a w^{1118} background, by P-element mediated transformation.

2.8.1 Generation of *UAS-miR-184* transgenic flies

To clone the *miR-184* sequence into the pUAST vector, restriction sites Not I and Xba I were chosen. Therefore, the primers with these restriction sites and a few overhangs were designed to PCR-amplify from genomic DNA of wild type CS flies as shown below.

2R CHROMOSOME WITH MIR-184 SEQUENCE HIGHLIGHTED IN GREEN

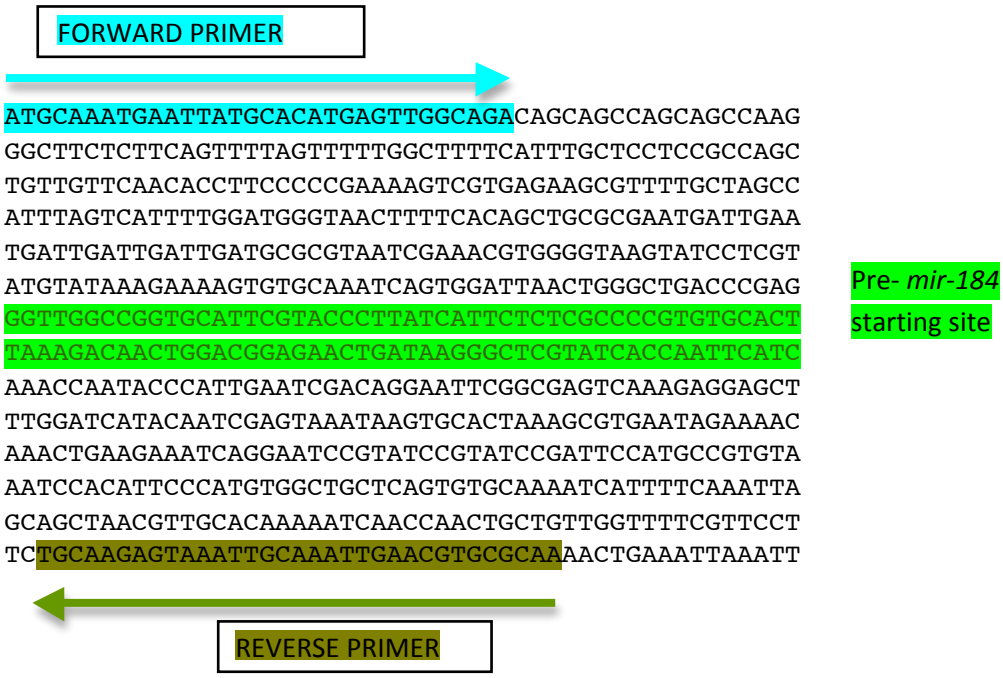

Forward Primer

5’-AAGAATGCGGCCGCATGCAAATGAATTATGCACATGAGTTGGCAGA-3’

(The NotI restriction site in green and the overhangs in black and the gene sequence in pink)

Reverse Primer

5’-TGCTCTAGATTGCGCACGTTCAATTTGCAATTTACTCTTGCA-3’

(The Xba I restriction site in green and the overhangs in black and the gene sequence in pink).

As described in section 2.7, the *miR-184* genomic region was amplified by Phusion Polymerase PCR by using a high-fidelity DNA polymerase, the Phusion Polymerase (BioLabs, Ipswich, MA). The correct size band of 685 bp was gel purified using Qiagen's Gel Purification kit protocol. This fragment was sub-cloned into the multicloning site of the intermediate vector, the pSC-B-amp/Kan vector using the Strataclone Blunt PCR Cloning Kit (STRATAGENE). The correct insert size was confirmed by ECoRI restriction digestion. One of the p-SCB- miR-184 clones were sent for sequencing at *SeqWright DNA Technology Service* and the sequences was confirmed by using M-13 forward and reverse primers. The *mir-184* fragment was excised from the p-SCB vector by Not I and Xba I digestion. Because of the difference in the efficiency of different restriction enzymes (Not I and Xba I), sequential restriction digestion reactions were performed.

Similarly, the vector pUAST was linearized by cutting with Not I and Xba I. The linearized pUAST vector was dephosphorylated by addition of heat-inactivated alkaline phosphatase (Promega). Insert and vector were gel purified. The ligation using the T4 DNA ligase was set up between the linearized pUAST vectors and linearized the *miR-184* fragment (NEB). The ligation product was transformed into NEB 5-alpha competent *E. coli* (High Efficiency) cells using the manufacturer's protocol from New England Biolabs.

Genomic Region of miR-184 amplified by Phusion Polymerase

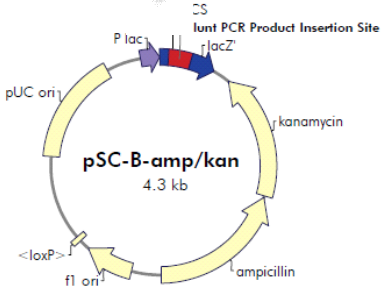

pSC-B + miR-184 construct

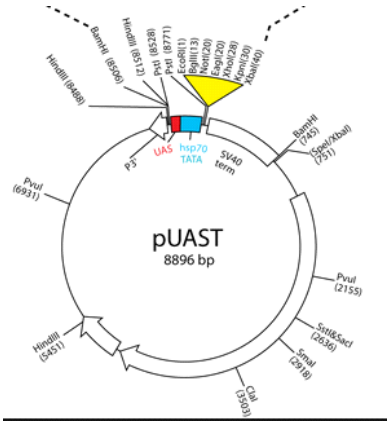

pUAST+ miR-184 construct

Injected into W^{1118} embryos

UAS-miR-184 transgenic

Figure 2.4: Flow diagram of creating the *UAS-miR-184* flies. The *miR-184* region was amplified from genomic DNA using Phusion Polymerase PCR. The sequence was cloned into an intermediate pSC-B vector and sequence verified. The sequence was then cloned from pSC-B into a pUAST vector downstream of the *UAS* sequence. The pUAST+ *miR-184* construct was injected into w^{1118} flies.

Once confirmed, the clone was sent for sequencing. The primers used for sequencing were pUAST forward (5'-ACT GCA ACT ACT GAA ATC TGC CA-3') and pUAST reverse (5'-TCC AAT TAT GTC ACA CCA CAG -3'). Once the sequencing result confirmed the sequence of the fragment, the clone # 7(2) was processed for large scale production of the DNA by using Qiagen plasmid midi kit followed by phenol: chloroform extraction. I sent the sample to Rainbow Transgenic Flies, Inc., CA for injection in TE buffer at least ≥ 35µg of total DNA sample. The injection was successful and I received ~260 larvae.

From the larvae, as soon as they eclosed, the P_0 virgin females were caught and crossed individually with male white eyed CS flies (w^{1118}) and similar but reciprocal crosses were set up for the male P_0 flies. The progeny F1 flies with orange eye color were collected and crossed to balance the transgene. Flies with the transgene on the 1st, 2nd or 3rd chromosome were balanced using FM6K or Cyo or TM3, Sb respectively. The chromosomal location of the UAS-miR-184 transgene was mapped in about thirty transgenic lines and the lines were finally established as homozygous stocks.

2.8.2 Generation of *UAS-miR-184 sponge (miR-184 sp)* transgenic flies

To study the effect of inhibition *of miR-184*, I generated *miR-184* sponge transgenic flies. The sponge was designed as follows: The sponge sequence is the complementary seed sequence of the target microRNA, the *miR-184*, with mismatches in positions 9-12 as shown in Figure 2.5. The sponge sequence was designed as described in Loya et al, 2009. Briefly, the miR-SP cassette was designed by placing 10 microRNA binding sites containing mismatches at positions 9–12 downstream of EGFP in a UAS-containing P-element vector (pUAST-EGFP). 10 repeats of the *miR-184* complementary

sequence (ACCTGCCTAACGACTATTCCC) with mismatches at position 9-12 and separated by a variable four-nucleotide linker (CGCG) were designed. To clone the sponge sequence, XbaI restriction sites were added on both ends of the construct. The sponge construct was synthesized by Biobasic Inc, Canada.

2.8.3 Cloning of the sponge cassette into PUAST-EGFP vector

We received the vector pUAST-EGFP as a gift from Dr. Tudor A. Fulga from the University of Oxford, UK. This vector was received on a filter paper marked with pencil. I cut the marked area with sterile razor blade into fine pieces and dissolved in TE buffer (10mM, pH7.5) and mixed well by vortexing. I used ~5µl of this sample to transform the NEB 5-alpha competent cells by following the manufacturer's protocol. I received many colonies and picked a few to proceed. The phenol: chloroform purified DNA from mini-preps was sent for sequencing. This confirmed the sequence and the orientation of the EGFP sequence. Once confirmed, I prepared more DNA and 20µg of this DNA was sent to Bio Basic Inc. for cloning of the synthesized sponge sequence. The company sent their sequence information that confirmed the vector sequences and the insert. The company sent the pUAST-EGFP miR-184 sponge vector back to our lab. I received about 4µg of DNA and dissolved it in Tris-EDTA, pH 7.5. The diluted sample (~50ng/µl) of this sample was used to transform supercompetent sure2 cells form STRATAGENE using the company protocol. These cells were chosen to avoid changes in repeat number due to recombination.

(A)

(B)

12 11 10 9 8 7 6 5 4 3 2 1

5'TCTAGACCCTTATCAAGCATCCGTCCACGCGCCCTTATCAAGCA

TCCGTCCACGCGCCCTTATCAAGCATCCGTCCACGCGCCCTTATC

AAGCATCCGTCCACGCGCCCTTATCAAGCATCCGTCCACGCGCCC

TTATCAAGCATCCGTCCACGCGCCCTTATCAAGCATCCGTCCACG

CGCCCTTATCAAGCATCCGTCCACGCGCCCTTATCAAGCATCCGT

CCACGCGCCCTTATCAAGCATCCGTCCACGCGTCTAGA-3'

Figure 2.5: ***miR-184 sponge* constructs** (Loya et al., 2009). A) Diagrammatic position of the sponge cassette in the pUAST-EGFP vector. B) 10 repeats of the *miR-184* complementary sequence (ACCTGCCTAACGACTATTCCC) with mismatches at position 9-12 and separated by a variable four-nucleotide linker (CGCG) were designed with Xba I restriction sites (shown in blue) and placed in the 3'UTR region of EGFP in pUAST-EGPF vector and cloned, seed region (position 1-6).

After successful transformation, individual colonies were used for minipreps and sent for sequencing to confirm the sequence. Since the previously used pUAST reverse primer was too close to the XbaI site, so I designed a new reverse primer - 5'-TTT TAT ATT TAC CTT AGA GCT TT-3'. Sequencing using the forward primer and the new reverse primer confirmed the sequence and the orientation of the *pUAST-EGFP- miR-184 sponge* vector. After confirmation, large scale production of DNA was achieved by Qiagen midi prep kit protocol and ≥ 35µg of phenol: chloroform purified DNA in TE was sent to Rainbow Transgenic Flies Inc., CA for injection. The successful injection resulted in ~240 larvae and 30 transgenic lines. The chromosomal location of the transgene, *UAS-miR 184 sponge* was identified as described previously for *UAS-miR-184* transgenic flies and homozygous stock of these transgenic lines were established.

2.8.4 Verification of the transgene in the flies

Verification of the expression of the transgene insertion in transgenic lines generated was done by RT-PCR. For this purpose, the transgenic fly lines were crossed to a heat inducible driver, hsp70-Gal4. CS wild type flies were used as control flies. The progenies from the crosses were subjected to heat shock at 37°C for 2 hours in over-night pre-warmed food vials. The flies were collected in a pre-cooled tube on dry ice and immediately stored in -80°C until processed for RNA extraction. RNA was extracted from these flies using the Trizol method from Invitrogen. RT reaction and cDNA synthesis were done as described below:

2.8.4.1 RT reaction and cDNA synthesis

For each sample, 2 µg of total RNA was digested using DNAse in DNAse buffer (Promega) and water in 20µl total volume by incubating at 37°C for 90 minutes. The reaction was stopped by adding 1µl of DNAse stop solution (Promega) and heating to 65°C for 10 min. Samples were then transferred to ice or at 4 °C for longer storage. Five microliter of DNAse treated RNA was mixed with 2µl of oligodT (Invitrogen), 2µl of 10mM dNTP mix and 5 µl DEPC water to make up the total volume of 12 µl. Two replicates of this mixture were prepared and were labeled as +RT and –RT samples. The purpose of including –RT sample was to check if there was any genomic DNA contamination in the final PCR reaction. Each mixture was incubated at 65°C for 5 min and quickly chilled on ice. The content was then briefly centrifuged. To each sample (12µl), 4µl of 5X first strand buffer, 2µl of 0.1M DTT (Invitrogen), and 1µl of RNAse in Ribonuclease Inhibitor (Promega) were mixed and incubated at 42°C for 2 min. The RT+ sample of each RNA sample was mixed with 1µl of SuperScript RT II (Invitrogen, Superscript-II-Reverse Transcriptase). The -RT sample was mixed with 1µl of DEPC water. All samples were incubated at 42°C for 50 min for the reverse transcription reaction. The reaction was inactivated by heating at 70°C for 15 min. The prepared cDNA was stored at -80°C until further processed.

2.8.4.2 PCR

The *miRNA-184* forward and miRNA reverse primers were used to amplify the cDNA of *UAS-miR-184* fly lines; the pUAST forward and pUAST reverse primers were used to amplify cDNA of the transgene *UAS-miR-184 Sponge*. PCR reaction using the cDNAs was performed for 25. The PCR condition was set as: Step 1: denaturation at

94°C for 2 minutes; Step 2: 25 cycles of denaturation at 94°C for 30 seconds, annealing at 55°C for 1 minute and extension at 72°C for 1 minute; and final extension at 72°C for 10 minutes followed by 4°C holding temperature overnight. 16 µl of the PCR product from each reaction were run on a 1.2% agarose gel and stained with ethidium bromide and visualized under a UV illuminator.

2.9 Behavioral assays

2.9.1 Courtship assay

The male flies to be tested were collected immediately after eclosion. The flies were then isolated in a fresh vial individually and allowed to mature to 4-7 days (depending upon the temperature at which they are grown). On the day of the assay, a male fly was placed in a small chamber of 10mm diameter together with a *Canton-S* virgin female (2-6 hours old) and their behavior was recorded for 10 min. The courting behavior of the male fly was measured as the courtship index, which was calculated as the fraction of time the male spent courting the female within the 10 minutes observation period.

2.9.2 Activity assay

The males were collected and reared individually in vials as described in section 2.9.1 for courtship assays. Each male was placed in a courtship chamber which had a line drawn at the centerline along the diameter of the chamber. The male was allowed to get used to the surroundings for the first 2 minutes. Then, the activity of the male was observed for the next 3 minutes. Activity was recorded as the number of times the male crossed the centerline of the chamber.

2.10 Temperature sensitive Gal80 flies

For all Gal80 temperature sensitive experiments, control and experimental flies were raised in an 18˚C incubator. Virgin male flies were collected immediately after eclosion and were kept for 7 days at 18˚C to reach adulthood. In order to induce the expression of the gene of interest, the flies (both the control and the experimental) were placed in a 32˚C incubator for 36-40 hours unless otherwise stated. After 36-40 hours, the flies were removed from the 32˚C incubator and allowed to rest for 3 hours at RT. Non-induced controls from 18˚C were also subjected to the same resting period of 3 hours at RT. The flies were then tested in behavioral assays.

2.11 Microinjection

2.11.1 Pulling needles for microinjection

Microinjections were performed with borosilicate glass capillaries (needles), 100mm in diameter (World Precision Inst., order number TW100-4). The needles were pulled using a Sutter needle puller (Model: PP-830, courtesy of Dr. Dryer). The temperature of the heater 1 was set to 70°C and the heater 2 was set at 50°C. The tip of the needles was broken to ~ 25 micron in diameter by tapping onto a glass surface using a Narishige Scientific Instrument Laboratory Microscope with an optical ruler (courtesy of Dr. Dryer).

2.11.2 Filling needles

The needles were backfilled using a micro loader pipette tip (Eppendorff's) without introducing any air bubbles.

2.11.3 Injecting

A Tritech Research micro injector was used to perform injection. Parameters that were used for microinjection are as follows:

Injection pressure: 20 psi
Injection time : 0.6-1 sec
Hold pressure : 1 psi

Flies were anesthetized on ice for 5-10 minutes before the microinjection. The needle was backfilled with 20 µl of 25 mg/ml Dextran conjugated with florescent Texas red dye (Invitrogen D-1863) in H_2O. The volume dispensed by the needle was first tested onto a parafilm. A tiny drop~100 nl of the dye was used for microinjections. A pre-cooled tube storage box (filled with frozen H_2O) was used to keep the flies anesthetized making them immobile during the microinjection procedure. A pre-cooled slide with a colored tape on it for contrast purpose was placed on top of the storage box. The anesthetized fly was placed on top of the slide facing the edge of another slide such that they did not move during injection). The needle was angled at 45 degrees and injection was performed into the scutellum of the fly.

2.11.4 Dye microinjection

Male flies of the desired age were injected with ~100 nl Texas red lysine fixable Dextran (25 mg/ml in H_2O). After injection the flies were placed in fresh food and allowed to recover overnight. Fly heads were separated by anesthetizing in CO2 and

subsequently fixed in 4% Paraformaldehyde (EM grade, Polysciences Inc.) in 1X PBHS for 30 minutes at RT. Then the proboscis was removed with the help of a sterile blade and the heads were fixed for an additional 5 minutes at RT. The brain was finally dissected and washed in 1X PBS 3 times for 30 minutes each. The brains were mounted on a coverslip using Vectashield mounting media with DAPI (VectorLab) and observed with a Leica SP8 confocal microscope. DAPI- stained cell nuclei were visualized at 405 nm, Texas red dextran at 633 nm.

2.12 Generation of *ΔmiR-184* flies

To generate the *miR-184* deletion fly lines, the methods described in Parks et al., 2004 and Iovino et al., 2009 were adopted. The *miR-184* gene is located on chromosome 2. The two FRT-bearing P-element insertion lines, f05119 (PBac{WH}f05119) and d08710 (P{XP}d08710) flanking the *miR 184* gene were selected. The *Δmir-184* deletion was created by FLP-mediated recombination of the two FRT-bearing P elements (PBacf05119 and P {XP} d08710). The deletion was detected by loss of w^+ and confirmed molecularly by loss of the *miR-184* coding sequence (Parks et al., 2004). The ribosomal protein *rp49* gene was used as an endogenous control. The crosses were set as shown in Figure 2.7.

Males containing element d08710 were crossed to females containing the FLP recombinase transgene. The resulting progeny male containing both the FLP recombinase and the d08710 element were crossed to females with the second element f05119. After

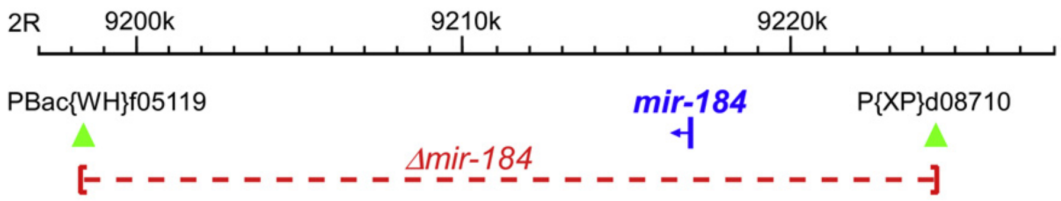

Figure 2.6: Organization of the *mir-184* locus, indicating the genomic coordinates of the mature miRNA and the *mir-184* deletion (Iovino et al., 2009). *mir-184* is a single copy gene and lies isolated within a 50 kb region on the right arm of the second chromosome (50A; 9217K). The FRT site-containing elements The FRT site-containing elements PBac{WH}f05119 and P{XP}d08710 (green triangles) were used to generate an FLP-induced deletion following established procedures (Parks et al., 2004).

48 hours, the vials with the parent flies were subjected to heat shock at 37°C for 1 hour. The parents were removed after 72 hours and for the next 4 days; the vials were heat shocked for 1 hour every day. The progenies were raised to adulthood and the virgin females were crossed to white-eyed double balancer males.

The progenies with white eyes were looked for along with orange-eyed progenies. These flies were individually crossed with double balancer flies to get flies with a balanced 2nd chromosome. Twenty-one individual lines with white eye color and 21 orange-eyed individual fly lines were selected and maintained for further examination.

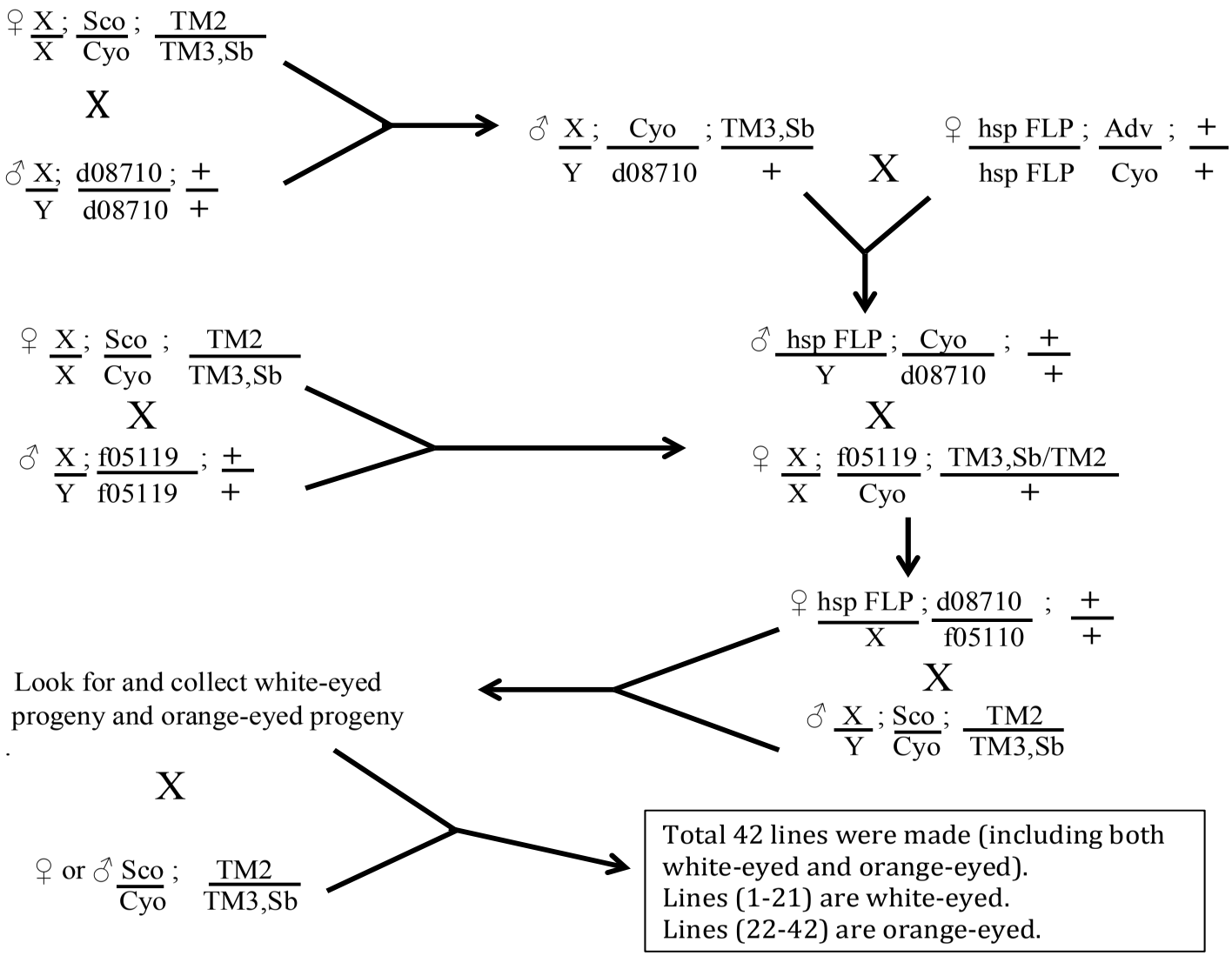

Figure 2.7: Crossing scheme for generating *Δmir-184 mutants*

2.12.1 Verification of *miR-184* deletion

A. By genomic PCR

To confirm the deletion, genomic DNA was isolated from these fly lines (DNAzol Reagents, Invitrogen). I performed PCR on the genomic DNAs of heterozygous and homozygous deletion candidate lines by using *miR-184* primers to confirm the absence of *miR-184* gene. An amplification of the ribosomal protein (*rp49*) gene was used as a control.

B. By assessing the egg/embryo morphology

One way of confirming the deletion of *miR-184* in these flies was by assessing the fertility of the females and of the morphology of the eggs laid by the *miR-184* deficient homozygous females. As described previously by Iovino et al., 2009, we expect that females with reduced fertility and that most of the *ΔmiR-184* eggs are smaller in size than control CS flies and that the dorsal appendages are short and not well developed.

2.13 qPCR (Quantitative Reverse Transcription Polymerase Chain Reaction)

TaqMan Universal PCR Master Mix with No AmpErase UNG (Part No 4324018) and TaqMan probes for *Sinu, rp49, miR-184 and 2S rRNA* and the RT primers were purchased from applied biosystems and the company protocol was followed (Applied Biosystems).

sinu probe- TaqMan assay ID= Dm02397874_gl. Sinu FAM PN431372, Size: 360 rxns. 20X Lot: P130627-004H09

rp49 probe- TaqMan assay ID= Dm02151827_gl. RPL32 VIC PL PN4448485; Size: 750µl rxns 20X, Lot: P130315-003H12

miR-184 probe-Taqman assay ID= TM 290 dme-miR-184 FAM; Size: 150µl rxns, 20X Real Time Lot: 1009007-□ F2

2S rRNA probe- Taqman assay ID= TM001766 2S rRNA FAM; Size: 150 µl rxns 20X Lot: P120622-003D05

miR-184 RT primer- Taqman assay ID= RT 290, dme-miR-184 FAM; Size: 150µl rxns, 5X RT primer Lot:1009007-□ F2

2s rRNA RT primer- Taqman assay ID=RT 001766 2S rRNA Pn 4427975; Size: 150µl rxns 5X Lot: P1200622-003D05.

2.13.1 RNA extraction and reverse transcription for detection of *sinu* expression

In order to examine the effect of overexpression of *UAS-miR 184* on the expression level of its target *sinu* in the bbb, a qPCR was performed. *miR-184* was expressed throughout the development and adulthood using the bbb specific driver, SPG-Gal4. A total of 300 brains from each genotype were dissected. The whole RNA was extracted (Trizol plus RNA purification kit, Ambion) from these brains. The reason for dissecting whole brains instead of bbb cells was that *sinu* is not expressed in the brain. Therefore, any effects on its RNA levels are likely to reflect the levels in the bbb. cDNA was synthesized from the 1µg of total RNA from each sample following the manufacturer's protocol for Taqman reverse transcription kit (part no N808-0234). The kit included Multiscribe^{TM} RT enzyme (50U/µl, Lot No 1301117), 10X Taqman RT buffer (PN 4319981), dNTP mix w/dTTp (100M total, PN 4367381), Random hexamers,

25mM Magnesium chloride and RNase inhibitor (200U/µl, Lot No 1211007). For a 50 µl RT reaction, 5 µl of 10X Taqman RT buffer, 11µl of 25mM of MgCl2, 10 µl of dNTPs, 2.5 µl of Random hexamers, 1 µl of RNAse inhibitor and 1.25 µl of Multiscribe™ reverse transcriptase were added. The remaining volume was nuclease free water minus the RNA volume. The RT reaction condition was: 25°C for 10 minutes; 48°C for 30 minutes; and 95°C for 5 minutes. Minus RT sample was also prepared in parallel to check for any genomic DNA contamination later in the real time PCR.

2.13.2 RNA extraction and reverse transcription for detection of *miR-184* expression

To verify the specificity of the function of the sponge transgene on *miR-184* expression, I measured the level of *miR-184* in sponge overexpressing cells by quantitative PCR (qPCR). In order to do so, a total of 50 whole brains were dissected per genotype and bbb cells expressing the sponge for *miR-184* (*UAS-miR-184 7.1 Sp*) were manually isolated and RNA was prepared by using the miRNA mini kit from Qiagen following the manufacturer's protocol for whole RNA extraction including the small RNAs from animal tissues. The lysis and the homogenization of the cells were carried out using a syringe and needle method (20 gauges). Complementary DNA (cDNA) was prepared from this RNA using the Taqman MicroRNA Reverse Transcription kit (PN 4366596) purchased from Applied Biosystems. The kit included Multiscribe™ RT enzyme (50U/µl, Lot No 1301117), 10X RT buffer (PN 4319981), dNTP mix w/dTTp (100M total, PN 4367381) and RNase inhibitor (200U/µl, Lot No 1211007). In a total of 15 µl RT reaction, 10 ng of total RNA in a 5 µl volume, 3 µl of 5X *miR-184* RT primer and 7 µl of master mix containing Multiscribe™ RT enzyme, 10X RT buffer), dNTP

mix, and RNAse inhibitor were reverse transcribed using the protocol described in the manual. The thermocycler conditions were: 16°C for 30 minutes; 42°C for 30 minutes, and 85°C for 5 minutes and holding at 4°C. A Minus RT sample for each genotype was also prepared to check for genomic contamination in the qPCR. For an internal control, a separate cDNA was prepared in parallel using the *2S rRNA* RT primer.

2.13.3 Establishing a standard curve and qPCR assay

A standard curve was established to determine the dynamic range for the target and the endogenous control targets. The cDNA from one of the control genotypes was used for this purpose for the quantification. A standard curves with 5 dilutions points (each dilution with 3 replicates) were generated using the dilutions of 1, 0.1, 0.01, 0.001, and 0.0001 of the cDNAs. Standard curves with slope value -3.3+/-0.2 were obtained.

After determining the dynamic range for each sample, the qPCR assay for each sample was performed in a 20 µl mix consisting of 10 µl TaqMan Master Mix (Applied Biosystems), 2 µl cDNA, 1 µl TaqMan probe and 7 µl of DEPC treated water. The samples were loaded in triplicate into a 96 well plate. The amplification was performed with the initial holding temperature at 95°C for 20 seconds followed by 40 cycles of cycling stages involving 95°C for 1 second followed by 60°C for 2 seconds in an Applied Biosystems StepOnePlus Real-Time PCR system. Triplicate of water sample was run as negative control and –RT cDNA for each sample in triplicate was used to see if there was any genomic DNA contamination.

2.13.4 Data analysis

The Comparative Threshold Cycle (ΔΔCt) method was used to analyze the relative expressions. The change in the target gene was calculated as fold change relative to the control. The ΔCt (normalized Ct) value was calculated as the difference between the average Ct (threshold cycle values) for the expression of the *target gene* and the endogenous control for each genotype. The endogenous control used for mRNA expression was the ribosomal protein gene, *rp49* and the endogenous control used for microRNA expression was small ribosomal RNA, *2SrRNA*. The calibrated ΔCt value for each sample (ΔΔCt) was calculated as the difference between the ΔCt values of the sample and the reference sample. The fold change for each sample relative to the calibrator was calculated as $2^{-\Delta\Delta Ct}$. The fold induction values for each genotype are plotted as a bar graph (Bookout and Mangelsdorf, 2003).

2.14 Statistical analysis

The data are presented as means + standard error of the means. Statistical comparisons between the genotypes were performed by one-way or two-way ANOVA followed by Bonferroni multiple comparison *post hoc* test. Statistical analyses were performed with the Statview (Adept Scientifics, Bethesda, MD) program.

Chapter III

Results

3.1 A genomic approach to identify sex-specific molecules in the bbb

In contrast to mammals, sex in *Drosophila* is determined cell autonomously (Baker and Ridge, 1980). The males and females express sex-specific forms of different proteins. By taking advantage of this system, the sexual identity of individual cells can be altered genetically. Previous studies done in our lab have shown that the sexual identity of the sub-perineural glial layer of the *Drosophila* blood brain barrier (bbb) is important for normal male courtship behavior. When the female specific protein TraF was specifically expressed in this layer of otherwise normal males, the courtship behavior was significantly reduced compared to the controls males with normal bbb (Hoxha et al., 2013). The courtship results of the bbb feminization confirmed that the bbb plays an important role in males for courtship behavior suggesting that these cells have sex-specific molecules that are controlled by *tra.* So, the next question was: what is the identity of these genes/molecules present in this layer that are important for courtship behavior? To address this question, I took three genomic approaches by carrying out the screens described in Figures 3.1a and 3.1b:

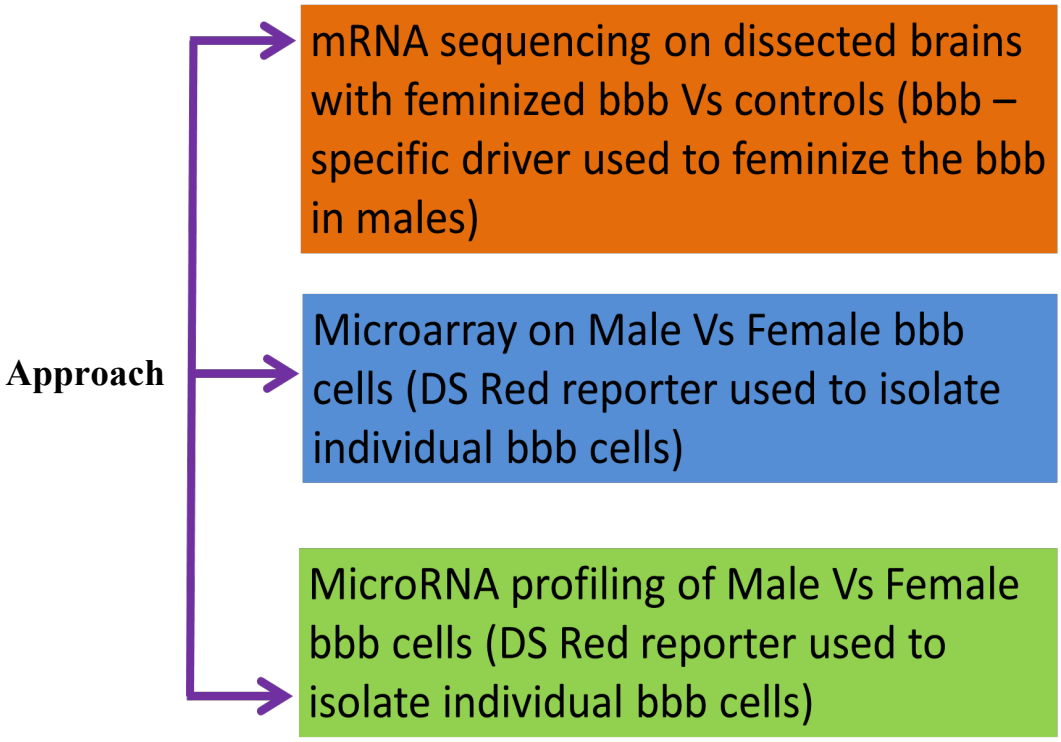

Figure 3.1a: Genomic approaches taken to identify sex-specific transcripts in the bbb.

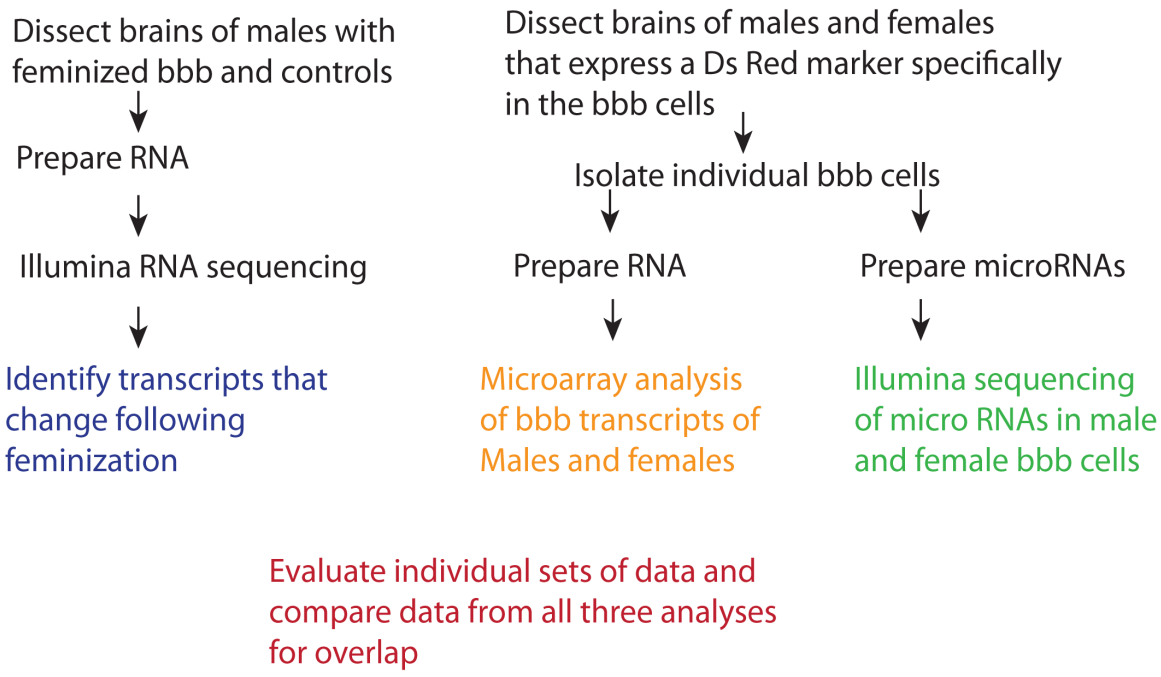

Figure 3.1b: Flow diagram of different genomic approaches for identification of bbb-specific genes/molecules.

3.2 mRNA sequencing of bbb-feminized male brains reveales numerous genes with differential expression in comparison to normal males

I started by first outcrossing the fly lines (two SPG-Gal4 driver lines and the UAS-TraF line) for 10 generations with white-eyed CS flies {w^{1118}*(CS)*} to normalize the genetic background. I then tested these fly lines to make sure they reproduced the earlier observation (Figure 3.2). I used the Gal4-UAS binary system to drive expression of TraF in the bbb of the normal males. The genotypes tested for courtship were as shown in Table 3.1.

Table 3.1: The following genotypes were created and used for courtship behavior

Flies	**Genotypes**
Control 1	*X/Y; +/SPG-Gal4 (B-4) Chr II; +/+*
Control 2	*X/Y; +/+; +/SPG-Gal4 (B-1) Chr III*
Control 3	*X/Y; +/+; +/UAS-TraF*
Experimental 1	*X/Y; +/SPG-Gal4 (B-4) Chr II; +/UAS-TraF*
Experimental 2	*XY/; +/+; SPG-Gal4 Chr III/UAS-TraF*

All the crosses were carried out at 25°C and the individual males were raised in food vials immediately after eclosion and matured for 4-5 days and then subjected to the courtship assays with young 4-6 hours virgin wild-type CS females in a courtship chamber. Their courtship index was measured as described in the Materials and Method section 2.9.1. The SPG-Gal4 driver line on the second chromosome was weaker than the one on the third chromosome. However, the third chromosome driver line showed some

additional insertion of Gal4 on the 4th chromosome that we were unable to isolate. So, to avoid variation at the strength level of driver, I continued using the SPG-Gal4 driver line on the 2nd chromosome for the bbb feminization experiments. In the courtship assay, the bbb feminized males showed all of the individual steps of courtship but less often than the normal control males.

The courtship results of the bbb feminization confirmed that the bbb plays an important role for male courtship behavior. This indicates that these cells have sex-specific molecules that are controlled by *tra.* To see if the feminization of the bbb brings about changes in gene expression, a mRNA sequencing experiment was conducted on whole brains of males with feminized bbb in comparison to the normal control males. For this experiment, the feminization of the bbb was carried out using the SPG-Gal4 on the second chromosome. The genotypes of the flies are shown in Table 3.2.

Table 3.2: The following genotypes were created and used for whole brain dissection

Flies	**Genotypes**
Control 1	*X/Y; +/SPG-Gal4 (B-4) Chr II; +/+*
Control 2	*X/Y; +/+; +/UAS-TraF*
Experimental	*X/Y; +/SPG-Gal4 (B-4) Chr II; +/UAS-TraF*

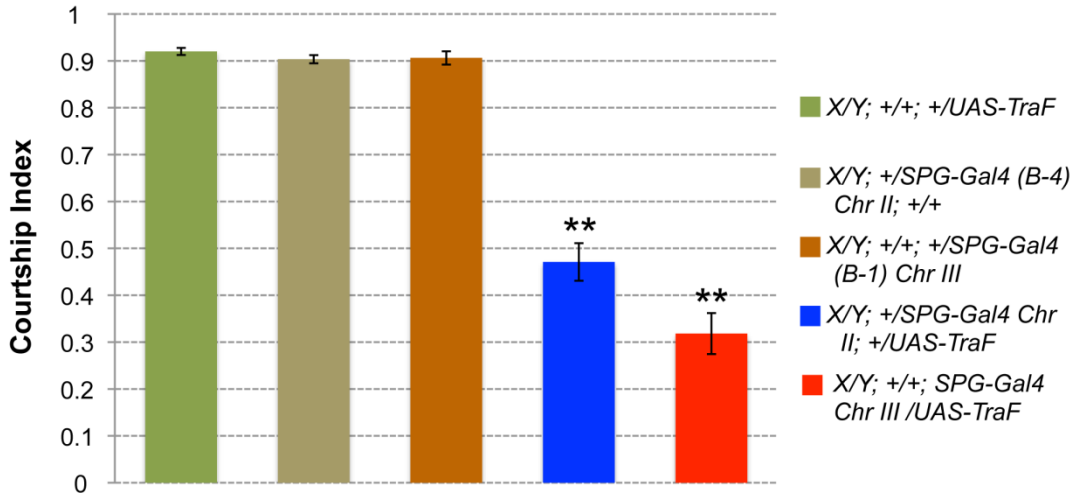

Figure 3.2: Courtship phenotype of flies is unchanged after outcrossing for 10 generations. The bbb of the males was feminized by the expression of the female-specific form of protein TraF in the bbb by using two different bbb –specific drives. The genotypes tested were the three control genotypes: *X/Y; +/SPG-Gal4 (B-4) Chr II; +/+*, *X/Y; +/+; +/SPG-Gal4 (B-1) Chr III)* and *X/Y; +/+; +/UAS-TraF* and the two experimental genotypes*: X/Y; +/SPG-Gal4(B-4) Chr II; +/UAS-TraF* and *X/Y; +/+; SPG-Gal4 Chr III/UAS-TraF*. The courtship index was measured as described in the Materials and Methods section 2.9.1. Before the behavioral tests, the Gal4 and the UAS lines were outcrossed for 10 generations with the w^{1118} CS flies to normalize the genetic background. As shown in the figure, the experimental genotypes showed a significant reduction in courtship index as compared to the controls as indicated. (ANOVA, **, $p<0.001$, $n=20$). Error bars represent the standard error of the means.

Whole brains were dissected from bbb-feminized males and the two controls. The brain dissection and RNA preparation protocols are described in section 2.2 of the Materials and Methods. mRNA sequencing was performed at the BCM Microarray Core Facility. Two biological replicates of total RNA of each genotype were submitted for sequencing with the goals to have the RNA sequencing samples prepared for paired end sequencing (75 bases) on the core's Illumina sequencer.

I submitted two biological replicates of these samples to the BCM core facility for mRNA sequencing; however, they used a wrong protocol without discussing this with our lab. Instead of sequencing from both the 3' and 5' end, they performed only 3' sequencing. This method limits the information that is obtained, especially in the case of alternatively spliced transcripts. As a result, I could not get the desired information from this experiment and had to submit two biological replicates of the brain RNA again to sequence with the correct method and protocol.

3.2.1 Data analysis

Once the raw data were received, the data analysis was done in collaboration with Peter Chang from the University of Southern California, Los Angeles, CA and Dr. Weimen Xiao from Dr. P. Gunaratne's lab at the University of Houston. Initially, the following comparisons were done (Table 3.3).

Table 3.3: Summary of data analysis

SN	Data analysis
1	An initial comparison was made between the two controls (+/SPG vs +/TraF)
2	Each control was independently compared to the experimental to identify differentially expressed genes.
3	The differentially expressed genes were compared to the Chang et al. (2011) study and based on their data the genes were classified as either sex-specific (i.e. different between males and females) and/or *tra*-dependent (difference between females and *tra* mutant females).

It is important to keep in mind the design of the experiment. The RNA of whole brains was sequenced, and the only difference among samples is that in the experimental, the bbb is feminized. 11,421 genes were identified as expressed overall in the entire brain samples. Initial RPKM (Reads Per Kilobase of transcript per Million mapped reads) correlation analysis for the samples showed that all samples that contained SPG-Gal4 grouped together, suggesting that the presence of this transgene affects the RNA profile. Since there were two independent controls for this experiment, we performed a comparison between the two controls (+/UAS and +/Gal4). We would expect that there are few differences since we outcrossed the two strains. However, 209 genes (out of 11,421 totals) were found to be differentially expressed between the two controls. However, it is worth noting that these differences between the controls are several orders of magnitude smaller than differences between the control and experimental samples.

Since we were interested in analyzing the changes in the experimental samples compared with the controls rather than the changes within the controls themselves, we focused our analysis on the differential expression of genes in the experimental samples compared to either of the controls. Based on these findings, we performed the following further analyses; the differentially expressed genes were categorized as group I, II, and III where;

I= Genes that are expressed differentially between +/ SPG and SPG/TraF

II= Genes that are differentially expressed between +/TraF and SPG/TraF

III= Overlap between I and II

A total of 114 genes were found to be differentially expressed in group I, 91 genes were differentially expressed in group II, and 40 genes were differentially expressed in group III. Figure 3.3 I, II, and III shows the heat maps of these genes.

We further compared our datasets with the data in Chang et al.'s (2011) study from Michelle N. Arbeitmen's lab (MNA data) (see Table 3.2 and Table 3.3). These authors had profiled whole heads to identify sex-specific transcripts. In addition, they examined the transcripts that were dependent on Tra regulation. While we have examined brains and they have examined whole heads, many transcripts are expected to overlap. We expect that our dataset identifies sex-specifically expressed transcripts. Since our experimental approach was feminization of the bbb by Tra, we expect to see a large number of transcripts in our set to overlap with the previously identified Tra-dependent transcripts. Table 3.4 and 3.5 show that this is indeed the case.

Table 3.4: Differentially expressed genes are classified as sex-specific (S) and Tra-dependent (T) (based on a comparison with Chang et al., 2011)

Group	Number of differentially expressed genes	Number of sex-specific genes (S)	Number of Tra-dependent genes (T)
I	114	57 (50%)	80 (69.56%)
II	91	47 (51.65%)	63 (69.23%)
II	40	21 (52.5%)	31 (77.5%)

Among all of the transcripts we identified, the percentage of sex-specific transcripts was 15.8% (1348/8735, see Table 3.5), very similar to the findings of Chang et al. This indicates that the transcript pool identified was similar in the two experiments, suggesting a good quality of our RNA sequencing runs. Among the differentially expressed transcripts in groups I, II, and III, this percentage is 50%, 51.65%, and 52.5% respectively (see Table 3.4). Figure 3.3 I, II, and III show the genes identified in our screen. We found that there are 114 genes in our group I, out of which 57 genes were classified as sex-specifically expressed by Chang et al, and 80 of them were *tra*-dependent genes in the Chang et al. study. In our group II, a total of 91 genes were present out of which 47 genes were identified as sex-specific and 63 genes were found to be *tra*-dependent in the Chang et al. study. Similarly, in our group III, 40 genes were found with 21 being classified as sex-specific and 31 as *tra*-dependent by Chang et al. As shown in Table 3.7, there was a significant enrichment for sex-specific and Tra-dependent transcripts in our identified groups of differentially expressed genes I, II, and III.

Table 3.5: Comparison of differentially expressed genes in category I, II, and III with the sex-specific genes and *tra*-specific genes in Chang et al. (2011) study (MNA Data)

	Differentially Expressed in MNA Data between F and M	Not Differentially Expressed	Hypergeometric Test for Enrichment
8896 Genes Expressed in MNA Data	1381	7515	
8735 Genes Expressed in MNA Data and Full Data Set	1348	7387	$p < 0.97$
114 Genes in "I"	57	52	**p = 0**
91 Genes in "II"	47	42	**p < 1.3e-15**
40 Genes in "III"	21	19	**p < 5.4e-08**
	Differentially Expressed in MNA Data between F and T-mutant	Not Differentially Expressed	Hypergeometric Test for Enrichment
8896 Genes Expressed in MNA Data	1850	7046	
8735 Genes Expressed in MNA Data and Full Data Set	1805	6930	$p < 0.99$
114 Genes in "I"	80	29	**p = 0**
91 Genes in "II"	63	26	**p < 1.0e-15**
40 Genes in "III"	31	9	**p < 1.7e-14**

Table 3.6: Differentially expressed genes from the group III gene list compared to the Chang et al. (2011) study shows that our differentially expressed mRNA data set contains many sex-specific (S) and *tra*-dependent (T) genes. The columns show the fold reduction FDR (False Discovery Rate) for the different comparisons that were carried out analyzing our data. Column 5 indicates whether the gene was identified as sex-specifically expressed (S) (Female vs male) in Michelle N. Arbeitman data (F vs M in MNA data). Column 6 shows whether the gene was differentially expressed in normal vs *tra*-mutant females (Females vs Tra mutant in MNA data, (F vs T in MNA data).

Name	FDR for +/SPG vs +/TraF	FDR for +/SPG vs SPG/TraF	FDR for +/TraF vs SPG/TraF	FvM in MNA Data	FvT in MNA Data
bnb	1	3.08E-232	3.06E-237		T
ATPsyn-beta	1	2.04E-108	6.87E-125	S	
CaMKII	1	1.12E-70	3.28E-78		T
cals	0.624567941	2.79E-54	5.14E-70		T
CR32477	1	1.13E-69	1.31E-66	S	T
CG11155	1	1.68E-42	1.61E-44		T
CG32017	1	3.10E-35	1.51E-39		T
plexA	1	1.42E-23	2.30E-20		T
CG31221	0.309772007	1.31E-09	8.31E-19	S	T
Zyx102EF	1	6.42E-13	4.74E-15		T
Tsf1	0.342328698	4.36E-07	4.74E-15	S	T
trol	1	1.26E-14	1.26E-11	S	T
Cam	0.361810643	0.000481563	1.89E-10	S	T
cpx	0.910456372	5.28E-05	3.38E-10	S	T
Actbeta	1	3.00E-10	5.45E-10		T
pho	1	1.85E-06	1.27E-09		T
Ggamma30A	0.405173209	0.00650065	1.90E-08	S	T
CG42613	1	4.08E-12	2.02E-08	S	
roX1	1	1.35E-07	4.39E-08	S	T
nrv3	0.417239001	1.21E-14	2.61E-07		T
CG11076	1	6.87E-06	2.57E-06		T
14-3-3zeta	1	1.54E-09	3.73E-06	S	T
CG10936	1	8.71E-05	3.83E-06		
Arf102F	1	0.000640231	5.23E-06		T
CG6329	1	5.03E-05	3.82E-05	S	T
CG16971	1	1.13E-06	3.90E-05	S	T
su(w[a])	1	6.52E-07	0.00122412	S	
chrb	1	0.004425367	0.003960116	S	T
Pitslre	1	4.20E-05	0.011677014	S	
CG10077	1	2.67E-05	0.013334628	S	
pUf68	1	8.56E-05	0.015420019	S	
pAbp	0.829729711	1.92E-06	0.015783358	S	T
Unr	1	0.023592448	0.01898344		T
B52	1	0.002947559	0.020633033	S	
CG9657	1	0.028661338	0.021227119		T
Kif3C	1	0.035608736	0.022660105		
Pif1B	0.458583847	1.28E-06	0.030165893	S	T
CG40498	1	0.046509825	0.033071059		T
CG2217	1	0.021759642	0.039946766		T
CG31705	0.065490365	1.46E-08	0.048812294		T

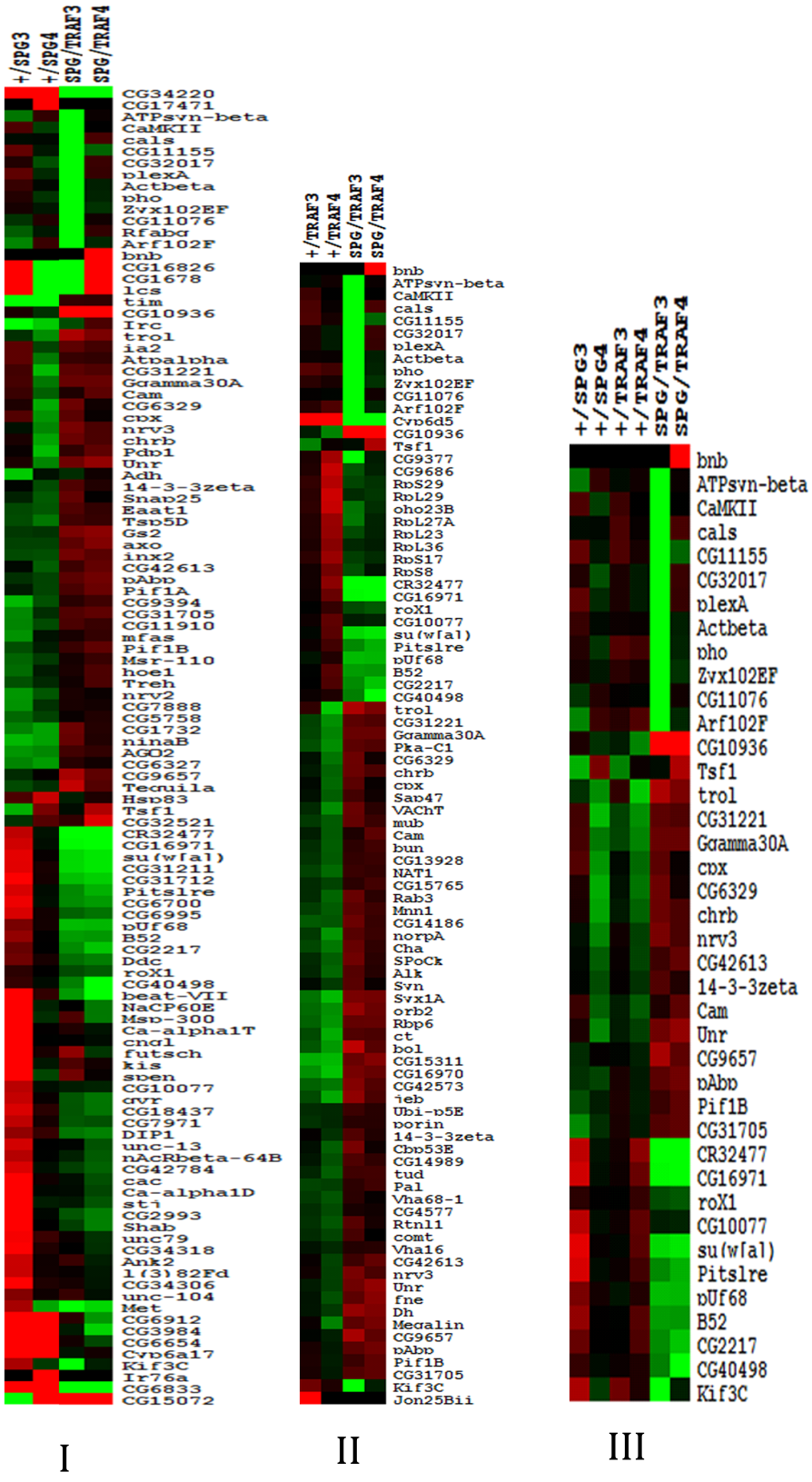
+/SPG3
+/SPG4
SPG/TRAF3
SPG/TRAF4
CG34220
CG17471
ATPsyn-beta
CaMKII
cals
CG11155
CG32017
plexA
Actbeta
pho
Zvx102EF
CG11076
Rfabg
Arf102F
bnb
CG16826
CG1678
lcs
tim
CG10936
Irc
trol
ia2
Atpalpha
CG31221
Ggamma30A
Cam
CG6329
cpx
nrv3
chrb
Pdp1
Unr
Adh
14-3-3zeta
Snap25
Eaat1
Tsp5D
Gs2
axo
inx2
CG42613
pAbp
Pif1A
CG9394
CG31705
CG11910
mfas
Pif1B
Msr-110
hoe1
Treh
nrv2
CG7888
CG5758
CG1732
ninaB
AGO2
CG6327
CG9657
Tecruila
Hsp83
Tsf1
CG32521
CR32477
CG16971
su(wfal)
CG31211
CG31712
Pitslre
CG6700
CG6995
pUf68
B52
CG2217
Ddc
roX1
CG40498
beat-VII
NaCP60E
Msp-300
Ca-alpha1T
cngl
futsch
kis
spen
CG10077
qvr
CG18437
CG7971
DIP1
unc-13
nAcRbeta-64B
CG42784
cac
Ca-alpha1D
sti
CG2993
Shab
unc79
CG34318
Ank2
l(3)82Fd
CG34306
unc-104
Met
CG6912
CG3984
CG6654
Cyp6a17
Kif3C
Ir76a
CG6833
CG15072
+/TRAF3
+/TRAF4
SPG/TRAF3
SPG/TRAF4
bnb
ATPsyn-beta
CaMKII
cals
CG11155
CG32017
plexA
Actbeta
pho
Zvx102EF
CG11076
Arf102F
Cyp6d5
CG10936
Tsf1
CG9377
CG9686
RpS29
RpL29
oho23B
RpL27A
RpL23
RpL36
RpS17
RpS8
CR32477
CG16971
roX1
CG10077
su(wfal)
Pitslre
pUf68
B52
CG2217
CG40498
trol
CG31221
Ggamma30A
Pka-C1
CG6329
chrb
cpx
Sap47
VAChT
mub
Cam
bun
CG13928
NAT1
CG15765
Rab3
Mnn1
CG14186
norpA
Cha
SPoCk
Alk
Syn
Syx1A
orb2
Rbp6
ct
bol
CG15311
CG16970
CG42573
jeb
Ubi-p5E
porin
14-3-3zeta
Cbp53E
CG14989
tud
Pal
Vha68-1
CG4577
Rtnl1
comt
Vha16
CG42613
nrv3
Unr
fne
Dh
Megalin
CG9657
pAbp
Pif1B
CG31705
Kif3C
Jon25Bii
+/SPG3
+/SPG4
+/TRAF3
+/TRAF4
SPG/TRAF3
SPG/TRAF4
bnb
ATPsyn-beta
CaMKII
cals
CG11155
CG32017
plexA
Actbeta
pho
Zvx102EF
CG11076
Arf102F
CG10936
Tsf1
trol
CG31221
Ggamma30A
cpx
CG6329
chrb
nrv3
CG42613
14-3-3zeta
Cam
Unr
CG9657
pAbp
Pif1B
CG31705
CR32477
CG16971
roX1
CG10077
su(wfal)
Pitslre
pUf68
B52
CG2217
CG40498
Kif3C
I
II
III

Figure 3.3: Heat map of differentially expressed genes in group I, II, and III. (I) Differentially expressed genes between +/SPG-Gal4 Vs SPG/TraF; (II) Differentially expressed genes between +/TraF Vs SPG/TraF; (III) Differentially expressed genes in both I and II. A total of 114, 91, and 40 genes were found to be differentially expressed in category I, II, and III respectively. Red indicates highest expression and green indicates least expression.

The observation that a majority of our differentially expressed genes were also found in Chang et al.'s differentially expressed gene lists provides strong support that our screen detects changes due to the feminization of the blood brain barrier.

Further analysis of the genes in group I, II, and III indicates that many of these genes are neuronal genes as shown by gene ontology classification using flymine (Flymine.org). This is not an unexpected outcome, because feminization of the bbb could bring about changes in the brain itself. I next examined how many of these genes our screen identified in category I, II, and III had previously been designated as "glial genes/functions", since the bbb is made up of glial cells. The pathway enrichment analysis of these genes shows that at least five genes: *Gs2, Syx1A, cpx, VAChT*, and *Sap25* are involved in glial cell function such as neurotransmitter uptake and metabolism in glial cells.

3.2.2 Identification of RNA isoforms

Since mRNA sequencing detects different isoform of the same gene, originating from differential splicing or alternative 5' or 3' end use, we next performed a similar analysis for our data sets. We again used the Chang et al. (2011) study for comparison. In that study, a total of 4368 gene isoforms were analyzed, and they found that 1370 were sex-specifically expressed and 1639 were *tra*-dependent genes in their data set. In our group I, a total of 411 gene isoforms were found to be expressed of which 90 were sex-specific and 114 were *tra*-dependent genes. In category II, a total of 252 gene isoforms were found, among which 58 were sex-specific and 57 were *tra*-dependent. In category III, a total of 45 gene isoforms were found, among which 13 gene isoforms were sex-specific (F vs M) and 15 gene isoforms were found to be *tra*-dependent (F vs T) (Table

3.7). Overall, there was a significant enrichment in our data sets for genes with alternative RNA isoforms. This is consistent with the fact that we expect changes in response to TraF that is a splicing regulator.

Table 3.7: Comparison of different gene isoform to the Chang et al. (2011) study

	Differentially Expressed in MNA Data between F and M	Not Differentially Expressed	Hypergeometric Test for Enrichment
4368 Alternative Transcripts Expressed in MNA Data	1370	2998	
411 Genes in "I"	90	86	**p <1.6e -08**
252 Genes in "II"	58	40	**p < 7.0e -09**
45 Genes in "III"	13	7	**p < 0.0019**
	Differentially Expressed in MNA Data between F and T-mutant	Not Differentially Expressed	Hypergeometric Test for Enrichment
4368 Alternative Transcripts Expressed in MNA Data	1639	2729	
411 Genes in "I"	114	62	**p < 2.0e -15**
252 Genes in "II"	57	41	**p < 5.7e -06**
45 Genes in "III"	15	5	**p < 0.00045**

3.2.3 Summary

The feminization of the bbb in otherwise normal males was achieved by the expression of the female specific protein TraF in otherwise normal males using the Gal4/UAS binary system. The RNA from whole brains of these males was subjected to mRNA sequencing and compared to RNA from normal males without feminized bbb. The results show that there are many genes that are differentially expressed in these bbb feminized males compared to the control males. Many of them are probably sex-specific transcripts that are present in the bbb. A study done by Chang et al. (2011) found that

many genes are sex-specifically expressed between males and females in whole heads and many of these genes are *tra*-dependent. When our mRNA seq data was compared to this study, the differentially expressed genes found in our study overlapped with many of their identified sex-specific and *tra*-dependent genes. This strongly suggests that the differential gene expression seen in our screen is indeed due to the effect of expression of TraF in the bbb of the experimental males. We have observed differences in gene expression between the two controls. There is also variation between the two biological replicates. This together with the number of biological replicates being low (n=2 in this study) sets limitations on our experiment and the data obtained.

3.3 Microarray analysis of male and female bbb cells shows expression of many sex-specific genes in the bbb of *Drosophila melanogaster*

In order to directly identify sex-specific transcripts in the bbb, I isolated bbb cells from males and females. Microarray analysis was performed using the RNA from these cells. Male and female bbb cells were isolated as described in the Materials and Method section 2.3. Flies bearing a transgene containing the UAS-regulated fluorescent reporter DS Red Stinger were crossed with flies bearing the bbb-specific driver (SPG-Gal4) to mark these cells. The fluorescent bbb cells from the surface of the brain were isolated and frozen immediately on dry ice frozen Trizol. The cells were submitted to GenUs Biosystems for RNA isolation and microarray analysis as described below. Approximately 1500 -3000 cells isolated from ~50 brains were used per sample. Three biological replicates of male or female bbb cells were provided

Figure 3.4: Isolated *Drosophila* brain. The nuclei of the subperineurial glial cells that form the bbb that ensheathes the brain are labeled by expression of DS Red stinger. The fluorescent cells were isolated from dissected brains to prepare RNA for microarray and miRNA sequencing analysis.

GenUs Biosystems performed the RNA isolation and microarray analysis using the following protocol: RNA was extracted and purified using RNeasy (Qiagen) and Ribopure (Ambion) RNA isolation. Total RNA samples were quantitated by UV spectrophotometry [OD260/280]. The quality of total RNA was assessed using an Agilent Bioanalyzer. First and second strand cDNA was prepared from the total RNA samples. cRNA was prepared from the DNA template and verified on the Bioanalyzer. cRNA was fragmented to uniform size and hybridized to Agilent Drosophila GE 4x44K arrays. Slides were washed and scanned on an Agilent G2565 Microarray Scanner. Data was analyzed with Agilent Feature Extraction and GeneSpring GX v7.3.1 software packages. Differentially expressed genes were identified with fold change > 1.5 fold and Welch T-test p-value < 0.05.

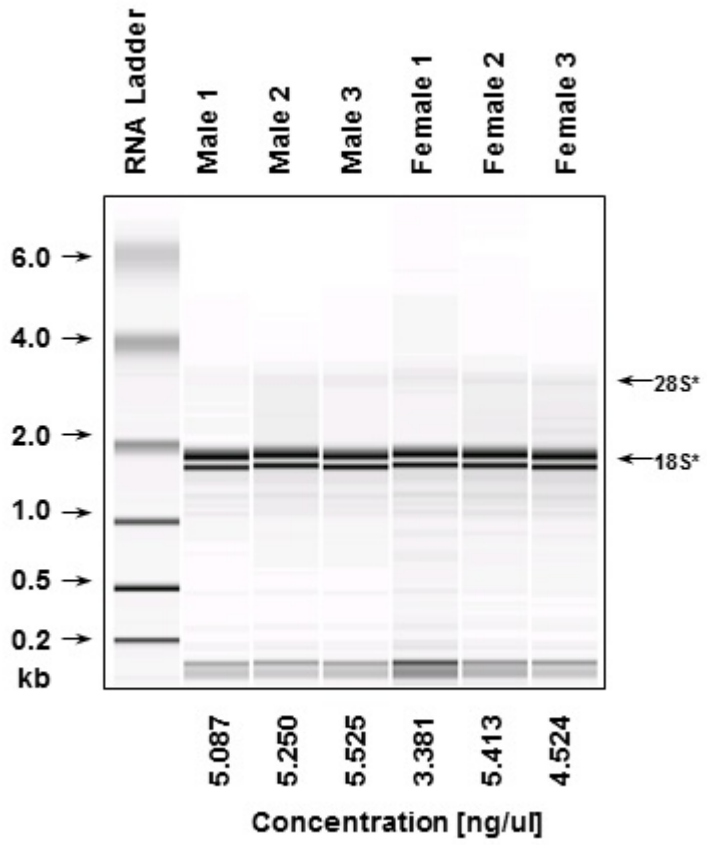

Figure 3.5: Total RNA quality analysis using the Agilent bioanalyzer. *Drosophila* 28S rRNA is cleaved into 2 fragments that migrate in a similar manner to human 18S rRNA (source: GenUs Biosystems).

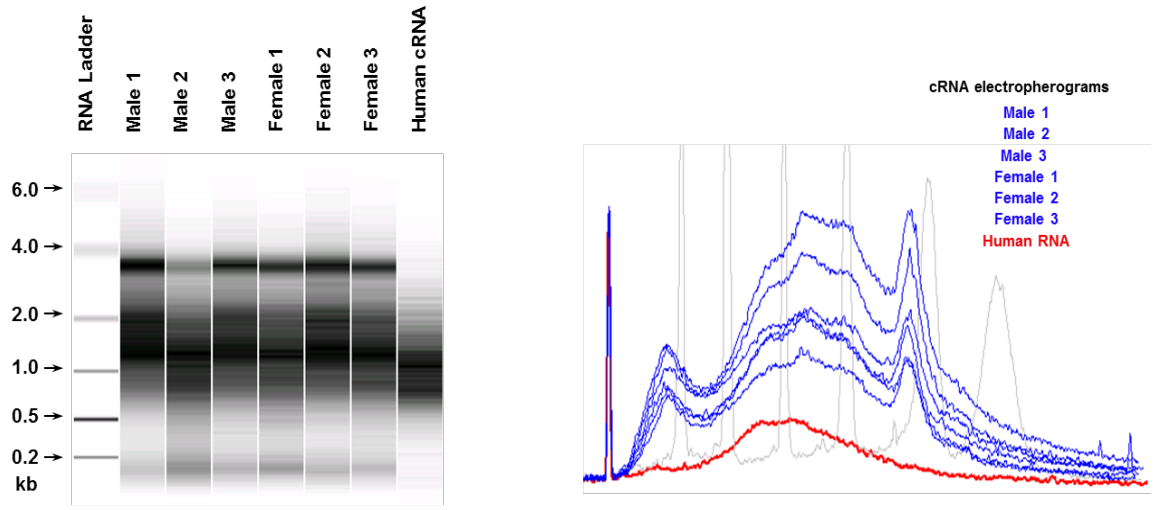

Figure 3.6: cRNA quality analysis. The analysis shows high amounts of *Drosophila* specific cRNA. Human RNA is used for comparison (source: GenUs Biosystems).

3.3.1 Several bbb genes are sex-specifically expressed

A total of 32,162 transcripts were found to be expressed in the bbb cells of males and female *Drosophila* (called "all genes" list). Among these ~284 genes were found to be differentially (sex-specifically) expressed in the bbb cells of males and females (>2 fold, T-test, p-value < 0.05, 284 probes). For this analysis, the intensity values were normalized to the 75th percentile intensity of each array and p-values are based on a Welch T-test. Table 3.8 and 3.9 show lists of differentially expressed genes (>2 fold) with highest expression in males or females respectively.

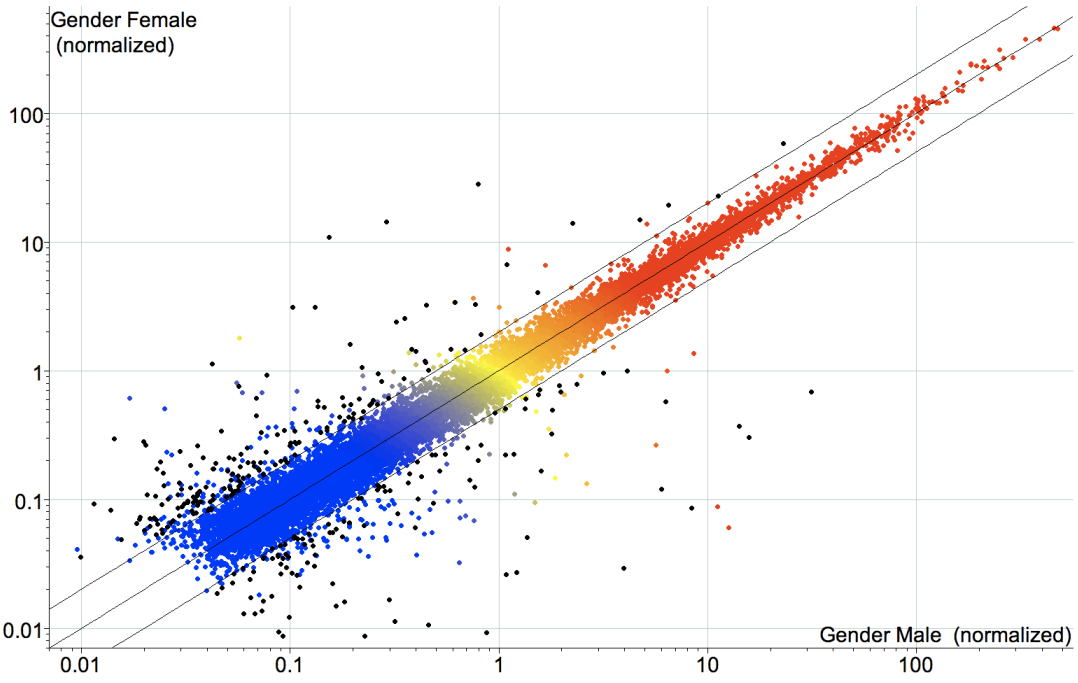

Figure 3.7: Probes present (above background) in all male or female samples are displayed as normalized to the 75th percentile intensity of each array (19,218 probes). Each spot is the mean of 3 samples from each condition. Black spots = differentially expressed genes (>2 fold, T-test p-value < 0.05, 284 probes). Red/orange=High expression, Yellow=Medium expression, Blue=Low expression (source: GenUs Biosystems).

Table 3.8: The top ranking female-specifically expressed genes in the bbb (from top to bottom)

P-value	Expression profile (males, females)	GeneName
4.03E-03		Yolk protein 1
6.60E-03		Yolk protein 3
6.53E-03	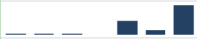	Yolk protein 2
2.27E-04		Chitinase 2
1.57E-03		CG14222 gene product from transcript CG14222-RA
4.65E-02		Chorion protein 36
4.91E-02		Drosophila melanogaster IP02756 full insert cDNA. [BT(
4.53E-03		Chorion protein b at 7F
1.21E-03		CG33238 gene product from transcript CG33238-RB
4.65E-07		Chorion protein b at 7F
1.15E-03		CG33246 gene product from transcript CG33246-RB
3.45E-02		deadhead
3.19E-02		Rep: Thioredoxin-1 - Drosophila melanogaster (Fruit fly)
4.68E-02		Chorion protein 15
3.58E-02		Jonah 99Fi
1.74E-03		CG33240 gene product from transcript CG33240-RB
2.26E-05		doublesex
6.25E-03		polar granule component
3.00E-02		Cyclin B
7.58E-03		Heat-shock-protein-70Aa
6.84E-03		Rep: Stellate protein CG33236/CG33244 - Drosophila r
1.59E-02		Heat-shock-protein-70Aa
3.90E-02		Drosophila melanogaster LP04080 full insert cDNA. [BT
1.73E-02		Chorion protein 19
3.06E-02		Heat-shock-protein-70Bb
2.66E-02		Cyclin B
1.90E-02		Drosophila melanogaster thioredoxin-like protein mRNA,
8.96E-03	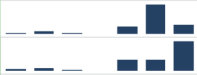	CG5834 gene product from transcript CG5834-RA
9.69E-03		CG8936 gene product from transcript CG8936-RA
3.67E-03		Chorion protein 16
2.48E-06		CG14075 gene product from transcript CG14075-RA
1.73E-03		EK024109.5prime Exelixis FlyTag CK01 pCDNA-SK+ D
6.82E-03		
1.63E-02		doublesex
3.63E-08		Checkpoint suppressor homologue
4.37E-02		Mucin 68D
4.97E-02		Rep: Probable 60S ribosomal protein L37-A - Drosophila
1.62E-02		CG4020 gene product from transcript CG4020-RA
3.33E-08		Chorion protein a at 7F
3.97E-02		CG17633 gene product from transcript CG17633-RA
4.71E-02		CG6824 gene product from transcript CG6824-RE
2.43E-02		CG4020 gene product from transcript CG4020-RA
1.63E-03		oskar
1.71E-03		CG14075 gene product from transcript CG14075-RA

Table 3.9: The top ranking male-specifically expressed genes in the bbb (from bottom to top)

P-value	Expression profile (males, females)	GeneName
2.39E-03		Calpain C
1.22E-02		CG34391 gene product from transcript CG34391-RC
1.02E-02		CG6356 gene product from transcript CG6356-RA
1.45E-02		DNA fragmentation factor-related protein 2
1.28E-02		Rep: CG11092-PA - Drosophila melanogaster (Fruit fly), co
1.82E-02		brother of iHog
1.37E-02		CG42340 gene product from transcript CG42340-RC
3.19E-02		CG8709 gene product from transcript CG8709-RK
4.46E-03		GB
2.52E-02		CG9576 gene product from transcript CG9576-RA
1.78E-03		no receptor potential A
4.43E-02		CG17838 gene product from transcript CG17838-RA
2.58E-02		odd skipped
7.77E-05		cAMP-dependent protein kinase R1
6.97E-04		Minichromosome maintenance 3
1.57E-02		Rep: Rab GTPase - Dictyostelium discoideum (Slime mold),
7.57E-04		
3.69E-03		Hormone receptor-like in 46
1.02E-02		CG42492 gene product from transcript CG42492-RA
3.53E-02		Dopamine 2-like receptor
1.78E-03		CG40351 gene product from transcript CG40351-RF
3.35E-02		CG11796 gene product from transcript CG11796-RA
9.09E-05		CG2681 gene product from transcript CG2681-RA
3.48E-06		Rep: IP15861p - Drosophila melanogaster (Fruit fly), partial (53%) [T
8.89E-04		
1.81E-03		Drosophila melanogaster stellate supressor (SuSte) mRNA exons 1-3
1.08E-07		RNA on the X 1
1.11E-04		CG13762 gene product from transcript CG13762-RB
1.98E-04		
1.08E-03		Rep: Ribonuclease H - Phaseolus vulgaris (Kidney bean) (French bea
3.94E-03		RNA on the X 1
4.92E-08		RNA on the X 1
1.64E-06		RNA on the X 2
2.12E-06		GB
1.06E-05		RNA on the X 1
4.52E-07		Rep: SD26211p - Drosophila melanogaster (Fruit fly), partial (14%) [T

As can be seen from the tables, there are a number of genes that are sex-specifically expressed. The three biological replicates show only modest variation. The presence of female specific genes such as the *yolk protein* gene most likely indicates contamination from the fat body around the brain although great care was taken to clean the brain while dissecting and isolating the cells. In addition, the presence of insulin-like peptide RNAs may indicate the presence of cells from the Pars intercebralis (P1), which are in close proximity to the bbb.

An additional comparative analysis was carried out at the level of 1.5 fold change in the level of gene expression between male and female bbb cells. At this threshold, we observed many more genes (711 genes), which are differentially expressed between males and females in this comparison (>1.5 fold, $p<0.05$, 711 probes) (Figure 3.8).

3.3.2 Gene ontology classifications of the differentially expressed genes

A gene ontology classification was carried out for the gene lists that appeared in the 1.5 fold change between male and female bbb cells (source: GenUS Biosystems). The results are shown in Table 3.10. The p-value is a measure of likelihood that it is a coincidence that this many genes were in both the gene list and the category. Some of the sex-specific genes are highlighted in Table 3.10. As expected, many sex-specific category genes were enriched in this analysis.

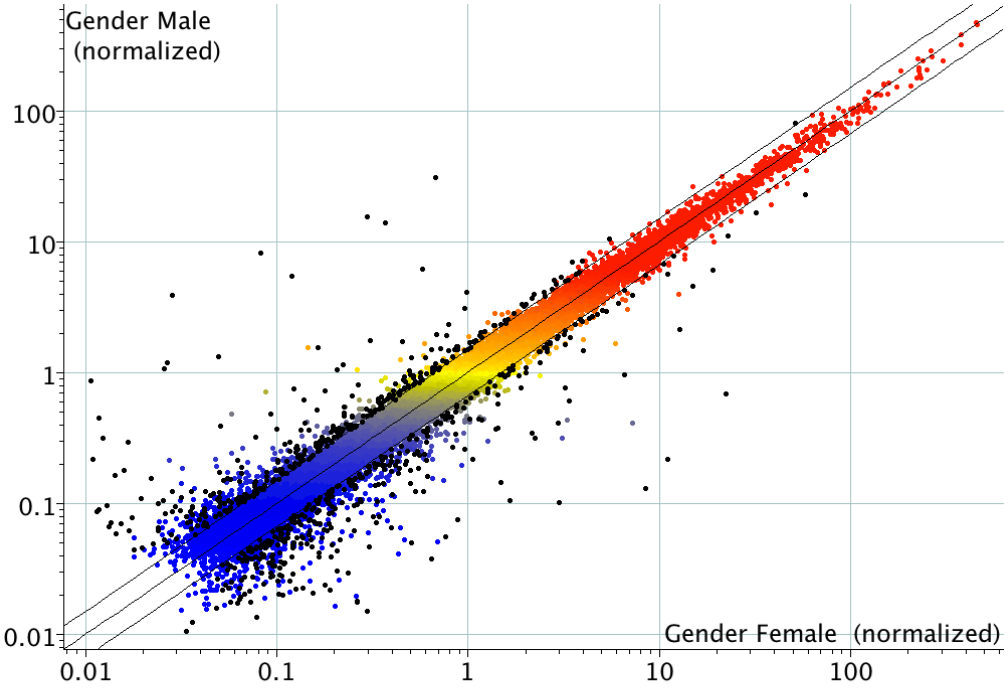

Figure 3.8: Probes present (above background) in all male or female samples are displayed as normalized to the 75th percentile intensity of each array (19,218 probes). Each spot is the mean of 3 samples from each condition. Black spots = differentially expressed genes (>1.5 fold, T-test p-value < 0.05, 711 probes). Red/orange=High expression, Yellow=Medium expression, Blue=Low expression (source: Genus Biosystems).

Table 3.10: Overlap of 711 genes differentially expressed (>1.5 fold, p<0.05) in BBB males vs. females with gene ontology classifications

Category=the name of the category within the ontology.			
Genes in Category=the total number of genes in the genome that have been assigned to the category			
Genes in List in Category=the total number of genes that are both in the selected gene list and in the category.			
P-value=a hypergeometric p-value without multiple testing corrections.			
This is a measure of the statistical significance of the overlap.			
i.e. the likelihood that it is a coincidence that this many genes were in both the gene list and the category.			
Biological Process			
Category	**Genes in Category**	**Genes in List in Category**	**p-Value**
GO:30237: female sex determination	28	11	2.53E-11
GO:19101: female somatic sex determination	21	9	6.76E-10
GO:7530: sex determination	62	13	2.71E-09
GO:7549: dosage compensation	48	11	1.71E-08
GO:19099: female germ-line sex determination	17	7	8.09E-08
GO:18992: germ-line sex determination	18	7	1.30E-07
GO:16457: dosage compensation complex assembly (sensu Insecta)	13	6	3.15E-07
GO:42714: dosage compensation complex assembly	13	6	3.15E-07
GO:18993: somatic sex determination	39	9	3.29E-07
GO:7548: sex differentiation	168	16	3.96E-06
GO:7541: sex determination, primary response to X:A ratio	20	6	6.16E-06
GO:9047: dosage compensation, by hyperactivation of X chromosome	22	6	1.14E-05
GO:35079: polytene chromosome puffing	7	4	1.19E-05
GO:35080: heat shock-mediated polytene chromosome puffing	7	4	1.19E-05
GO:7538: primary sex determination	34	7	1.56E-05
GO:3: reproduction	1571	64	3.11E-05
GO:7446: imaginal disc growth	82	10	3.17E-05
GO:9790: embryonic development	1099	49	3.35E-05
GO:50789: regulation of biological process	3422	117	3.64E-05
GO:48025: negative regulation of nuclear mRNA splicing, via spliceosome	18	5	5.77E-05
GO:7539: primary sex determination, soma	31	6	9.30E-05
GO:7422: peripheral nervous system development	422	24	1.26E-04
GO:51253: negative regulation of RNA metabolism	21	5	1.29E-04
GO:50686: negative regulation of mRNA processing	21	5	1.29E-04
GO:40029: regulation of gene expression, epigenetic	214	15	2.72E-04
GO:19102: male somatic sex determination	6	3	2.80E-04
GO:45496: male analia morphogenesis (sensu Endopterygota)	6	3	2.80E-04
GO:45497: female analia morphogenesis (sensu Endopterygota)	6	3	2.80E-04
GO:6563: L-serine metabolism	6	3	2.80E-04
GO:51305: chromosome movement towards spindle pole	6	3	2.80E-04
GO:31324: negative regulation of cellular metabolism	420	23	2.99E-04
GO:51243: negative regulation of cellular physiological process	707	33	3.15E-04
GO:7275: development	4315	136	3.37E-04
GO:19953: sexual reproduction	1413	55	3.94E-04
GO:42026: protein refolding	15	4	3.97E-04
GO:45934: negative regulation of nucleobase, nucleoside, nucleotide and r	348	20	4.00E-04
GO:48086: negative regulation of pigmentation	7	3	4.80E-04
GO:43118: negative regulation of physiological process	726	33	5.03E-04
GO:7296: vitellogenesis	16	4	5.19E-04
GO:46660: female sex differentiation	44	6	6.82E-04

Table 3.10 (Cont.)

Category	Genes in Category	Genes in List in Category	p-Value
GO:7617: mating behavior	186	13	7.05E-04
GO:6950: response to stress	1055	43	7.24E-04
GO:30238: male sex determination	8	3	7.55E-04
GO:281: cytokinesis after mitosis	8	3	7.55E-04
GO:40007: growth	598	28	8.57E-04
GO:17148: negative regulation of protein biosynthesis	63	7	8.71E-04
GO:48523: negative regulation of cellular process	906	38	8.86E-04
GO:31327: negative regulation of cellular biosynthesis	64	7	9.58E-04
GO:9892: negative regulation of metabolism	458	23	9.88E-04
GO:50896: response to stimulus	2125	74	9.92E-04
GO:7350: blastoderm segmentation	268	16	1.00E-03
GO:51084: posttranslational protein folding	19	4	1.04E-03
GO:10004: gastrulation (sensu Insecta)	65	7	1.05E-03
GO:9890: negative regulation of biosynthesis	65	7	1.05E-03
GO:9408: response to heat	128	10	1.24E-03
GO:7276: gametogenesis	1385	52	1.31E-03
GO:1703: gastrulation (sensu Protostomia)	68	7	1.37E-03
GO:9070: serine family amino acid biosynthesis	10	3	1.56E-03
GO:48519: negative regulation of biological process	1001	40	1.62E-03
GO:380: alternative nuclear mRNA splicing, via spliceosome	134	10	1.75E-03
GO:7079: mitotic chromosome movement towards spindle pole	3	2	1.78E-03
GO:19098: reproductive behavior	206	13	1.79E-03
GO:9880: embryonic pattern specification	341	18	2.01E-03
GO:398: nuclear mRNA splicing, via spliceosome	456	22	2.10E-03
GO:377: RNA splicing, via transesterification reactions with bulged adenosi	456	22	2.10E-03
GO:45471: response to ethanol	94	8	2.20E-03
GO:375: RNA splicing, via transesterification reactions	458	22	2.21E-03
GO:48071: sex-specific pigmentation	12	3	2.76E-03
GO:40008: regulation of growth	352	18	2.82E-03
GO:8595: determination of anterior/posterior axis, embryo	120	9	2.84E-03
GO:7351: regional subdivision	120	9	2.84E-03
GO:48024: regulation of nuclear mRNA splicing, via spliceosome	144	10	2.98E-03
GO:9266: response to temperature stimulus	144	10	2.98E-03
GO:42386: hemocyte differentiation (sensu Arthropoda)	78	7	3.04E-03
GO:8380: RNA splicing	471	22	3.11E-03
GO:7354: zygotic determination of anterior/posterior axis, embryo	59	6	3.20E-03
GO:16071: mRNA metabolism	596	26	3.44E-03
GO:35282: segmentation	359	18	3.48E-03
GO:7126: meiosis	303	16	3.48E-03
GO:6999: nuclear pore organization and biogenesis	4	2	3.51E-03
GO:45448: mitotic cell cycle, embryonic	80	7	3.51E-03
GO:7486: female genitalia morphogenesis (sensu Endopterygota)	13	3	3.52E-03
GO:30540: female genitalia morphogenesis	13	3	3.52E-03
GO:7487: analia morphogenesis (sensu Endopterygota)	13	3	3.52E-03
GO:35010: encapsulation of foreign target	13	3	3.52E-03
GO:9792: embryonic development (sensu Metazoa)	660	28	3.60E-03

Table 3.10 (Cont.)

Category	Genes in Category	Genes in List in Category	p-Value
GO:50684: regulation of mRNA processing	148	10	3.63E-03
GO:16199: axon midline choice point recognition	81	7	3.76E-03
GO:51327: M phase of meiotic cell cycle	306	16	3.83E-03
GO:45924: regulation of female receptivity	43	5	3.92E-03
GO:6417: regulation of protein biosynthesis	150	10	3.99E-03
GO:86: G2/M transition of mitotic cell cycle	27	4	4.04E-03
GO:16545: male courtship behavior (sensu Insecta), wing vibration	44	5	4.33E-03
GO:45433: male courtship behavior (sensu Insecta), song production	44	5	4.33E-03
GO:51321: meiotic cell cycle	311	16	4.48E-03
GO:48149: behavioral response to ethanol	84	7	4.60E-03
GO:7281: germ cell development	399	19	4.75E-03
GO:16542: male courtship behavior (sensu Insecta)	45	5	4.78E-03
GO:48065: male courtship behavior (sensu Insecta), wing extension	45	5	4.78E-03
GO:35186: syncytial blastoderm mitotic cell cycle	45	5	4.78E-03
GO:1666: response to hypoxia	45	5	4.78E-03
GO:51252: regulation of RNA metabolism	179	11	4.81E-03
GO:7154: cell communication	2733	87	4.94E-03
GO:31326: regulation of cellular biosynthesis	155	10	5.03E-03
GO:7485: male genitalia morphogenesis (sensu Endopterygota)	15	3	5.39E-03
GO:35263: genital disc sexually dimorphic development	15	3	5.39E-03
GO:35076: ecdysone receptor-mediated signaling pathway	15	3	5.39E-03
GO:45498: sex comb development	15	3	5.39E-03
GO:7155: cell adhesion	494	22	5.45E-03
GO:48042: regulation of oviposition, post-mating	5	2	5.75E-03
GO:1715: ectodermal cell fate specification	5	2	5.75E-03
GO:1712: ectodermal cell fate commitment	5	2	5.75E-03
GO:6564: L-serine biosynthesis	5	2	5.75E-03
GO:46785: microtubule polymerization	5	2	5.75E-03
GO:45839: negative regulation of mitosis	5	2	5.75E-03
GO:92: mitotic anaphase B	5	2	5.75E-03
GO:7610: behavior	1596	55	6.03E-03
GO:9889: regulation of biosynthesis	160	10	6.26E-03
GO:51244: regulation of cellular physiological process	2500	80	6.36E-03
GO:48589: developmental growth	268	14	6.68E-03
GO:578: embryonic axis specification	137	9	6.79E-03
GO:7362: terminal region determination	49	5	6.89E-03
GO:16198: axon choice point recognition	91	7	7.11E-03
GO:6397: mRNA processing	538	23	7.33E-03
GO:51640: organelle localization	165	10	7.73E-03
GO:30522: intracellular receptor-mediated signaling pathway	17	3	7.77E-03
GO:30518: steroid hormone receptor signaling pathway	17	3	7.77E-03
GO:7127: meiosis I	93	7	7.99E-03
GO:50000: chromosome localization	33	4	8.40E-03
GO:51303: establishment of chromosome localization	33	4	8.40E-03
GO:8608: attachment of spindle microtubules to kinetochore	6	2	8.48E-03
GO:8037: cell recognition	118	8	8.71E-03
GO:8038: neuron recognition	118	8	8.71E-03
GO:45944: positive regulation of transcription from RNA polymerase II pron	96	7	9.44E-03
GO:50794: regulation of cellular process	2913	90	9.56E-03
GO:7131: meiotic recombination	53	5	9.57E-03

Table 3.10 (Cont.)

Cellular Component			
Category	**Genes in Category**	**Genes in List in Category**	**p-Value**
GO:805: X chromosome	18	6	2.58E-06
GO:803: sex chromosome	20	6	5.18E-06
GO:46536: dosage compensation complex	21	6	7.11E-06
GO:16456: dosage compensation complex (sensu Insecta)	21	6	7.11E-06
GO:45495: pole plasm	31	6	7.89E-05
GO:19908: nuclear cyclin-dependent protein kinase holoenzyme complex	13	4	1.93E-04
GO:307: cyclin-dependent protein kinase holoenzyme complex	14	4	2.65E-04
GO:5956: protein kinase CK2 complex	15	4	3.55E-04
GO:5634: nucleus	3133	99	9.41E-04
GO:5875: microtubule associated complex	700	30	1.38E-03
GO:43186: P granule	22	4	1.67E-03
GO:17122: UDP-N-acetylglucosamine-peptide N-acetylglucosaminyltransfe	4	2	3.31E-03
GO:5623: cell	10006	257	4.09E-03
GO:15630: microtubule cytoskeleton	874	33	5.99E-03
GO:43229: intracellular organelle	5737	159	6.05E-03
GO:43226: organelle	5737	159	6.05E-03
GO:791: euchromatin	18	3	8.45E-03
GO:5622: intracellular	7566	201	8.63E-03
GO:43232: intracellular non-membrane-bound organelle	2013	64	8.72E-03
GO:43228: non-membrane-bound organelle	2013	64	8.72E-03
Molecular Function			
Category	**Genes in Category**	**Genes in List in Category**	**p-Value**
GO:19207: kinase regulator activity	97	13	4.64E-07
GO:19887: protein kinase regulator activity	93	12	1.94E-06
GO:48027: mRNA 5'-UTR binding	13	5	8.00E-06
GO:5213: structural constituent of chorion (sensu Insecta)	10	4	5.81E-05
GO:5158: insulin receptor binding	24	5	2.13E-04
GO:16538: cyclin-dependent protein kinase regulator activity	38	6	2.47E-04
GO:3729: mRNA binding	430	23	2.50E-04
GO:8187: poly-pyrimidine tract binding	28	5	4.56E-04
GO:3730: mRNA 3'-UTR binding	64	7	7.70E-04
GO:900: translation repressor activity, nucleic acid binding	33	5	9.98E-04
GO:3723: RNA binding	743	31	1.64E-03
GO:30371: translation repressor activity	37	5	1.70E-03
GO:8266: poly(U) binding	25	4	2.64E-03
GO:16262: protein N-acetylglucosaminyltransferase activity	6	2	7.88E-03
GO:5302: L-tyrosine transporter activity	6	2	7.88E-03
GO:8083: growth factor activity	74	6	8.13E-03
GO:3727: single-stranded RNA binding	53	5	8.21E-03

3.3.3 Comparison of differentially expressed bbb genes to Chang et al. (2011)

Further characterization of the 1.5 fold change gene list was carried out by comparing it with the male and female specific transcripts identified in whole heads (Chang et al., 2011).

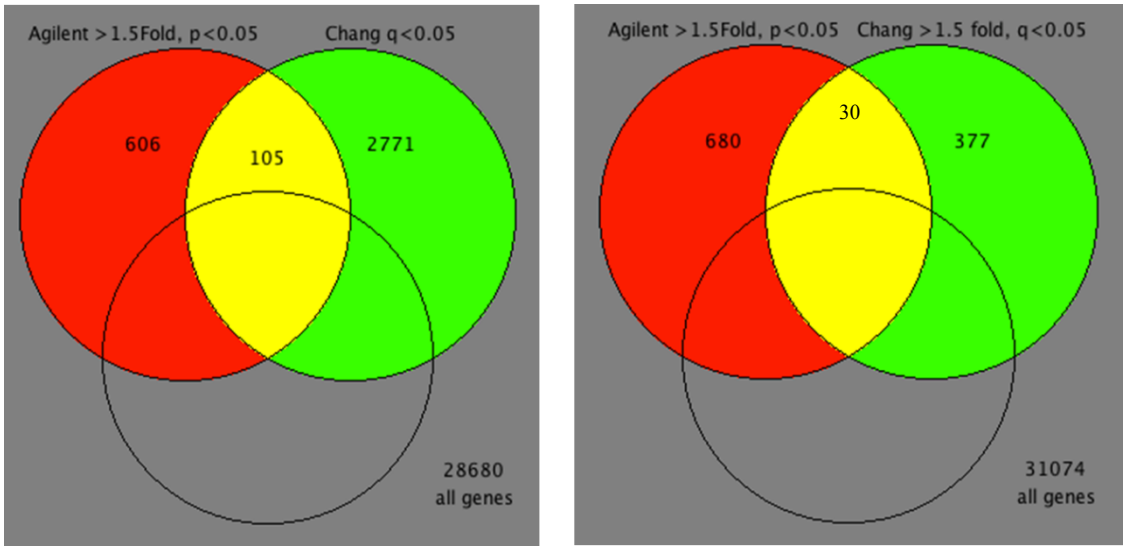

Figure 3.9: Venn diagram overlaps of Agilent results >1.5 fold, p<0.05 with the Chang et al. (2011), list of F vs. M q<0.05 (left) and F vs. M > 1.5 FC and q<0.05 (right). A total of 105 sex-specific transcripts in our Agilent results are included in the Chang q<0.05 list of sex-specific transcripts, and 30 overlap with transcripts that change more than 1.5X in their data (Data analyzed by GenUs Biosystems).

We found that a total of 105 genes from the set of differentially expressed genes showing at least a 1.5 fold change in male vs female lists from our microarray results overlapped with the genes reported in the Chang et al. (2011) study. And among them 30 genes were expressed >1.5 fold in their male vs. females comparison. Of these, 19 genes

showed similar directional change (i.e. change in expression in the same sex) as in Chang et al. (2011), whereas only 4 genes showed the opposite directional change (i.e. change in expression in the opposite sex). These genes are shown in Table 3.11.

In summary, the microarray analysis of isolated male and female bbb cells demonstrated that there are a number of sex-specific transcripts in the bbb. This confirms our findings from the behavioral feminization experiments. These identified sex-specific transcripts are candidate genes for a role in sex-specific behavior.

Table 3.11: 30 Agilent probes >1.5 fold, p<0.05 and >1.5 fold, q<0.05 in Chang et al. (2011). 23 probes (19 genes) go in the same direction. 7 probes (4 genes) go in opposite directions.

Agilent P-value	Expression profile (males, females)	GeneName
4.03E-03		Yolk protein 1
6.60E-03		Yolk protein 3
6.53E-03		Yolk protein 2
3.80E-03		Insulin-like peptide 3
1.40E-02		Insulin-like peptide 3
4.25E-02		CG4259 gene product from transcript CG4259-RA
7.59E-05		CG7607 gene product from transcript CG7607-RA
2.30E-04		CG42259 gene product from transcript CG42259-RA
1.35E-02		Flavin-containing monooxygenase 2
9.95E-03		fruitless
3.29E-02		diminutive
6.70E-03		CG3939 gene product from transcript CG3939-RA
2.07E-03		male-specific lethal 2
3.24E-03		CG2889 gene product from transcript CG2889-RA
8.76E-05		CG2691 gene product from transcript CG2691-RA
1.59E-03		CG1753 gene product from transcript CG1753-RA
7.62E-03		CG3132 gene product from transcript CG3132-RA
2.07E-06		trynity
1.08E-07		RNA on the X 1
3.94E-03		RNA on the X 1
4.92E-08		RNA on the X 1
1.64E-06		RNA on the X 2
1.06E-05		RNA on the X 1
4.75E-03		Heat shock protein 27
8.08E-03		Heat shock protein 27
6.35E-03		Heat shock protein 27
5.17E-03		Heat shock protein 27
1.95E-02		CG14221 gene product from transcript CG14221-RB
1.96E-02		Troponin C at 41C
1.81E-02		CG12643 gene product from transcript CG12643-RA

3.4 Candidate gene *Hr46*

Given our question of how soluble circulating molecules might signal through the bbb to influence brain courtship circuits, we were particularly interested in potential signaling molecules. One gene that caught my attention was ***Hormone-receptor-like in 46*** **(*Hr46***, also called *DHR3*).

Hr46 was one of the genes that were expressed significantly higher in male bbb than the females (>2 fold, T-test p-value < 0.05). Its RNA is male-preferentially expressed in bbb cells. *Hr46* has characteristics of steroid nuclear hormone receptors and plays an important role in development. The protein is expressed in response to the steroid hormone ecdysone and acts as transcriptional regulator of target genes (Carney et al., 1997; Koelle et al., 1992; Lam et al., 1999). One of them is *ftz-f1*. Significantly among other functions, Ftz-f1 has recently been found to bind to Met, a transcriptional regulator that binds Juvenile Hormone (JH) and is thought to mediate JH regulated gene expression (Bernardo and Dubrovsky, 2012; Dubrovsky et al., 2011). This places *Hr46* as a potential player in the integration of signals from both ecdysone and JH, the two main hormones in *Drosophila*. Much less is known about the functions of these hormones in adults beyond their roles in fertility, although a role of ecdysone in learning and memory has been shown (Ishimoto et al., 2009). These findings point to a role of hormonal signaling in adult bbb. Therefore, I hypothesize that *Hr46* signaling may contribute to the sex-specific function including courtship behavior of these cells.

A role for *Hr46* in the adult male courtship behavior was tested by bbb-specific expression of *Hr46* RNAi using the conditional $Gal80^{ts}$/Gal4/UAS system as described in

section 2.10 of Materials and Methods. I used two RNAi lines (*UAS-Hr46-RNAi 27254* and *UAS-Hr46-RNAi 27253*.

The genotypes used for the courtship behavior assay using the first RNAi line were two controls: *X/Y; +/+; +/UAS-Hr46-RNAi 27253 and X/Y; +/Gal80^{ts10}; +/SPG-Gal4* and the experimental genotype, *X/Y; +/Gal80^{ts10}; SPG-Gal4/UAS-Hr46-RNAi 27253*. The behavioral experiment using the second RNAi lines involved the control genotypes: *X/Y; +/+; +/UAS-Hr46-RNAi 27254 and X/Y; +/Gal80^{ts10}; +/SPG-Gal4* and the experimental genotype *X/Y; +/Gal80^{ts10}; SPG-Gal4/UAS-Hr46-RNAi 27254*. The crosses were raised at 18°C and individual eclosing males were raised in isolation for 7 days at 18°C.

For induction, all the control and the experimental genotypes were placed at 32°C for 2 days and on the second day the induced as well as the uninduced control flies from the 18°C incubator were kept at RT for 3 hours before testing. The use of the temperature sensitive Gal80^{ts} system ensured that the gene *Hr46* is only knocked down in adult bbb and not disrupted during development. This was especially important given the role of *Hr46* in development. Interestingly, post-developmental reduction of *Hr46* expression in the SPG layer resulted in significant reduction of normal courtship behavior (Figure 3.10 A and B). The reduced courtship is statistically significant (ANOVA, $p<0.0001$) in both the RNAi lines tested. This demonstrates that normal physiological level of *Hr46* in the bbb cells is required for normal courtship behavior.

Taken together, these results suggest that *Hr46* signaling in the blood brain barrier plays an important physiological role in male courting behavior in *Drosophila*. It also

demonstrates that our microarray results are an excellent tool for identifying sex-specific transcripts that are important for courtship.

3.5 Summary

Microarray analysis of transcripts from bbb cells of male and female *Drosophila* shows that many sex-specific transcripts are present in the bbb. Presence of many male-specific transcripts from dosage compensation genes such as *roX1, roX2* only in the male samples and the presence of the female forms of genes such as *chorionic protein 16, yolkless, ovarian tumor* only in the female samples validates the sex-specificity of the result of our screen.

The gene ontology classification of the sex-specific genes, which were differentially expressed between males and females (>1.5 fold, $p<0.05$) showed that many genes belonging to sex-specific processes and cellular signaling are present among the sex-specific transcripts identified in the bbb. One of the sex-specific genes, which was present in the male bbb at >2 fold higher levels than in females, was the candidate gene *hormone-receptor-like in 46* (*Hr46)*. A role of this gene in the bbb for adult male courtship behavior was tested by using the conditional Gal4/Gal80^{ts}/UAS system. The conditional RNAi mutant data shows that this gene is required in the bbb for normal male courtship behavior.

(A)

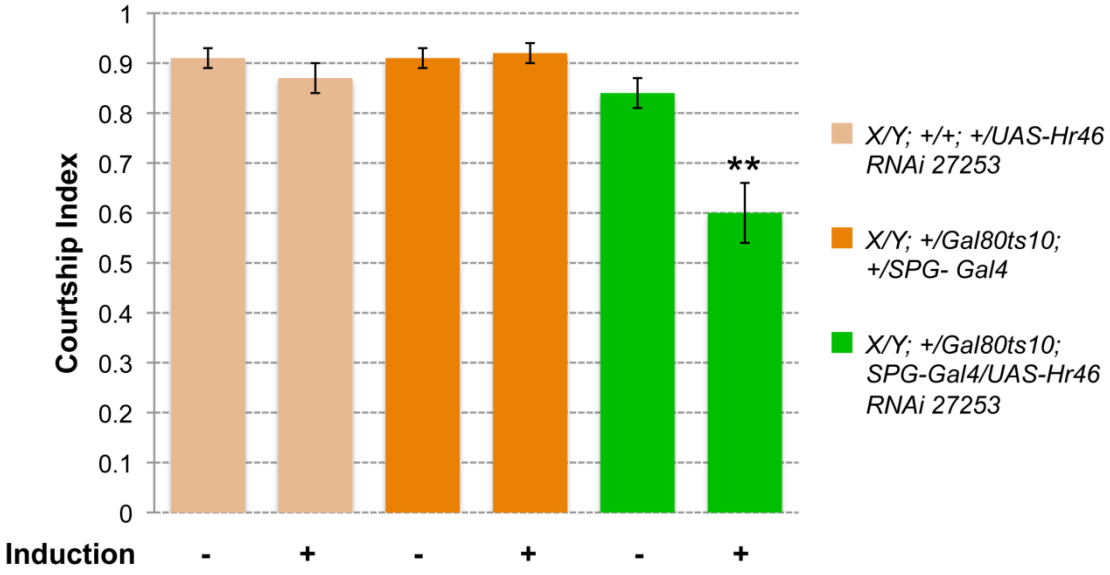
Courtship Index
1
0.9
0.8
0.7
0.6
0.5
0.4
0.3
0.2
0.1
0
**
Induction
- + - + - +
X/Y; +/+; +/UAS-Hr46 RNAi 27253
X/Y; +/Gal80ts10; +/SPG- Gal4
X/Y; +/Gal80ts10; SPG-Gal4/UAS-Hr46 RNAi 27253

(B)

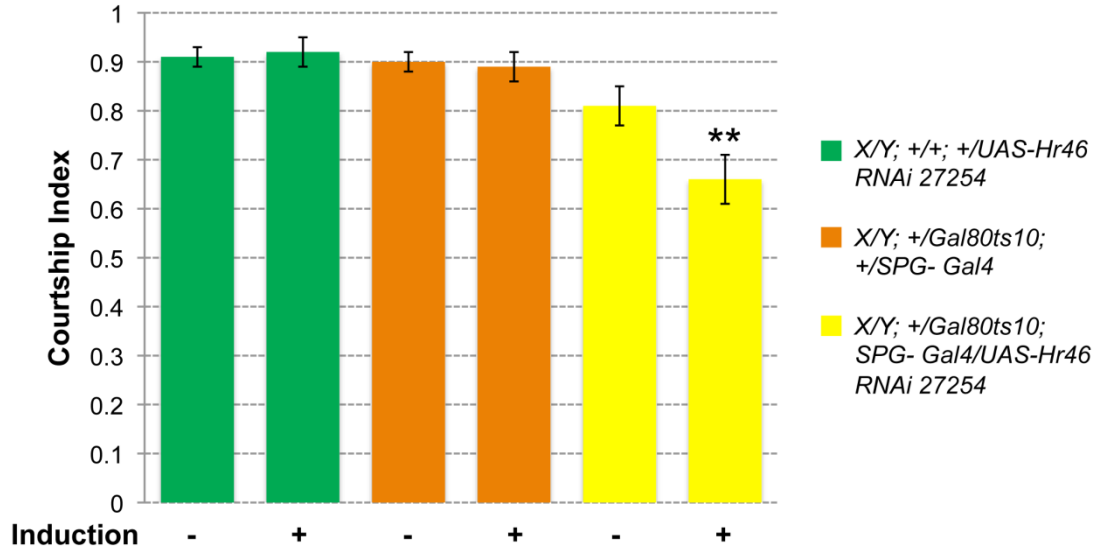
Courtship Index
1
0.9
0.8
0.7
0.6
0.5
0.4
0.3
0.2
0.1
0
**
Induction
- + - + - +
X/Y; +/+; +/UAS-Hr46 RNAi 27254
X/Y; +/Gal80ts10; +/SPG- Gal4
X/Y; +/Gal80ts10; SPG- Gal4/UAS-Hr46 RNAi 27254

Figure 3.10: Conditional knockdown of *Hr46* by RNAi in the adult bbb reduces male courtship behavior of *Drosophila melanogaster*. The Gal^{80ts}/Gal4/UAS system was used in order to control the temporal and spatial expression of *UAS-Hr46-RNAi* in the bbb of the tested males. Two RNAi lines targeting *Hr46* were used to knockdown expression of the gene: *UAS-Hr46-RNAi 27253* and the *UAS-Hr46-RNAi 27254*. **(A)** The genotypes used in the first RNAi line were two controls: *X/Y; +/+; +/UAS-Hr46-RNAi 27253 and X/Y; +/*$Gal80^{ts10}$*; +/SPG-Gal4* and the experimental genotype, *X/Y; +/*$Gal80^{ts10}$*; SPG-Gal4/UAS-Hr46-RNAi 27253*. Both the genetic controls and the mutant were reared and kept at 18°C. At this temperature the expression of the *UAS-Hr46-RNAi* is suppressed by the presence of $Gal80^{ts}$, which is active at this temperature resulting in normal behavior of the courting male. However, when the flies are induced at 32°C, the $Gal80^{ts}$ gets inactivated leaving Gal4 free for binding to the Upstream Activating Sequence (UAS sequence) and leading to the expression of *Hr46-RNAi.* This resulted in the significant reduction of the courtship index of experimental males compared to the uninduced experimental genotype and the two uninduced and induced control genotypes (ANOVA with post-hoc Bonferroni multiple comparison; **, $p<0.0001$, n=25). **(B)** The behavioral experiment using the second RNAi lines involved the control genotypes: *X/Y; +/+; +/UAS-Hr46-RNAi 27254 and X/Y; +/*$Gal80^{ts10}$*; +/SPG-Gal4* and the experimental genotype *X/Y; +/*$Gal80^{ts10}$*; SPG-Gal4/UAS-Hr46-RNAi 27254*. As described for the first RNAi line, the second RNAi line also showed significant reduction in the courtship behavior of the induced mutant male towards a virgin female compared to the uninduced experimental as well as compared to the two controls under induced and uninduced condition (Two way ANOVA with post-hoc Bonferroni multiple comparisons test; **, $p<0.0001$, n=23). Error bars denote standard error of the means. **(+)** = Induction of male flies for 48 hr in 32°C incubator before the assay. **(-)** = Male flies were kept constantly at 18°C.

Chapter IV

microRNA profiling of the bbb cells of *Drosophila*

4.1 Illumina sequencing to characterize microRNAs in male and female bbb cells

MicroRNAs (miRNA) are one of the major classes of small non-coding RNAs that are involved in post-transcriptional regulation of gene expression in multi-cellular organisms largely by interacting with the 3'UTR of their targets affecting both the stability and translation of mRNAs (Hutvagner and Zamore, 2002). MicroRNAs have the potential to regulate sets of cell- or function-specific proteins. Therefore, I hypothesized that microRNAs play an important role in the bbb of male *Drosophila* for their courtship behavior.

In order to test this hypothesis, individual bbb cells from 50 male and 50 female brains were isolated as described in Materials and Methods section 2.3. Small RNAs was isolated from these bbb cells (see section 2.6 of Materials and Methods) and small RNA libraries for Illumina platform sequencing were prepared as described in Materials and Method section 2.6.2. Small RNA library constructs were gel purified as described in section 2.6.5 of Materials and Methods. The precipitated smRNA library was analyzed and quantified by Picogreen assay as describe in section 2.6.7 of Materials and Methods. Finally, the samples were submitted to the UH sequencing center with 3 biological replicates for male and female samples.

The protocols used for microRNA sequencing were adopted from the method developed by Benham A, (2011). However, the protocols were optimized for extremely low starting RNA material because we had a very small amount of RNA (see section 2.6.1).

4.2 Small RNA mapping

4.2.1 Small RNA sequencing and mapping

Small RNA sequencing was performed by the UH sequencing core using the Illumina Genome Analyzer 1 (GA-1), according to the manufacturer's protocol for small RNA sequencing. For analysis of the resulting data, those reads containing insert sequence along with the adapter sequence (the read length being 36nt) were selected and used for miRNA mapping. A non-redundant Fasta file was created for the full set of unique sequences with copy number information for each unique tag. The unique sequence was filtered for potential contamination by *E. coli* sequence using BLAST against the *E.coli* sequence database. Each sequence read which did not pass the Illumina and no-calls filter was removed. Reads with copy number less than 4, insert length less than 10nt or more than 10 consecutive, repetitive nucleotides were removed. Reads with exact match or loose match were observed. Up to three mismatches were allowed for loose matches in a single alignment. The remaining validated reads were aligned using the miRNA reference database miRBase 17 (www.mirbase.org). Sequences aligning with the mature miRNA sequence with 3 base overhangs on the 5' end and a 6 base overhang on the 3' end were considered. Read counts were then normalized to the total number of miRNAs identified to give the relative abundance of each miRNA in the dataset. This was labeled as "microRNA expression profile" of the sample.

The sequencing results were analyzed by Dr. Weimen Xiao in Dr. Preethi Gunaratne's lab. A total of 413 miRs were identified in the raw data of which only 173 miRs were found in miRBase 17.0. The rest are currently considered putative novel miRNAs. The cutoff for identified miRs was: The read of one miR > 1 in at least one of

the six samples. The other 240 miRs in the database showed 0 read in all the six samples, indicating that they are not expressed in the bbb.

Within the three biological replicates for the male and female samples, the expression of each microRNA was normalized to the expression of *dme-mir-10-5p*. This mir was randomly chosen as a "midlevel" expression mir in the sample. Statistical analysis was carried out to see if any of these microRNAs is sex-specifically present between male and female bbb cells. Student t-test was used to compare males with females. None of the miRNAs was found to be sex-specific in the bbb. This indicates that if there are differences in the microRNA expression between males and females at all, it is likely to be very small. Figure 4.1 shows a heat map of the top 19 most highly abundant microRNAs and Table 4.1 shows their abundance.

Therefore, from this experiment, we conclude that there are many miRNAs that are expressed in the blood brain barrier of male and female *Drosophila*. Some of the microRNAs are present in high abundance suggesting that they are important in the tight regulation of their target proteins in the bbb. For the work presented in this chapter we focused on *dme-mir-184* (referred to as *miR-184* hereafter), which is the most abundant microRNA in the bbb of both male and female flies.

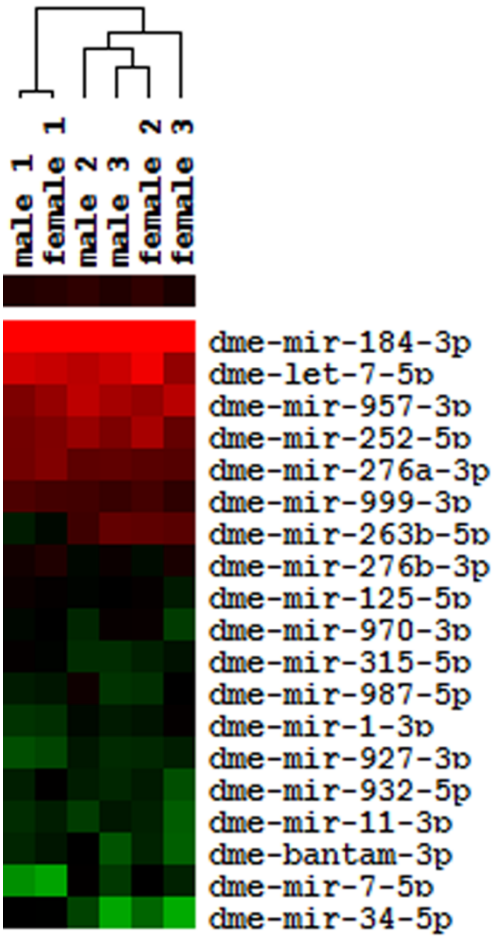

Figure 4.1: Illumina sequencing results revealed more than 173 mature miRNAs and no significant sex-specific difference was found between male and female bbb cells. Shown are the top 19 most abundant microRNAs from male and female bbb cells.

Table 4.1: The abundance of the top 19 miRNAs as relative copy number

Mature miRNA	Average relative # of copies in males in three biological replicates	Average relative # of copies in females in three biological replicates
dme-mir-184-3p	2595.99204	3153.31356
dme-let-7-5p	130.939113	161.259032
dme-mir-957-3p	67.3469944	71.5744169
dme-mir-252-5p	44.4316402	56.1344716
dme-mir-276a-3p	31.4109534	36.563184
dme-mir-999-3p	18.3339099	18.4254396
dme-mir-263b-5p	13.0967399	16.9031734
dme-mir-276b-3p	7.74620617	9.27560376
dme-mir-125-5p	7.14824993	7.17038391
dme-mir-970-3p	5.71717805	6.69441522
dme-mir-315-5p	5.26553248	5.71344911
dme-mir-987-5p	5.09174611	4.91781244
dme-mir-932-5p	4.13695905	5.54164484
dme-mir-34-5p	4.12669807	4.06156311
dme-mir-1-3p	4.10292471	4.80687383
dme-bantam-3p	4.09167394	4.235416
dme-mir-11-3p	3.554474	4.02181808
dme-mir-927-3p	3.08704047	3.3607557
dme-mir-7-5p	2.84463805	3.38474196

4.3 Role of *miR-184* in courtship behavior of *Drosophila melanogaster*

Among the top 19 most abundant miRNAs, *miR-184-3p* was by far the most abundant microRNA (present in high copy number ~ 3 million copies) in the bbb of both males and females (Figure 4.1). The role of *miR-184* during development has been studied and it has been found that this miRNA is important for microRNA-mediated regulation in major developmental transitions of the female germ line (Iovino et al., 2009, Li et al., 2011). It is unknown what its role might be in other tissues. The presence of such a significant amount of this miRNA in the adult bbb indicates the importance of its

role beyond development and suggests tight regulation of its target protein levels in the adult bbb. Table 4.2 shows the predicted targets of *miR-184* (http://www.targetscanfly.org). Intriguingly, its predicted targets include *sinu* and *Neurexin*. These proteins have already been shown to be important for the development of the bbb and they are important components of the adult bbb (Wu et al., 2004; Baumgartner et al., 1996; Stork et al., 2008). Furthermore, it has already been shown *in vitro* that *miR-184* regulates the protein levels of several predicted targets, including *sinu* and *Neurexin* (Iovino et al., 2009). Importantly, many of the potential *miR-184* targets were found to be present in the bbb in our microarray characterization of bbb transcripts. The high level of this miRNA in the bbb indicates that these proteins have a function beyond development.

Table 4.2: Predicted targets of *miR-184*

Gene	Symbol	Gene Identifier
CG10217	CG10217	FBgn0039113
CG10620	Tsf2	FBgn0036299
CG10624	sinu	FBgn0010894
CG10710	CG10710	FBgn0036377
CG1105	CG1105	FBgn0037465
CG11059	Cals	FBgn0039928
CG11516	Ptp99A	FBgn0004369
CG12766	CG12766	FBgn0035476
CG14059	Ilp8	FBgn0036690
CG14505	CG14505	FBgn0034327
CG15186	CG15186	FBgn0037448
CG17816	CG17816	FBgn0037525
CG2341	Ccp84Ad	FBgn0004780
CG2727	emp	FBgn0010435
CG31195	CG31195	FBgn0051195
CG33472	qvr	FBgn0260499
CG33556	form3	FBgn0053556
CG34361	Dgk	FBgn0085390
CG3903	Gli	FBgn0001987
CG42250	lqfR	FBgn0261279
CG42277	rn	FBgn0259172
CG42342	CG42342	FBgn0259244
CG4313	CG4313	FBgn0025632
CG43367	CG43367	FBgn0263110
CG43689	CG43689	FBgn0263772
CG43738	cpo	FBgn0263995
CG43780	CG43780	FBgn0264302
CG43781	CG43781	FBgn0264303
CG43921	CG43921	FBgn0264542
CG4467	CG4467	FBgn0039064
CG5753	stau	FBgn0003520
CG6114	sff	FBgn0036544
CG6312	Rfx	FBgn0020379
CG6446	Sema-1b	FBgn0016059
CG6583	CG6583	FBgn0032420
CG6827	Nrx-IV	FBgn0013997
CG7586	Mcr	FBgn0264800
CG7650	CG7650	FBgn0036519
CG7713	CG7713	FBgn0038545
CG7921	Mgat2	FBgn0039738
CG8121	CG8121	FBgn0037680
CG9796	CG9796	FBgn0038149

Therefore, I hypothesize that *miR-184* and its bbb specific target proteins have roles in the adult bbb. In this chapter, I present work to examine whether *miR-184* and some of its target genes contribute to the role of the bbb in the regulation of courtship behavior of *Drosophila*.

I examined the role of *miR-184* in courtship using two different approaches;

1) By overexpressing it in the bbb. This is expected to lower the amount of its target proteins.
2) Using a *miR-184* "sponge" transcript that is expected to lead to mis-regulation of specific targets.

4.3.1 Generation of *UAS- miR-184* transgenic flies

I generated transgenic flies containing the *UAS-miR-184* transgene to alter the level of *miR-184* by taking advantage of the Gal4-UAS binary system, a very common tool used in fly genetics (Brand and Perrimon, 1993). Moreover, the temporal restricted expression of *miR-184* was achieved using the Gal4/ $Gal80^{ts}$/ UAS (TARGET) system to observe the effect at the post-developmental/physiological level rather than throughout development (McGuire et al., 2003; Roman, 2004).

A 685 bp genomic fragment containing *miR-184* was amplified and sub-cloned into the multicloning site of the pSC-B vector (Stratagene) and subsequently cloned in to the pUAST transformation vector (Figure 4.2). The sequence was verified by appropriate restriction digestions as well as by sequencing. Finally the construct was injected into embryos of w^{1118} flies by Rainbow Transgenic Flies Inc., CA to generate the *UAS-miR-184* transgenic flies. The transgenic lines were mapped for the chromosomal location of

the transgene and balanced and homozygosed. A total of 34 transgenic lines were established as shown in Table 4.3.

Table 4.3: Mapping of the chromosomal location of the transgene in *UAS-miR-184* transgenic lines

Chromosomal Location	**Transgenic Lines (*UAS-miR-184*)**
X Chromosome	12.1
2nd Chromosome	1.2, 2.1, 2.2, 3.1,4.1, 6.1, 9.1, 13.1, 15.1, 16.1, 18.1, 19.1, 20.1, 21.1, 23.1, 25.2, 28.1, 29.2
3rd Chromosomes	1.3, 5.1, 7.1, 10.1, 11.1, 12.1, 14.1, 17.1, 22.1, 24.1, 26.1, 27.1, 27.2, 29.1, 30.1

4.3.2 Verification of transgene expression in the transgenic flies

Confirmation of transgene expression in the *UAS-miR 184* transgenic lines was done by RT-PCR using the primers that were used to clone the *miR-184* fragment. For this purpose, the transgenic fly lines were crossed to flies expressing the heat inducible driver, hsp70-Gal4. The progenies and the wild-type control CS flies were subjected to heat shock. The RNA was then extracted and cDNA was synthesized as described in section 2.8.4.1 of Materials and Methods. PCR reactions were performed at a low cycle number (section 2.8.4.2) and the product was run on a 1.2% agarose gel and visualized under a UV illuminator (Figure 4.3, Gel I and Gel II).

(A)

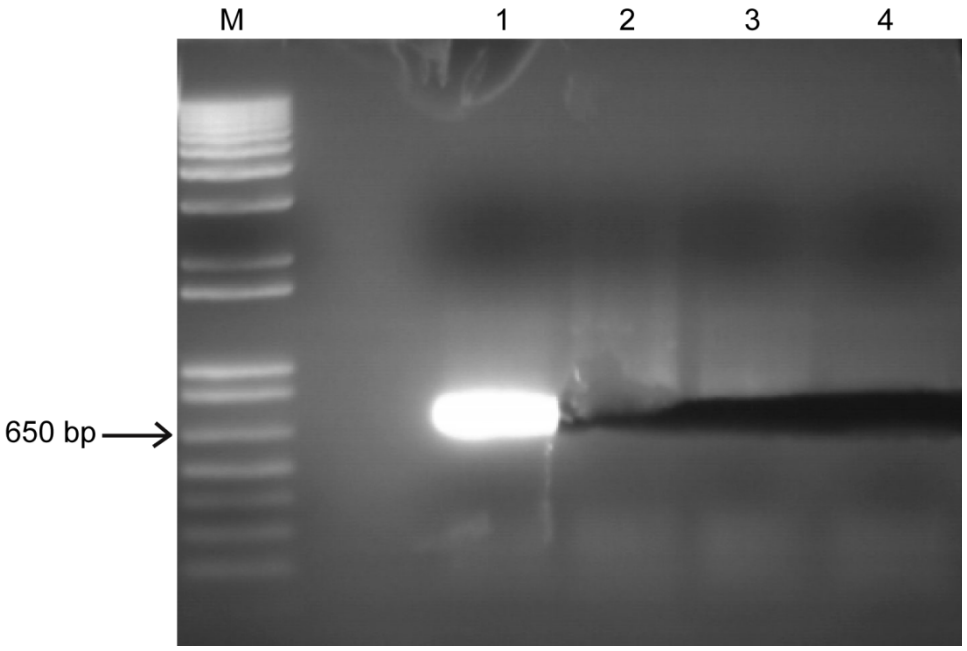

(B)

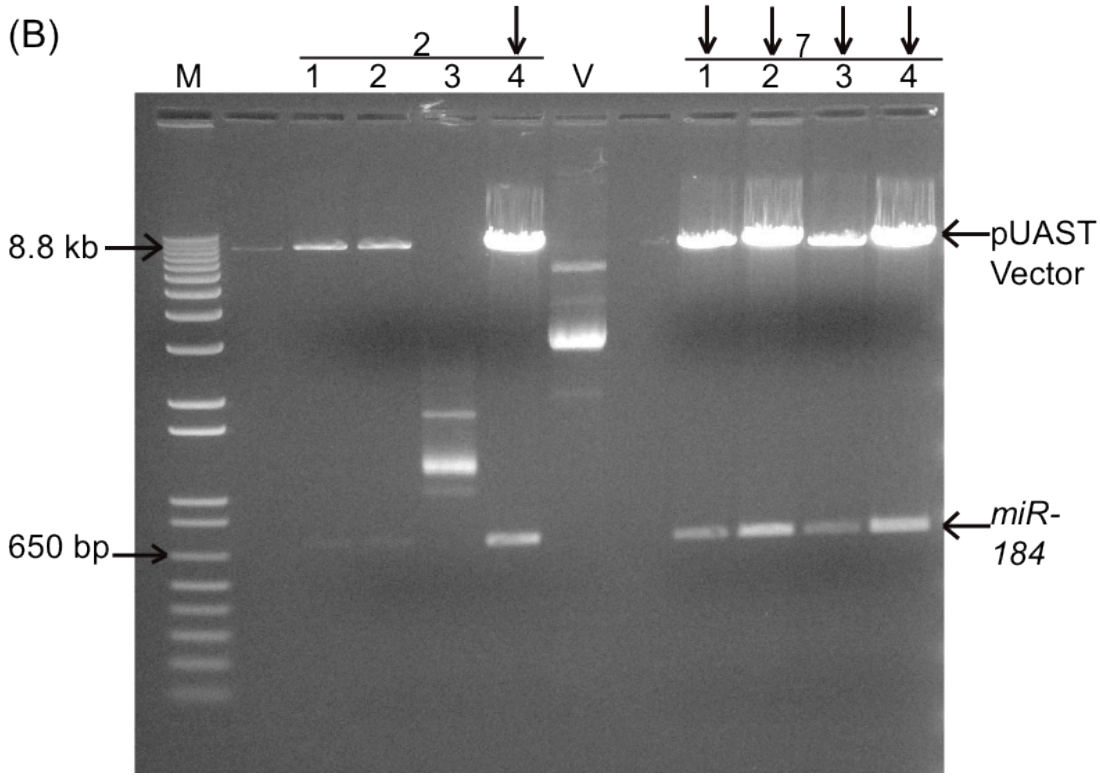

Figure 4.2: Cloning of the *mir-184* fragment into the pUAST vector. (A) Amplification of the *miR-184* genomic region using high fidelity Phusion DNA polymerase. M= Marker (1 Kb Plus ladder); 1-4 (PCR reaction samples), samples 2-4 were cut and gel purified for further experiments. Arrow indicates band of 650 bp lengths. (B) The cloning of the 685 bp *miR-184* fragment into the 8.8 KB pUAST vector. The cloning was verified by subjecting the construct to a restriction test digest, using Not1 and Xba1. Several mini-preps were prepared 2(1-4) and 7(1-4) and the colonies subjected to a restriction test digest. This resulted in the release of the 685 bp insert from the pUAST vector. Samples 2 (4), 7(1), 7(2), 7 (3) and 7(4) have inserts of the expected size. V=vector only. Sample 7 (2) was used for sequencing and subsequent generation of transgenic flies.

Most transgenic lines showed robust expression of the transgene *UAS-miR-184* as a 685 bp fragment. A second smaller fragment seen is likely due to a reduced size PCR product caused by secondary structure. Minus RT samples did not show any amplification showing that there was no genomic contamination in the RNA samples. No product was visible in CS wild-type flies although these flies do have the *miR-184* gene. This indicates that the endogenous level in whole wild type flies was low in comparison to the hsp70-Gal4 directed overexpression in the transgenics.

4.3.3 Overexpression of *miR-184* in bbb affects courtship

The ultimate goal of the transgenic lines generated was to use them to alter the expression level of miR-184 in the bbb and see the effect of this manipulation on behavior. I chose line 27.2 (referred as *UAS-miR-184 27.2* hereafter) to carry out the behavioral tests.

The courtship assay was performed as described in section 2.9.1 of Materials and Methods. *miR-184* overexpression in the bbb was achieved by crossing *UAS-miR-184* flies to flies containing the bbb-specific SPG-Gal4 in addition to a copy of a temperature-sensitive Gal80 ($Gal80^{ts}$). Experimental flies contained two copies of SPG-Gal4 (one on the second (II), and one on the third (III) chromosome, and two $Gal80^{ts}$ transgenes ($Gal80^{ts10}$ and $Gal80^{ts20}$). The genotypes tested in the courtship assay are shown in Table 4.4.

Gel I

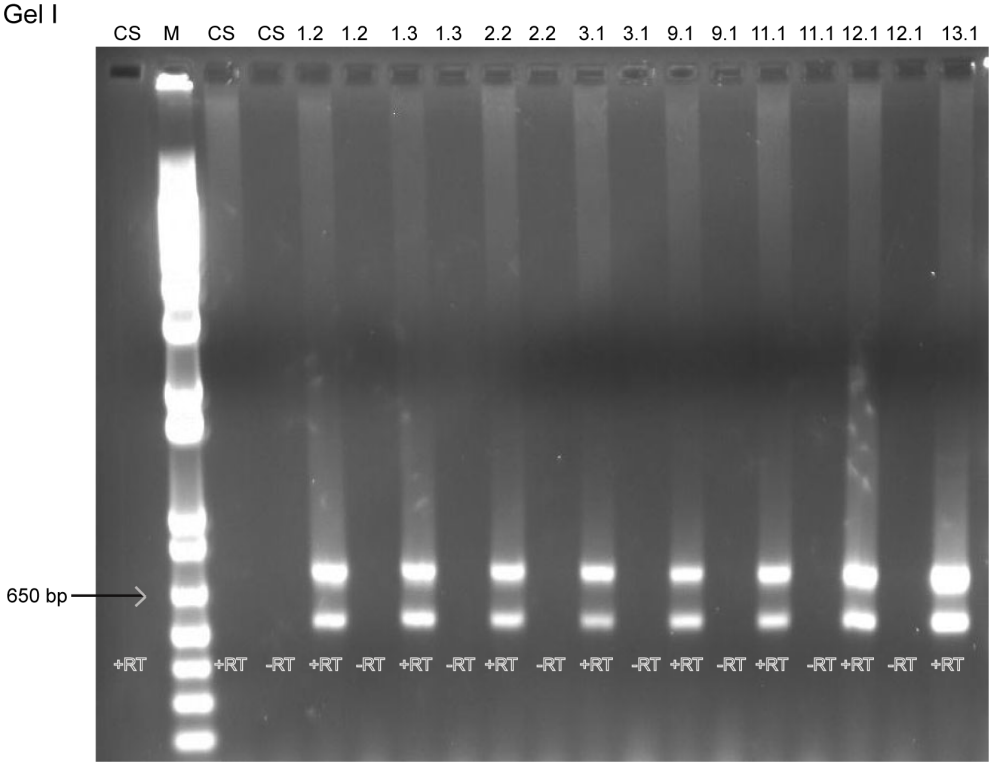
CS M CS CS 1.2 1.2 1.3 1.3 2.2 2.2 3.1 3.1 9.1 9.1 11.1 11.1 12.1 12.1 13.1
650 bp
+RT +RT -RT +RT -RT +RT -RT +RT -RT +RT -RT +RT -RT +RT -RT +RT -RT +RT -RT +RT

Gel II

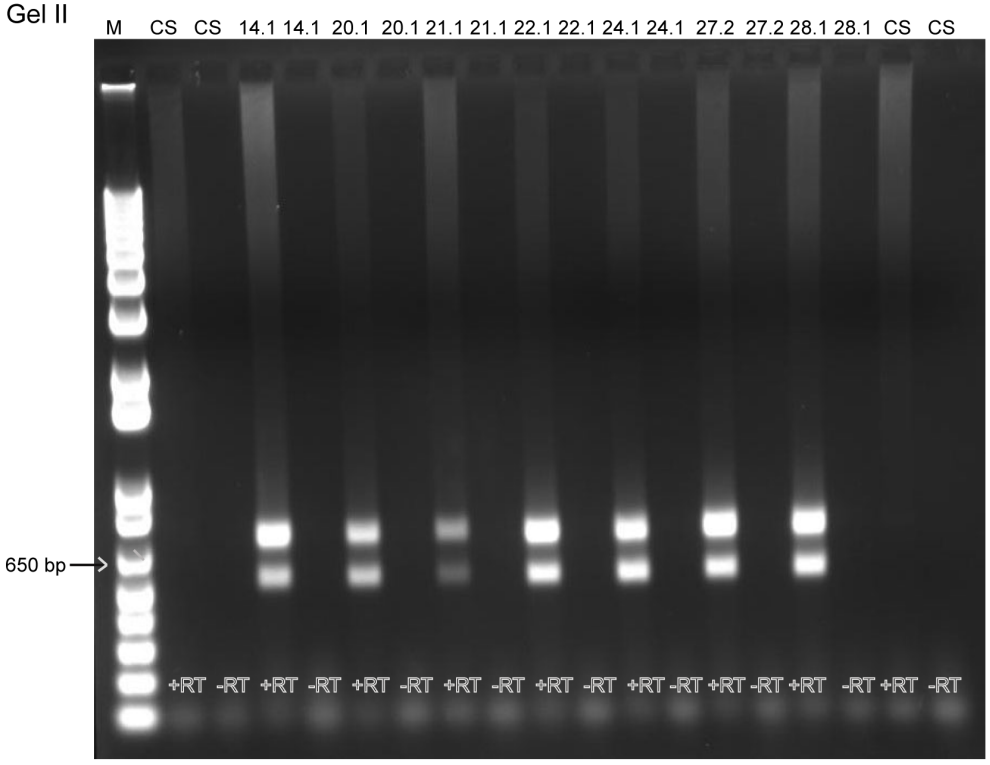
M CS CS 14.1 14.1 20.1 20.1 21.1 21.1 22.1 22.1 24.1 24.1 27.2 27.2 28.1 28.1 CS CS
650 bp
+RT -RT +RT -RT +RT -RT +RT -RT +RT -RT +RT -RT +RT -RT +RT -RT +RT -RT +RT -RT

Figure 4.3: Verification of transgene *UAS-miR-184* expression in *hsp70-Gal4/UAS miR-184* transgenic lines by RT PCR. M=1 Kb plus ladder. The progenies of the cross involving several of the transgenic (*UAS-miR-184*) lines with the *hsp70-Gal4* line were heat shocked at 37°C for 2 hours followed by RNA extraction and cDNA synthesis. Low cycle PCR (25 cycles) amplification of the cDNA using *miR-184* forward and reverse primers shows the expression of the UAS-transgene in most lines (Gel I and Gel II). Absence of expression in the CS flies and the –RT sample confirms the absence of genomic DNA contamination in the fly lines tested.

Table 4.4: The following genotypes were created and used for behavioral assays

Flies	**Genotypes**
Control 1	*X/Y; +/Gal80^{ts10}; +/UAS-miR-184 (27.2)*
Control 2	*X/Y; +/SPG-Gal4-II, Gal80^{ts20}; +/SPG-Gal4-III*
Experimental	*X/Y; SPG-Gal4-II, Gal80^{ts20}/Gal80^{ts10}; SPG-Gal4-III/UAS-miR-184 (27.2)*

Following induction, the experimental flies that overexpressed *miR-184* showed statistically significant reduction in the courtship index compared to the uninduced experimental and the controls (ANOVA, $p<0.0001$). The results are shown in Figure 4.4. Table 4.4 shows the genotypes that were tested in the courtship assay.

The courtship indices of induced and uninduced controls were not significantly different suggesting that the effect observed in the induced experimental is not some non-specific effect, rather it is due to the physiological effect of *miR-184* being overexpressed and that the effect is real. When tested for locomotor activity, the experimental and control flies did not show any significant difference in their locomotion index suggesting that the behavioral phenotype observed in the mutant flies is not due to locomotion defects (Figure 4.4 B).

(A)

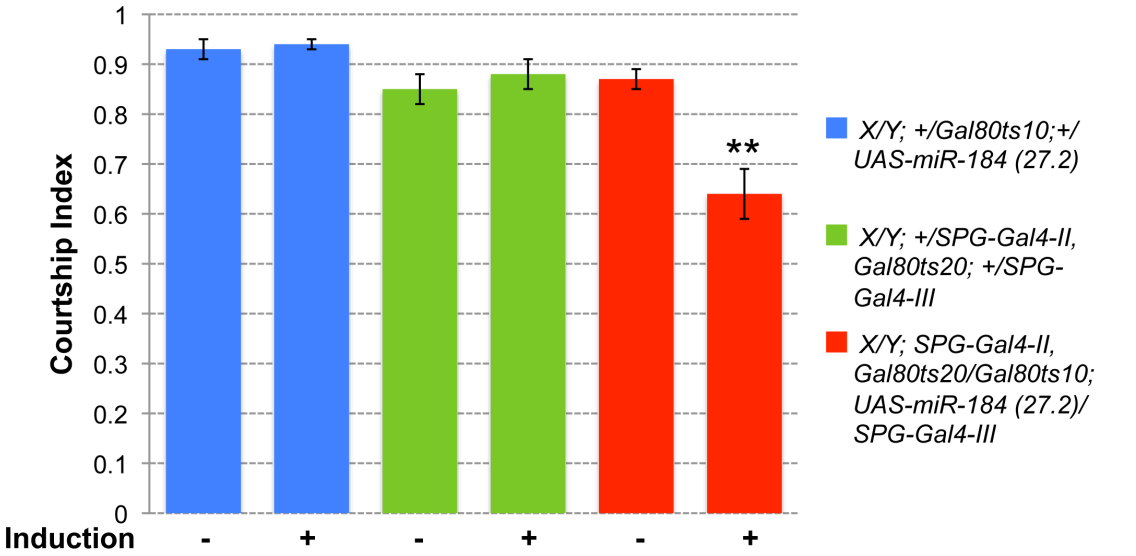
Courtship Index
1
0.9
0.8
0.7
0.6
0.5
0.4
0.3
0.2
0.1
0
**
Induction
- + - + - +
X/Y; +/Gal80ts10;+/ UAS-miR-184 (27.2)
X/Y; +/SPG-Gal4-II, Gal80ts20; +/SPG-Gal4-III
X/Y; SPG-Gal4-II, Gal80ts20/Gal80ts10; UAS-miR-184 (27.2)/ SPG-Gal4-III

(B)

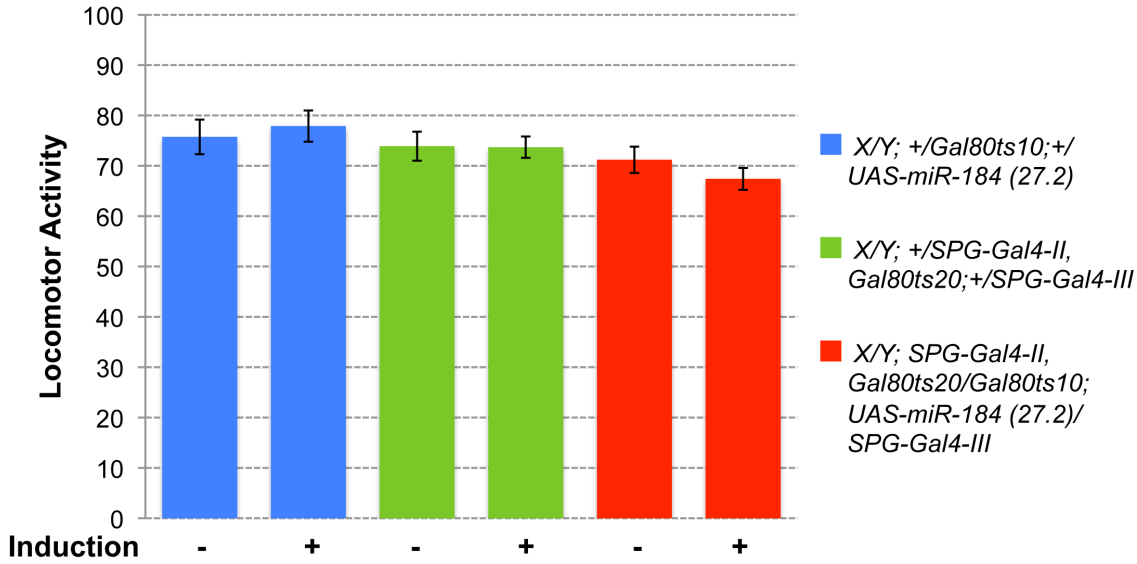
Locomotor Activity
100
90
80
70
60
50
40
30
20
10
0
Induction
- + - + - +
X/Y; +/Gal80ts10;+/ UAS-miR-184 (27.2)
X/Y; +/SPG-Gal4-II, Gal80ts20;+/SPG-Gal4-III
X/Y; SPG-Gal4-II, Gal80ts20/Gal80ts10; UAS-miR-184 (27.2)/ SPG-Gal4-III

Figure 4.4: Conditional overexpression of *miR-184* mutant reduces male courtship behavior. (A) The temporal and spatial expression of *miR-184* in the adult bbb was achieved by using the $Gal80^{ts}$/Gal4/UAS system. The genotypes used were: a) *X/Y; +/*$Gal80^{ts10}$*; +/UAS-miR-184 (27.2)* b) *X/Y; +/SPG-Gal4-II,* $Gal80^{ts20}$*; +/SPG-Gal4-III*; c) *X/Y; SPG-Gal4-II,* $Gal80^{ts20}$*/*$Gal80^{ts10}$*; SPG-Gal4-III/UAS-miR-184 (27.2)*. Both the genetic controls and the mutant were reared and kept at 18°C. At this temperature the expression of *UAS-miR-184* is suppressed by the expression of $Gal80^{ts}$, which is active at this temperature resulting in normal behavior of the courting male. However, when the flies are induced at 32°C, the $Gal80^{ts}$ gets inactivated leaving Gal4 free for binding to the Upstream Activating Sequence (UAS sequence) leading to the expression of *miR-184.* This resulted in the significant reduction of courtship index of experimental males compared to the uninduced experimental genotype (Two way ANOVA with post-hoc Bonferroni multiple comparisons test; **, $p<0.0001$, n=25). The courtship index of the control genotypes at induced condition was not significantly different from the uninduced control as well as the uninduced experimental proving that the reduced courtship index in induced experimental is a physiological effect of *miR-184* overexpression rather than some non-specific effects due to the induction process. **(B)** The flies were treated in the same way as described above before subjecting them to the activity assay which is a measure of the locomotion activity of the flies measured as an index of how many times a fly crosses a midline drawn along the diameter of the mating wheel. All the genotypes with and without induction showed no significant difference in this assay. ANOVA analysis of the activity assay data for all genotypes showed no significant difference (n=20). Error bars denote standard error of the means. (+) = Induction of male flies for 48 hr in a 32°C incubator before the assay. (-) = Male flies were kept in the 18°C incubator.

4.3.4 *miR-184* overexpression affects the RNA levels of its target gene *sinu*

sinu is one of the top predicted targets of *miR-184* and it has been shown previously *in vitro* that *sinu* is one of the targets of *miR-184* (Iovino et al., 2009). In addition, *sinu* is an important component of the tight bbb system in flies. Therefore, overexpression and/or silencing of *miR-184* is expected to have an effect on the level of its target *sinu*. In order to examine this, I overexpressed the transgene *UAS-miR 184* throughout development and adulthood using the bbb specific driver, SPG-Gal4. The relevant control crosses were also set up. The genotypes of the controls were: *X/Y; +/+; +/SPG-Gal4 and X/Y; +/+; +/UAS-miR-184 (27.2)*. The experimental genotype was *X/Y; +/+; SPG-Gal4/ UAS-miR-184 (27.2)*. Around 300 brains from each genotype were dissected in 1X PBS and immediately stored on a frozen droplet of Trizol reagent (Ambion) followed by storage at -80°C until processed further. Total RNA was extracted (Trizol plus RNA purification kit, Ambion) from these brains. The reason for dissecting whole brains instead of bbb cells is that *sinu* is not expressed in the brain (Wu et al., 2004). Therefore, any effects on its RNA levels are likely to reflect the levels in the bbb.

cDNA was synthesized from 1µg of total RNA as described in section 2.13. 1of Materials and Methods. Following RT reaction, qPCRs were performed with TaqMan Gene Expression Assay. The dynamic range for both *sinu* and the endogenous control *rp49* was determined using the standard curve method. The standard curves had a slope of -3.8 for *rp49* and -3.4 for *sinu* and were determined to be good. Based on the standard curve, I chose to use a 1/10 dilution of each cDNA sample for the qPCR reaction.

The comparative ΔΔCt method was used to quantify the expression as described in section 2.13.4 of Materials and Methods. The ΔCt (normalized Ct) value was

calculated as the difference between the average Ct (threshold cycle values) for the expression of the *sinu* gene and the endogenous control, *rp49* for each genotype. The calibrated ΔCt value for each sample (ΔΔCt) was calculated as the difference between the ΔCt values of the sample and the reference/calibrator sample (the +/UAS control). The fold change for each sample relative to the calibrator was calculated as $2^{-\Delta\Delta Ct}$. The fold induction values for each genotype are plotted as a bar graph. I found that when *miR-184* was overexpressed throughout development and adulthood, the mRNA expression level of its target gene, *sinu* was significantly increased (almost doubled) compared to the genetic controls (Figure 4.5, $p<0.0001$, $n=3$).

Our expectation was that having more *miR-184* might decrease *sinu* mRNA levels. The result obtained by qPCR was opposite to what was expected. However, this result indirectly confirms that *miR-184* affects the expression of one of its target, *sinu*. One of the explanations for this result is that the increase in *sinu* mRNA might be the result of the feedback system trying to overcome the effect of the overwhelmingly abundant *miR-184*, as Sinu proteins are likely to be tightly controlled for proper functionality of the bbb. Or the increase in *sinu* expression could be the result of complex feedback loops with other targets such as suppressors for *sinu* or indirect downstream effectors. Also the effect could be apparent at the translational level rather than at the transcriptional level and further experiments measuring the level of Sinu protein would be more relevant to address the question of whether amount of the *miR-184* target *sinu*

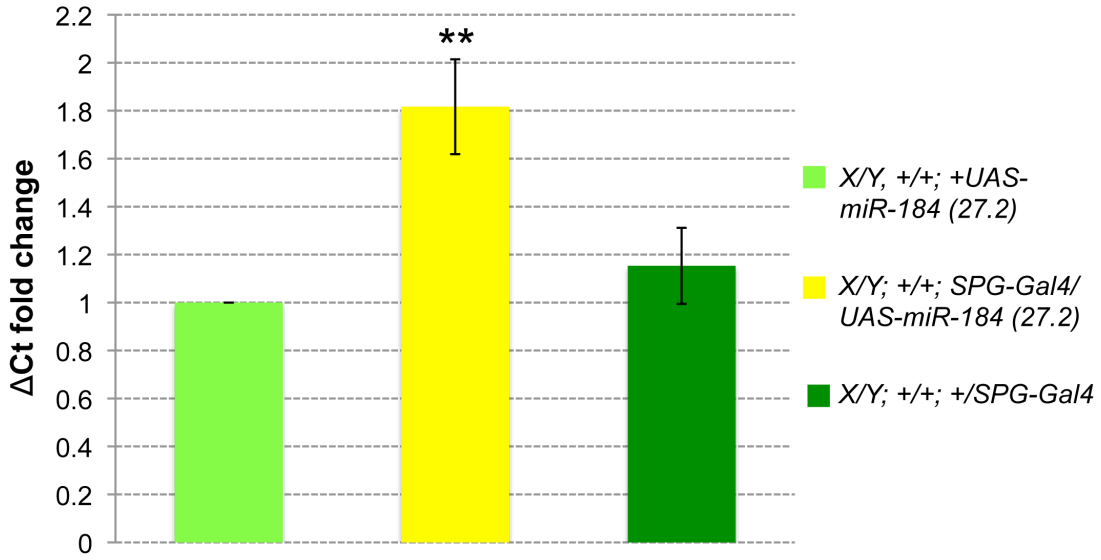

Figure 4.5: Expression of *miR-184* target *sinu* is altered by overexpression of *miR-184* in the bbb of male flies. The fold change was normalized to the *UAS-miR-184* control genotype. The change in expression of *sinu* is statistically significant compared to the controls (ANOVA, $p<0.0001$, $n=3$). Error bars represent the standard error of means.

decreases post *miR-184* manipulation or not. Unfortunately, we have so far not been successful in obtaining Sinu antibodies to examine this hypothesis.

4.4 Generation of *UAS-miR-184 sponge* transgenic flies

The reduction of *miR-184* was achieved by using microRNA sponge. In order to reduce *miR-184*, I generated transgene that contained a "sponge construct" to reduce the function of the endogenous *miR-184*. A microRNA sponge consists essentially of multiple repeats of a modified complementary sequence of the target microRNA of interest. In principle, it would bind to the target microRNA and prevent its function as a regulator of the target genes. The sponge construct is shown in Figure 4.6 (For details see Materials and Methods sections 2.8.2, 2.8.3, and 2.8.4). A total of 30 transgenic lines were established as shown in the Table 4.5.

12 11 10 9 8 7 6 5 4 3 2 1

5'TCTAGACCCTTATCAAGCATCCGTCCACGCGCCCTTATCAAGCATCCGTCCA

CGCGCCCTTATCAAGCATCCGTCCACGCGCCCTTATCAAGCATCCGTCCACGC

GCCCTTATCAAGCATCCGTCCACGCGCCCTTATCAAGCATCCGTCCACGCGCC

CTTATCAAGCATCCGTCCACGCGCCCTTATCAAGCATCCGTCCACGCGCCCTT

ATCAAGCATCCGTCCACGCGCCCTTATCAAGCATCCGTCCACGCGTCTAGA-3'

Figure 4.6: ***miR-184 sponge* constructs (Loya et al., 2009).** 10 repeats of 21 bp length each containing the *miR-184* seed (1-6) complementary sequence and containing mismatches at positions 9-12 were designed with Xba I restriction sites (shown in blue) on both ends, and was placed in the 3'UTR region of EGFP in the pUAST-EGFP vector and cloned.

Table 4.5: Mapping of the chromosomal location of the transgene in *UAS-miR-184 sponge* transgenic lines

Chromosomal Location	**Transgenic Lines (*UAS-miR-184 sponge*)**
X chromosome	3.1, 17.1, 26.1, 28.1
2nd Chromosome	1.1, 2.1, 4.1, 11.1, 13.1, 14.1, 15.1, 18.1, 20.1, 21.1, 24.1, 25.1, 30.1
3rd Chromosome	5.1, 6.1, 7.1, 8.1,9.1, 10.1, 12.1,16.1, 19.1, 22.1, 23.1,27.1, 29.1

4.4.1 Verification of transgene expression in the flies

Confirmation of transgene expression in the *UAS-miR 184 sponge* transgenic lines was done by RT-PCR. The pUAST forward and reverse primers were used for RT-PCR (the same primers that were used to sequence the initial sponge transgene in the pUAST-EGFP vector). The transgenic fly lines were crossed to flies expressing the heat inducible driver, hsp70-Gal4. The progenies and the wild-type control CS flies were subjected to heat shock as described in section 2.8.4 of Materials and Methods.. The RNA was then extracted and cDNA was synthesized as described in section 2.8.4.1 of Materials and Methods. PCR reactions were performed at a low cycle number (section 2.8.4.2) and the product was run on a 1.2% agarose gel and visualized under a UV illuminator (Figure 4.7, Gel I and Gel II). An expected product of >1000 bp was obtained. The smaller sized bands likely correspond to a shorter PCR product due to secondary structure. Lines in which the PCR products are smaller may be lines with fewer repeats in the sponge sequence due to unequal crossover in the repeats. No product was visible in CS wild-type flies. Minus RT samples did not show any amplification showing that there was no

genomic contamination in the RNA samples. The transgenic line 7.1 (referred as *UAS-miR-184 sponge (7.1 sp)* hereafter*)* was selected for behavioral assays.

4.4.2 *miR-184 sponge* silences the expression of *miR-184* in bbb

To verify the specificity of the function of the sponge transgene on *miR-184* expression, I measured the level of *miR-184* in sponge overexpressing cells. In order to do so, I specifically generated flies expressing the sponge in the bbb along with the fluorescent marker DS Red stinger. Briefly, the flies bearing the *UAS-miR-184 sponge* and the *UAS-DS Red marker* were crossed to the SPG-Gal4 driver. The genotype of these flies was: X/Y; +/ *UAS-DS Red stinger; SPG-Gal4/UAS-miR-184 sponge 7.1.* The control flies were made by crossing the flies bearing only the UAS-DS Red stinger reporter with the SPG-Gal4 driver. The genotype of the control flies was: *X/Y; +/UAS-DS Red stinger; +/SPG-Gal4.* The flies were grown at 25°C and the progeny males were collected on day one and aged for 4-5 days. Then the whole brain was dissected from these animals and bbb cells expressing the sponge for *miR-184* (*UAS-miR-184 7.1 Sp*) were manually isolated and RNA was prepared by using the miRNA mini kit from Qiagen following the manufacturer's protocol. The lysis and the homogenization of the cells were carried out using a syringe and needle method (20 gauges). The same sized needles had been used to isolate miRNAs for sequencing. Three biological replicates were prepared for each genotype and the bbb cells from 50 brains were isolated for each sample. Complementary DNA (cDNA) was prepared with miRNA-specific stem-loop RT primers from this RNA

Gel I

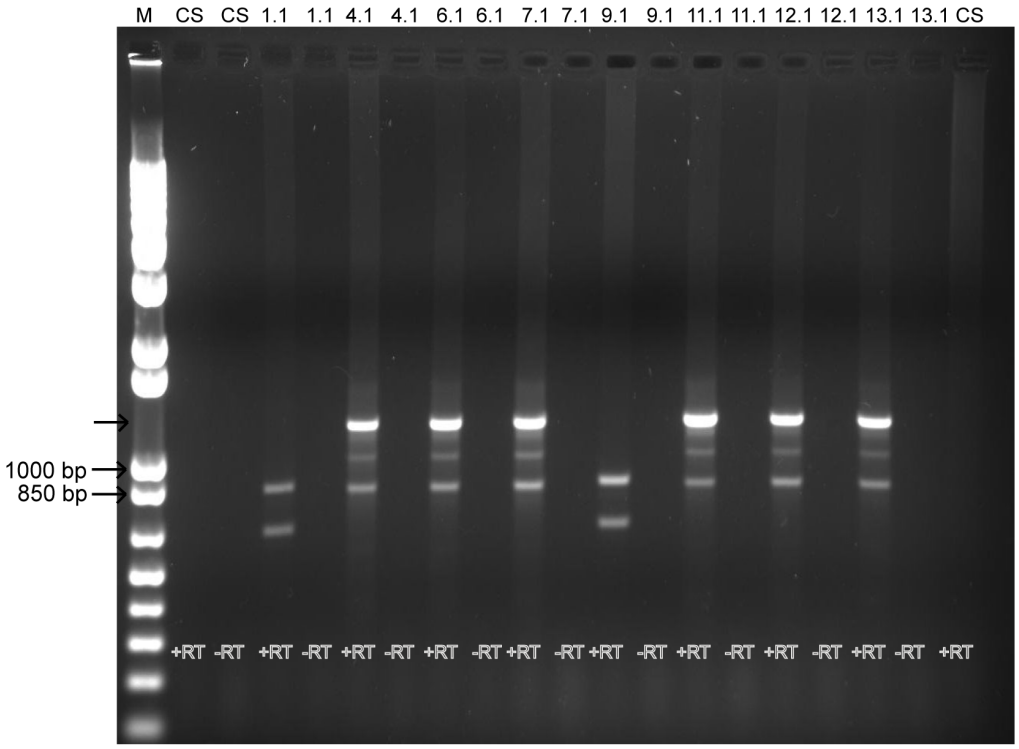
M CS CS 1.1 1.1 4.1 4.1 6.1 6.1 7.1 7.1 9.1 9.1 11.1 11.1 12.1 12.1 13.1 13.1 CS
1000 bp
850 bp
+RT -RT +RT -RT +RT -RT +RT -RT +RT -RT +RT -RT +RT -RT +RT -RT +RT -RT +RT

Gel II

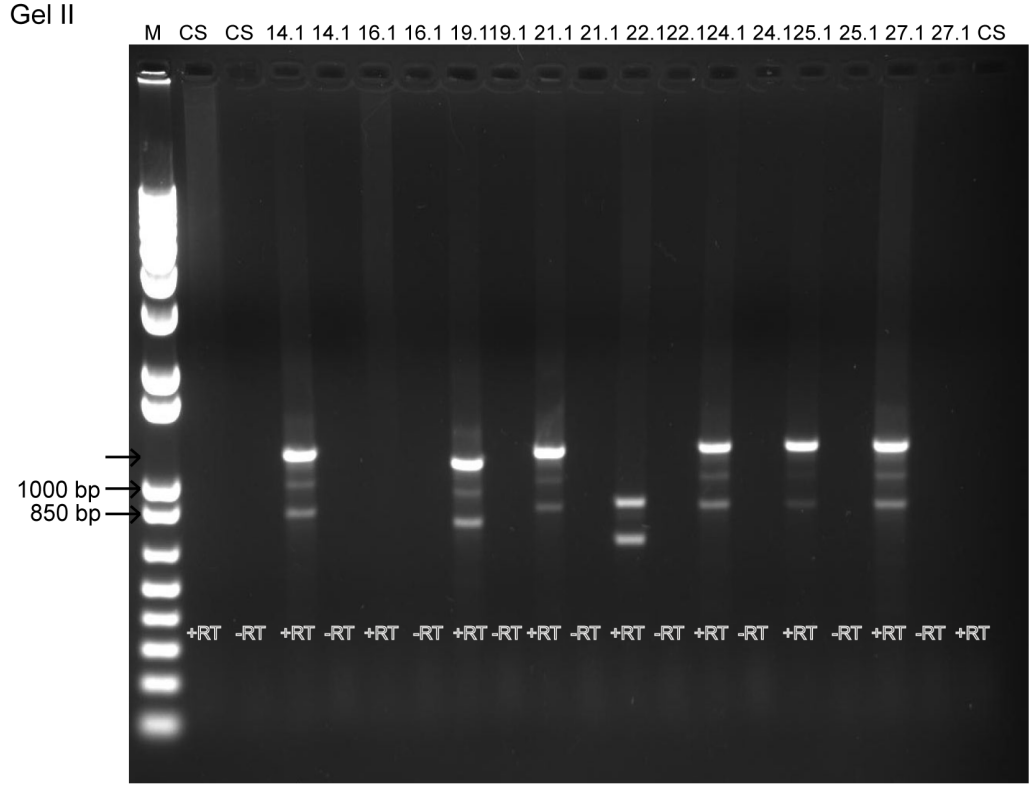
M CS CS 14.1 14.1 16.1 16.1 19.1 19.1 21.1 21.1 22.1 22.1 24.1 24.1 25.1 25.1 27.1 27.1 CS
1000 bp
850 bp
+RT -RT +RT -RT +RT -RT +RT -RT +RT -RT +RT -RT +RT -RT +RT -RT +RT -RT +RT

Figure 4.7: Verification of transgene *UAS-miR-184 sponge* expression in transgenic lines by RT PCR. M=1 Kb plus ladder. The progenies of the cross involving several of the transgenics (*UAS-miR-184 sponge*) lines with the heat shock promotor hsp-gal4 line were heat shocked at 37°C for 2 hours followed by RNA extraction and cDNA synthesis. Using pUAST forward and reverse primer, low cycle PCR (25 cycles) amplification of the cDNA shows the expression of the UAS-transgene in several lines; Gel I, Gel II. Absence of a PCR product in –RT sample confirms the absence of genomic DNA contamination.

using the Taqman MicroRNA Reverse Transcription kit (PN 4366596) as described in section 2.13.2 of Materials and Methods. qPCRs were described in section 2.13.2 of Materials and Methods. qPCRs were performed in an Applied Biosystems StepOne Plus Real-Time PCR System using the comparative ΔΔCt method as described in section 2.13.4 of Materials and Methods. The ΔCt (normalized Ct) value was calculated as the difference between the average Ct (threshold cycle values) for the expression of *miR-184* and the endogenous control, *2S rRNA* for each genotype. The calibrated ΔCt value for each sample (ΔΔCt) was calculated as the difference between the ΔCt values of the sample and the reference/calibrator sample (the SPG-Gal4/UAS-DS Red control). The fold change for each sample relative to the calibrator was calculated as $2^{-\Delta\Delta Ct}$. The fold induction values for each genotype are plotted as a bar graph (Figure 4.8).

4.4.3 Establishing the standard curve

Quantitative PCR of the one of the control genotype cDNA was performed initially to establish the dynamic range for the *miR-184-3p* and the endogenous control *2S rRNA* using the standard curve method. The standard curves had a slope of -3.7 for *miR-184-3p* and -3.8 for *2S rRNA* and were determined to be good. Based on the result, a 1/10 dilution of the *miR-184-3p* cDNA and a 1/100 dilution of the endogenous control *2S rRNA* cDNA were chosen to perform the relative quantitation of *miR-184-3p* expression using the comparative ΔΔCt method.

Three biological replicates for each genotype sample were examined with three technical replicates of each sample. The fold change of *miR-184* expression and endogenous control *2s rRNA* for 3 biological replicates was averaged and plotted against the genotype. The results show that the expression of *miR-184* is significantly reduced in

the bbb cells expressing the *miR-184 sponge* (Figure 4.8, $p<0.0001$, n=3) compared to the control fly only expressing the fluorescent marker, the DS Red stinger. This shows that the sponge construct is specific and functioning as expected in the bbb.

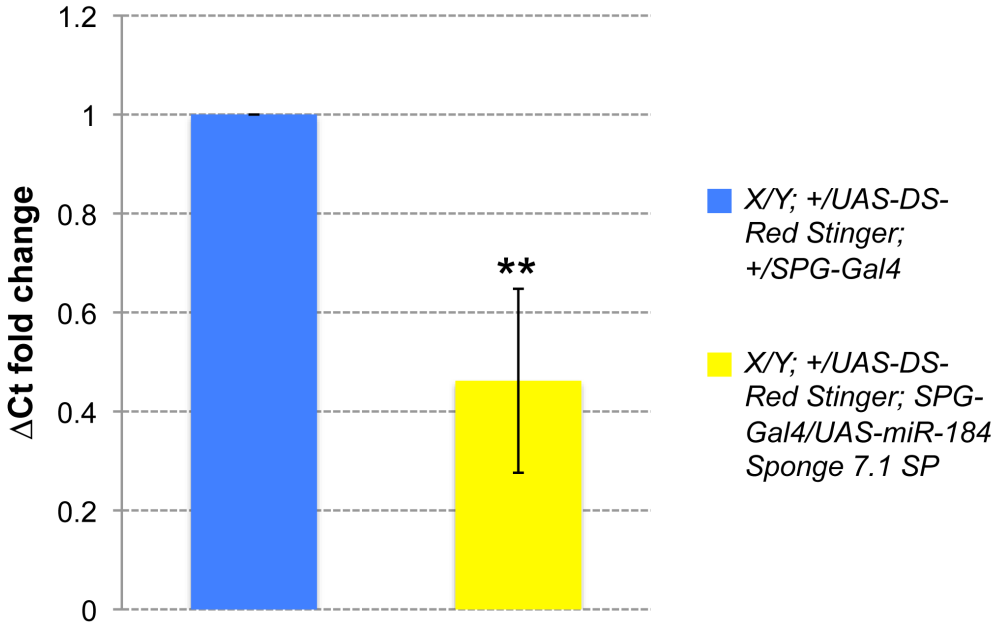

Figure 4.8: Examination of *miR-184* knockdown in the bbb by sponge expression, using qPCR. qPCR was performed on three biological replicates of sponge overexpressing bbb cells of male flies in which knockdown was performed throughout development. Three technical replicates of each sample with a total of 3 biological replicates each were run. The fold change of *miR-184* expression and endogenous control *2s rRNA* for 3 biological replicates was averaged and plotted against the genotype. The result shows the silencing of *miR-184* levels by the sponge (n=3). Error bar represents the standard error of the means.

4.4.4 Silencing of *miR-184* in the bbb by sponge affects the courtship behavior

As the courtship result from the *miR-184* overexpressing experiment suggested that optimal expression of the *miR-184* is important for normal male courtship behavior, I wanted to investigate if reducing the levels of *miR-184* in the bbb cells would also have an effect on male courtship behavior of *Drosophila*. For this purpose the transgenic line 7.1 Sp was crossed to the $Gal80^{ts}$/SPG-Gal4 driver line to specifically knock down the *miR-184* in the bbb post developmentally. The silencing of *miR-184* in the bbb was obtained by crossing *UAS-miR-184 sponge 7.1 sp* flies to flies containing the bbb-specific SPG-Gal4 in addition to a copy of a temperature-sensitive Gal80 ($Gal80^{ts}$). Experimental flies contained two copies of SPG-Gal4 (one on the second (II), and one on the third (III) chromosome, and two $Gal80^{ts}$ transgenes ($Gal80^{ts10}$ and $Gal80^{ts20}$). The genotypes used are shown in Table 4.6. The courtship assay was performed as described in section 2.9.1 of Materials and Methods.

Table 4.6: The following genotypes were created and used for behavioral assays

Flies	**Genotypes**
Control 1	*X/Y; +/$Gal80^{ts10}$; UAS-miR-184 Sponge (7.1sp)*
Control 2	*X/Y; +/SPG-Gal4-II, $Gal80^{ts20}$; +/SPG-Gal4-III*
Experimental	*X/Y; SPG-Gal4-II, $Gal80^{ts20}$/$Gal80^{ts10}$; SPG-Gal4-III/UAS-miR-184 Sponge (7.1sp)*

(A)

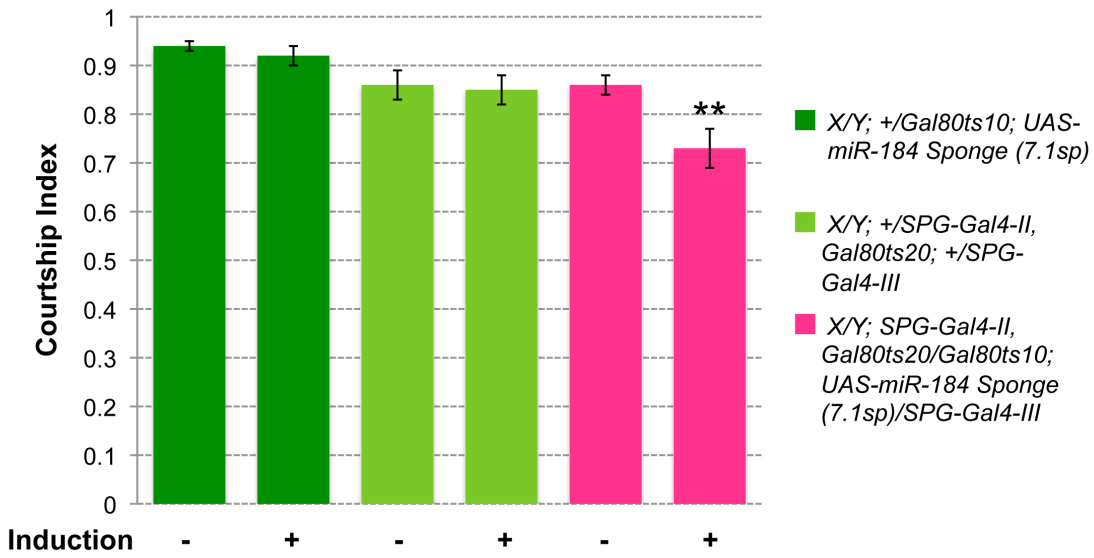
Courtship Index
1
0.9
0.8
0.7
0.6
0.5
0.4
0.3
0.2
0.1
0
**
Induction
- + - + - +
X/Y; +/Gal80ts10; UAS-miR-184 Sponge (7.1sp)
X/Y; +/SPG-Gal4-II, Gal80ts20; +/SPG-Gal4-III
X/Y; SPG-Gal4-II, Gal80ts20/Gal80ts10; UAS-miR-184 Sponge (7.1sp)/SPG-Gal4-III

(B)

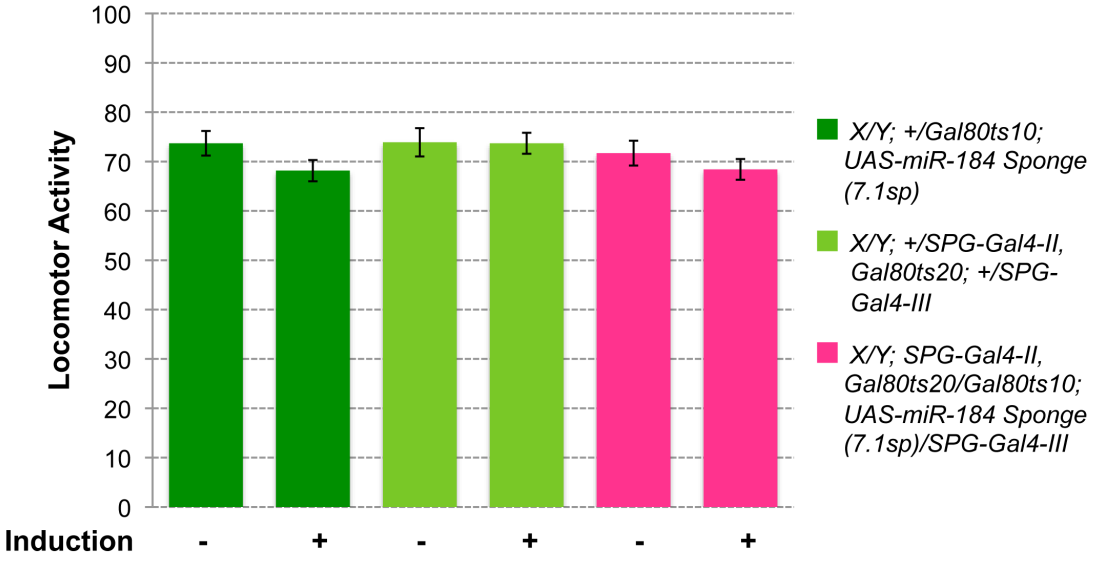
Locomotor Activity
100
90
80
70
60
50
40
30
20
10
0
Induction
- + - + - +
X/Y; +/Gal80ts10; UAS-miR-184 Sponge (7.1sp)
X/Y; +/SPG-Gal4-II, Gal80ts20; +/SPG-Gal4-III
X/Y; SPG-Gal4-II, Gal80ts20/Gal80ts10; UAS-miR-184 Sponge (7.1sp)/SPG-Gal4-III

Figure 4.9: **Reduction of *miR-184* expression in the bbb by *miR-184 sponge* reduces male courtship. (A)** The Gal80^{ts}/Gal4/UAS system was used in order to control the temporal and spatial expression of the *miR-184 sponge* to silence the endogenous miR-184 expression in adult male bbb. The genotypes used were: a) *X/Y; +/Gal80^{ts10}; UAS-miR-184 Sponge (7.1sp)* b) *X/Y; +/SPG-Gal4-II,Gal80^{ts20}; +/SPG-Gal4-III*, c) *X/Y; SPG-Gal4-II, Gal80^{ts20}/Gal80^{ts10}; SPG-Gal4-III/UAS-miR-184 Sponge (7.1sp).* The two genetic controls and the mutant were reared 18°C and induced at 32°C for 3 days and then observed for courtship behavior towards a virgin female after 3 hours of resting period at RT. The induced mutant genotype expressing *miR-184 sponge (7.1sp)* showed a significantly reduced courtship index as compared to both induced and un-induced genetic controls (Two way ANOVA with Bonferroni multiple comparisons test; **, $p<0.0001$, n=25) as well as with un-induced experimental (Two way ANOVA with post-hoc Bonferroni multiple comparisons test; **, $p<0.0001$). (**B**) Shows the locomotion activity of all genotypes with and without induction. ANOVA analysis of the activity assay for all genotypes shows no significant difference among each other (n=20). Error bars denote standard error of the means. **(+)** = Induction of male flies to 3 days in 32°C incubator before the assay. **(-)** = Male flies were not induced and kept at 18°C.

As seen in Figure 4.9 A, the courtship assay shows that the courtship index of the male fly towards a female is significantly reduced when *miR-184* expression is reduced in the bbb by the expression of the *miR-184 sponge*. This result confirms our earlier observations that indicate that optimal levels of *miR-184* in the bbb are required for normal male courtship behavior. Statistical analysis showed that this effect is significant (Two way ANOVA with Bonferroni multiple comparisons test; **, $p<0.0001$). The locomotion assay showed that this effect is not due to defects in the locomotion as indicated in Figure 4.9 B. There was no significant difference between the locomotor activities of the control flies and the experimental flies.

4.5 Role of predicted *miR-184* targets, *sinu* and *Neurexin* in courtship behavior

Since we observed an effect of altered *miR-184* expression on courtship behavior, we next examined whether the reduction of some of its target genes affects courtship. Interestingly, s*inu* and *Neurexin* are predicted and demonstrated *miR-184* targets *in vitro* (Iovino et al., 2009) and their role in the development of the bbb has been described (Wu et al., 2004, Baumgartner et al., 1996). The independent courtship role of these genes in the adult bbb was examined by creating specific and conditional mutations by using lines that contain RNAi transgenes against these genes. Temporal control of expression of the RNAi was again achieved by using the UAS/Gal80ts/Gal4 system (Brand and Perrimon, 1993; McGuire et al., 2003; Roman, 2004). This is important since these genes have been shown to be required during development.

4.5.1 Test the hypothesis that *sinu* and *Neurexin* have a dynamic role in the function of the adult bbb

Rationale: A developmental role for *sinu* in the set-up of a functional bbb has been described (Wu et al., 2004; Stork et al., 2008), but its adult function is unknown. As expected, our microarray analysis of bbb cells showed that *sinu* and *Neurexin* transcripts are present in the bbb of adult flies. The high levels of *miR-184* in the bbb and the fact that *sinu* is one of the top predicted (and *in vitro* verified in dual luciferase assay in lysates of transiently transfected S2 cells, Iovino et al. (2009)) *miR-184* target suggest that the amount of Sinu protein in adults is tightly regulated. Sinu belongs to the group of Claudin proteins, transmembrane proteins that are essential components of the mammalian bbb (see introduction). The following genotypes were created and tested in the courtship assay as described previously.

Table 4.7: Genotypes used for courtship assays

Flies	**Genotypes**
Control 1	*X/Y; +/UAS-sinu-RNAi; +/+*
Control 2	*X/Y; +/Gal80^{ts10}; +/SPG-Gal4*
Experimental	*X/Y; Gal80^{ts10}/UAS-sinu-RNAi; +/SPG-Gal4*

(A)

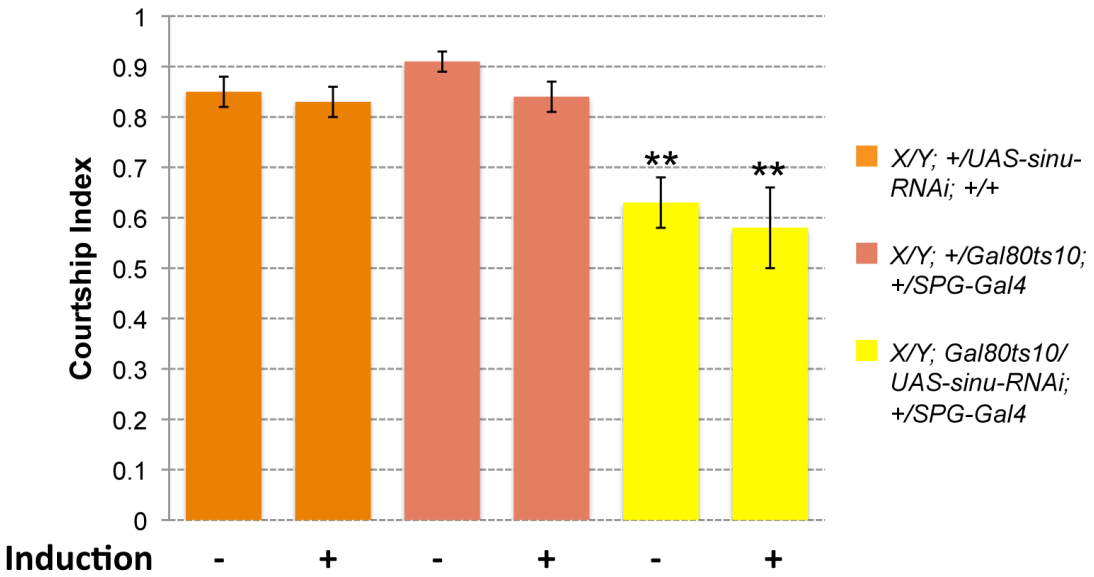
Courtship Index
1
0.9
0.8
0.7
0.6
0.5
0.4
0.3
0.2
0.1
0
**
**
Induction
-
+
-
+
-
+
X/Y; +/UAS-sinu-RNAi; +/+
X/Y; +/Gal80ts10; +/SPG-Gal4
X/Y; Gal80ts10/ UAS-sinu-RNAi; +/SPG-Gal4

(B)

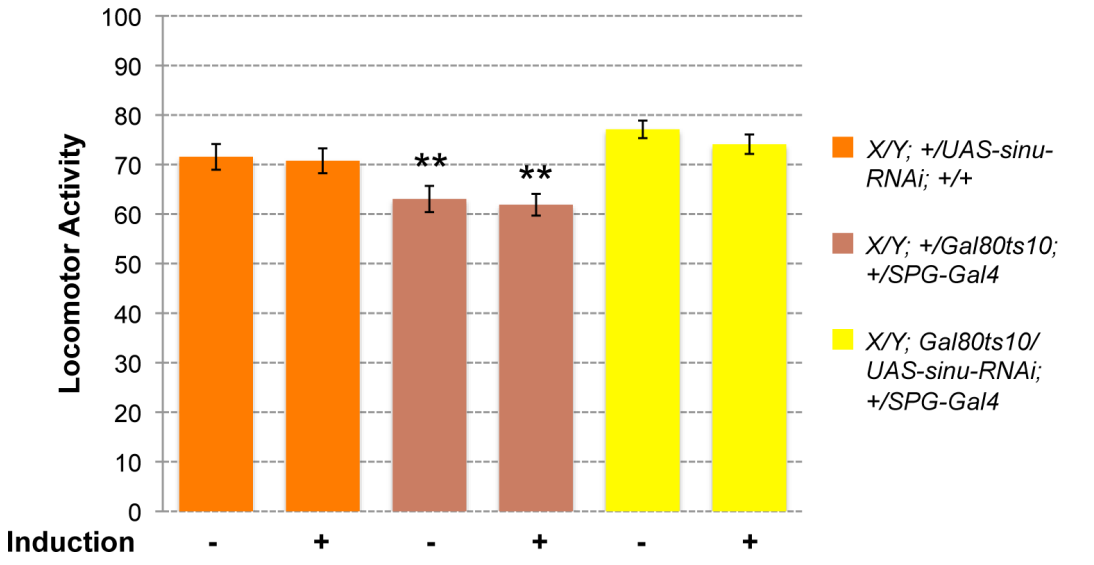
Locomotor Activity
100
90
80
70
60
50
40
30
20
10
0
**
**
Induction
-
+
-
+
-
+
X/Y; +/UAS-sinu-RNAi; +/+
X/Y; +/Gal80ts10; +/SPG-Gal4
X/Y; Gal80ts10/ UAS-sinu-RNAi; +/SPG-Gal4

Figure 4.10: Expression of *sinu-RNAi* in the bbb reduces male courtship behavior. **(A)** The temporal and spatial expression of *sinu-RNAi* in the adult bbb was achieved using the Gal80^{ts}/Gal4/UAS system. The genotypes used were: a) *X/Y; +/UAS-sinu-RNAi; +/+ b) X/Y; +/Gal80^{ts10}; +/SPG-Gal4; c) X/Y; Gal80^{ts10}/UAS-sinu-RNAi; +/SPG-Gal4*. Both the genetic controls and the mutant were reared and kept at 18°C. At this temperature the expression of *UAS-sinu RNAi* is suppressed because Gal80^{ts} is active at this temperature. However, when the flies are induced at 32°C, the Gal80^{ts} gets inactivated leaving Gal4 free for binding to the Upstream Activating Sequence (UAS sequence) leading to the expression of *sinu-RNAi.* The courtship index of the control genotypes at induced condition was not significantly different from the uninduced control. However, the courtship index of the uninduced experimental was also significantly reduced as compared to the induced and uninduced controls. This suggests a leaky repression by the single copy of Gal80^{ts} present in these flies. (Two way ANOVA with post-hoc Bonferroni multiple comparisons test; **, $p<0.0001$, n=25). **(B)** The flies were treated in the same way as described above before subjecting them to the activity assay which is a measure of the locomotion activity of the flies measured as an index of how many times a fly crosses a midline drawn along the diameter of the mating wheel. One of the control genotypes, the *X/Y; +/Gal80^{ts10}; +/SPG-Gal4* showed significant reduction in its activity compared to the experimental flies and the other control (ANOVA with post hoc Bonferroni multiple comparisons test, **$p<0.001$, n=20). Error bars denote standard error of the means. **(+)** = Induction of male flies for 48 hr in 32°C incubator before the assay. **(-)** = Male flies were kept at 18°C incubator. The experimental flies show a statistically significant increase in locomotor activity ($p<0.001$, n=20).

As shown in Figure 4.10A, expression of *sinu-RNAi* resulted in a significantly reduced courtship index of the experimental flies compared to the controls (ANOVA, $p<0.0001$). However, the courtship index of the uninduced experimental flies was also statistically significantly ($p<0.0001$) reduced. It is not uncommon for $Gal80^{ts}$ repression to be a little "leaky" i.e. some Gal4 is active. In the future, this experiment needs to be re-done with two copies of $Gal80^{ts}$. These results show that *sinu* has a role in courtship behavior, but at this point do not answer the question whether this is a developmental or physiological effect. When tested for locomotion, the control and experimental flies showed a similar level of overall activity (Figure 4.10 B, ANOVA, <0.001).

4.5.2 Test the hypothesis that *Neurexin* has a dynamic role in the function of the adult bbb

Neurexin has been verified to be a *miR-184* target *in vitro*. It plays a very important role in the development of bbb (Baumgartner et al., 1996). Therefore, I checked the adult role of this gene in the bbb for male courtship behavior. As described for *sinu*, I performed conditional knockdown of *Neurexin* specifically in the bbb using the Gal4/ $Gal80^{ts}$/ UAS system. The conditional mutation was created by using three different RNAi lines (UAS- RNAi lines 9039, 8353 and 108128, VDRC stock center). None of the RNAi lines tested showed a statistically significant reduction in the courtship indices, suggesting that *Neurexin* may not have an adult role in courtship behavior of *Drosophila*, besides its structural role during development and in adult (Figure 4.11 A, B, and C). The reduction achieved by expression of the RNAi constructs may not be sufficient to significantly affect the structural role of *Neurexin*. It is possible that the turnover rate for this protein is slow, so that the RNAi reduction would not be efficient in

the time frame we used. This suggests that courtship defects I have observed for *sinu* indicate a specific role in courtship, and courtship defects are not simply caused by disturbing proteins that contribute to structural bbb functions.

4.5.3 The bbb is intact in *miR-184* mutants and *sinu* mutants we have used in the study

In order to examine whether the courtship defects that I observed in the *mir-184* mutants and *sinu* mutants is due to structural changes in the integrity of the bbb, I performed dye exclusion experiments using an assay that was previously established in our lab by Hoxha et al. (2013) to see if the permeability of the bbb in these mutants is changed. This issue is immensely important because if the bbb is compromised, the blood of the fly, the hemolymph will have unrestricted access to the brain and hence may have some unwanted effects in behavior including unspecific courtship defects. Therefore, to assess the bbb properties in the mutant males that showed courtship defects is very important. The dye exclusion assay involves microinjection of (~100nl) a fluorescently labeled dextran molecule of 10kDa into the body of a fly through the scutellum. Since the flies have an open circulatory system, the dye will enter the circulating hemolymph. Because of the bbb, the dye does not enter the brain, and accumulation of the dye can be observed as clear red line at the bbb. The flies were allowed to recover overnight. The next day, the brain was dissected and fixed in 4% PFA followed by mounting in medium containing 4', 6-diamidino-2-phenylindole (DAPI) to stain the nuclei.

(A)

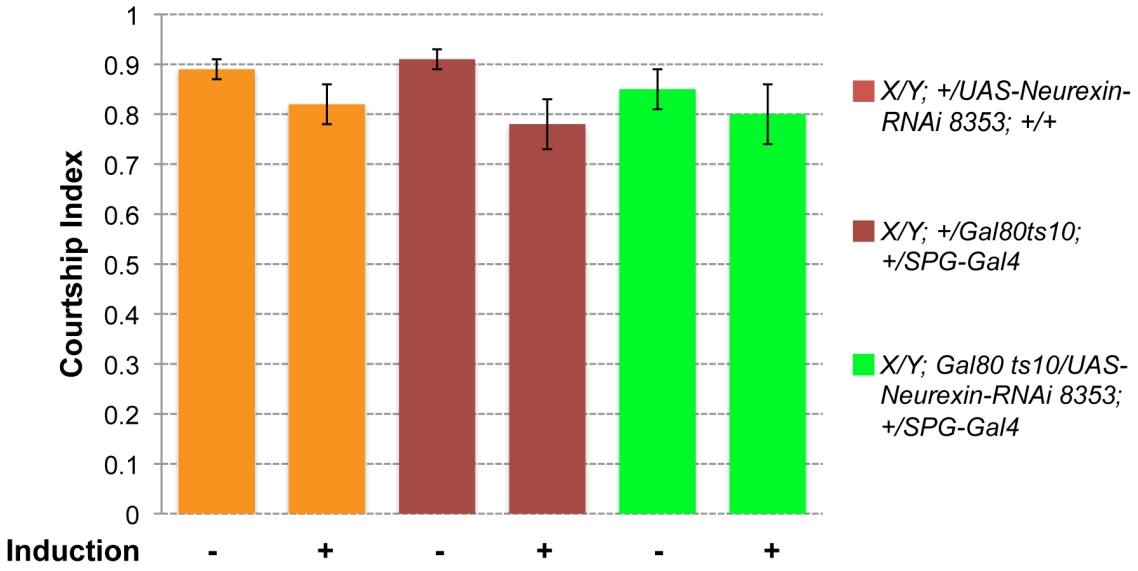
Courtship Index
1
0.9
0.8
0.7
0.6
0.5
0.4
0.3
0.2
0.1
0
Induction
- + - + - +
X/Y; +/UAS-Neurexin-RNAi 8353; +/+
X/Y; +/Gal80ts10; +/SPG-Gal4
X/Y; Gal80 ts10/UAS-Neurexin-RNAi 8353; +/SPG-Gal4

(B)

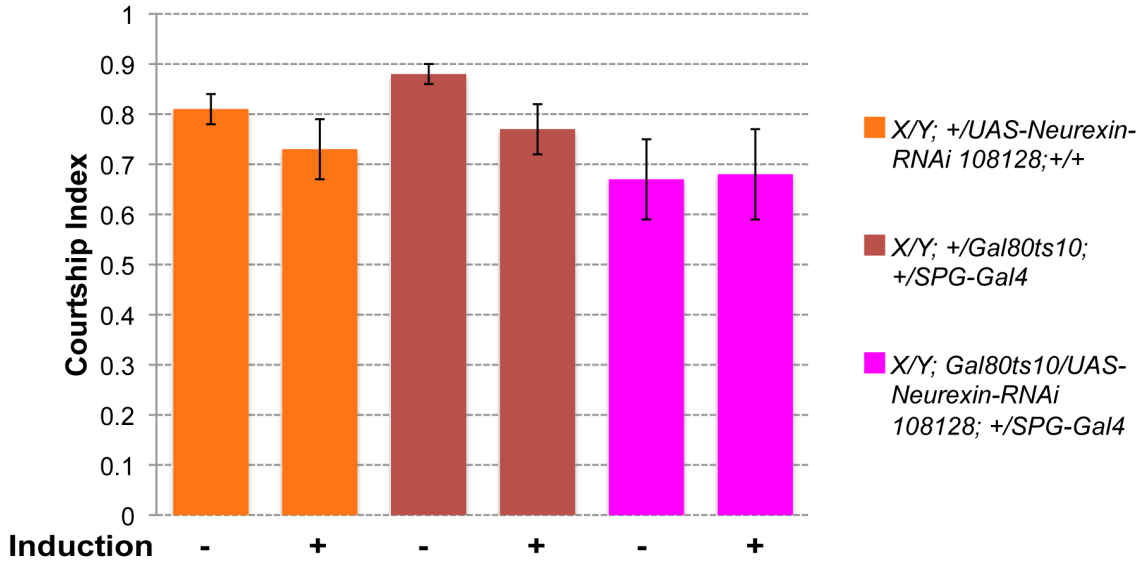
Courtship Index
1
0.9
0.8
0.7
0.6
0.5
0.4
0.3
0.2
0.1
0
Induction
- + - + - +
X/Y; +/UAS-Neurexin-RNAi 108128;+/+
X/Y; +/Gal80ts10; +/SPG-Gal4
X/Y; Gal80ts10/UAS-Neurexin-RNAi 108128; +/SPG-Gal4

(C)

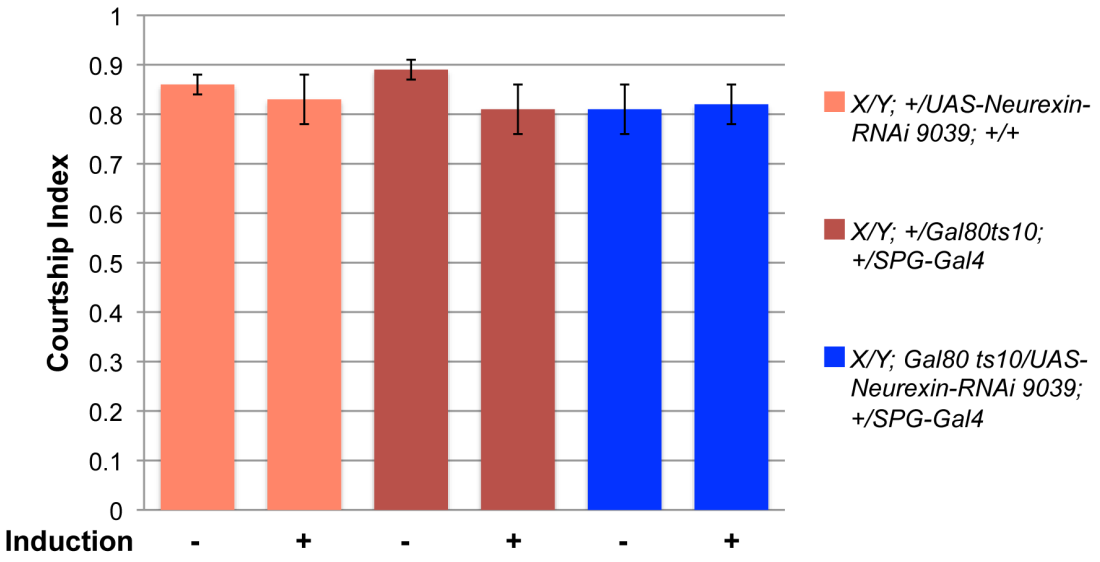

Figure 4.11: Conditional expression of *Neurexin-RNAi* in the adult bbb does not reduce male courtship behavior. The temporal and spatial expression of *Neurexin-RNAi* in the adult bbb was achieved using the Gal80^{ts}/Gal4/UAS system. Three RNAi lines were tested. The genotypes used were: A) two controls: *X/Y; +/UAS-Neurexin-RNAi 8353; +/+* and *X/Y; +/Gal80^{ts10}; +/SPG-Gal4* and one experimental *X/Y; Gal80^{ts10}/UAS-Neurexin-RNAi 8353; +/SPG-Gal4* for the first RNAi line; B) two controls: *X/Y; +/UAS-Neurexin-RNAi 108128; +/+* and *X/Y; +/Gal80^{ts10}; +/SPG-Gal4* and one experimental *X/Y; Gal80^{ts10}/UAS-Neurexin-RNAi 108128; +/SPG-Gal4* for the second RNAi line; and C) two controls: *X/Y; +/UAS-Neurexin-RNAi 9039; +/+* and *X/Y; +/Gal80^{ts10}; +/SPG-Gal4* and one experimental *X/Y; Gal80^{ts10}/UAS-Neurexin-RNAi 9039; +/SPG-Gal4* for the third RNAi line. The two genetic controls and the mutant for each RNAi line were reared at 18°C and induced at 32°C for 2 days and then observed for courtship behavior towards a virgin female after 3 hours of resting period at RT. No significant difference in the courtship index between the controls and experimental flies was observed; indicating that conditional knock down of *Neurexin* in the adult bbb shows no effect on male courtship behavior.

Flies with intact bbb will have no penetration of the dye into the brain; the dye will be accumulated around the bbb of the brain. In contrast in the flies with compromised bbb, the dye will penetrate inside of the brain. DAPI is used for better visualization of the brain cell bodies that are situated in the brain periphery underneath the blood brain barrier. As shown in Figure 4.12 A, the bbb of wild-type CS flies is intact as evidenced by the formation of a red line around the brain. For comparison purpose, a fly with impaired bbb from a previous study done in our lab is shown in Figure 4.12 B. In case of a leaky bbb, as can be seen in Figure 4.12 B, the dye penetrates the blood brain barrier and intersperses between the neuronal nuclei.

I examined control and experimental genotypes at the induced (32°C) and at the uninduced temperature (18°C). I found that none of the genotypes tested in this assay had compromised bbb permeability as evidenced by the observation that the dextran-conjugated Texas red dye was prevented from reaching the brains in all of them. This indicates that neither overexpression (Figure 4.12 C-G) nor reduction of *miR-184* (Figure 4.12 H-K) in the bbb has an adverse effect on the structural integrity/permeability of the blood brain barrier, as evidenced by this assay. We cannot exclude small effects that would not be visible in our assay. Likewise, reduction of *sinu* expression in the adult bbb also had no effect on the permeability of the bbb (Figure 4.12 L-O). These results indicate that the behavioral courtship defects observed in these flies is a physiological response rather than due to defects in the tightness of the blood brain barrier.

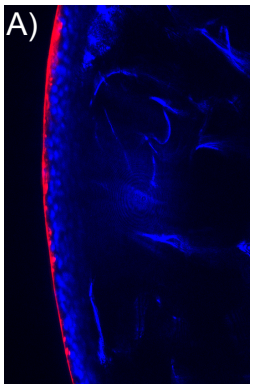

Canton S (CS)

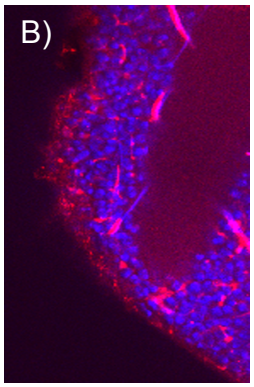

moody null mutant

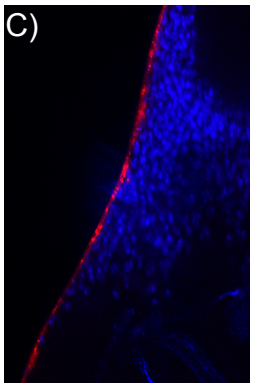

X/Y; +/Gal80^{ts10}; +/UAS-mir-184 (27.2) (U)

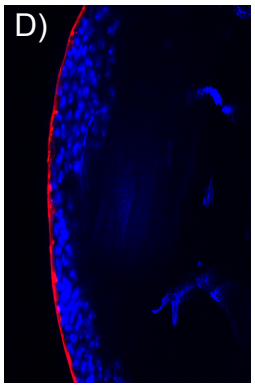

X/Y; +/Gal80^{ts10}; +/UAS-mir-184 (27.2) (I)

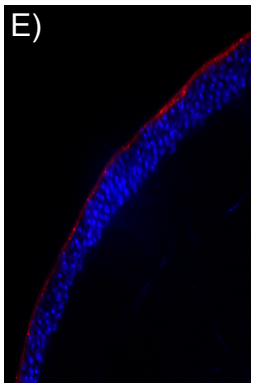

X/Y; SPG-Gal4-II, Gal80^{ts20}/ Gal80^{ts10}; SPG-Gal4-III/ UAS-miR-184 (27.2) (U)

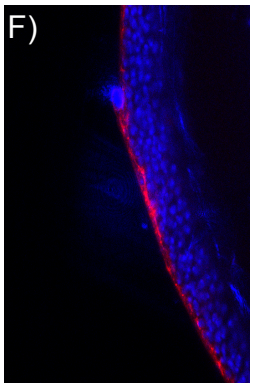

X/Y; SPG-Gal4-II, Gal80^{ts20}/ Gal80^{ts10}; SPG-Gal4-III/ UAS-miR-184 (27.2) (I)

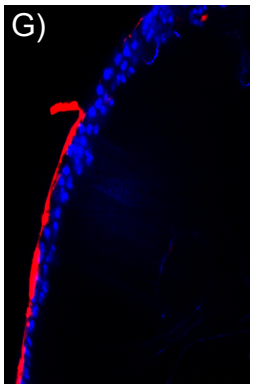

X/Y; +/+; SPG-Gal4/UAS-miR-184 27.2 (25°C)

bbb integrity of *miR-184* overexpressed mutants and controls

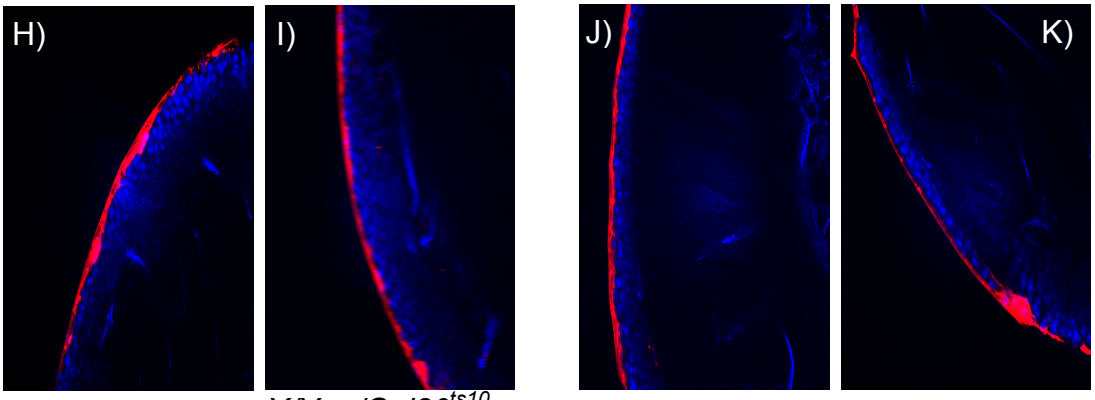

X/Y; +/Gal80^{ts10}; +/ UAS-miR-184 Sponge (7.1sp) (U)

X/Y; +/Gal80^{ts10}; +/ UAS-miR-184 Sponge (7.1sp) (I)

X/Y; SPG-Gal4-II, Gal80^{ts20}/ Gal80^{ts10}; UAS-miR-184 Sponge (7.1sp)/SPG-Gal4-III (U)

X/Y; SPG-Gal4-II, Gal80^{ts20}/ Gal80^{ts10}; UAS-miR-184 Sponge (7.1sp)/SPG-Gal4-III (I)

bbb integrity of *miR-184* sponge expressed mutants and controls

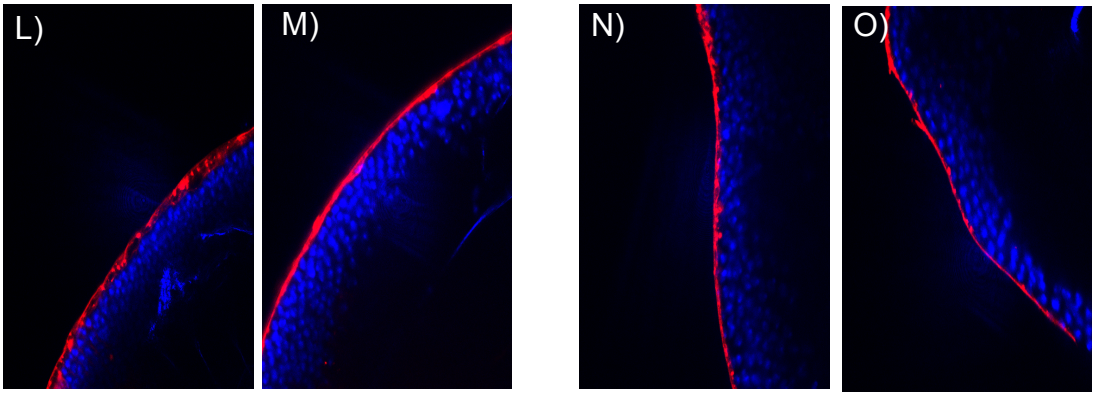

X/Y; +/UAS-sinu-RNAi; +/+ (U)

X/Y; +/UAS-sinu-RNAi; +/+ (I)

X/Y; Gal80^{ts10}/UAS-sinu-RNAI; +/SPG-Gal4 (U)

X/Y; Gal80^{ts10}/UAS-sinu-RNAI; +/SPG-Gal4 (I)

bbb integrity of *sinu-RNAi* mutants and controls

Figure 4.12: The Integrity of the blood brain barrier (BBB) in mutant flies is not compromised. In order to examine the permeability of the blood brain barrier, mutants as well as control flies were injected with 10KD dextran conjugated to Texas red florescent dye, and dye penetration into or exclusion from the brain was observed by confocal cross sectional images. DAPI (blue), which specifically stains neuronal nuclei, was used to better visualize Texas Red (red) penetration or exclusion from the brain. (A) Negative Control, Canton S- wild type flies, which show a tight blood brain barrier, seen here as a red line on the surface of the brain indicating that Texas Red is completely excluded from the brain. (B) *moody* null flies show leaky blood brain barrier (Hoxha et al., 2013). Texas Red is no longer a red line on the surface of the brain, but it penetrates and intersperses between the neuronal nuclei. (C-F) Overexpression of *miR-184* in the bbb does not have an effect on the permeability of the BBB. At 18°C, both the genetic controls and the mutants show a clear red line outside the brain and no penetration of Texas Red dye as noted in figure C and E. Conditional expression at 32°C didn't lead to any change in BBB permeability as shown in figure D and F. Additionally, overexpression of *miR-184* throughout the development of the fly doesn't affect the permeability of the bbb (G). (H-K) Silencing of *miR184* in the bbb by *the miR-184* sponge does not have an effect on the integrity of the bbb. At 18°C, both the genetic control and the mutant flies expressing *UAS-mir-184 sponge (7.1sp)* showed no penetration of Texas dye inside the brain, confirming the integrity of the BBB (Figure H and J). Conditional induction at 32°C did not compromise the bbb of *UAS-mir-184 sponge (7.1sp)* expressing control and mutant flies (figure I and K). (L-O). *sinu* mutant flies show intact bbb. At 18 °C, the uninduced controls as well as the mutant flies have intact bbb as shown by no penetration of Texas Red dye into the brain and the red line staying outside the brain (Figure L and N). M and O show that conditional induction of control as well as the mutant at 32°C also didn't affect the integrity of the BBB. U=Uninduced, flies were kept at 18°C, I= flies were induced at 32°C.

4.6 Generation of *ΔmiR-184* mutants

When I used the *miR-184 sponge* to silence *miR-184* in the bbb, the courtship phenotype of the male flies was significantly reduced. As the q-PCR results show, the reduction is significant, but not complete. It is therefore desirable to support these results by characterization of loss of function mutants. In a null mutant, we expect to see at least the same but perhaps also a more pronounced effect. We also expect that the courtship defects should be stronger if a heterozygous loss of *miR-184* (lacking one copy of *miR-184*) is combined with the *UAS-miR-184 sponge* than the defects observed by using the sponge alone. In order to investigate this, I generated a *miR-184* deletion mutant (*ΔmiR-184*) by using the method described by Iovino et al. (2009) and Parks et al. (2004).

The *miR-184* gene is located on chromosome 2 (Figure 4.13). Two FRT-bearing P-element insertion lines, f05119 (PBac{WH}f05119) and d08710 (P{XP}d08710) flanking the *miR-184* gene were selected. The *Δmir-184* deletion was created by FLP-mediated recombination of FRT-bearing P elements (PBac{WH}f05119) and P {XP}d08710). The deletion was detected by loss of w^+ and confirmed molecularly by genomic PCR (Parks et al., 2004). The *rp49* gene was used as an endogenous control.

Males containing one element (d08710) were crossed to a females containing FLP recombinase transgene. The resulting progeny male containing both the FLP recombinase and d08710 were crossed to females with the second element (f05119). After 48 hours, the vials with the parent flies were subjected to heat shock at 37°C for 1 hour. The parents were removed after 72 hours and for the next 4 days; the vials were heat shocked for 1 hour every day. The progenies were raised to adulthood and the virgin females were crossed to white eyed double balancer flies. The progenies with white eye color as

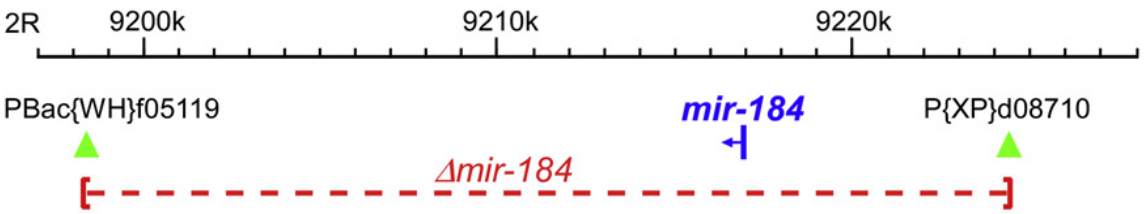

Figure 4.13: Organization of the *mir-184* locus, indicating the genomic coordinates of the mature miRNA and the *mir-184* deletion (Iovino et al., 2009). *mir-184* is a single copy gene and lies isolated within a 50 kb region on the right arm of the second chromosome (50A; 9217K). The FRT site-containing elements PBac{WH}f05119 and P{XP}d08710 (green triangles) were used to generate an FLP-induced deletion following established procedures (Parks et al., 2004).

well as orange eye color were selected. Orange-eyed flies were recovered in addition to white-eyed flies because it is possible that the removal might be incomplete. 21 individual lines with white eye color and 21 orange-eyed individual fly lines were maintained for further examination. These flies were individually crossed with double balancer flies to get the balanced 2nd chromosome.

4.6.1 Verification of *miR-184* deletion

A. Verification by PCR on genomic DNA

To confirm the deletion, genomic DNA was isolated from these fly lines (DNAzol Reagents, Invitrogen). I performed PCR on the genomic DNAs of heterozygous and homozygous deletion fly lines by using *miR-184* primers to detect *miR-18*4. I did not see amplification of the *miR-184* sequences in the flies homozygous for the deletion whereas heterozygous lines always showed the *miR-184* PCR product. As an internal control, the ribosomal protein (*rp49*) gene was present in all samples (Figure 4.14). These results confirm that *miR-184* genomic sequences are absent in the deletion lines.

B. Verification by assessing the egg/embryo morphology

An alternative way of confirming the deletion of *miR-184* in these flies was done by assessing the morphology of eggs laid by the *miR-184* deficient homozygous females. As described previously by Iovino et al., 2009, most of the *ΔmiR-184* eggs were smaller in size; the dorsal appendages were smaller and not well developed (Figure 4.15). In addition, most of the egg surface looked rougher than the wild-type control CS flies.

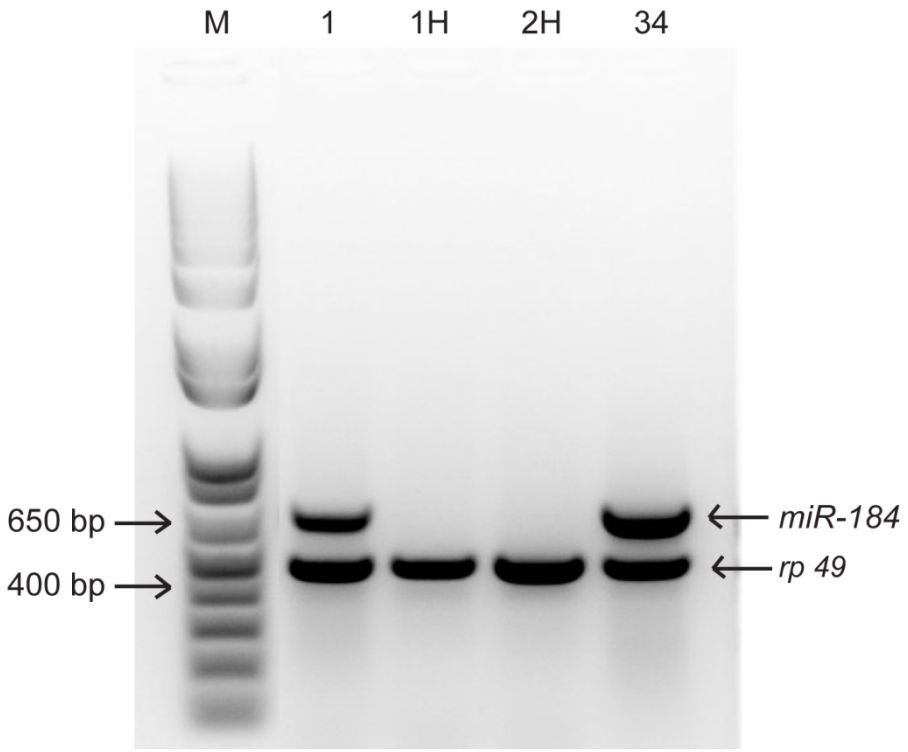

Figure 4.14: PCR of genomic DNA of *ΔmiR-184* fly lines. M=1 Kb plus ladder. *miR-184* forward and reverse primers and *rp49* primers were used. Presence of *miR-184* amplification in the stock line1 (heterozygotes) but its absence in the stock line 1H (homozygous) confirms the deletion of *miR-184* in the genome of these flies. Stock line 2H (homozygous) also shows the deletion by the absence of *mir-184* amplification. As a comparison, line 34, which was an orange-eyed stock, didn't show *miR-184* deletion. *rp49* was visible in all samples.

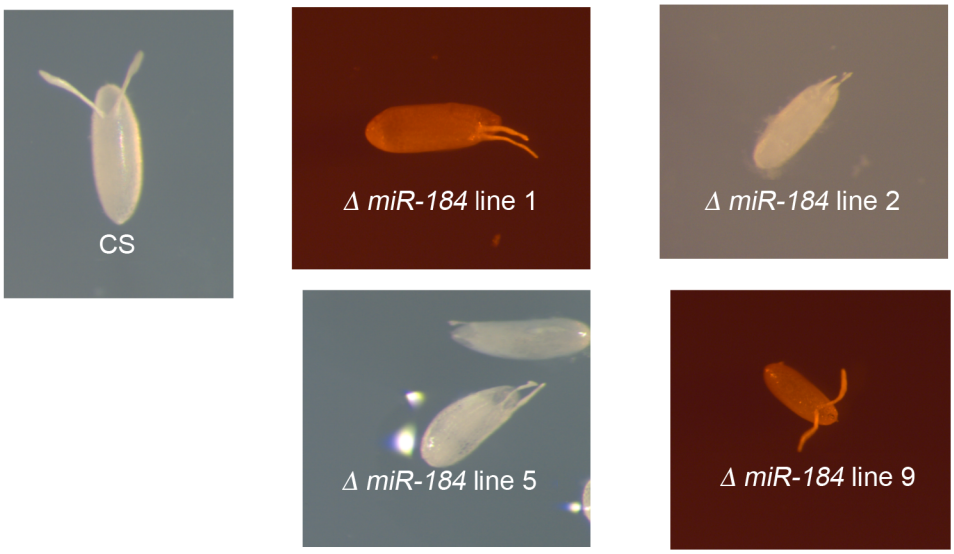

Figure 4.15: Abnormal phenotype of eggs/embryo in *Δmir-184* flies. Eggs laid by *Δ mir-184* females were often smaller than wild-type CS, a phenotype that is indicative of defects in vitellogenesis (Iovino et al., 2009). In addition, the dorsal appendages in most eggs were shortened and not well developed compared to wild-type.

Therefore, both genomic PCR data and the morphology of the eggs from *ΔmiR-184* flies confirm the deletion of *miR-184* in these flies. They will be used in future experiments to further study the role of *miR-184* in courtship.

4.7 Summary

From the microRNA Illumina sequencing results, it was found that there are many microRNAs present in the bbb of male and female flies. More than 173 microRNAs were found to match identified miRNAs present in the fly miRBase database. Among them, the top 19 microRNAs were identified in the bbb cells and *miR-184* was found to be the most abundant one.

To study the role of *miR184* in the bbb for the male courtship behavior, two transgenic lines were generated; one to overexpress (*UAS-miR-184*) and the other to silence (*UAS-miR-184 sponge*). The results show that both the overexpression and the silencing of *miR-184* in the adult bbb have a significant effect on male courtship behavior of *Drosophila*. This shows that optimal levels of this microRNA and its targets are required in the bbb of adult flies for the normal behavior. The results obtained in the behavioral tests using the sponge will be further corroborated by the combining the sponge with the loss of function mutant analysis using the *ΔmiR-184* fly lines I have generated.

In addition to its structural function in glial cells, the *miR-184* target, *sinu* is required for normal courtship behavior as shown by the courtship assay. That *sinu* is a target of *miR-184* is verified in vivo by qPCR on whole brains of males that overexpress *miR-184* in the bbb. The courtship defects observed in these mutant flies (*miR-184* and *sinu* mutants) were neither due to locomotor defects (as shown by activity assay) nor due to a compromised blood brain barrier as evidenced by their tight barrier in the dye exclusion assay.

Chapter V

Study of overlapping genes in the three genomic screens

5.1 Comparison of the three genomic screens for identifying bbb-specific molecules of *Drosophila melanogaster*

Individual sets of data from all the three screens were studied and a comparison of overlapping genes among the three screens was performed (see Table 5.1) using Flymine v 38.0 (flymine.org).

Table 5.1: Data used for the comparison

SN	Date Source/Approach	Gene lists used for comparison
1	mRNA sequencing of brains of normal males vs males with feminized bbb.	Differentially expressed genes from groups I, II, and III (see page 85).
2	Microarray analysis of isolated bbb cells of males and females.	All genes identified in the bbb cells (bbb repertoire).
3	miRNA sequencing of isolated bbb cells of males and females.	Predicted target genes of the top 19 most abundant miRNAs expressed in the bbb.

The results are shown in Figure 5.1. This analysis shows that;

- Most of the differentially expressed genes (160 of 164) identified in the RNA sequencing data are also found in the bbb sample
- Most of the top 19 miR predicted targets are present in the bbb sample
- 53 genes are found in all the three datasets, indicating that they are present in the bbb, changed in response to bbb feminization, and are potentially regulated by miRNAs in the bbb. A list of these 53 genes is shown in Table 5.2.

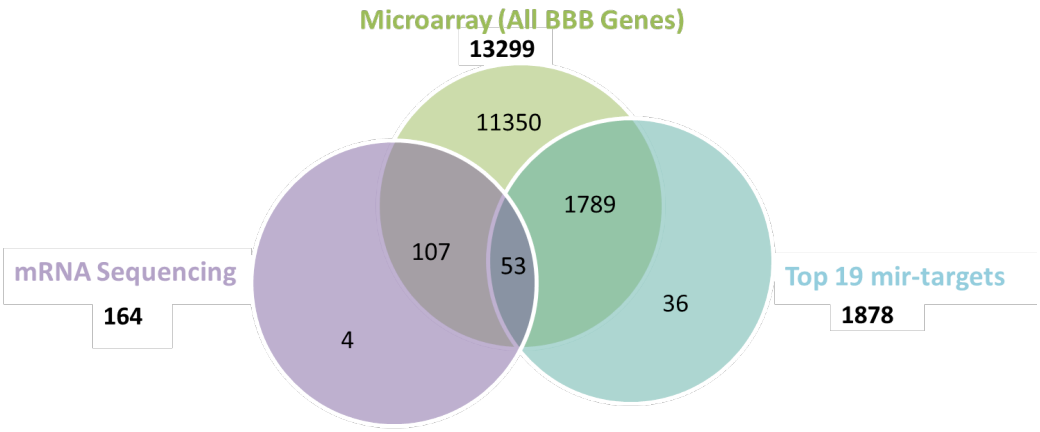

Figure 5.1: Overlap of expressed genes in the three genomic approaches to identify bbb-specific genes/molecules.

Analysis of the 53 genes shows that a number of genes are involved in transport activity either as a channel protein or a transporter protein in the brain. Many genes are predicted to be express in the "brain" or "thoraco-abdominal ganglion" (see Table 5.2). Since both of these structures are surrounded by bbb cells, we would also expect bbb-specific gene expression to be classified there. Examples are *nAcRbeta-64B, ca-alpha1T, cpx, Nacp60E, Eaat1, porin*. Other genes were found to be involved in DNA- or RNA-binding functions such as *Pif1A, Pdp1, Spen,* and *Orb2*. Other genes in the list are predicted to be protein binding, metal ion binding, receptors or involved in enzymatic activity. The functions of a number of genes in this list are not known yet.

Table 5.2: List of all 53 genes that overlap in all three categories. The gene name is shown, together with information about possible biological function and expression (data obtained from Flybase)

Symbol	Gene Name	Molecular Function	Biological Processes	Expression(male/female)	Expression (organ/tissue)
nAcRbeta-64B	nicotinic Acetylcholine Receptor beta 64B	nicotinic acetylcholine-activated cation-selective channel activity	ion transport. Protein features are: Neurotransmitter-gated ion-channel; Neurotransmitter-gated ion-channel ligand-binding;	mod. High male adult	high in brain,thoracoabdominal
Ca-alpha1T	Ca-alpha1T	low voltage-gated calcium channel activity	regulation of calcium ion transport via voltage-gated calcium channel activity.	mod. High male adult	brain
cpx	complexin	neurotransmitter transporter activity	regulation of neurotransmitter secretion; synaptic growth at neuromuscular junction; synaptic vesicle exocytosis	mod. High male adult	brain, thoracoabdominal, eye,head
NaCP60E	Na channel protein 60E	voltage-gated sodium channel activity	olfactory behavior	mod. In males, low in femals	brain
Eaat1	Excitatory amino acid transporter 1	L-glutamate transmembrane transporter activity; glutamate:sodium symporter activity; L-aspartate transmembrane transporter activity.	regulation of excitatory postsynaptic membrane potential involved in skeletal muscle contraction	high in yound male adults	fat body,brain, thoracoabdominal, eye
porin	porin	voltage-gated anion channel activity	sperm mitochondrion organization; sperm individualization; ion transport; mitochondrion organization.	very high in both	everyhere
CG7888		amino acid transmembrane transporter activity.	amino acid transmembrane transport	mod. High for both, more in males	brain, thoracoabdominal, hind gut
Shab	Shaker cognate b	delayed rectifier potassium channel activity.	regulation of action potential; synaptic transmission; regulation of heart contraction; larval locomotory behavior; regulation of synaptic activity	NA	NA
CG13928		zinc ion binding	Not known	mod.high in males	brain, thoracoabdominal, eye
CG15311		magnesium ion binding; inorganic diphosphatase activity.	phosphate-containing compound metabolic process	low	brain
Cbp53E	Calbindin 53E	calcium ion binding	cellular calcium ion homeostasis	mod. High 1 day male. Mod., more in males	brain, thoracoabdominal
cals	calsyntenin-1	calcium ion binding	synaptic transmission; calcium-dependent cell-cell adhesion.	mod. High 1 day male. Moderate in both	high in brain,thoracoabdominal
Megalin	Megalin	low-density lipoprotein receptor activity	unknown	mod. In both	thoracoabdominal, male accessary gland
CG31221		lipoprotein particle receptor activity.	unknown	mod. In males	brain, thoracoabdominal

Table 5.2 (Cont.)

Symbol	Gene Name	Molecular Function	Biological Processes	Expression(male/female)	Expression (organ/tissue)
ct	cut	DNA binding; sequence-specific DNA binding transcription factor activity	process; cellular process involved in reproduction; cell cycle; sensory perception of mechanical stimulus; multicellular organism reproduction	mod. In males, low in femals	brain, thoracoabdominal, malpigian tubules
Pif1A	PFTAIRE-interacting factor 1A	sequence-specific DNA binding transcription factor activity; sequence-specific DNA binding.	regulation of transcription, DNA-dependent.	Very High in Male	brain, thoracoabdominal, eye,head
Pdp1	PAR-domain protein 1	DNA binding	growth; circadian rhythm; mitosis; DNA endoreduplication; response to nutrient.	Mod. High in young male adults	brain, thoracoabdominal
spen	split ends	nucleotide binding; nucleic acid binding.	biological regulation; system development; cell fate commitment; cellular process; neuroblast fate commitment;sensory organ development;	more in females than males	brain
orb2		mRNA binding	ong-term memory; male courtship behavior.	NA	NA
mub	mushroom-body expressed	poly(C) RNA binding.	regulation of alternative nuclear mRNA splicing, via spliceosome.	NA	NA
su(w[a])	suppressor of white-apricot	RNA binding.	nuclear mRNA splicing, via spliceosome.	mod. High for both	
futsch	futsch	protein binding; microtubule binding	olfactory learning; neurofilament cytoskeleton organization; negative regulation of neuron apoptosis; dendrite morphogenesis; microtubule cytoskeleton organization; axonogenesis; axon cargo transport; regulation of synaptic growth at neuromuscular junction.	mod. In males	eye, brain
bun	bunched	protein homodimerization activity.	ovarian follicle cell development; programmed cell death; multicellular organism reproduction; positive regulation of biological process; gamete generation; gland morphogenesis; sensory organ development.	mod. High for both	brain, thoracoabdominal
tim	timeless	protein binding	circadian behavior; locomotor rhythm; mating behavior; copulation.	mod., more in males than females	
14-3-3zeta	14-3-3zeta	protein binding; protein heterodimerization activity; protein homodimerization activity.	germarium-derived oocyte fate determination; mitotic cell cycle, embryonic; learning or memory; protein stabilization; chromosome segregation; oocyte microtubule cytoskeleton polarization; protein folding	mod. High for both	brain, thoracoabdominal, eye,head
comt	comatose	**ATPase activity.**	Golgi organization; regulation of short-term neuronal synaptic plasticity; phagocytosis, engulfment.	mod. High male adult	brain, thoracoabdominal, eye,head
Ggamma30A	G protein gamma30A	**GTPase activity.**	phototransduction	Very High in Male	eye, brain, head
Rab3	Rab-protein 3	**GTPase activity**	maintenance of presynaptic active zone structure.	mod. In males, low in femals	
unc-13	unc-13	diacylglycerol binding	synaptic transmission; synaptic vesicle exocytosis.	mod. In both	brain, thoracoabdominal
qvr	quiver	GPI anchor binding	regulation of synaptic transmission, cholinergic; positive regulation of circadian sleep/wake cycle, sleep.	mod. In males	

Table 5.2 (Cont.)

Symbol	Gene Name	Molecular Function	Biological Processes	Expression(male/female)	Expression (organ/tissue)
Dh44	Diuretic hormone 44	neuropeptide hormone activity.	body fluid secretion	mod. In males, very low in females	brain
RpL27A	Ribosomal protein L27A	structural constituent of ribosome	mitotic spindle elongation; mitotic spindle organization.	hgh in female	salivry gland
Treh	Trehalase	trehalase activity.	trehalose metabolic process	high in both, more in males	brain, thoracoabdominal, salivary gland
kis	kismet	ATP-dependent helicase activity.	neuron differentiation; immune response; embryonic pattern specification; pattern specification process; post-embryonic organ morphogenesis; segment specification; short-term memory.	mod. High in females	brain, thoracoabdominal
Syn	Synapsin	ATP binding; ligase activity	olfactory learning; memory; response to heat; optomotor response; behavioral response to ethanol; male courtship behavior.	mod. In males	brain, thoracoabdominal
CG10077		RNA helicase activity	Not known	Very High in Male	brain, thoracoabdominal, male accessary gland
CG42856		protein serine/threonine kinase activity.	protein phosphorylation.	NA	NA
2mit		Unknown	unknown	low in male, very low in female	
CG34306		Unknown	unknown	low in both	
CG31712		Unknown	unknown	mod. In both	brain, thoracoabdominal
CG42613		Unknown	unknown	mod. High male adult	brain
CG42784		unknown	unknown	NA	NA
beat-VII	beat-VII	Unknown	unknown	low in male, very low in female	brain, thoracoabdominal
CG32521		Unknown	unknown	High in males, mod. high in females	ovary, head
Rtnl1	Rtnl1	Unknown	inter-male aggressive behavior; olfactory behavior.	same in both	everyhere
Tsp5D	Tetraspanin 5D	Unknown	unknown	mod., more in males than females	brain, thoracoabdominal
CG6327		Unknown	unknown	mod. High in females, mod. In male	thoracoabdominal, salivary, brain
CG6329		Unknown	unknown	mod. In males, low in femals	NA
CG2217		unknown	unknown	mod. In males	brain, thoracoabdominal
CG6700		Unknown	unknown	mod. In both	brain
chrb	charybde	Unknown	negative regulation of growth; head involution; cell death	mod. High in females, mod. In male	eye, head, heart
Msr-110	Msr-110	Unknown	unknown	Very high in adult male n 1 day female	Head, brain, male accessory gland
Mnn1	Menin 1	unknown	response to stress; biological regulation; response to DNA damage stimulus; response to stimulus; response to abiotic stimulus; determination of adult lifespan; post-embryonic organ morphogenesis; DNA repair; proboscis development.	more in females than males	brain

5.2 Candidate gene *qvr/sleepless*

One of the expressed genes in the overlapping intersection of the gene lists was the gene ***quiver (qvr),*** also known as ***sleepless***. *qvr* was present in the "all bbb genes" list of the bbb microarray experiment. Further, this gene was among the targets of the most abundant microRNA, *miR-184* in the bbb. Interestingly, in the mRNA sequencing result, *quiver* was one of the genes whose expression was down regulated in the brains of male with feminized bbb. In addition, this gene was also found by Chang et al. (2011) to be *tra*-dependent gene. Modencode data suggest that this gene is male preferentially expressed in adult flies (Flybase.org).

qvr has previously been isolated in two screens: In one for altered response to ethanol (LaFerriere et al., 2008), and in another as a gene that is required for normal wake/sleep cycles (it is therefore also called *sleepless*) (Koh et al., 2008). The QVR protein is a GPI-anchored protein linked to the plasma membrane and is predicted to belong to the Ly-6/neurotoxin family of proteins. These proteins can act as receptors, but also, upon GPI cleavage, as signaling molecules that can change the activity of various ion channels. In fact, in *Drosophila*, *qvr* has been shown to interact with and modulate Shaker potassium channels (Dean et al., 2011; Wu et al., 2010). It would therefore be attractive to speculate that *qvr* can act as a bbb effector that can modulate the excitability of brain neurons in behavioral circuits. Given the presence of this gene in the bbb (known from the microarray all gene list); being the target of *miR-184,* the most abundant microRNA in the bbb; and being *tra*-dependent and a down-regulated gene in mRNA sequencing experiment, I hypothesized that *qvr* has a role in the bbb for male courtship

behavior. Therefore, I investigated whether *qvr* has a role in the bbb for normal male courtship behavior.

5.2.1 Effect of *qvr* mutation on male courtship behavior

In order to investingate the role of *qvr* in courtship behavior, different *qvr* mutant alleles were tested for their courtship towards a young virgin female. Three different mutant alleles known as *P1*, *P2*, and *Ex40* lines (courtesy of Amita Sehgal) and their heteroallelic combinations were tested. *P1* is a severe hypomorph/null, *P2* is a hypomorph and *Ex40* is also a null mutant. As shown in Figure 5.2, the courtship index of the *P1/P2* mutant combination as well as the courtship index of the *P1/Ex40* combination is significantly reduced in comparison to their control counterparts.

The *qvr* mutants showed significant reduction in courtship behavior compared to the heterozygous control group. However, the mutant flies had locomotion problems, as described previously for these mutants (Koh et al., 2008). All of these mutants affect *quiver* in all the cells where it is expressed. It is likely that the locomotion problems are caused by *quiver* reduction in other cells than the bbb. In order to assess a possible role for *quiver* in the bbb, I next performed experiments in which I expressed *quiver* RNAi only in the bbb.

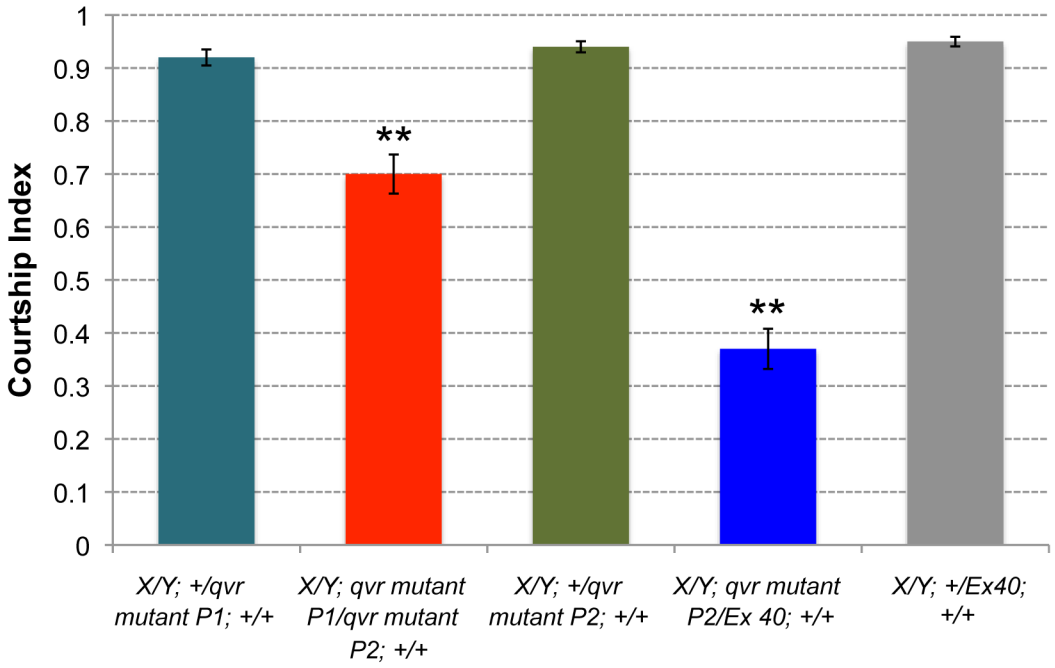

Figure 5.2: Effect of *qvr* mutations on male courtship behavior: In order to investigate the role of *qvr* in courtship behavior, different *qvr* mutant allele males were tested for their courtship index towards a young virgin female. Three different mutant alleles known as *P1*, *P2* and *Ex40* lines (courtesy of A. Sehgal) and their heteroallelic combinations were tested. All the crosses were grown at RT and the courtship assays were performed (as described previously) with 5-6 days old males grown and reared at RT. As indicated by ANOVA analysis with Bonferroni multiple comparisons test, the courtship index of the *P1/P2* mutant combination as well as the courtship index of the *P1/Ex40* combination is significantly reduced to their control counterparts ($p<0.0001$, $n=16$). Error bar represents the standard error of the means.

5.2.2 Reduction of *qvr* in the bbb throughout development and adulthood affects normal courtship behavior

To address the question of if this effect of *qvr* mutation is due to a signal coming from the bbb or somewhere else, I tested two RNAi lines against *qvr* using the bbb specific driver *SPG-Gal4*. The genotypes of two RNAi lines were: *UAS-qvr-RNAi 104533/KK* and *UAS-qvr-RNAi 16792/GD*. The crosses were set at RT and the virgin male progenies were placed at RT in individual food vials and matured for 5-6 days before testing for courtship. The genotypes for the first RNAi line tested were: two control genotypes: *X/Y; +/+; +/SPG-Gal4* and *X/Y; +/UAS-qvr-RNAi 104533/KK; +/+* and one experimental genotype: *X/Y; +/UAS-qvr-RNAi 104533/KK; +/SPG-Gal4*. The courtship index of the experimental flies was significantly reduced compared to the two control genotypes (Figure 5.3A, ANOVA, Fisher's test, $p<0.01$, for the Gal4 control and $p<0.02$ for the RNAi control). With the second RNAi line, the genotypes tested were the two controls: *X/Y; +/+; +/SPG-Gal4* and *X/Y; +/+; +/UAS-qvr-RNAi 16792/GD* and the experimental genotype: *X/Y; +/+; SPG-Gal4/UAS-qvr-RNAi 16792/GD*. The second RNAi line didn't show any significant reduction in the courtship index of the mutant compared to the controls (Figure 5.3B).

(A)

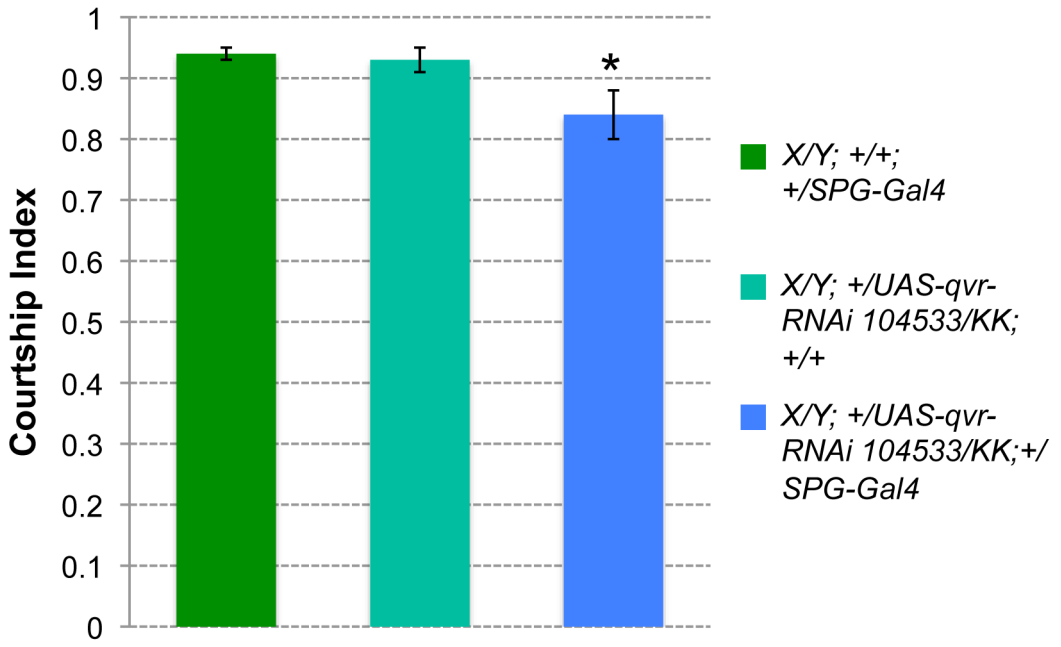
Courtship Index
1
0.9
0.8
0.7
0.6
0.5
0.4
0.3
0.2
0.1
0
*
X/Y; +/+; +/SPG-Gal4
X/Y; +/UAS-qvr-RNAi 104533/KK; +/+
X/Y; +/UAS-qvr-RNAi 104533/KK;+/ SPG-Gal4

(B)

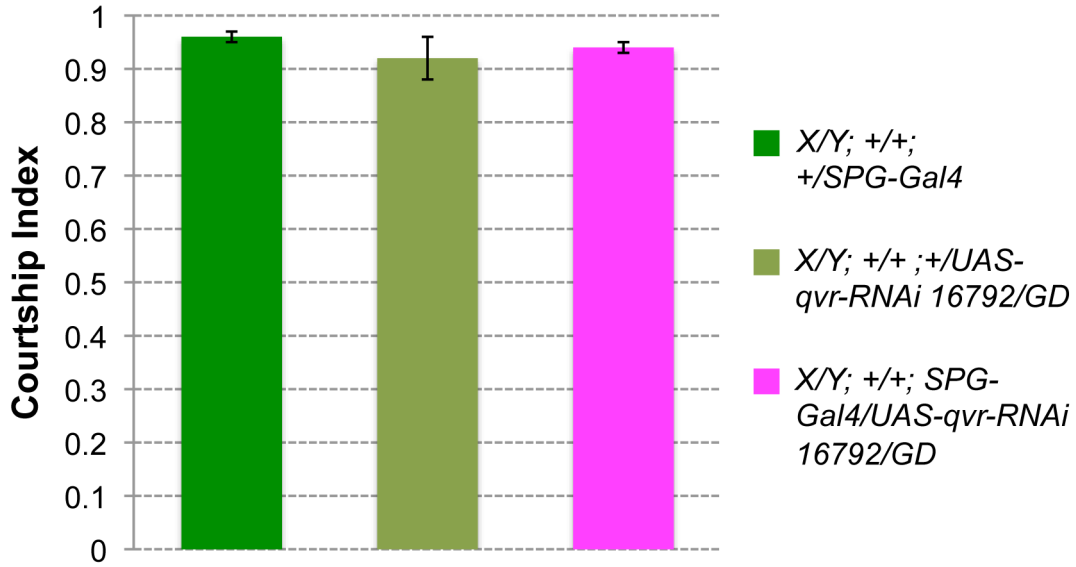
Courtship Index
1
0.9
0.8
0.7
0.6
0.5
0.4
0.3
0.2
0.1
0
X/Y; +/+; +/SPG-Gal4
X/Y; +/+ ;+/UAS-qvr-RNAi 16792/GD
X/Y; +/+; SPG-Gal4/UAS-qvr-RNAi 16792/GD

Figure 5.3: Expression of *qvr* RNAi in the bbb throughout development and adulthood affects normal courtship behavior. In order to test the role of *qvr* in the bbb, the RNA was targeted by using the two RNAi lines available: *UAS-qvr-RNAi 104533/KK* and *UAS-qvr-RNAi 16792/GD*. The crosses were set at RT and the virgin male progenies were reared at RT in individual food vials and matured for 5-6 days before testing for courtship assay. **(A)** The genotypes for the first RNAi line tested were: two control genotypes: *X/Y; +/+; +/SPG-Gal4 and X/Y; +/UAS-qvr-RNAi 104533/KK; +/+* and one experimental genotype: *X/Y; +/UAS-qvr-RNAi 104533/KK; +/SPG-Gal4*. The courtship index of the experimental flies was significantly reduced compared to the two control genotypes (Fisher's test, $p<0.01$, for the Gal4 control and $p<0.02$ for the RNAi control). **(B)** With the second RNAi line, the genotypes tested were the two controls: *X/Y; +/+; +/SPG-Gal4* and *X/Y; +/+; +/UAS-qvr-RNAi 16792/GD* and the experimental genotype: *X/Y; +/+; SPG-Gal4/UAS-qvr-RNAi 16792/GD*. The second RNAi line didn't show any significant reduction in the courtship index of the mutant compared to the controls. Error bar represents the standard error of the means.

5.2.3 Knockdown of *qvr* in a *qvr* mutant background leads to reduced male courtship behavior

This result from the RNAi experiments described above suggests that *qvr* has a role in the bbb for normal male courting behavior. Since this effect is relatively weak, I next explored whether RNAi expression in a *qvr* heterozygous mutant background would further reduce courtship. I combined the mutant allele *P1* with the RNAi line 104533/KK. In order to test the effect of RNAi-mediated knock down of *qvr* in the bbb in a *qvr* heterozygous mutant background, the bbb-specific driver, SPG-Gal4 was used to express q*vr-RNAi (UAS-qvr-RNAi 104533/KK*) in a *P1/+* mutant background. In addition, *Dicer* was also expressed in these flies to augment the function of RNAi. The genotypes used were: *Dicer/Y; +/UAS-qvr-RNAi 104533/KK; +/+, X/Y; +/qvr mutant (P1); SPG-Gal4/+,* and *Dicer/y; qvr mutant (P1)/UAS-qvr-RNAi 104533/KK; +/SPG-Gal4*. There was a significant reduction of courtship by the flies expressing RNAi in the heterozygous *qvr P1* mutant background compared to the controls. These data indicate the importance of *qvr* in the bbb for male courtship behavior (Fishers' test; compared to the Gal4 control, $p<0.02$; compared to RNAi control, $p<0.05$,). The heterozygous *qvr* mutant showed normal courtship (Figure 5.4). The observed courtship index in the *P1/qvr RNAi* flies is lower than by just *quiver RNAi* itself (Figure 5.3 A). This could be an effect of the heterozygous *qvr-P1* mutation, but since we added dicer to the genotype, this could also be due to enhanced RNAi efficiency due to the presence of UAS-Dicer.

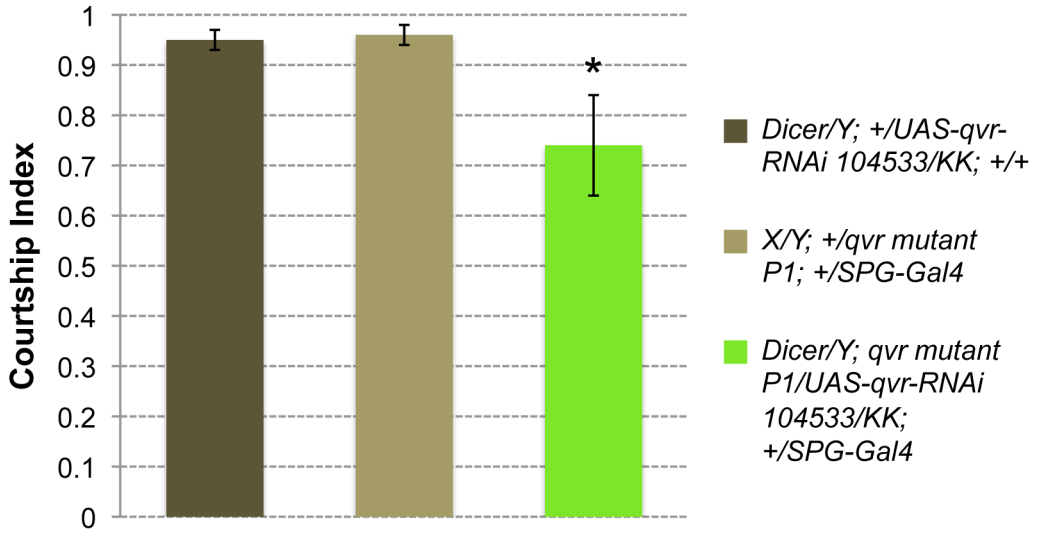

Fig 5.4: Knockdown of *qvr* in the bbb in a *qvr* mutant background results in reduced male courtship behavior. In order to test the effect of expressing q*vr-RNAi* in the bbb in a *qvr* mutant background, the bbb-specific driver, SPG-Gal4 was used to express *qvr-RNAi (UAS-qvr-RNAi 104533/KK* -in a *P1* mutant background. In addition, *Dicer* was also expressed. The genotypes used were: *Dicer/Y; +/UAS-qvr-RNAi 104533/KK; +/+, X/Y; +/qvr mutant (P1); SPG-Gal4/+,* and *Dicer/y; qvr mutant (P1)/UAS-qvr-RNAi; +/SPG-Gal4*. The courtship index of flies expressing qvr RNAi in the heterozygous *qvr* mutant background is significantly reduced compared to the controls (Fishers' test; compared to the Gal4 control, $p<0.02$; compared to RNAi control, $p<0.05$, $n=10$). The courtship index of the heterozygous *qvr* mutants is normal. Error bar represents the standard error of means.

5.2.4 Conditional knockdown of *qvr* in the adult bbb shows no effect on male courtship behavior

In the previous experiments (the mutant *P1/P2, P2/Ex40*) and the RNAi experiments), *qvr* is reduced/absent throughout development and adulthood. However, since we are interested in the adult role of *qvr*, I investigated the role of *qvr* in an adult male courtship behavior by conditionally expressing *qvr* RNAi only in adults using the $Gal80^{ts}$ system as described in Materials and Methods. The temporal and spatial expression of *qvr* was achieved by use of the Gal 80^{ts}/Gal4/UAS system. Two RNAi lines were driven by the bbb-specific driver, SPG-Gal4 in the presence of $Gal80^{ts}$**.** In the first RNAi line tested (Figure 5.5A), the genotypes tested were: *X/Y; +/*$Gal80^{ts10}$*; +/SPG-Gal4, X/Y; +/UAS-qvr-RNAi 104533/KK, +/+,* and *X/Y;* $Gal80^{ts10}$*/UAS-qvr-RNAi 104533/KK; +/SPG-Gal4*. Genotypes tested with the second RNAi line were: *X/Y; +/*$Gal80^{ts10}$*; +/SPG-Gal4, X/Y; +/+; +/UAS-qvr-RNAi 16792/GD, and X/Y; +/*$Gal80^{ts10}$*; SPG-Gal4/qvr-RNAi 16792/GD* (Figure 5.5B). The flies were induced for 2 days at 32°C and allowed to rest along with the uninduced flies from 18°C for at least 3 hours before testing them for courtship. Under these experimental conditions, conditional expression of *qvr RNAi* in the bbb did not reduce male courtship behavior (n=10, $p>0.05$).

(A)

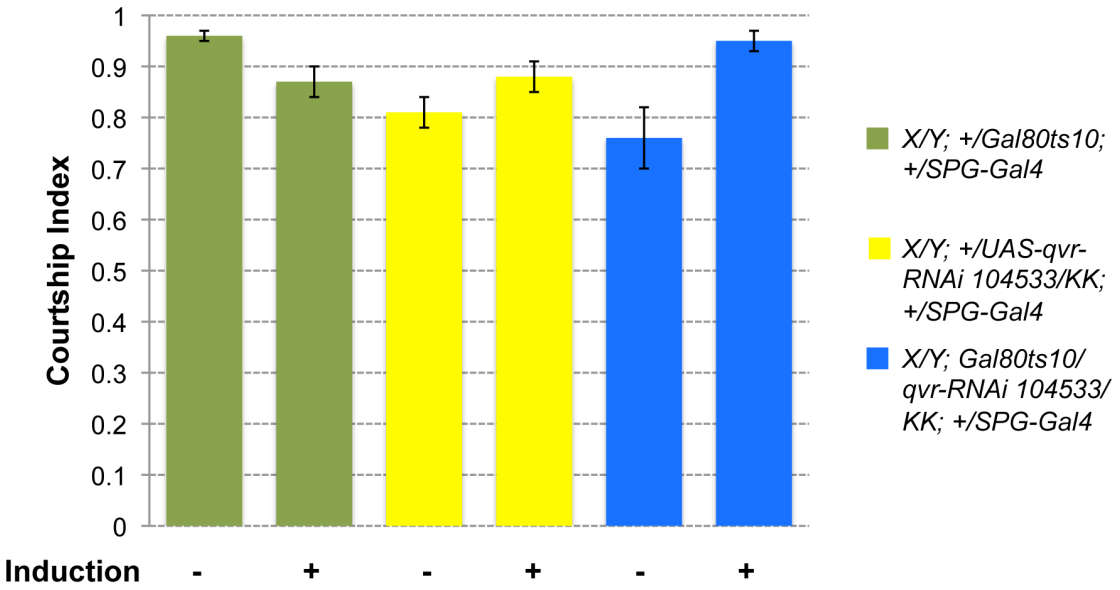
Courtship Index
1
0.9
0.8
0.7
0.6
0.5
0.4
0.3
0.2
0.1
0
Induction - + - + - +
X/Y; +/Gal80ts10; +/SPG-Gal4
X/Y; +/UAS-qvr-RNAi 104533/KK; +/SPG-Gal4
X/Y; Gal80ts10/ qvr-RNAi 104533/ KK; +/SPG-Gal4

(B)

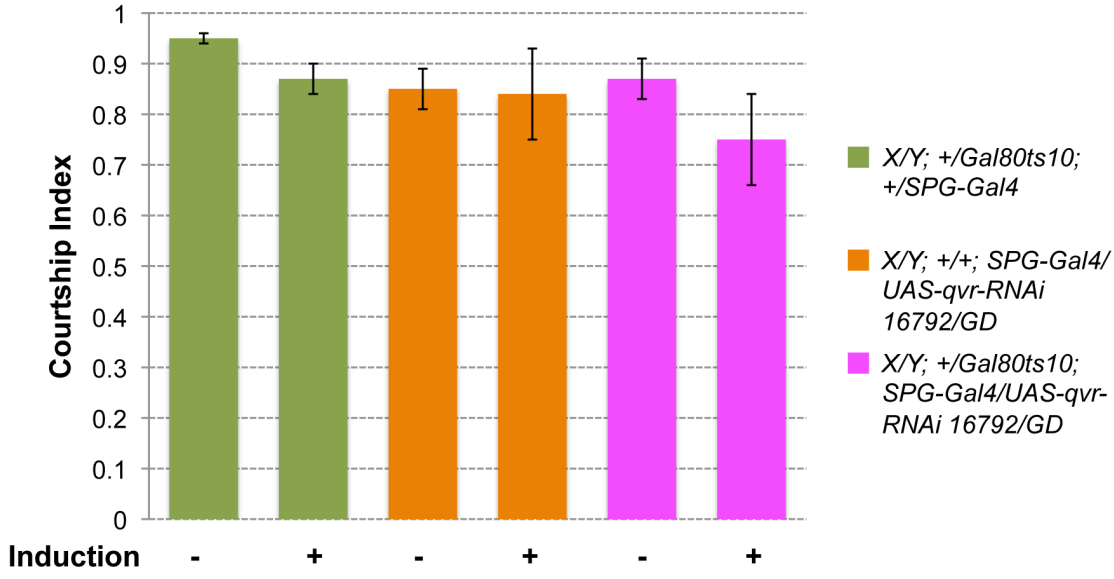
Courtship Index
1
0.9
0.8
0.7
0.6
0.5
0.4
0.3
0.2
0.1
0
Induction - + - + - +
X/Y; +/Gal80ts10; +/SPG-Gal4
X/Y; +/+; SPG-Gal4/ UAS-qvr-RNAi 16792/GD
X/Y; +/Gal80ts10; SPG-Gal4/UAS-qvr-RNAi 16792/GD

Figure 5.5: Conditional knockdown of *qvr* in the adult bbb shows no effect on male courtship behavior. The temporal and spatial expression of *qvr* was achieved by use of the Gal 80^{ts}/Gal4/UAS system. Two RNAi lines were tested for an adult role of *qvr* in the bbb for male courtship behavior. The two genetic controls and the mutant were reared at 18°C and induced at 32°C for 2 days and then observed for courtship behavior towards a virgin female after 3 hours of resting period at RT. **(A)** The genotypes tested for the first RNAi line were: *X/Y; +/Gal80^{ts10}; +/SPG-Gal4, X/Y; +/UAS-qvr-RNAi 104533/KK; +/+,* and *X/Y; Gal80^{ts10}/UAS-qvr-RNAi 104533/KK; +/SPG-Gal4* for the first RNAi line tested. **(B)** The genotypes tested for the second RNAi line used were: *X/Y; +/Gal80^{ts10}; +/SPG-Gal4, X/Y; +/+; +/UAS-qvr-RNAi 16792/GD, and X/Y; +/Gal80^{ts10}; SPG-Gal4/UAS-qvr-RNAi 16792/GD*. Conditional expression of *qvr RNAi* in the bbb does not reduce male courtship behavior (n=10, $p>0.05$).). Error bar represents the standard error of the means.

This result suggests that *qvr* has a role during development rather than in adult physiology. Alternatively, there could be experimental reasons for the absence of a courtship phenotype in these flies. The driver may not be strong enough to reduce levels of *qvr* specifically in the bbb, or the reduction may be too small to cause a behavioral phenotype under the condition tested. Further experiments involving more than one driver and possibly more RNAi transgene copies could be used. A dicer transgene could be added, or the experiment could be done in the presence of a heterozygous *quiver* mutant.

5.3 Summary

In conclusion, *qvr* mutants show courtship defects in our assay, showing the importance of *qvr* in courtship behavior. This was demonstrated using heteroallelic combinations of *qvr* mutants, but also by expression of *qvr* RNAi specifically in the bbb. In contrast, conditional expression of RNAi only in adult males did not lead to a courtship phenotype. This may be due to the experimental conditions chosen, or it could indicate that the main role of *quiver* is during development.

Chapter VI

Discussion

6.1 Feminization of the bbb results in differential expression of many sex-specific (*tra*- dependent) genes

The blood brain barrier is an important selective interface between circulating factors and the brain. The existence of a sexually dimorphic bbb between males and female has been suspected based on the evidence of differential blood brain barrier permeability in the two sexes in rats (Oztas et al., 1992). Many studies in mammals suggest that bbb permeability is regulated by reproductive hormones (Oztas and Kaya, 1998; Saija et al., 1990) and a role of serum gonadotropins has been related to the cerebropathophysiology of age-related neurodegenerative diseases such as stroke and Alzheimer's disease (Wilson et al., 2008). Moreover, modifications of blood brain barrier function in a variety of diseases have been reported such as in stroke (Sandoval and Witt, 2008), epilepsy (Diler et al., 2007) and seizures (Oztas, 1998). These studies show that the blood brain barrier is modulated in health and diseases in a sex-dependent manner. Moreover, a beneficial effect of optimal ethanol concentration on bbb integrity through the altered expression of tight junction proteins (zonula occludens-1 and laminin) after stroke has been shown (Peng et al., 2013). On the other hand, a negative effect of alcohol on bbb function has been documented. Interestingly, a recent study from our lab has suggested that the bbb itself is sexually dimorphic in *Drosophila* (Hoxha et al., 2013). This study shows that the bbb plays a crucial role in the regulation of male courtship behavior in *Drosophila*. When the bbb is feminized in an otherwise normal male, the courtship index drops significantly, indicating the presence of male-specific factors and processes in these cells. Importantly, while some of these sex-specific factors may affect sex-specific development of the bbb, the same study demonstrated that feminization of

the bbb exclusively in the adult is sufficient to reduce male courtship. Thus, male-specific factors are physiologically required in courting males. Yet, it is not known what sex-specific genes/molecules are present in the bbb which are important for bbb function including the courtship behavior. In this dissertation, I investigated these factors by using a genomic approach, mRNA sequencing of dissected whole male brains with feminized bbb and comparing it to control male brains with the normal bbb. The feminization of a specific tissue and/or organ is possible in *Drosophila* because in this organism the sex of the somatic cell is controlled cell-autonomously. Therefore, one can manipulate the sex of the blood brain barrier layer without affecting the sexual identity of the surrounding cells. Hence, ectopic expression of the female transcription factor *transformer* (TraF) produces feminization of the cells in which it is expressed (Ferveur et al., 1995).

Our RNA seq analysis of male brains with feminized bbb in comparison to control males identified a number of differentially expressed transcripts. To assess the nature of these transcripts, we compared these results from our screen to the results obtained in a previous study done by Chang et al. (2011). In that study, the authors were investigating the changes in the transcriptomes in the heads of *tra* mutant (*tra*-dependent gene expression) flies with the transcriptomes of fly heads of female vs male flies (sex-specific gene expression). The screen by Chang et al. differs from ours in that they were examining whole heads. This means that their sample includes the fat body that surrounds the brain that has already been shown to express many sex-specific transcripts. The fat body is absent in our samples which consists of entire brains that were carefully cleaned of other cells. The comparison of our data with their data demonstrates that a majority of the transcripts identified in our screen was previously identified as sex-specifically

expressed. Even more importantly, a large proportion of genes identified have been identified by Chang et al. (2011) as genes regulated by *tra*. Since in our experiment, we feminized the bbb by expression of *tra*, this is the type of transcripts we would expect to find.

A number of the differentially expressed genes in our data have been classified as genes primarily expressed in the brain. This is not an unexpected outcome because the changes in the bbb (by feminization) could result in gene expression changes within the brain itself. Alternatively these genes may function in both the brain and the bbb. Since the feminization of the bbb was carried out throughout development and adulthood, the changes in gene expression could be due to a developmental as well as a physiological effects. Currently, we cannot distinguish between the two possibilities. In contrast, the microarray experiments identify transcripts in adult heads.

Several other previous studies have suggested that there are many sex-specifically expressed genes in different tissues or cells or organs outside of reproductive tissues. In an elegant experiment, Lazareva et al. (2007) have shown that feminization of adult fat body affects male courtship behavior implying the importance of sexual identity of the fat body and sex-specific factors in the fat body for normal male courtship behavior. These factors have not identified yet. Similarly, gene expression profiling of *Drosophila* heads suggested a role for fat body cells in the generation of sex-specific distinct physiological conditions in male and female head (Fuji and Amrein, 2002). Many sexually dimorphic genes have been found in liver, adipose, muscle and brain tissues of mammals (Yang et al., 2006). Sex and segment specific gene expression profiles of *Drosophila* have been

carried out to identify dimorphic bristle patterns of first and second legs between males and females (Barmina et al., 2005).

One of the most recent studies by Chang et al. (2011) has shown that there are many sex-specific transcriptome differences between the adult male and female head tissues. In addition, they found that many sex-specific gene isoforms differ between males and females. Interestingly, differential gene expression was also observed in several experiments that examined changes in head gene expression of flies after exposure to conspecific flies of the same or the opposite sex (Ellis and Carney, 2009, 2010, 2011).

While we clearly identified relevant transcripts in our screen, the screen also has a few limitations, which may have affected the results we obtained. For sex-specifically expressed bbb genes that are also fairly strongly expressed in the brain, a small change in the bbb cells may not be significant enough to be detected. This issue would be enhanced if the datasets show a lot of variability. Despite this potential limitation, we have observed a number of sex-specific and *tra*-dependent transcripts from the screen. The biological replicas in our RNA seq were n=2, and each of the replicas was only sequenced once on the Illumina sequencer. Biological replicas of 3 of more would decrease variability. In the future, more biological replicas would be desirable. New bar-coding techniques are available that allow to run several samples in one slot of the sequencing machine and thus reduce costs.

6.2 Microarray analysis of male and female bbb cells showed expression of many sex-specific genes in the bbb of *Drosophila melanogaster*

Our previous behavior data from males with feminized bbb suggested that sex-specific transcripts in the bbb exist and contribute to courtship behavior. I studied the genes expressed in the bbb of males and females by using the bbb driver SPG-Gal4 (Stork et al., 2008) to express the fluorescent DS Red protein and have isolated bbb cells by brain dissection and selection of fluorescent cells (Figure 3.2). RNA extracted from these cells of males and females was then used in a microarray experiment to identify bbb transcripts, specifically the ones that differ between males and females.

Out of a total of 32,162 identified transcripts in the bbb, we found 112 genes that were enriched over 2 fold in males and 172 genes that were enriched over two fold in females. When the cutoff is set at 1.5 fold enrichment, the numbers are 372 and 339 respectively in males and females. For this analysis, the intensity values were normalized to the 75th percentile intensity of each array and p-values are based on a Welch T-test. Among those transcripts are some that would be expected to be identified; *roX1* and *roX2*, two non-coding RNAs with a crucial role in male dosage compensation, which have previously been shown to be preferentially present in males. In addition, *dsx* was identified in both male and female: CG11094-RA *dsx*M and CG11094-RB *dsx* F. While the microarray platforms we utilized do not distinguish between spliced versions, they do recognize different 3' ends. The male and female *dsx* transcripts differ in their 3'ends in addition to their internal alternative splicing, which explains why sex-specific *dsx* transcripts were identified in the microarray screen. The presence of many female specific genes such as *yolk protein* gene may indicate the contamination from the fat

body around the brain during the manual isolation of the bbb cells. Only a few cells would lead to their identification since they are exclusively expressed in females in high abundance.

In the future, Fluorescent Activated Cell Sorting (FACs sorting) techniques could be used to avoid this type of contamination. However the presence of many signature genes such as the dosage compensation gene *roX1* and *roX2* only in the males as sex-specific genes indicate that the results we are observing in our microarray of bbb cells are genuine results. We believe that the quality of this screen and the data is good. Our screen identifies a number of sex-specific transcripts. The three biological replicas for each sex show little variation. The RNA was amplified only once prior to probe generation (by generating the cDNA which give rise to cRNA used as probe) and predicted transcripts were identified.

The gene ontology (GO) classification of the genes that are sex-specifically expressed in the bbb shows enrichment in genes involved in biological processes such as sex-determination, dosage compensation, courtship behavior, male/female genitalia morphogenesis and behavior. In terms of cellular components, the sex-specific genes are found to be expressed in X-chromosome, dosage compensation complexes, intracellular membrane bound organelles, microtubule associated complexes, and many protein kinase complexes. In terms of molecular function, many of the sex-differentially expressed genes are linked to kinase regulator activity, mRNA binding, 3' and 5'-UTR binding, growth factor binding, and insulin receptor binding function.

Of interest is also the presence of GO groups indicating involvement of actin and other cytoskeletal components. *moody*, a bbb-specific G-protein coupled receptor

(GPCR) has been shown to be involved in the organization of the actin cytoskeleton of the bbb during development (Hatan et al., 2011). The identification of neuronal transcripts may indicate some contaminations of the RNA prep with neuronal cells. However, channels and signaling molecules that may have been described in neurons previously, may also be components of the bbb. There is an increasing appreciation that glial cells have important signaling functions that are required for neuronal function. A number of splicing factors such as *Suv(a)* and *B52* belonging to the SR protein family of splicing factors were also present it the screen. We also compared the identified sex-specifically expressed genes (>1.5 fold) in our screen with the prior Chang et al. study (2011). We found that 30 genes were shared.

Many previous studies have shown sex-specifically expressed genes in different tissues or organs in *Drosophila* (Arbeitman et al., 2004; Barmina et al., 2005; Boltz et al., 2007; Dauwalder et al., 2002; Fujii and Amrein, 2002; Lazareva et al., 2007). Males and females seem to respond differently to genetic and environmental manipulations in terms of life span and aging phenotypes. Sexual differentiation in *Drosophila* has been implicated in life span and aging processes (Shen et al., 2009; Tower, 2006). For example, the *tudor* mutation increases life span in males but not in females (Shen et al., 2009). Furthermore, a differential response of males and females to alcohol related aggressive behaviors have been described in mice models (Lisciotto et al., 1990). In the future, the role of differentially expressed genes in the blood brain barrier could be studied in longevity, apoptosis, or aggression. As discussed earlier, the mammalian blood brain barrier permeability is under the influence of sexual differentiation. We could study the roles of genes in *Drosophila* relevant to human diseases such as epilepsy, seizures,

and neuronal injury. This could be a further step in better understanding of the genes that make diseases more pronounced in one sex than the other. Therefore, in the future, it would be interesting to investigate the relevance of a sexually dimorphic blood brain barrier for other behaviors and diseases.

6.3 BBB-specific *Hr46* is required for normal courtship behavior

One of the candidate genes identified from the microarray of bbb cells was the gene *Hr46*. Its RNA is male-preferentially expressed in bbb cells (>2 fold, T-test, p-value < 0.05). We found that conditional reduction of *Hr46* in the bbb reduced courtship, using two different drivers. This suggests that *Hr46* plays an active role in the bbb. *Hr46* has the characteristics of a steroid nuclear hormone receptor and plays an important role in development. The protein is expressed in response to the steroid hormone ecdysone and acts as transcriptional regulator of target genes (Carney et al., 1997; Koelle et al., 1992; Lam et al., 1999). One of its targets is *ftz-f1*. Significantly among other functions, Ftz-f1 has recently been found to bind to Met, a transcriptional regulator that binds Juvenile hormone (JH) and is thought to mediate JH regulated gene expression (Bernardo and Dubrovsky, 2012; Dubrovsky et al. 2011). These interactions are shown in Figure 6. 1. This places *Hr46* as a potential player in the integration of signals from both ecdysone and JH, the two main hormones in *Drosophila*. Little is known about the functions of JH

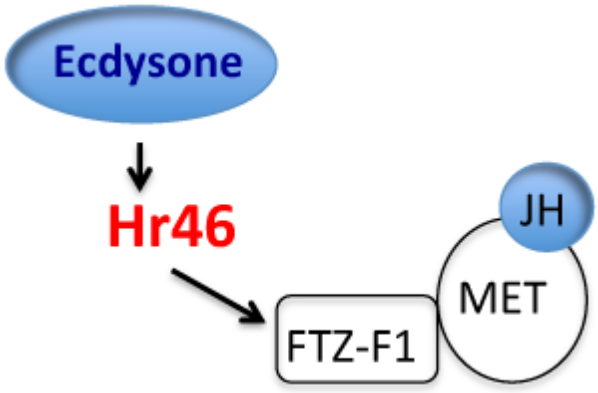

Figure 6.1: *Hr46* might link ecdysone and JH signals by regulating Ftz-f1 that acts in the JH pathway.

and ecdysone in adults beyond their roles in fertility, although a role of ecdysone in learning and memory has been shown (Ishimoto et al., 2009). Our findings point to a role of hormonal signaling in adult bbb. This is of particular interest to us, since our lab has shown recently that JH plays a role in male courtship (Wijesekera, dissertation, 2013). In addition, we have found that *ftz-f1* and *Met* transcripts are present in the bbb, as seen in the microarray characterization of these cells. Furthermore, Met is identified as down-regulated gene in one of the comparisons of the RNA seq experiment. It will be of interest to examine in the future whether these pathways play a role in the bbb for courtship. Several predicted splice forms of *Hr46* exist which are partly confirmed by cDNA sequences. RNA seq data in Flybase (http://flybase.org) suggest the sex-specific use of alternatively spliced exons. These RNAs are predicted to code for different protein isoforms that might contribute to the courtship function that we observed in our behavior data. The likely reason why *Hr46* was not identified in the feminized bbb RNA seq

experiment is the fact that *Hr46* is also expressed in the brain, so we may not have seen a small change in the bbb.

Further diagnostics of the predicted alternative exons can be accomplished by performing RT-PCR using isoform-specific primers on RNA isolated from bbb cells of males, females, and males expressing TraF in the bbb. The functional significance of the isoforms can be tested to rescue the *Hr46* courtship phenotype. Since *Hr46* is positioned as an integral part of intracellular JH response by regulating FTZ-F1, in the future, potential genetic interaction between the JH pathway and *Hr46* in courtship behavior could be tested. *Hr46* in the bbb may interact directly or indirectly with *fru* (a master regulator of courtship behavior in males) for normal male courtship behavior. Such an interaction is suggested from a very recent study from the Arbeitman lab where *Hr46* has been shown as one of the predicted downstream targets of *fru,* an observation from a global transcriptional response study as a result of overexpression of individual Fru^M isoforms in *fru* expressing neurons (Dalton et al., 2013). Therefore, in the future interaction studies could be performed by knocking down *Hr46* in a *fru* mutant background.

6.4 Many miRNAs are expressed in the bbb

MicroRNAs (miRNA) are one of the classes of small non-coding RNAs that are involved in post transcriptional regulation of gene expression in multi-cellular organisms largely by interacting with the 3'UTR of their targets affecting both the stability and translation of mRNAs (Hutvagner and Zamore, 2002). MicroRNAs have the potential to regulate sets of cell/tissue- or function-specific proteins. Therefore, a sex-specific role for

microRNAs in the bbb of male *Drosophila melanogaster* for their courtship behavior was examined. Statistical analysis showed that none of the miRNAs was sex-specifically enriched in the bbb of the male and female bbb cells. Interestingly, the most abundant, *miR-184,* is present with a large copy number (~3 million copies). The presence of such a significant amount of this miRNA in the adult bbb signifies the importance of its role beyond development and suggests tight regulation of its target protein levels in the adult bbb.

6.4.1 Role of *miR-184* in courtship behavior of *Drosophila melanogaster*

Intriguingly, several *miR-184* predicted targets are proteins with established important functions in the bbb; the prominent ones being *sinu* and *Neurexin*. It has already been shown *in vitro* that *miR-184* regulates the protein levels of *sinu* and *Neurexin* (Iovino et al., 2009. The importance of Sinu and Neurexin proteins is well established for the development of the bbb and they are important components of the septate junctions of the bbb. Mutations in *Neurexin* genes cause the breakdown of the septate junctions in the blood brain barrier (Baumgartner et al., 1996).

Similarly, *sinuous* mutants have a reduced number of septa and fragmented septate junction ribbons resulting in compromised paracellular barrier function (Wu et al., 2004, Stork et al., 2008). In addition, other predicted targets may have important roles in the bbb, *Tsf2* codes for Transferrin 2 and Transferrins have been shown to be essential for iron transport through the bbb. Tsf2 has been shown to interact with Neurexin IV. A mutation in *Tsf2* affects epithelial septate junctions in embryos (Tiklova et al., 2010). Recently, modified Transferrin has been explored as a “vehicle” to transport drugs

through the blood brain barrier into the brain and into other specific tissues such as cancer cells (Li et al., 2009; Liu et al., 2013).

Gli, gliatactin is another septate junction associated protein in vertebrate glial cells (Gilbert et al., 2001). *Gli* encodes a transmembrane protein of the serine esterase family that is homologous to the neuroligin 3 protein expressed. A mutation in *Gli* disrupts the septae normally located between the membranes and reduces its number as well as disrupts the paracellular barrier in the embryonic salivary gland (Genova and Fehon, 2003).

quiver, another *miR-184* target, has interesting properties as a signaling molecule and as a modulator of ion channels (see later). These findings suggest that *miR-184* plays an important role in the regulation of the adult bbb. The high level of this miRNA in the bbb in adults indicates that these proteins have a function beyond development.

An adult role for *miR-184* in the bbb for the regulation of male courtship in *Drosophila* was examined by altering the level of this miRNA by overexpressing and/or silencing it in the bbb. The overexpression of this miRNA in the bbb resulted in significant reduction in the courtship indices of the experimental flies compared to the controls suggesting the significance of optimal *miR-184* level in the bbb for the normal courtship behavior.

The silencing of *miR-184* in the bbb was achieved by designing and generating a transgenic microRNA sponges (miR-SPs), a *miR-184 "sponge"* by placing modified microRNA complementary oligonucleotides downstream of repetitive upstream activation sequences (UASs). Silencing of *miR-184* in the adult bbb resulted in significant reduction in the courtship index, again supporting the suggestion that optimal

levels of *miR-184* are required for normal courtship behavior.

In conclusion, both the courtship results from both the overexpression and the silencing of *miR-184* as well as a very high abundance of *miR-184* in the bbb suggest that the target proteins of this miRNA are tightly regulated. An important point to be noted is that none of the *miR-184* mutant flies exhibited locomotion defects, as evidenced in an activity assay. In addition, none of the mutants tested had compromised bbb permeability as evidenced by the observation that the dextran conjugated Texas red dye was prevented from reaching the brains. This indicates that neither overexpression nor silencing of *miR-184* in the adult bbb has an adverse effect on the structural integrity of the blood brain barrier; as assessed by this assay. However, we cannot exclude small effects that would not be visible in our assay.

When I used the *miR-184 sponge* to silence *miR-184* in the bbb, the courtship phenotype of the male flies was significantly reduced. The reduction of *miR-184* by sponge in the bbb is significant, but not complete as shown by the q-PCR results. It is therefore desirable to support these results by characterization of the *miR184* loss of function mutants I generated. In a null mutant, we expect to see at least the same but perhaps also a more pronounced effect. We also expect that the courtship defects should be stronger if a heterozygous loss of *miR-184* (lacking one copy of *miR-184*) is combined with the *UAS-miR-184 sponge* than the defects observed by using the sponge alone.

Overexpression of *miR-184* is expected to have an effect on the level of its target *sinu* since it has been shown previously *in vitro* that *sinu* is one of the targets of *miR-184* (Iovino et al., 2009). When *miR-184* was overexpressed throughout development and in adulthood using the bbb -specific driver, the mRNA expression level of its target gene,

sinu was significantly increased (almost doubled) compared to the genetic controls Our expectation was that having more *miR-184* would decrease *sinu* mRNA levels. One of the explanations for this result is that the increase in *sinu* mRNA might be the result of a feedback system trying to overcome the effect of the overwhelmingly abundant *miR-184*, as Sinu proteins are likely to be tightly controlled for proper functionality of the bbb. Or the increase in *sinu* expression could be the result of complex feedback loops with other targets (such as a suppressor of *sinu*) or indirect downstream effectors. Further experiments measuring the level of Sinu protein would be more relevant to address the question of whether the *miR-184* target, Sinu decreases post *miR-184* manipulation. Alternatively, the effect of *miR-184* overexpression on the expression of *sinu* could be examined by conditionally expressing *miR-184* only during adulthood because it is possible that the feedback mechanism that tries to keep Sinu protein levels constant is more pronounced throughout development.

6.4.2 *sinu* but *Neurexin* has a dynamic role in the adult blood brain barrier function

Our data show that manipulations of *miR-184* affect courtship. If these effects are because of changes in the abundance of *miR-184* targets, we would predict to see courtship defects when we affect their levels. Therefore, independent roles for the *miR-184* targets *sinu* and *Neurexin* in the regulation of courtship behavior were examined. Conditional RNAi knockdown of *sinu* showed a significant reduction in the courtship behavior of *Drosophila*. The adult role of *Neurexin*, another *miR-184* target was examined for male courtship behavior in the bbb by using the similar strategy as used for *sinu*. None of the RNAi lines tested showed a statistically significant reduction in

courtship indices, suggesting that *Neurexin* may not have an adult role in courtship behavior, besides its structural role during development and in adult. This suggests that courtship defects I have observed for *sinu* indicate a specific role in courtship and courtship defects are not simply caused by disturbing proteins that contribute to the bbb function. In support of this interpretation, reduction of *sinu* expression in the adult bbb had no effect on bbb permeability. However, we cannot exclude subtle effects that would not be visible in our assay.

6.4.3 Role of *quiver* in male courtship behavior

In addition to *sinu* and *Neurexin*, another *miR-184* putative target gene, *quiver* was examined for its role in regulation of male courtship behavior. The *qvr* was identified as one of the genes expressed in the microarray experiment. Interestingly, *qvr* was one of the genes whose expression was significantly down regulated in the brains of male with feminized bbb. In addition, this gene was also identified in the Chang et al. (2011) study as a *tra* dependent gene, suggesting that this is a sex-specific gene. Furthermore, the Flybase expression profile suggests that *qvr* is male preferentially expressed in flies (Flybase.org). The *qvr* mutants showed significant reduction in courtship behavior compared to the heterozygous control group. However, the mutant flies have locomotion problems as described previously for these mutants (Koh et al., 2008). Therefore, from these results, it is hard to distinguish whether the courtship phenotype observed in these mutants is due to the locomotion issues. The locomotor assay that we routinely do in our lab may not be able to address this question because we measure the overall activity as a total number of times that a fly crosses the mid line drawn along the diameter of the courtship chamber in a 3 minutes observation period. In the future, the locomotion could

be measured as the total distance walked by the fly in a given period of time. Of the two RNAi lines tested one showed a significant reduction in courtship index.

Flies in which *qvr-RNAi* was combined with the mutant allele *P1* also showed reduction in courtship index which was stronger than that observed with just RNAi alone. In contrast, an adult knockdown of *qvr* in the bbb did not have an effect on courtship behavior. The absence of the behavioral phenotype could indicate that *qvr* has a mostly developmental function, or it could be due to insufficient lowering of *qvr* in the adult time window used for RNAi expression. Further experiments involving more than one driver and possibly more than two RNAi lines could be used to further examine a physiological role of *qvr* for male courtship behavior in the bbb.

qvr has previously been isolated in two screens: In one for altered response to ethanol (LaFerriere et al., 2008), and in another as a gene that is required for normal wake/sleep cycles (Koh et al., 2008). It is therefore also called *sleepless*. Interestingly, the bbb has been implicated in the ethanol response (Peng et al., 2013; Zeng et al., 2012), and *moody*, a bbb-specific gene, was isolated based on the altered alcohol tolerance of the mutant (Bainton et al., 2005). The Qvr protein is a GPI-anchored protein linked to the plasma membrane and is predicted to belong to the Ly-6/neurotoxin family of proteins. These proteins can act as receptors, but also, upon GPI cleavage, as signaling molecules that can change the activity of various ion channels. They are therefore attractive molecules that can receive signals and pass them on. In fact, in *Drosophila*, *qvr* has been shown to interact with and modulate *Shaker* potassium channels (Wu et al., 2010, Dean et al., 2011).

Since *qvr* is a target of *miR-184* which is the most abundant microRNA in the bbb, the effect of conditionally knocking down *qvr* by RNAi in *miR-184* overexpressing background could be tested for courtship behavior. If the courtship defects get worse under these conditions, it will argue for a role of *qvr* in the bbb for adult male courtship behavior. At present, my results suggest a role for a *quiver* in the bbb during development/adulthood but an adult physiological involvement is less clear. *qvr* was identified as a bbb transcript, but it did not appear expressed sexually dimorphic in these cells. In contrast, in the feminization experiments, *quiver* was identified as a gene with altered expression. Sex-specific expression is also consistent with Flybase data. It is possible that the expression of *qvr* in the brain is sex-specific, but perhaps not in the bbb. In this case, it could be one of the transcripts in the brain that changes when the bbb is feminized.

In addition to the three predicted (*sinu, Neurexin, and quiver*) and verified targets of *miR-184*, interestingly the gene ontology classification of the remaining predicted targets indicates that they are glial-specific genes. These genes comprise a group with diverse function as predicted by Gene Ontology annotations. For example *Tsf2, Cals Ptp99A, emp, Gli, CG4313, Stau,* and *Sema-1b*, are genes which function either as anchored membrane protein, a membrane channel, or plasma membrane proteins. They have been predicted to function in different biological processes such as septate junction assembly, apical junction assembly, cell-cell junction assembly, all very common features of the bbb structure. Since the bbb is a very tightly regulated structure surrounding the brain, the presence of predicted target genes belonging to the structural constituents of the intact barrier suggests that the presence of highly abundant *miR-184* in

the bbb would be required to regulate the very tight control of these targets.

6.5 Summary

Overall, our data show that *miR-184* plays an important regulatory role in the adult bbb in the regulation of courtship behavior. Disturbing its abundance, either by overexpression or removal, affects courtship behavior, we have not observed a difference in the amount of *miR-184* in male and female bbb, but this does not mean that it cannot affect target genes differently. If target genes are present in differing amounts, regulation by *miR-184* could result in different overall levels. We have shown that two *miR-184* target genes, *sinu* and *quiver* are involved in the regulation of courtship. Remarkably, although *sinu* is best known for its contribution to the bbb barrier function, it appears to also play a more physiological role in behavior. Mutants with reduced *sinu* did not have obvious bbb defects. This could still indicate that *sinu* regulates bbb permeability in subtle ways that cannot be observed in our assay. *sinu* belongs to the class of claudins, an important family of proteins that are also important for the mammalian bbb. Its domain motifs are classified as "facilitator superfamily domain" and general substrate transporter.

This is the first time a microRNA has been identified with a role in the adult bbb and the first microRNA that affects male-female courtship. The only other example of a microRNA whose role in male courtship has been studied is *miR-124* (*miR-124* is not present among the top 19 bbb miRNAs we identified). *miR-124* is expressed throughout the brain. *miR-124* mutant males had reduced mating success with females and elicited mating from other males due to aberrant pheromone production. The same phenotype was observed when *miR-124* was removed by the expression of *miR-124* sponge in *dsx-*

expressing cells. *tra* RNA was shown to have putative *miR-124* binding sites and increased amounts of *tra* RNA was found in the mutants. The mutant phenotype could be rescued by lowering *tra* in *miR-124* mutants (Weng and Cohen, 2012). Although *tra* functions by alternative splicing of its pre-mRNA, the authors suggest that due to "noise" in that regulation, *miR-124* functions to buffer the abundance of mRNA.

While *miR-184* is by far the most abundant microRNA in the bbb, the following is a short description of the other miRNAs identified as well as some of their predicted targets.

6.6 Role of other miRNAs expressed in the bbb other than *miR-184*

Besides *miR-184*, among the other highly expressed 19 miRNAs that were found in the bbb cells, many have been implicated in major *Drosophila* developmental processes, although a few adult roles have been suggested.

Drosophila miR-315 has been shown to regulate *wnt* signaling by targeting the two important genes: *Notum* and *Axim*. *miR-315* inhibits *Axin* and *Notum*, which encode essential, negatively acting components of the Wg pathway (Silver et al., 2007).

The Dystrophin Glycoprotein Complex (DGC) is at the center of significant inheritable diseases, such as muscular dystrophies that can be fatal and impair neuronal function in addition to muscle degeneration. Recent evidence has shown that microRNAs such as *miR-252* are regulated via a Dystroglycan-Dystrophin-Syntrophin dependent pathway (Marrone et al., 2012). This miRNA was found to be expressed throughout the development and adulthood of silkworm (Liu et al., 2009).

miR-263a/b are members of a conserved family of microRNAs that are expressed in peripheral sense organs across the animal kingdom. A role for *miR-263a* and *miR-263b* in protecting *Drosophila* mechanosensory bristles from apoptosis by down-regulating the pro-apoptotic gene head involution defective (*hid*) has been shown previously. Both microRNAs are expressed in the bristle progenitors, and in *miR-263a* and *miR-263b* deletion mutants, loss of bristles appears to be sporadic, suggesting that the role of the microRNAs may be to ensure robustness of the patterning process by promoting survival of these functionally specified cells (Hilgers et al., 2010). Despite a difference in their seed sequence, they share this key common target *hid*, however, the high abundance of only *miR-263b* compared to *miR-263a* in the bbb sequencing results may suggest that its function is specific to the bbb and/or signaling. In silkworm, *miR-263b* (*bmo-miR-263b*) abundance significantly changes during the developmental transition from larvae to pupae (Liu et al., 2010).

A recent study has shown an essential role of *miR-276a* in the mushroom body neurons for memory formation and in ellipsoid body for naïve behavioral responses to odor in *Drosophila* (Li et al., 2013). Both the roles of *miR-276a* were found to be mediated by the dopamine receptor (*DopR*). A mutation of *Drosophila* dopamine receptor *DopR* induces male-male courtship behavior (Chen et al., 2012). Our data show that *DopR* is expressed in the bbb, and *miR-276a* is expressed at high copy number as seen in our Illumina sequencing results; it would be interesting to examine whether *miR-276a* mediates male-male/male-female courtship behavior via *DopR* in the bbb of *Drosophila*. Additionally, one of the predicted targets of *miR-276a* is the gene *lov.* The mutation in this gene causes aberrant courtship behavior of adult males (not directed towards the

target female) (Bjorum et al., 2013). Therefore, it would be interesting to see if *lov* is required in the bbb and *miR-276a* regulates *lov* in the bbb for male courtship since *lov* is found in our list of bbb transcripts.

The *Drosophila* let-7 complex (let-7-C) is a polycistronic locus encoding three miRNAs: *let-7*, *miR-100* and *miR-125.* The role of these miRNAs in the regulation of the innate immunity response has been shown to be regulated by 20-hydroxyecdysone (Garbuzov and Tatar, 2010). Ecdysone was shown to directly activate this locus and affect the expression of these miRNAs. The let-7-C mutation affected adult behaviors such as flight, motility and fertility as evidenced by the phenotypes from the knockout flies. In addition, *let-7* was required for remodeling of the *Drosophila* neuromusculature during larval to adult transition (Chawla and Sokol, 2012; Sokol et al., 2008). A role for the *Drosophila let-7* and *miR-125* locus has been shown in the regulation of transcription factors that control the temporal cell fate in the mushroom body (MB) lineage (Wu et al., 2012b).

In vertebrates, *miR-34* has been associated with many cancer diseases as a tumor suppressor by inducing apoptosis, senescence, and cell cycle arrest. (Hermeking, 2010). *Drosophila miR-34* displays multiple isoforms that differ at the 3' end, (Liu et al., 2011). A neuroprotective role of *miR-34* has been shown in aging in the *Drosophila* brain via regulation of *Eip74EF*, a transcription factor regulated by ecdysone (Liu et al., 2012). The role of this miRNA in the *Drosophila* bbb for aging and perhaps for male courtship behavior could be tested in future.

miR-1 has previously been found exclusively in cardiac muscles, where it regulates cardiac differentiation in *Drosophila* (Kwon et al., 2005). *Cdc42*, a Rho GTPase

is a directly repressed by *miR-1* causing the imbalance in gene expression tipping it towards deregulated cardiac function (Qian et al., 2011).

A role for *miR-7* has been described in oogenesis (Huang et al., 2013). In addition, a role of *miR-7* in photoreceptor differentiation of *Drosophila* eye has been shown previously (Li and Carthew, 2005). A hemopoietic role of *miR-7* has been described in lymph gland of *Drosophila* (Tokusumi et al., 2011).

bantam plays a positive role in the regulation of tissue growth control (Zhang and Lai, 2013), such as in *Drosophila* wing disc development (Zhang et al., 2013). *bantam* is critical for optic lobe development and proliferation of glial cells during development (Li et al., 2012). A circadian role of *bantam* has been implicated in the regulation of clock genes in *Drosophila* (Kadener et al., 2009). An adult role of *bantam* in the glial cells of the bbb could be an interesting area to examine in future.

miR-11 is a member of the largest family of miRNAs in *Drosophila*; the miR-2 family. *miR-11* specifically modulates pro-apoptotic functions to limit the level of apoptosis during *Drosophila* embryonic development. *miR-11* mutants showed embryonic lethality and defects in the central nervous system (CNS) (Truscott et al., 2011).

6.7 Predicted target genes of the top 18 miRNAs in the bbb cells

Gene ontology classification of the predicted targets of the remaining 18 miRNAs from our top 19 miRNA list are analyzed and explained as shown in Table 6.1.

Table 6.1: Top 18 miRNAs and functions of the predicted target genes

miRNA	**Predicted functions of the target genes**
let-7	The predicted targets of miRNA *let-7* shows that these genes are predominantly targeting nucleic acid/ sequence-specific DNA binding transcription factors such as *Atf3, cwo, Eip93F, bin, ac, ab, apt, h, rib, hkb*. The role of some of these genes has been implicated in regulation of circadian rhythm, morphogenesis of dendritic neurons, and glial cell differentiation.
miR-252	The predicted *miR-252* target genes are mainly found to be involved in biological processes such as organ development, system development, neuronal differentiation, metamorphosis, wing disc development, segmentation, signaling, cell differentiation, cell communication, sensory organ development, signal transduction, chemotaxis, and sex differentiation. *miR-252* targets have been predicted to be involved in protein binding, active transmembrane transporter activity, metal ion transmembrane, and transporter activity. As an example, *CG11897* and *MRP* are involved in xenobiotic transporting and ATPase activity, *Nha2* is a potassium antiporter, and *CG33310* has sodium: potassium exchanging ATPase activity. These molecules might play an important role in the bbb. In fact, the glial-specific *Hr46, sinu,* and *fray* are among the predicted targets of *miR-252*.
miR-276a	*miR-276a* targets are predicted to be involved in organ developments and regulation of biological and cellular processes. For example, *NPFR1* is involved in a G-protein coupled receptor signaling pathway; *pirk* is involved in negative regulation of innate immune response, *svp* regulates steroid hormone mediated signaling pathways, and *esc* is a chromatin/gene silencing gene.
miR-999	*miR-999* predicted targets genes are mainly enriched in developmental processes.

Table 6.1 (Cont.)

miRNA	Predicted functions of the target genes
miR-263b	*miR-263b* predicted genes are predicted to be involved in neurogenesis, axonogenesis, cell morphogenesis, chemotaxis, cell differentiation, cell adhesion, and signaling. In terms of molecular function, the target genes are enriched for receptor activity such as G-protein coupled receptor, neuropeptide receptor, transmembrane receptor, ionotropic glutamate receptor, scavenger receptor activity, and dopamine neurotransmitter activity.
miR-970	*miR-970* predicted targets are predicted to be involved in processes such as *Or85b* for sensory perception of smell, *drl* for learning and memory, *Scram2* and *Ace* for synaptic transmission, Rab6 and *Rab3* for neurotransmitter secretion.
miR-315	*miR-315* predicted target genes are predicted to be involved in many biological processes such as neuronal development, metamorphosis, and signal transduction. The majority of these genes are involved in cellular components such as plasma membrane, neuron part, cell periphery and plasma membrane part. Sequence-specific binding, GTPase regulator activity and Zn ion binding are major molecular functions of these target genes.
miR-987	*miR-987* predicted targets are predicted to be involved in cellular processes such as transmembrane transport, synapse organization, heterophilic cell-cell adhesion, cell fate specification, and photoreceptor differentiation.
miR-1	*miR-1* predicted targets are predicted to be involved in major developmental processes and cell communication, signaling, cell-cell junction organization, neuronal development, endocytosis, morphogenesis, sensor organ development, and neurotransmitter secretion. Interestingly, *miR-1* may also target bbb-specific genes such as *sinu, Neurexin, Gli, sna, aPKC, Cont, yrt*.

Table 6.1 (Cont.)

miRNA	Predicted functions of the target genes
miR-927	*miR-927* target genes are predicted to be involved in major biological and cellular processes, for example serotonin signaling pathway, cell division, and clathrin mediated endocytosis.
miR-932	*miR-932* target genes are predicted to be involved in processes in the plasma membranes and cell periphery. For example *pHCI*, a glycine gated chloride; *stan, tipE kek3, Dscam4* are intrinsic to the plasma membrane.
miR-11	*miR-11* target genes are predicted to be involved in biological processes such as signal transduction, cell communication, signaling, regulation of cellular and biological processes, generation of neurons and differentiation. The majority of these genes are involved in cell communication processes such as Notch signaling (*fng*), neurotransmitter secretion (*Syt12)*, cell-cell signaling (*fj*), and G-protein coupled receptor signaling (*Galphaf*).
bantam	Predicted targets of *bantam* are enriched for organ morphogenesis, sensory organ development. These genes are mostly expressed on the cell surface and enriched for DNA binding transcription factor activity.
miR-7	*miR-7* target genes are predicted to be involved in organ development, regulation of biological and cellular processes, single organism developmental process. These genes are mostly expressed on the cell surface and enriched for DNA binding transcription factor activity.
miR-34	*miR-34* target genes are predicted to be involved in anatomical morphogenesis, response to external stimuli, metamorphosis, taxis and neuron projection guidance. A number of these genes belong to a class of genes required for axonal guidance implicating the importance of *miR-34* in the regulation of development and regeneration of neurons. These genes are predominantly expressed in the basal lamina.

6.8 Many genes are commonly present in all three genomic screens

Individual sets of data from all the three screens were studied and overlapping comparisons of genes among the three screens were performed. All genes from bbb cells, 164 differentially expressed genes in bbb feminized whole brains and the predicted targets of the top most abundant 19 miRNAs in the bbb were used for the comparison. A total of 53 genes are found in all the three datasets, indicating that they are present in the bbb, changed in response to bbb feminization, and are potentially regulated by miRNAs in the bbb. Among the differentially expressed 164 genes in bbb-TraF mRNAseq, 160 were also present in the bbb cells. The remaining 4 are the genes that might be changing in the brain in response to bbb feminization. They are *CG43693*, *CG43729*, *CG43778*, and *CG43902*. From Flybase expression profile, these genes are found to be express mostly in fly heads. *CG43693* has a predicted amino acid transporter activity, *CG43729* is predicted to be involved in intracellular signal transduction, and the functions of the other two genes are not yet identified.

A majority of sex-specific genes in the bbb are not found in the differentially expressed genes in the bbb-TraF mRNAseq of whole brains. Only 15 genes of the 1.5 fold difference between males and females were common with the differentially expressed 164 genes in RNA seq. This could be because some genes are *tra*- independent and sex–specifically expressed or the differential expression seen in the bbb feminized brains might be a dominant effect of TraF on the expression of these genes. In addition, the comparison between the whole brain genes and the bbb genes is difficult because the methods used for identification of these genes are different. And of course the predicted

targets of the miRNAs in the bbb are identified based on computational analysis only. Therefore, they would need to be verified by *in vitro* or *in vivo* experiments. In addition, the presence of sex-specific transcripts at the transcriptional level may not necessarily indicate a functional difference of the gene at a particular space and time.

Appendix

Appendix I: 114 differentially expressed genes between the +/Gal4 control and the experimental (Gal4/TraF)

Gene	FDR for +/SPG vs +/TraF	FDR for +/SPG vs SPG/TraF (114 Genes)	FDR for +/TraF vs SPG/TraF
bnb	1	3.08E-232	3.06E-237
ATPsyn-beta	1	2.04E-108	6.87E-125
CaMKII	1	1.12E-70	3.28E-78
CR32477	1	1.13E-69	1.31E-66
CG17471	8.43E-57	1.18E-56	1
cals	0.624567941	2.79E-54	5.14E-70
CG11155	1	1.68E-42	1.61E-44
Rfabg	0.000882407	1.25E-36	2.78E-66
CG32017	1	3.10E-35	1.51E-39
Gs2	0.034676533	9.07E-31	2.89E-15
plexA	1	1.42E-23	2.30E-20
CG34220	1.78E-57	1.02E-22	8.87E-131
CG1732	3.00E-10	9.55E-18	0.825226699
futsch	8.02E-39	2.62E-15	0.000144639
CG16826	9.45E-06	2.68E-15	0.038961936
nrv3	0.417239001	1.21E-14	2.61E-07
trol	1	1.26E-14	1.26E-11
unc-13	3.14E-05	3.67E-14	0.093405478
Zyx102EF	1	6.42E-13	4.74E-15
CG42613	1	4.08E-12	2.02E-08
nrv2	1.34E-08	1.72E-11	1
CG9394	1.91E-05	9.46E-11	0.948315904
NaCP60E	1.69E-06	1.08E-10	1
qvr	0.009815598	1.41E-10	0.03591759
Actbeta	1	3.00E-10	5.45E-10
CG18437	0.004008899	9.32E-10	0.180806576
CG31221	0.309772007	1.31E-09	8.31E-19
14-3-3zeta	1	1.54E-09	3.73E-06
Atpalpha	5.78E-19	1.23E-08	1.95E-56
CG31705	0.065490365	1.46E-08	0.048812294
Eaat1	0.030241906	3.16E-08	0.139157217
CG7971	0.014236227	4.55E-08	0.25203576
unc79	4.41E-08	6.04E-08	1
ia2	1.58E-42	1.07E-07	1.01E-89
roX1	1	1.35E-07	4.39E-08
tim	1.23E-09	1.74E-07	1
Tsf1	0.342328698	4.36E-07	4.74E-15
CG6912	2.05E-07	6.04E-07	1
su(w[a])	1	6.52E-07	0.00122412
CG16971	1	1.13E-06	3.90E-05
Pif1B	0.458583847	1.28E-06	0.030165893
Msr-110	0.000742782	1.31E-06	1
pho	1	1.85E-06	1.27E-09
pAbp	0.829729711	1.92E-06	0.015783358
Irc	2.53E-14	5.19E-06	0.199594967

Gene	FDR for +/SPG vs +/TraF	FDR for +/SPG vs SPG/TraF (114 Genes)	FDR for +/TraF vs SPG/TraF
CG11076	1	6.87E-06	2.57E-06
CG11910	0.051935302	1.11E-05	0.781125007
CG10077	1	2.67E-05	0.013334628
Snap25	0.019822868	3.08E-05	1
Pitslre	1	4.20E-05	0.011677014
Ca-alpha1T	1.13E-06	4.56E-05	1
CG6329	1	5.03E-05	3.82E-05
cpx	0.910456372	5.28E-05	3.38E-10
cac	0.003674988	8.56E-05	1
pUf68	1	8.56E-05	0.015420019
CG10936	1	8.71E-05	3.83E-06
CG5758	0.006897739	9.90E-05	1
CG1678	0.107412299	0.000176501	1
Adh	1.44E-13	0.00021751	0.05098334
lcs	0.34755928	0.000381653	0.665364842
Hsp83	4.97E-10	0.000456216	0.497980065
Cam	0.361810643	0.000481563	1.89E-10
mfas	0.322101288	0.000508049	0.819212268
axo	1	0.000604582	0.111792973
Arf102F	1	0.000640231	5.23E-06
DIP1	0.668062658	0.000720653	0.429322491
AGO2	0.069265101	0.000802831	1
CG6700	1	0.000881168	0.072751963
Msp-300	0.003109687	0.000881168	1
CG31211	1	0.001147871	0.098650579
Ank2	2.74E-08	0.001147871	0.948103898
CG3984	0.007135898	0.002263432	1
B52	1	0.002947559	0.020633033
nAcRbeta-64B	0.426619921	0.003452269	1
inx2	1	0.00428845	0.499868547
chrb	1	0.004425367	0.003960116
CG6654	0.00205089	0.004425367	1
CG15072	7.42E-08	0.005926175	6.25E-20
Ggamma30A	0.405173209	0.00650065	1.90E-08
kis	6.48E-10	0.007009314	0.113187681
beat-VII	1	0.008581303	0.860137216
CG6833	1	0.008778128	0.278348814
CG2993	1	0.010361611	0.846127048
Treh	0.668062658	0.01041774	1
Ddc	1	0.01199546	0.060187694
Shab	0.372370751	0.012008455	1
Ca-alpha1D	0.237305328	0.012795124	1
CG31712	1	0.01307254	0.406680933
Pdp1	1	0.014977404	0.191969657
Ir76a	0.010743343	0.015995644	1
CG7888	0.111975789	0.017227444	1

Gene	FDR for +/SPG vs +/TraF	FDR for +/SPG vs SPG/TraF (114 Genes)	FDR for +/TraF vs SPG/TraF
hoe1	0.661171914	0.017227444	1
ninaB	0.168470192	0.01832121	1
Tsp5D	0.379734354	0.019992313	1
CG6995	1	0.021147988	0.696873769
CG2217	1	0.021759642	0.039946766
CG32521	0.000425168	0.022470883	2.54E-14
cngl	0.029002891	0.023592448	1
Unr	1	0.023592448	0.01898344
CG42784	1	0.027682757	1
CG9657	1	0.028661338	0.021227119
Cyp6a17	2.91E-06	0.029692116	0.966875327
CG34318	0.033211496	0.029692116	1
stj	1	0.034098873	1
Kif3C	1	0.035608736	0.022660105
CG34306	7.60E-06	0.039045428	1
Met	3.48E-12	0.042311172	1.62E-26
spen	3.66E-11	0.043285977	0.007904677
Pif1A	1	0.043285977	0.528829809
CG6327	0.124785356	0.044316114	1
CG40498	1	0.046509825	0.033071059
Tequila	1	0.046940589	0.248735995
unc-104	4.59E-16	0.046940589	1.06E-05
l(3)82Fd	0.019235501	0.04913942	1

Appendix II: 91 differentially expressed genes between the +/TraF control and the experimental (Gal4/TraF)

Gene	FDR for +/SPG vs +/TraF	FDR for +/SPG vs SPG/TraF	FDR for +/TraF vs SPG/TraF (91 genes)
bnb	1	3.08E-232	3.06E-237
ATPsyn-beta	1	2.04E-108	6.87E-125
CaMKII	1	1.12E-70	3.28E-78
cals	0.624567941	2.79E-54	5.14E-70
CR32477	1	1.13E-69	1.31E-66
CG11155	1	1.68E-42	1.61E-44
CG32017	1	3.10E-35	1.51E-39
plexA	1	1.42E-23	2.30E-20
CG31221	0.309772007	1.31E-09	8.31E-19
Zyx102EF	1	6.42E-13	4.74E-15
Tsf1	0.342328698	4.36E-07	4.74E-15
trol	1	1.26E-14	1.26E-11
Cam	0.361810643	0.000481563	1.89E-10
cpx	0.910456372	5.28E-05	3.38E-10
Actbeta	1	3.00E-10	5.45E-10
pho	1	1.85E-06	1.27E-09
Ggamma30A	0.405173209	0.00650065	1.90E-08
CG42613	1	4.08E-12	2.02E-08
roX1	1	1.35E-07	4.39E-08
nrv3	0.417239001	1.21E-14	2.61E-07
Sap47	0.063857893	0.420098523	6.65E-07
VAChT	0.12603966	0.261165448	8.11E-07
CG11076	1	6.87E-06	2.57E-06
CG9686	0.09192515	0.62550664	3.40E-06
14-3-3zeta	1	1.54E-09	3.73E-06
CG10936	1	8.71E-05	3.83E-06
Arf102F	1	0.000640231	5.23E-06
Rab3	0.073701595	1	6.48E-06
Syx1A	0.099365265	1	1.51E-05
CG6329	1	5.03E-05	3.82E-05
CG16971	1	1.13E-06	3.90E-05
CG9377	1	0.064106712	7.74E-05
Rbp6	0.281228027	1	0.000122791
Pka-C1	0.343083692	1	0.000236374
CG14989	1	0.143377159	0.000374733
Cbp53E	1	0.069671767	0.001137584
fne	1	0.067643965	0.001192005
su(w[a])	1	6.52E-07	0.00122412
RpS29	0.132505488	1	0.001284858
bun	0.446712921	1	0.001294961
CG15311	0.142744719	1	0.001317055
Cyp6d5	1	0.463309158	0.001681804
RpL27A	0.189750836	1	0.003781269
chrb	1	0.004425367	0.003960116

Gene	FDR for +/SPG vs +/TraF	FDR for +/SPG vs SPG/TraF	FDR for +/TraF vs SPG/TraF (91 genes)
Ubi-p5E	0.961492161	1	0.004055668
mub	0.328368336	1	0.004400524
Pal	0.648363826	1	0.005305229
RpL29	0.07597658	1	0.006781355
norpA	0.058046062	1	0.007114384
RpL23	0.289763099	1	0.010311129
Vha68-1	0.179727245	1	0.010904681
CG13928	0.170340719	1	0.01144219
Pitslre	1	4.20E-05	0.011677014
orb2	1	1	0.011677014
RpL36	0.132505488	1	0.011814058
Mnn1	0.51890156	1	0.01288611
NAT1	0.134799519	1	0.013313706
CG10077	1	2.67E-05	0.013334628
RpS17	0.051101729	1	0.01344923
Cha	0.155427449	1	0.014063041
porin	1	1	0.015420019
pUf68	1	8.56E-05	0.015420019
pAbp	0.829729711	1.92E-06	0.015783358
CG4577	0.230149428	1	0.018829142
bol	1	1	0.01898344
Unr	1	0.023592448	0.01898344
SPoCk	0.098162769	1	0.019324883
RpS8	0.118256605	1	0.020010876
B52	1	0.002947559	0.020633033
CG9657	1	0.028661338	0.021227119
CG16970	0.140892719	1	0.021227119
Dh	1	0.251480309	0.021310252
Kif3C	1	0.035608736	0.022660105
Megalin	1	0.290345488	0.022919251
Alk	0.112644345	1	0.023993183
CG15765	0.168088715	1	0.024130311
tud	1	1	0.024491491
Rtnl1	0.997188512	1	0.027793314
Pif1B	0.458583847	1.28E-06	0.030165893
comt	0.643305218	1	0.030834006
Jon25Bii	0.138517756	1	0.032905119
CG40498	1	0.046509825	0.033071059
Syn	0.174346223	1	0.036702609
CG42573	0.052917467	1	0.0398766
CG2217	1	0.021759642	0.039946766
oho23B	0.612474636	1	0.040439016
jeb	0.118299748	1	0.040439016
CG14186	0.720635135	1	0.040439016
Vha16	1	1	0.040446733
ct	0.799167649	1	0.046718657
CG31705	0.065490365	1.46E-08	0.048812294

Appendix III: 40 differentially expressed genes common between the group I and group II in Appendix I and II

Name	FDR for +/SPG vs +/TraF	FDR for +/SPG vs SPG/TraF	FDR for +/TraF vs SPG/TraF (40 genes)
bnb	1	3.08E-232	3.06E-237
ATPsyn-beta	1	2.04E-108	6.87E-125
CaMKII	1	1.12E-70	3.28E-78
cals	0.624567941	2.79E-54	5.14E-70
CR32477	1	1.13E-69	1.31E-66
CG11155	1	1.68E-42	1.61E-44
CG32017	1	3.10E-35	1.51E-39
plexA	1	1.42E-23	2.30E-20
CG31221	0.309772007	1.31E-09	8.31E-19
Zyx102EF	1	6.42E-13	4.74E-15
Tsf1	0.342328698	4.36E-07	4.74E-15
trol	1	1.26E-14	1.26E-11
Cam	0.361810643	0.000481563	1.89E-10
cpx	0.910456372	5.28E-05	3.38E-10
Actbeta	1	3.00E-10	5.45E-10
pho	1	1.85E-06	1.27E-09
Ggamma30A	0.405173209	0.00650065	1.90E-08
CG42613	1	4.08E-12	2.02E-08
roX1	1	1.35E-07	4.39E-08
nrv3	0.417239001	1.21E-14	2.61E-07
CG11076	1	6.87E-06	2.57E-06
14-3-3zeta	1	1.54E-09	3.73E-06
CG10936	1	8.71E-05	3.83E-06
Arf102F	1	0.000640231	5.23E-06
CG6329	1	5.03E-05	3.82E-05
CG16971	1	1.13E-06	3.90E-05
su(w[a])	1	6.52E-07	0.00122412
chrb	1	0.004425367	0.003960116
Pitslre	1	4.20E-05	0.011677014
CG10077	1	2.67E-05	0.013334628
pUf68	1	8.56E-05	0.015420019
pAbp	0.829729711	1.92E-06	0.015783358
Unr	1	0.023592448	0.01898344
B52	1	0.002947559	0.020633033
CG9657	1	0.028661338	0.021227119
Kif3C	1	0.035608736	0.022660105
Pif1B	0.458583847	1.28E-06	0.030165893
CG40498	1	0.046509825	0.033071059
CG2217	1	0.021759642	0.039946766
CG31705	0.065490365	1.46E-08	0.048812294

Appendix IV: 173 mirs mapped to the miRbase database

mature miRNA	Male 1 bbb	Male 2 bbb	Male 3 bbb	Female 1 bbb	Female 2 bbb	Female 3 bbb
dme-mir-281-3p	0	0	0	0	0	3.161709296
dme-mir-4952-5p	0	3.7880798	0	0	0	0
dme-mir-4956-3p	0	3.7880798	0	0	0	0
dme-mir-4963-3p	0	3.7880798	0	0	0	0
dme-mir-316-3p	0	4.5456958	0	0	0	0
dme-mir-4911-3p	0	4.5456958	0	0	0	0
dme-mir-4952-3p	0	4.5456958	0	0	0	0
dme-mir-283-3p	0	0	0	0	0	4.742563944
dme-mir-6-3p	0	0	0	0	0	4.742563944
dme-mir-87-5p	0	0	0	0	0	4.742563944
dme-mir-307a-5p	0	0	0	0	0	5.532991268
dme-mir-375-3p	0	0	0	0	0	5.532991268
dme-mir-1010-5p	0	0	0	0	6.151146951	0
dme-mir-1001-5p	0	0	0	0	0	6.323418592
dme-let-7-3p	7.0787153	0	0	0	0	0
dme-mir-999-5p	0	0	0	0	0	7.113845916
dme-mir-286-5p	0	0	0	0	0	7.90427324
dme-mir-958-3p	0	0	0	0	0	7.90427324
dme-mir-315-3p	0	0	0	0	0	8.694700564
dme-mir-4961-3p	0	4.5456958	0	0	5.272411673	0
dme-mir-1013-3p	9.9102015	0	0	0	0	0
dme-mir-282-3p	0	0	0	0	10.54482335	0
dme-mir-9b-3p	0	10.606624	0	0	0	0
dme-mir-976-3p	0	0	0	0	4.393676394	6.323418592
dme-mir-12-3p	11.325945	0	0	0	0	0
dme-mir-954-3p	11.325945	0	0	0	0	0
dme-mir-983-5p	8.4944584	0	0	0	0	3.161709296
dme-mir-7-3p	0	0	0	0	4.393676394	7.90427324
dme-mir-2535b-3p	0	7.5761597	5.5810121	0	0	0
dme-mir-982-5p	0	14.394703	0	0	0	0
dme-mir-285-5p	0	9.8490076	0	0	0	4.742563944
dme-mir-100-3p	0	0	0	0	14.93849974	0
dme-mir-1016-3p	9.9102015	0	0	0	5.272411673	0
dme-mir-13b-2-5p	0	7.5761597	0	0	0	7.90427324
dme-mir-13b-1-5p	0	6.0609278	0	0	0	10.27555521
dme-mir-1007-3p	0	0	6.5111808	10.0904957	0	0

mature miRNA	Male 1 bbb	Male 2 bbb	Male 3 bbb	Female 1 bbb	Female 2 bbb	Female 3 bbb
dme-mir-137-5p	11.325945	0	0	0	0	5.532991268
dme-mir-929-3p	8.4944584	0	7.4413495	0	0	3.95213662
dme-mir-33-3p	0	7.5761597	0	0	6.151146951	6.323418592
dme-mir-966-5p	15.573174	0	0	0	7.908617509	0
dme-mir-971-5p	16.988917	7.5761597	0	0	0	0
dme-mir-252-3p	19.820403	0	0	0	0	5.532991268
dme-mir-996-5p	16.988917	9.0913916	0	0	0	0
dme-mir-957-5p	7.0787153	15.152319	0	0	5.272411673	0
dme-mir-2b-1-5p	12.741688	0	0	16.14479311	0	0
dme-mir-969-5p	19.820403	6.8185437	0	0	0	5.532991268
dme-mir-79-5p	9.9102015	0	0	0	8.787352788	19.7606831
dme-mir-4940-3p	11.325945	6.0609278	0	10.0904957	12.3022939	0
dme-mir-4958-5p	26.899118	7.5761597	0	0	6.151146951	0
dme-mir-993-5p	7.0787153	0	0	10.0904957	4.393676394	19.7606831
dme-mir-184-5p	16.988917	0	4.6508435	22.19909053	0	0
dme-mir-971-3p	12.741688	6.0609278	0	10.0904957	7.908617509	7.113845916
dme-mir-304-5p	15.573174	13.637087	0	16.14479311	0	0
dme-mir-311-3p	0	17.425167	0	10.0904957	5.272411673	12.64683718
dme-mir-980-5p	18.40466	18.182783	0	0	12.3022939	0
dme-mir-305-5p	11.325945	4.5456958	0	20.18099139	4.393676394	8.694700564
dme-mir-79-3p	12.741688	18.182783	0	0	5.272411673	17.38940113
dme-mir-210-3p	22.651889	9.8490076	0	18.16289225	7.02988223	0
dme-mir-286-3p	22.651889	8.3337757	5.5810121	0	7.02988223	18.17982845
dme-mir-13a-3p	11.325945	21.213247	5.5810121	0	7.02988223	20.55111042
dme-mir-981-5p	28.314861	6.0609278	0	12.10859483	16.6959703	5.532991268
dme-mir-2489-3p	39.640806	0	5.5810121	20.18099139	4.393676394	0
dme-mir-193-5p	32.562091	20.455631	0	28.25338795	13.18102918	0
dme-mir-995-5p	38.225063	12.879471	0	22.19909053	10.54482335	13.43726451
dme-mir-133-5p	42.472292	15.152319	7.4413495	28.25338795	9.666088066	0
dme-mir-998-5p	28.314861	18.182783	9.3016869	14.12669397	7.908617509	26.87452902
dme-mir-4969-5p	31.146347	32.577487	8.3715182	10.0904957	12.3022939	11.06598254
dme-mir-969-3p	33.977834	9.0913916	12.092193	14.12669397	10.54482335	26.08410169
dme-mir-318-3p	7.0787153	25.758943	5.5810121	18.16289225	11.42355862	42.6830755
dme-mir-1006-3p	33.977834	23.486095	0	30.27148709	10.54482335	12.64683718
dme-mir-279-3p	39.640806	13.637087	9.3016869	22.19909053	12.3022939	19.7606831
dme-mir-996-3p	60.876952	12.879471	0	32.28958623	9.666088066	5.532991268
dme-mir-1011-3p	45.303778	40.153646	0	30.27148709	12.3022939	0
dme-mir-4940-5p	9.9102015	40.911262	10.231856	0	34.27067587	33.98837493
dme-mir-4962-3p	18.40466	19.698015	8.3715182	16.14479311	47.45170505	23.71281972

mature miRNA	Male 1 bbb	Male 2 bbb	Male 3 bbb	Female 1 bbb	Female 2 bbb	Female 3 bbb
dme-mir-2500-3p	33.977834	12.121856	12.092193	24.21718967	15.81723502	37.15008423
dme-mir-965-3p	42.472292	33.335103	4.6508435	18.16289225	12.3022939	27.66495634
dme-mir-219-5p	7.0787153	28.789407	8.3715182	0	11.42355862	82.99486902
dme-mir-92a-3p	31.146347	29.547023	0	32.28958623	21.08964669	35.56922958
dme-mir-4973-5p	86.360327	0	0	36.3257845	0	32.40752029
dme-mir-1003-3p	67.955667	15.909935	5.5810121	40.36198278	13.18102918	14.22769183
dme-mir-5-5p	26.899118	34.092719	6.5111808	22.19909053	29.87699948	40.31179353
dme-mir-1009-3p	62.292695	42.426494	0	46.4162802	7.02988223	3.95213662
dme-mir-219-3p	29.730604	78.792061	0	30.27148709	30.75573476	10.27555521
dme-mir-125-3p	59.461209	19.698015	10.231856	32.28958623	28.11952892	34.77880226
dme-mir-31b-5p	28.314861	39.39603	9.3016869	20.18099139	26.36205836	61.65333127
dme-mir-986-5p	55.21398	10.606624	10.231856	44.39818106	8.787352788	56.12034001
dme-bantam-5p	82.113098	37.880798	5.5810121	38.34388364	15.81723502	15.80854648
dme-mir-2b-2-5p	65.124181	30.304639	5.5810121	36.3257845	23.72585253	38.73093888
dme-mir-967-5p	53.798237	34.092719	14.882699	22.19909053	40.42182282	36.35965691
dme-mir-317-5p	101.9335	15.152319	11.162024	46.4162802	14.05976446	16.5989738
dme-mir-9a-5p	19.820403	4.5456958	0	0	9.666088066	177.8461479
dme-mir-956-3p	25.483375	95.459612	0	28.25338795	10.54482335	71.92888649
dme-mir-2a-3p	70.787153	53.033118	0	40.36198278	42.17929338	28.45538367
dme-mir-277-5p	53.798237	60.609278	14.882699	34.30768537	61.51146951	25.29367437
dme-mir-929-5p	89.191813	80.307293	10.231856	50.45247848	32.51320531	0
dme-mir-993-3p	46.719521	100.00531	14.882699	32.28958623	44.81549922	24.50324705
dme-mir-2a-2-5p	32.562091	63.639741	45.578266	24.21718967	91.38846899	10.27555521
dme-mir-970-5p	16.988917	184.10068	11.162024	0	46.57296977	31.61709296
dme-mir-995-3p	101.9335	30.304639	28.835229	88.79636212	28.9982642	28.45538367
dme-mir-9b-5p	59.461209	50.76027	5.5810121	34.30768537	21.96838197	135.9534997
dme-mir-954-5p	144.40579	10.606624	7.4413495	80.72396556	46.57296977	33.98837493
dme-mir-190-5p	158.56322	65.154973	4.6508435	78.70586643	12.3022939	19.7606831
dme-mir-92a-5p	128.83262	43.941726	19.533543	84.76016384	49.20917561	33.98837493
dme-mir-1005-3p	165.64194	9.8490076	9.3016869	127.1402458	28.9982642	71.92888649
dme-mir-11-5p	131.66411	71.973517	34.416242	84.76016384	53.602852	67.18632254
dme-mir-988-5p	99.102015	88.641068	27.905061	40.36198278	75.57123397	173.103584
dme-mir-124-3p	253.41801	40.911262	13.95253	139.2488406	40.42182282	35.56922958
dme-mir-281-2-5p	128.83262	123.4914	38.136916	96.86875868	104.5694982	72.71931381
dme-mir-124-5p	137.32708	120.46094	25.114555	92.8325604	57.11779312	134.3726451
dme-mir-1017-3p	210.94572	121.21856	12.092193	151.3574354	48.33044033	47.42563944
dme-mir-12-5p	237.84484	56.063582	13.95253	224.0090044	35.14941115	46.63521212
dme-mir-998-3p	243.50781	59.851662	13.95253	205.8461122	72.05629286	40.31179353
dme-mir-306-5p	76.450126	212.89009	86.505688	36.3257845	100.1758218	271.1165721

mature miRNA	Male 1 bbb	Male 2 bbb	Male 3 bbb	Female 1 bbb	Female 2 bbb	Female 3 bbb
dme-mir-990-5p	332.69962	81.064909	39.997254	177.5927242	111.5993804	61.65333127
dme-mir-4960-3p	249.17078	146.9775	61.391134	121.0859483	141.4763799	105.9172614
dme-mir-92b-3p	328.45239	112.88478	29.765398	209.8823105	117.7505274	57.70119465
dme-mir-2b-3p	271.82267	231.83049	20.463711	189.7013191	107.205704	42.6830755
dme-mir-306-3p	339.77834	96.974844	30.695567	175.5746251	137.0827035	132.7917904
dme-mir-278-3p	161.39471	196.22254	40.927422	96.86875868	107.205704	328.0273395
dme-mir-2c-5p	75.034383	637.15503	33.486073	0	110.7206451	143.0673457
dme-mir-312-3p	9.9102015	506.84508	27.905061	14.12669397	93.14593955	392.0519527
dme-mir-932-3p	198.20403	245.46757	88.366026	135.2126423	277.6803481	196.0259764
dme-mir-1000-3p	351.10428	348.50335	57.670459	131.176444	208.2602611	65.60546789
dme-mir-1004-3p	535.15088	94.701996	51.159278	363.257845	72.05629286	53.74905803
dme-mir-989-3p	96.270529	452.29673	51.159278	106.9592544	207.3815258	286.9251186
dme-mir-31a-5p	237.84484	459.11528	51.159278	163.4660303	202.9878494	146.2290549
dme-mir-965-5p	389.32934	378.05037	46.508435	205.8461122	195.9579672	104.3364068
dme-mir-13b-3p	342.60982	389.41461	53.949784	274.4614829	145.8700563	154.9237555
dme-mir-4951-5p	549.30831	184.8583	96.737544	205.8461122	228.4711725	355.6922958
dme-mir-307a-3p	706.45579	95.459612	249.28521	448.0180089	197.7154377	351.7401592
dme-mir-34-3p	635.66864	672.00536	68.832483	383.4388364	235.5010547	181.0078572
dme-mir-305-3p	148.65302	907.62393	184.1734	46.4162802	579.965284	329.6081941
dme-mir-10-3p	295.8903	972.7789	111.62024	135.2126423	452.5486686	280.6017
dme-mir-100-5p	668.23073	490.93515	292.07297	448.0180089	288.2251714	328.8177668
dme-mir-284-5p	518.16196	1874.3419	66.041977	238.1356984	252.197025	531.1671618
dme-mir-1012-3p	1788.0835	1134.9087	164.63986	904.1084143	475.3957858	209.4632409
dme-mir-9c-5p	1155.2463	587.90999	162.77952	611.4840392	393.6734049	1770.557206
dme-mir-278-5p	709.28728	2744.8427	176.73205	488.3799917	897.1887196	196.0259764
dme-mir-14-3p	1765.4316	751.55504	332.07022	928.325604	677.5048999	789.6368967
dme-mir-8-3p	1230.2807	1619.0253	237.19302	1204.805186	798.7703684	721.6601468
dme-mir-133-3p	2493.1235	725.03848	157.19851	1507.520057	559.7543726	406.2796446
dme-mir-10-5p	927.31171	1225.8226	509.73244	482.3256943	667.8388119	2258.250865
dme-mir-1000-5p	2292.088	1012.9326	452.99215	1206.823285	964.8513361	776.1996322
dme-mir-317-3p	2188.7388	983.38553	291.1428	1828.39782	349.7366409	1123.987655
dme-mir-14-5p	998.09886	1463.7141	609.26049	496.4523882	1837.435468	1378.505253
dme-mir-988-3p	2607.7987	1303.8571	237.19302	1412.669397	896.3099843	593.6109204
dme-mir-277-3p	2197.2332	1885.7061	216.72931	1614.479311	698.5945466	497.9692141
dme-mir-275-3p	1465.2941	2334.2148	316.25736	809.2577548	1678.384382	518.5203246
dme-mir-137-3p	2290.6723	1523.5657	375.78815	1372.307415	975.3961594	699.5281818
dme-mir-8-5p	1104.2796	2278.9088	583.21577	785.0405651	1264.500066	1889.911732
dme-mir-927-5p	3263.2878	1178.8504	342.30208	1836.470217	717.0479875	754.8580945
dme-mir-981-3p	2501.618	845.49942	554.38054	748.7147806	883.1289552	3262.093566

mature miRNA	Male 1 bbb	Male 2 bbb	Male 3 bbb	Female 1 bbb	Female 2 bbb	Female 3 bbb
dme-mir-1010-3p	1959.3884	2609.987	379.50883	1342.035928	835.6772501	1740.520968
dme-mir-11-3p	4863.0774	2638.7764	1665.002	3289.501597	2912.128714	1998.200275
dme-mir-927-3p	2927.7567	4464.6309	1254.7976	1854.633109	2655.538012	5105.370086
dme-mir-34-5p	9321.2524	2372.8532	199.98627	4982.686774	1053.603599	624.437586
dme-mir-7-5p	1121.2685	6547.3172	1011.0934	458.1085046	4729.35327	4793.94172
dme-bantam-3p	5331.6884	6348.0642	686.46449	3705.230019	2790.863245	1908.881988
dme-mir-932-5p	5950.3681	4155.5236	1327.3507	5192.569085	3182.77918	2469.29496
dme-mir-1-3p	4384.5563	5482.8668	1584.0773	2589.221195	3555.362938	8420.422283
dme-mir-315-5p	9890.3811	3350.1778	1222.2417	4817.202645	2989.457418	6044.397747
dme-mir-970-3p	8350.0526	3649.4361	2635.1679	5109.82702	5377.859906	3243.913738
dme-mir-987-5p	6198.1231	7916.3293	1087.3672	3713.302416	2385.766282	7863.961447
dme-mir-125-5p	11112.167	5965.4681	2342.1648	5497.302055	5150.267469	5423.912298
dme-mir-276b-3p	12222.11	5650.2999	2777.4837	8088.54135	3975.398401	11526.80167
dme-mir-263b-5p	6210.8648	15791.747	10046.752	4492.288684	19109.85611	28863.24416
dme-mir-999-3p	28705.606	16689.522	5316.8442	13866.35918	13087.88324	15649.67059
dme-mir-276a-3p	50768.546	25121.03	9680.2656	34461.0609	17480.6809	27249.982
dme-mir-252-5p	51279.63	59676.652	14941.3	33423.75794	55938.53038	34654.70517
dme-mir-957-3p	59968.045	103661.56	26917.222	46755.32086	43279.46995	119643.8223
dme-let-7-5p	205473.87	97704.428	46655.401	97280.4509	168033.5175	68828.83052
dme-mir-184-3p	3057584.5	2964022.5	1056518.2	1413430.221	2909173.527	4908063.617

Appendix V: Differentially expressed genes in BBB from males vs females (>1.5 Fold, p<0.05, 711 probes). Intensity values are normalized to the 75th percentile intensity to each array. P-values are based on a Welch T-test.

Systematic	GeneSymbol	P-value	Expression profile (males, females)
A_09_P010076	Yp1	4.03E-03	
A_09_P010081	Yp3	6.60E-03	
A_09_P011441	Yp2	6.53E-03	
A_09_P033016	Cht2	2.27E-04	
A_09_P040561	CG14222	2.59E-03	
A_09_P041791	Cp36	4.65E-02	
A_09_P046876		4.91E-02	
A_09_P047621	Cp7Fb	4.53E-03	
A_09_P017246	Ste:CG33238	1.21E-03	
A_09_P030341	Cp7Fb	4.65E-07	
A_09_P017282	Ste:CG33246	1.15E-03	
A_09_P029356	dhd	3.45E-02	
A_09_P166400		3.19E-02	
A_09_P061401	Jon99Fi	1.82E-02	
A_09_P017256	Ste:CG33240	1.74E-03	
A_09_P042086	dsx	2.26E-05	
A_09_P031461	pgc	7.20E-03	
A_09_P119000	CycB	3.13E-02	
A_09_P198615	Hsp70Aa	7.58E-03	
A_09_P017276		6.84E-03	
A_09_P029571	Hsp70Aa	1.59E-02	
A_09_P063611		3.90E-02	
A_09_P041786	Cp19	1.73E-02	
A_09_P029581	Hsp70Bb	3.06E-02	
A_09_P041876	CycB	2.66E-02	
A_09_P218800		1.90E-02	
A_09_P059675	Hsp70Bbb	8.96E-03	
A_09_P108115	Arpc3B	9.69E-03	
A_09_P041776	Cp16	3.67E-03	
A_09_P113130	CG14075	2.48E-06	
A_09_P176625		1.73E-03	
A_09_P171040		6.82E-03	
A_09_P119565	dsx	1.63E-02	
A_09_P148580	CHES-1-like	3.63E-08	
A_09_P160665		3.44E-02	
A_09_P149325		4.97E-02	
A_09_P067431	CG4020	1.62E-02	
A_09_P030336	Cp7Fa	3.33E-08	
A_09_P021206	CG17633	3.97E-02	
A_09_P134245	ovo	4.71E-02	

Systematic	GeneSymbol	P-value	Expression profile (males, females)
A_09_P112275	CG4020	2.43E-02	
A_09_P043951	osk	1.63E-03	
A_09_P034456	CG14075	1.71E-03	
A_09_P212665		9.97E-03	
A_09_P042706	hfw	5.03E-07	
A_09_P040936	r-cup	7.35E-04	
A_09_P054086	CG5804	2.13E-02	
A_09_P078091	CG6133	2.03E-02	
A_09_P010936	yl	1.68E-02	
A_09_P190865		8.12E-03	
A_09_P030346	Cp7Fc	3.03E-03	
A_09_P078056	Mipp2	3.14E-02	
A_09_P075131	CG3509	2.89E-02	
A_09_P077971	CG2652	2.47E-02	
A_09_P002691	CG17672	1.59E-04	
A_09_P168703		4.61E-06	
A_09_P043966	otu	1.02E-02	
A_09_P178935		7.48E-03	
A_09_P169159		1.97E-02	
A_09_P040376	Mec2	4.36E-02	
A_09_P180690		1.16E-02	
A_09_P019306	Ir25a	2.28E-02	
A_09_P070536	CG6733	3.65E-02	
A_09_P204080		4.72E-02	
A_09_P065356	CG7916	2.66E-02	
A_09_P123280		3.03E-02	
A_09_P078881	XRCC1	5.93E-06	
A_09_P203785		4.11E-02	
A_09_P130245	CG32755	2.33E-02	
A_09_P174050		2.71E-02	
A_09_P009321	CG18190	3.55E-02	
A_09_P056706	Ilp3	3.80E-03	
A_09_P184695		8.26E-03	
A_09_P181000		2.10E-03	
A_09_P213545		1.03E-02	
A_09_P039541	CG13008	7.75E-05	
A_09_P038616	CG11674	1.43E-02	
A_09_P051371	4-Muh.	2.70E-03	
A_09_P221105		1.84E-03	
A_09_P113000	Ilp3	1.40E-02	
A_09_P222415	tlk	1.77E-06	
A_09_P188255	CG12826	1.97E-02	
A_09_P149005		2.49E-04	
A_09_P191550	Lsd-2	7.80E-03	
A_09_P207745	up	2.56E-02	
A_09_P167837		9.37E-03	

Systematic	GeneSymbol	P-value	Expression profile (males, females)
A_09_P170820	ImpE1	4.67E-02	
A_09_P110435	pgc	7.13E-03	
A_09_P186555	CG15445	1.75E-05	
A_09_P064396	yellow-g	1.22E-02	
A_09_P209795	CG15308	1.94E-02	
A_09_P061806	CG2003	3.22E-03	
A_09_P169610		2.15E-03	
A_09_P010301	alphaTub67C	3.91E-02	
A_09_P197060		1.81E-02	
A_09_P051331		1.17E-02	
A_09_P034446	CG3819	7.86E-03	
A_09_P077296	Ant2	6.14E-04	
A_09_P048456		2.84E-02	
A_09_P224810		5.80E-04	
A_09_P226515		6.98E-03	
A_09_P012496	mtrm	2.44E-02	
A_09_P209100		2.79E-04	
A_09_P013416	RnrS	8.54E-03	
A_09_P044156	plu	2.97E-03	
A_09_P090090	CR33963	4.77E-03	
A_09_P042801	Hsp27	4.75E-03	
A_09_P038581	CG1368	1.58E-04	
A_09_P162875		5.63E-05	
A_09_P188290		2.52E-03	
A_09_P004446	CG34437	5.20E-04	
A_09_P189675	CG34417	8.66E-03	
A_09_P206870	Hsp27	8.08E-03	
A_09_P184930		9.79E-05	
A_09_P180530		1.94E-03	
A_09_P153540	Hml	2.83E-02	
A_09_P026966	CG3906	1.82E-02	
A_09_P009566	stg	3.57E-03	
A_09_P194885	Hsp27	6.35E-03	
A_09_P060721	CG14523	1.77E-02	
A_09_P067096	CG2861	4.88E-03	
A_09_P067446	CG3011	4.28E-02	
A_09_P017711	Cyp6t1	3.06E-02	
A_09_P111075	CG30345	1.83E-02	
A_09_P205005	Lsd-2	1.97E-02	
A_09_P071556	CG11878	8.59E-03	
A_09_P210930	CG13056	4.89E-02	
A_09_P196605	Osi7	1.95E-02	
A_09_P198270		9.45E-03	
A_09_P167565		9.42E-03	
A_09_P012081	Myo61F	2.87E-02	
A_09_P079121	inx7	4.04E-02	

Systematic	GeneSymbol	P-value	Expression profile (males, females)
A_09_P066931	CG6414	8.57E-03	
A_09_P172440		1.06E-02	
A_09_P161555		3.62E-02	
A_09_P038241	CG12716	4.90E-03	
A_09_P039486	CG13012	2.61E-05	
A_09_P066806	CG3603	7.59E-04	
A_09_P038871	RpL37a	2.00E-03	
A_09_P195970		2.62E-02	
A_09_P071976	CG14237	4.17E-02	
A_09_P000686	His1:CG33804	3.10E-02	
A_09_P166070		1.18E-03	
A_09_P031456	nompA	2.44E-03	
A_09_P115600		1.06E-02	
A_09_P025191	CG42326	9.66E-03	
A_09_P172890		4.76E-02	
A_09_P203140	CG42849	1.63E-02	
A_09_P196265		3.09E-04	
A_09_P042291	exu	1.11E-02	
A_09_P119495	dl	3.31E-02	
A_09_P063581		4.37E-03	
A_09_P125675	Rrp4	4.26E-02	
A_09_P115535	CG9897	4.36E-02	
A_09_P052731	CG11350	2.59E-02	
A_09_P035931	CG12582	2.49E-02	
A_09_P125740	CG9293	5.13E-03	
A_09_P069956	CG15497	4.97E-05	
A_09_P186545	Hsp27	5.17E-03	
A_09_P187970		1.38E-02	
A_09_P031116	CycB3	1.94E-03	
A_09_P018421	CG4259	4.25E-02	
A_09_P007436	CG6347	6.56E-04	
A_09_P062806	CG3526	2.90E-02	
A_09_P215595	CG9812	3.93E-02	
A_09_P114075	CG15579	1.11E-03	
A_09_P054871	CG7607	7.59E-05	
A_09_P177560		5.21E-03	
A_09_P002011	CG32335	1.04E-03	
A_09_P101550	CG4041	2.06E-02	
A_09_P041991	dl	5.12E-04	
A_09_P213435		3.63E-02	
A_09_P106105	fog	8.24E-04	
A_09_P180505	CG4325	4.75E-02	
A_09_P163855		1.03E-03	
A_09_P008146	CG8399	4.78E-02	
A_09_P048886	Tango13	1.91E-03	
A_09_P049981	CycE	6.06E-03	

Systematic	GeneSymbol	P-value	Expression profile (males, females)
A_09_P117300	retn	2.08E-02	
A_09_P175960	CG3603	4.21E-02	
A_09_P045561	DIPI	3.72E-03	
A_09_P063771	CG15579	4.43E-03	
A_09_P141770	drd	1.97E-03	
A_09_P189230		9.20E-03	
A_09_P054556	Ilp2	3.09E-02	
A_09_P193270		3.33E-02	
A_09_P006491	CG7777	2.97E-02	
A_09_P044016	peb	2.04E-02	
A_09_P041276	Antp	5.99E-03	
A_09_P209825		9.53E-03	
A_09_P040736	CG9572	1.19E-03	
A_09_P009216	CG15071	3.12E-02	
A_09_P005471		2.53E-02	
A_09_P010431	Klp67A	3.79E-03	
A_09_P195595		3.98E-02	
A_09_P179840		1.55E-02	
A_09_P142260		6.76E-03	
A_09_P186880		1.05E-03	
A_09_P009636	CG42259	2.30E-04	
A_09_P024441	Fmo-2	1.35E-02	
A_09_P215765	CG30492	3.72E-02	
A_09_P179350	baz	1.04E-02	
A_09_P180430	CG11073	6.33E-03	
A_09_P050981	Sxl	4.97E-03	
A_09_P116310	Kr-h1	2.76E-02	
A_09_P045511		4.40E-03	
A_09_P212819		4.49E-02	
A_09_P188570		2.22E-02	
A_09_P034291		6.20E-03	
A_09_P003406	CG34247	8.44E-03	
A_09_P041871	CycA	1.19E-02	
A_09_P038351	CG15747	9.25E-06	
A_09_P056806	Proct	1.71E-03	
A_09_P020121	TTLL3A	1.34E-03	
A_09_P079026	CG4302	3.71E-02	
A_09_P057921	CG30217	6.71E-04	
A_09_P222855		3.81E-04	
A_09_P018706	daw	4.07E-04	
A_09_P225910		6.26E-04	
A_09_P110370	CG42345	2.85E-02	
A_09_P037086	CG2641	4.90E-02	
A_09_P003666	CG34299	1.44E-02	
A_09_P039716	CG5010	8.85E-03	
A_09_P210485	CG14221	1.95E-02	

Systematic	GeneSymbol	P-value	Expression profile (males, females)
A_09_P067321	CG4078	4.37E-03	
A_09_P009301	CG15083	5.86E-04	
A_09_P201700		4.80E-02	
A_09_P116815	dbr	5.42E-04	
A_09_P044821	so	9.29E-03	
A_09_P065326	mol	3.74E-02	
A_09_P046426	fru	9.95E-03	
A_09_P069676	CG17271	2.66E-02	
A_09_P196315		2.01E-02	
A_09_P011746	Cry	2.43E-02	
A_09_P142380		6.78E-03	
A_09_P058296	CG30389	1.74E-02	
A_09_P037726		1.10E-03	
A_09_P033476	CG13067	1.18E-02	
A_09_P112040	CG4101	1.10E-02	
A_09_P140095		1.37E-02	
A_09_P091360	fus	1.69E-02	
A_09_P068201	sni	4.31E-03	
A_09_P212460		1.98E-03	
A_09_P107820		4.63E-02	
A_09_P135990		1.80E-02	
A_09_P189415		1.25E-02	
A_09_P038961	CG11655	2.80E-02	
A_09_P154115	Nup153	5.35E-04	
A_09_P021296	CG4709	3.77E-02	
A_09_P063156	CG11686	3.50E-02	
A_09_P130015		3.37E-02	
A_09_P065926	nimC4	3.43E-02	
A_09_P034196	CG5290	1.26E-02	
A_09_P207085	CG15083	9.60E-03	
A_09_P197425		2.41E-02	
A_09_P023806	CG9317	1.38E-02	
A_09_P195635		1.80E-02	
A_09_P066306	Spn27A	2.11E-02	
A_09_P054181	CG13314	1.38E-03	
A_09_P006521	CG13196	3.29E-02	
A_09_P076586	CG17778	3.81E-04	
A_09_P186905		6.26E-03	
A_09_P143460	Sxl	1.69E-02	
A_09_P038851	CG5599	4.38E-05	
A_09_P023966	CG9248	3.23E-02	
A_09_P223195		2.06E-02	
A_09_P077646	CG13369	2.47E-04	
A_09_P008841	CG6410	2.83E-02	
A_09_P015881	CG32573	4.93E-02	
A_09_P042016	dm	3.29E-02	

Systematic	GeneSymbol	P-value	Expression profile (males, females)
A_09_P117735	LIMK1	1.12E-02	
A_09_P016516	CG32813	4.48E-02	
A_09_P111140	CG31288	3.88E-02	
A_09_P037846	CG9360	2.87E-02	
A_09_P026721	nahoda	3.18E-03	
A_09_P079951	Gr2a	7.97E-04	
A_09_P056756	TotZ	3.20E-02	
A_09_P002831	CG41452	2.85E-02	
A_09_P011626	lola	4.24E-06	
A_09_P045386		1.62E-02	
A_09_P090515	CG32214	4.50E-02	
A_09_P174030		3.04E-03	
A_09_P178445		2.56E-03	
A_09_P062986	CG3939	6.70E-03	
A_09_P035186	Rcd2	4.92E-02	
A_09_P010321	scra	1.55E-03	
A_09_P034756	Cyp305a1	1.40E-02	
A_09_P038611	CG11590	1.17E-02	
A_09_P045566	CG11739	3.32E-03	
A_09_P178620	CG3011	3.60E-02	
A_09_P101930	CG13314	3.38E-03	
A_09_P000631	CG33777	2.44E-02	
A_09_P067691	Pink1	9.72E-03	
A_09_P076546	CG3191	9.54E-04	
A_09_P041521	btd	2.00E-03	
A_09_P133750	trbl	2.52E-02	
A_09_P069301	CG11453	2.40E-02	
A_09_P031936	lok	4.10E-03	
A_09_P163030		1.80E-02	
A_09_P039631	CG4880	2.45E-03	
A_09_P066886	HIP-R	3.85E-02	
A_09_P055376	Smyd4	4.05E-02	
A_09_P130075	CG13005	4.58E-02	
A_09_P201810		1.61E-02	
A_09_P187585		7.30E-04	
A_09_P067421	CG3016	4.16E-06	
A_09_P042306	e(y)2	1.30E-02	
A_09_P128265	CG17778	2.38E-03	
A_09_P035101	CG5910	2.45E-04	
A_09_P030816	hoip	1.15E-02	
A_09_P199365	Tsp3A	1.41E-03	
A_09_P224245		4.94E-03	
A_09_P193735	RhoGAP18B	3.35E-02	
A_09_P016351	CG32732	1.47E-03	
A_09_P040856	CG1812	2.96E-03	
A_09_P114800	CG13843	3.31E-02	

Systematic	GeneSymbol	P-value	Expression profile (males, females)
A_09_P001881	zwilch	4.96E-02	
A_09_P050251	N	2.82E-03	
A_09_P039976	CG6847	1.78E-03	
A_09_P146770		4.88E-02	
A_09_P009461	CG11961	8.63E-04	
A_09_P037531	CG11160	3.59E-02	
A_09_P117340	CG4050	1.41E-03	
A_09_P071591	CG10550	1.82E-02	
A_09_P117295		5.14E-03	
A_09_P121720	Cdk4	3.07E-03	
A_09_P022111	CG16965	4.47E-03	
A_09_P220590		2.41E-02	
A_09_P141755	SPR	1.19E-03	
A_09_P042156	Edg78E	2.79E-02	
A_09_P020616	CG8673	2.05E-02	
A_09_P162350		1.39E-02	
A_09_P042406	fog	3.79E-03	
A_09_P103570	hop	2.44E-02	
A_09_P009701	term	4.26E-02	
A_09_P114000	CG14695	1.63E-02	
A_09_P143120	CG14850	1.92E-02	
A_09_P066631	CG13373	1.37E-02	
A_09_P037041	CG14598	3.25E-02	
A_09_P192580		5.19E-03	
A_09_P052946	Lkr	1.44E-02	
A_09_P044251	ptr	1.93E-03	
A_09_P149230		1.28E-02	
A_09_P028376	CG13926	4.01E-02	
A_09_P041946	Pkg21D	1.02E-03	
A_09_P124815	CG3842	2.27E-03	
A_09_P109290	RpS18	3.10E-02	
A_09_P013011	HLH4C	9.25E-03	
A_09_P009796	tra	4.87E-02	
A_09_P198340	CG17778	1.01E-02	
A_09_P037471	CG2157	2.62E-02	
A_09_P002101	GlcAT-I	1.67E-04	
A_09_P067671	CG3224	7.52E-03	
A_09_P070841	CG13599	2.15E-02	
A_09_P073626	CG4570	2.54E-03	
A_09_P074611	CG7966	3.38E-04	
A_09_P016496	CG32803	7.76E-04	
A_09_P065496	l(2)05510	2.47E-02	
A_09_P199735	Pkcdelta	4.28E-02	
A_09_P076526	CG3587	2.37E-04	
A_09_P020016	CG9542	5.66E-03	
A_09_P177570		3.67E-03	

Systematic	GeneSymbol	P-value	Expression profile (males, females)
A_09_P066626	CG13373	1.06E-02	
A_09_P032236	CG4050	1.53E-04	
A_09_P146530	CG15210	4.91E-02	
A_09_P032106	stet	5.26E-03	
A_09_P160675		3.80E-02	
A_09_P067241	SPR	2.02E-03	
A_09_P206270		2.18E-02	
A_09_P169560		1.17E-02	
A_09_P048586	del	1.54E-02	
A_09_P039591	ppk28	4.98E-03	
A_09_P161590		2.11E-03	
A_09_P201960	CG13124	3.07E-03	
A_09_P043801	na	4.98E-02	
A_09_P040841	CG1695	4.09E-02	
A_09_P223395		3.74E-02	
A_09_P225680	fas	3.04E-02	
A_09_P046961	sqd	1.05E-02	
A_09_P222355		1.06E-02	
A_09_P164890	CG3008	2.63E-03	
A_09_P040141	CG6470	4.11E-03	
A_09_P196145		1.77E-02	
A_09_P162210		8.20E-03	
A_09_P220365	CG6422	2.87E-02	
A_09_P183530		5.81E-03	
A_09_P177645	dally	4.01E-03	
A_09_P186860	CG32473	8.87E-03	
A_09_P186195	llp6	1.34E-02	
A_09_P187915		3.90E-02	
A_09_P050551	Hcf	2.60E-02	
A_09_P224945	CG4747	1.92E-03	
A_09_P050521	cpo	2.90E-02	
A_09_P198610	msl-2	2.07E-03	
A_09_P195190		4.07E-03	
A_09_P037361	CG2889	3.24E-03	
A_09_P187850		3.13E-02	
A_09_P050646	CG33936	1.71E-03	
A_09_P195860		2.83E-02	
A_09_P173875		1.17E-02	
A_09_P201580		7.73E-03	
A_09_P224725	scyl	2.63E-02	
A_09_P184420	TM9SF4	2.06E-03	
A_09_P015511	shep	3.49E-04	
A_09_P019781	Tsp26A	1.41E-02	
A_09_P179280	CG31191	1.61E-02	
A_09_P215760	CycG	1.75E-03	
A_09_P166170	Adar	4.88E-02	

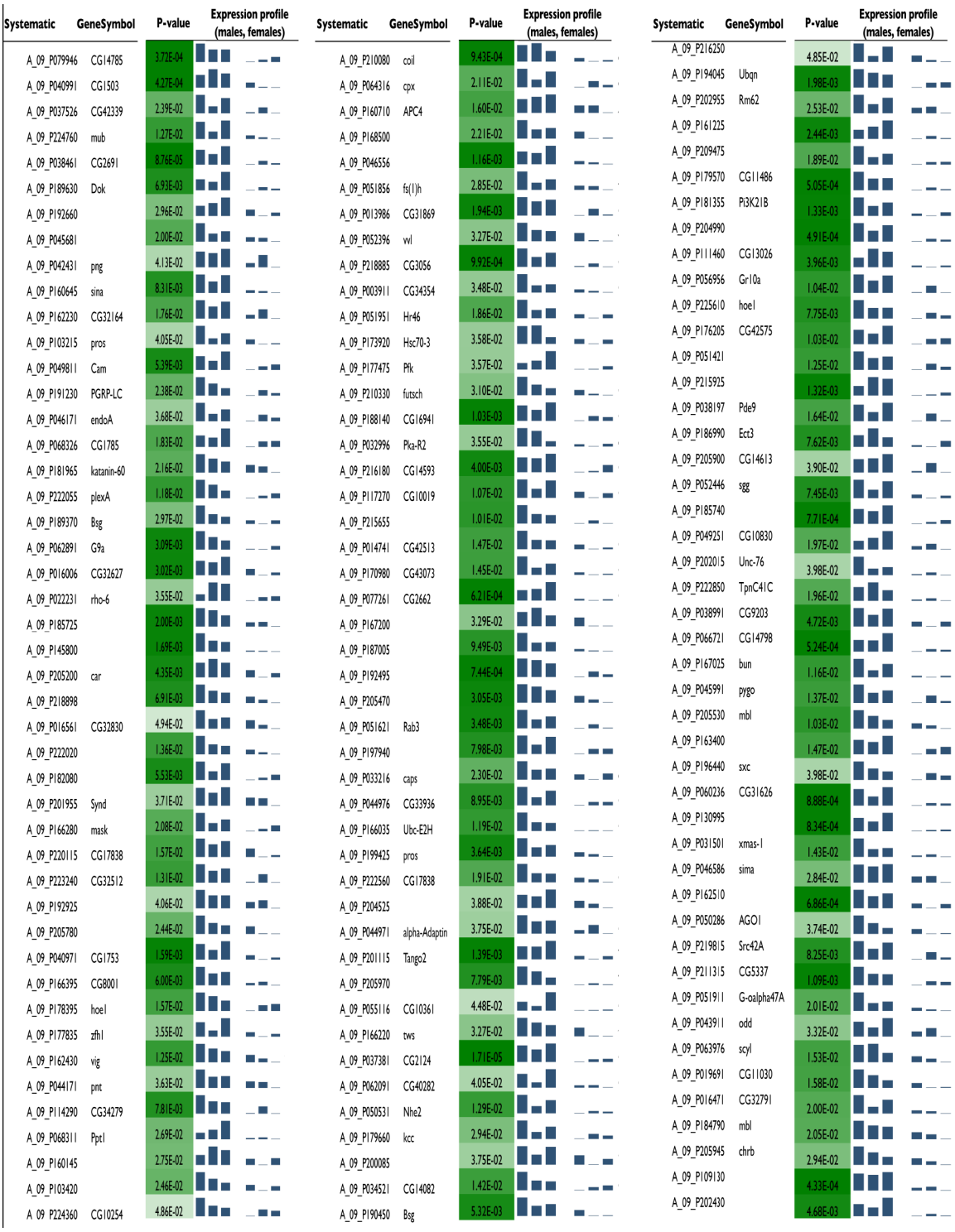
Systematic GeneSymbol P-value Expression profile (males, females)
A_09_P079946 CG14785 3.72E-04
A_09_P040991 CG1503 4.27E-04
A_09_P037526 CG42339 2.39E-02
A_09_P224760 mub 1.27E-02
A_09_P038461 CG2691 8.76E-05
A_09_P189630 Dok 6.93E-03
A_09_P192660 2.96E-02
A_09_P045681 2.00E-02
A_09_P042431 png 4.13E-02
A_09_P160645 sina 8.31E-03
A_09_P162230 CG32164 1.76E-02
A_09_P103215 pros 4.05E-02
A_09_P049811 Cam 5.39E-03
A_09_P191230 PGRP-LC 2.38E-02
A_09_P046171 endoA 3.68E-02
A_09_P068326 CG1785 1.83E-02
A_09_P181965 katanin-60 2.16E-02
A_09_P222055 plexA 1.18E-02
A_09_P189370 Bsg 2.97E-02
A_09_P062891 G9a 3.09E-03
A_09_P016006 CG32627 3.02E-03
A_09_P022231 rho-6 3.55E-02
A_09_P185725 2.00E-03
A_09_P145800 1.69E-03
A_09_P205200 car 4.35E-03
A_09_P218898 6.91E-03
A_09_P016561 CG32830 4.94E-02
A_09_P222020 1.36E-02
A_09_P182080 5.53E-03
A_09_P201955 Synd 3.71E-02
A_09_P166280 mask 2.08E-02
A_09_P220115 CG17838 1.57E-02
A_09_P223240 CG32512 1.31E-02
A_09_P192925 4.06E-02
A_09_P205780 2.44E-02
A_09_P040971 CG1753 1.59E-03
A_09_P166395 CG8001 6.00E-03
A_09_P178395 hoe1 1.57E-02
A_09_P177835 zfh1 3.55E-02
A_09_P162430 vig 1.25E-02
A_09_P044171 pnt 3.63E-02
A_09_P114290 CG34279 7.81E-03
A_09_P068311 Ppt1 2.69E-02
A_09_P160145 2.75E-02
A_09_P103420 2.46E-02
A_09_P224360 CG10254 4.86E-02
Systematic GeneSymbol P-value Expression profile (males, females)
A_09_P210080 coil 9.43E-04
A_09_P064316 cpx 2.11E-02
A_09_P160710 APC4 1.60E-02
A_09_P168500 2.21E-02
A_09_P046556 1.16E-03
A_09_P051856 fs(1)h 2.85E-02
A_09_P013986 CG31869 1.94E-03
A_09_P052396 vvl 3.27E-02
A_09_P218885 CG3056 9.92E-04
A_09_P003911 CG34354 3.48E-02
A_09_P051951 Hr46 1.86E-02
A_09_P173920 Hsc70-3 3.58E-02
A_09_P177475 Pfk 3.57E-02
A_09_P210330 futsch 3.10E-02
A_09_P188140 CG16941 1.03E-03
A_09_P032996 Pka-R2 3.55E-02
A_09_P216180 CG14593 4.00E-03
A_09_P117270 CG10019 1.07E-02
A_09_P215655 1.01E-02
A_09_P014741 CG42513 1.47E-02
A_09_P170980 CG43073 1.45E-02
A_09_P077261 CG2662 6.21E-04
A_09_P167200 3.29E-02
A_09_P187005 9.49E-03
A_09_P192495 7.44E-04
A_09_P205470 3.05E-03
A_09_P051621 Rab3 3.48E-03
A_09_P197940 7.98E-03
A_09_P033216 caps 2.30E-02
A_09_P044976 CG33936 8.95E-03
A_09_P166035 Ubc-E2H 1.19E-02
A_09_P199425 pros 3.64E-03
A_09_P222560 CG17838 1.91E-02
A_09_P204525 3.88E-02
A_09_P044971 alpha-Adaptin 3.75E-02
A_09_P201115 Tango2 1.39E-03
A_09_P205970 7.79E-03
A_09_P055116 CG10361 4.48E-02
A_09_P166220 tws 3.27E-02
A_09_P037381 CG2124 1.71E-05
A_09_P062091 CG40282 4.05E-02
A_09_P050531 Nhe2 1.29E-02
A_09_P179660 kcc 2.94E-02
A_09_P200085 3.75E-02
A_09_P034521 CG14082 1.42E-02
A_09_P190450 Bsg 5.32E-03
Systematic GeneSymbol P-value Expression profile (males, females)
A_09_P216250 4.85E-02
A_09_P194045 Ubqn 1.98E-03
A_09_P202955 Rm62 2.53E-02
A_09_P161225 2.44E-03
A_09_P209475 1.89E-02
A_09_P179570 CG11486 5.05E-04
A_09_P181355 PI3K21B 1.33E-03
A_09_P204990 4.91E-04
A_09_P111460 CG13026 3.96E-03
A_09_P056956 Gr10a 1.04E-02
A_09_P225610 hoe1 7.75E-03
A_09_P176205 CG42575 1.03E-02
A_09_P051421 1.25E-02
A_09_P215925 1.32E-03
A_09_P038197 Pde9 1.64E-02
A_09_P186990 Ect3 7.62E-03
A_09_P205900 CG14613 3.90E-02
A_09_P052446 sgg 7.45E-03
A_09_P185740 7.71E-04
A_09_P049251 CG10830 1.97E-02
A_09_P202015 Unc-76 3.98E-02
A_09_P222850 TpnC41C 1.96E-02
A_09_P038991 CG9203 4.72E-03
A_09_P066721 CG14798 5.24E-04
A_09_P167025 bun 1.16E-02
A_09_P045991 pygo 1.37E-02
A_09_P205530 mbl 1.03E-02
A_09_P163400 1.47E-02
A_09_P196440 sxc 3.98E-02
A_09_P060236 CG31626 8.88E-04
A_09_P130995 8.34E-04
A_09_P031501 xmas-1 1.43E-02
A_09_P046586 sima 2.84E-02
A_09_P162510 6.86E-04
A_09_P050286 AGO1 3.74E-02
A_09_P219815 Src42A 8.25E-03
A_09_P211315 CG5337 1.09E-03
A_09_P051911 G-oalpha47A 2.01E-02
A_09_P043911 odd 3.32E-02
A_09_P063976 scyl 1.53E-02
A_09_P019691 CG11030 1.58E-02
A_09_P016471 CG32791 2.00E-02
A_09_P184790 mbl 2.05E-02
A_09_P205945 chrb 2.94E-02
A_09_P109130 4.33E-04
A_09_P202430 4.68E-03

Systematic	GeneSymbol	P-value	Expression profile (males, females)
A_09_P196070	CG17193	1.02E-02	
A_09_P203810		6.86E-03	
A_09_P167340	cngl	2.47E-02	
A_09_P178895		4.56E-02	
A_09_P004756		3.32E-02	
A_09_P067201	CG3309	2.29E-03	
A_09_P207340	dpr12	2.20E-02	
A_09_P050331		1.16E-02	
A_09_P178285	CG11486	1.90E-03	
A_09_P217965		3.08E-02	
A_09_P154340	CG31688	1.69E-03	
A_09_P190920	Sur-8	1.97E-02	
A_09_P059121	CG31140	1.70E-02	
A_09_P183325	zfh1	3.47E-02	
A_09_P190110	Appl	1.95E-02	
A_09_P149460		9.95E-03	
A_09_P101490		2.33E-02	
A_09_P161965		3.20E-03	
A_09_P004256	tlk	3.91E-02	
A_09_P202515	pAbp	1.88E-04	
A_09_P033681	nxf2	2.16E-02	
A_09_P038481	CG15760	2.01E-02	
A_09_P071031	CG6356	1.45E-04	
A_09_P015726	CG32512	4.08E-02	
A_09_P179355	tral	1.35E-02	
A_09_P194925	bel	3.50E-04	
A_09_P012876	bol	1.86E-02	
A_09_P041261	CG2650	4.27E-03	
A_09_P135535		7.75E-03	
A_09_P224640		4.28E-04	
A_09_P139860	CG14778	2.84E-03	
A_09_P066396	cngl	3.05E-02	
A_09_P076886	Mcm3	1.72E-04	
A_09_P118775	Sema-1a	5.45E-03	
A_09_P199400	G9a	9.21E-03	
A_09_P204765		1.75E-02	
A_09_P040766	obst-A	9.69E-03	
A_09_P061846	RhoGAP102A	5.90E-05	
A_09_P042161	Edg84A	4.89E-02	
A_09_P004761		3.36E-02	
A_09_P186420		2.76E-03	
A_09_P167940	dpr9	8.58E-03	
A_09_P037816	CG2444	3.08E-02	
A_09_P162090	larp	1.23E-02	
A_09_P225570	dpr9	3.18E-03	
A_09_P204155		1.08E-04	

Systematic	GeneSymbol	P-value	Expression profile (males, females)
A_09_P058026	CG30284	4.20E-02	
A_09_P030306	Vps26	9.91E-04	
A_09_P016491	CG32801	1.23E-03	
A_09_P161725		1.57E-02	
A_09_P018361	c-cup	2.18E-02	
A_09_P041701	cin	1.81E-06	
A_09_P148695	RhoGAP1A	8.24E-04	
A_09_P220545		3.06E-02	
A_09_P059916	CG31462	2.36E-02	
A_09_P039381	CalpC	2.39E-03	
A_09_P197010	CG34391	1.22E-02	
A_09_P174340	CG6356	1.02E-02	
A_09_P123675	Drep-2	1.45E-02	
A_09_P118705		1.28E-02	
A_09_P166290	boi	1.82E-02	
A_09_P067621	CG42340	1.37E-02	
A_09_P180500	CG8709	3.19E-02	
A_09_P197225		4.46E-03	
A_09_P040746	CG9576	2.52E-02	
A_09_P145565	norpA	1.78E-03	
A_09_P211350	CG17838	4.43E-02	
A_09_P131435	odd	2.58E-02	
A_09_P182195	Pka-R1	7.77E-05	
A_09_P104655	Mcm3	6.97E-04	
A_09_P192270		1.57E-02	
A_09_P219135		7.57E-04	
A_09_P226155	Hr46	3.69E-03	
A_09_P191475	CG42492	1.02E-02	
A_09_P000101	D2R	3.53E-02	
A_09_P204390	CG40351	1.78E-03	
A_09_P035096	CG11796	3.35E-02	
A_09_P197265	CG2681	9.09E-05	
A_09_P071831	CG5948	1.60E-03	
A_09_P003491	CG34264	1.68E-02	
A_09_P164055	CG34306	1.37E-02	
A_09_P216680	CG42492	9.79E-03	
A_09_P069291	CG11391	1.77E-03	
A_09_P072621	CG42796	1.54E-02	
A_09_P043891	nod	1.80E-02	
A_09_P193985		2.01E-05	
A_09_P220670		4.00E-02	
A_09_P078831	l(1)G0045	3.01E-02	
A_09_P053166	CG6602	4.60E-02	
A_09_P090165	CG4857	2.30E-03	
A_09_P185440		2.76E-05	
A_09_P011896	GstD5	1.06E-03	

Systematic	GeneSymbol	P-value	Expression profile (males, females)
A_09_P063791	CG42492	2.43E-03	
A_09_P178841	CG40813	1.32E-02	
A_09_P176495		4.22E-02	
A_09_P224960		4.00E-03	
A_09_P221790		2.06E-02	
A_09_P210670	CG34205	1.06E-02	
A_09_P035611	CG14567	3.20E-03	
A_09_P181920		3.44E-02	
A_09_P205240		2.43E-02	
A_09_P066711	CG14778	7.67E-05	
A_09_P066186	CG31672	4.06E-02	
A_09_P090472		8.65E-04	
A_09_P203005	Nc73EF	3.32E-02	
A_09_P211035	CG13375	1.22E-02	
A_09_P066466	tyn	2.07E-06	
A_09_P066706	CG14770	9.18E-05	
A_09_P013826	CG31816	8.70E-03	
A_09_P039951	CG6788	3.45E-02	
A_09_P077961	RhoGAP1A	2.59E-07	
A_09_P225685	CG7852	2.69E-02	
A_09_P009671	Sxl	2.38E-05	
A_09_P032696	Crg-1	3.83E-03	
A_09_P058106	CG30334	1.62E-02	
A_09_P013211	Cyp4d2	3.45E-06	
A_09_P038441	Ndc80	8.05E-04	
A_09_P171335	CG42492	9.35E-03	
A_09_P004731		1.22E-02	
A_09_P062881	CG13375	2.82E-04	
A_09_P067481	CG5966	2.26E-02	
A_09_P063846	CG12643	1.81E-02	
A_09_P072221	CG17189	2.29E-02	
A_09_P075926	CG17560	2.29E-02	
A_09_P113455	CG17189	3.32E-02	
A_09_P184910		2.31E-05	
A_09_P042081	dsx	1.27E-05	
A_09_P062741	CG3706	6.26E-04	
A_09_P036646	CG1077	1.33E-02	
A_09_P214560		7.84E-03	
A_09_P001411		8.69E-04	
A_09_P074216	CG12256	3.74E-02	
A_09_P171190		9.23E-03	
A_09_P047886		1.00E-04	
A_09_P217945	CG11391	1.21E-02	
A_09_P067806	CG4586	4.91E-05	
A_09_P210350		6.59E-03	
A_09_P205860		1.48E-02	

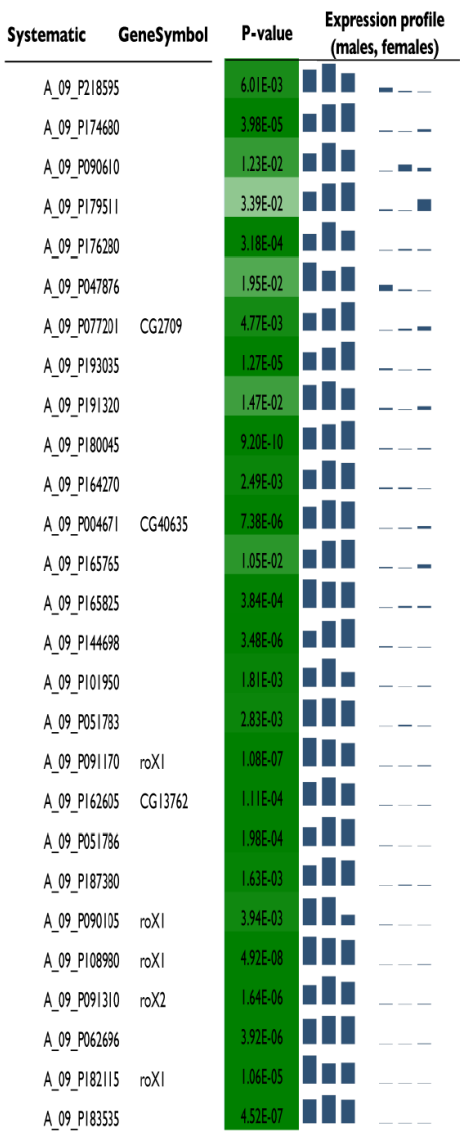

Systematic	GeneSymbol	P-value	Expression profile (males, females)
A_09_P218595		6.01E-03	
A_09_P174680		3.98E-05	
A_09_P090610		1.23E-02	
A_09_P179511		3.39E-02	
A_09_P176280		3.18E-04	
A_09_P047876		1.95E-02	
A_09_P077201	CG2709	4.77E-03	
A_09_P193035		1.27E-05	
A_09_P191320		1.47E-02	
A_09_P180045		9.20E-10	
A_09_P164270		2.49E-03	
A_09_P004671	CG40635	7.38E-06	
A_09_P165765		1.05E-02	
A_09_P165825		3.84E-04	
A_09_P144698		3.48E-06	
A_09_P101950		1.81E-03	
A_09_P051783		2.83E-03	
A_09_P091170	roX1	1.08E-07	
A_09_P162605	CG13762	1.11E-04	
A_09_P051786		1.98E-04	
A_09_P187380		1.63E-03	
A_09_P090105	roX1	3.94E-03	
A_09_P108980	roX1	4.92E-08	
A_09_P091310	roX2	1.64E-06	
A_09_P062696		3.92E-06	
A_09_P182115	roX1	1.06E-05	
A_09_P183535		4.52E-07	

References

Abbott, N.J. (1991). Permeability and transport of glial blood brain barriers. Ann N Y Acad Sci *633*, 378-394.

Aboobaker, A.A., Tomancak, P., Patel, N., Rubin, G.M., and Lai, E.C. (2005). *Drosophila* microRNAs exhibit diverse spatial expression patterns during embryonic development. Proceedings of the National Academy of Sciences of the United States of America *102*, 18017-18022.

Aravin, A.A., Lagos-Quintana, M., Yalcin, A., Zavolan, M., Marks, D., Snyder, B., Gaasterland, T., Meyer, J., and Tuschl, T. (2003). The small RNA profile during *Drosophila melanogaster* development. Dev Cell *5*, 337-350.

Arbeitman, M.N., Fleming, A.A., Siegal, M.L., Null, B.H., and Baker, B.S. (2004). A genomic analysis of *Drosophila* somatic sexual differentiation and its regulation. Development *131*, 2007-2021.

Arbeitman, M.N., Kopp, A., Siegal, M.L., and Van Doren, M. (2010). Everything you always wanted to know about sex ... in flies. Sex Dev *4*, 315-320.

Auld, V.J., Fetter, R.D., Broadie, K., and Goodman, C.S. (1995). Gliotactin, a novel transmembrane protein on peripheral glia, is required to form the blood-nerve barrier in *Drosophila*. Cell *81*, 757-767.

Awasaki, T., Lai, S.L., Ito, K., and Lee, T. (2008). Organization and postembryonic development of glial cells in the adult central brain of *Drosophila*. J Neurosci *28*, 13742-13753.

Bainton, R.J., Tsai, L.T., Schwabe, T., DeSalvo, M., Gaul, U., and Heberlein, U. (2005). moody encodes two GPCRs that regulate cocaine behaviors and blood brain barrier permeability in *Drosophila*. Cell *123*, 145-156.

Baker, B.S. (1989). Sex in flies: the splice of life. Nature *340*, 521-524.

Baker, B.S., and Ridge, K.A. (1980). Sex and the single cell. I. On the action of major loci affecting sex determination in *Drosophila melanogaster*. Genetics *94*, 383-423.

Baker, B.S., Taylor, B.J., and Hall, J.C. (2001). Are complex behaviors specified by dedicated regulatory genes? Reasoning from *Drosophila*. Cell *105*, 13-24.

Ballabh, P., Braun, A., and Nedergaard, M. (2004). The blood brain barrier: an overview:

structure, regulation, and clinical implications. Neurobiol Dis *16*, 1-13.

Banerjee, S., Pillai, A.M., Paik, R., Li, J., and Bhat, M.A. (2006). Axonal ensheathment and septate junction formation in the peripheral nervous system of *Drosophila*. J Neurosci *26*, 3319-3329.

Barmina, O., Gonzalo, M., McIntyre, L.M., and Kopp, A. (2005). Sex- and segment-specific modulation of gene expression profiles in *Drosophila*. Developmental Biology *288*, 528-544.

Baumgartner, S., Littleton, J.T., Broadie, K., Bhat, M.A., Harbecke, R., Lengyel, J.A., Chiquet-Ehrismann, R., Prokop, A., and Bellen, H.J. (1996). A *Drosophila* neurexin is required for septate junction and blood-nerve barrier formation and function. Cell *87*, 1059-1068.

Bernardo, T.J., and Dubrovsky, E.B. (2012). The *Drosophila* juvenile hormone receptor candidates methoprene-tolerant (MET) and germ cell-expressed (GCE) utilize a conserved LIXXL motif to bind the FTZ-F1 nuclear receptor. J Biol Chem *287*, 7821-7833.

Benham, A.L. (2011). MicroRNA: Discovery, family dynamics, and functional implications. (Unpublished doctoral dissertation). University of Houston, Houston, TX.

Bhardwaj, A., Singh, S., and Singh, A.P. (2010). MicroRNA-based cancer therapeutics: Big hope from small RNAs. Mol Cell Pharmacol *2*, 213-219.

Bhat, M.A., Rios, J.C., Lu, Y., Garcia-Fresco, G.P., Ching, W., St Martin, M., Li, J., Einheber, S., Chesler, M., Rosenbluth, J.*, et al.* (2001). Axon-glia interactions and the domain organization of myelinated axons requires neurexin IV/Caspr/Paranodin. Neuron *30*, 369-383.

Billeter, J.C., and Goodwin, S.F. (2004). Characterization of *Drosophila* fruitless-gal4 transgenes reveals expression in male-specific fruitless neurons and innervation of male reproductive structures. J Comp Neurol *475*, 270-287.

Billeter, J.C., Rideout, E.J., Dornan, A.J., and Goodwin, S.F. (2006). Control of male sexual behavior in *Drosophila* by the sex determination pathway. Curr Biol *16*, R766-776.

Bjorum, S.M., Simonette, R.A., Alanis, R., Jr., Wang, J.E., Lewis, B.M., Trejo, M.H., Hanson, K.A., and Beckingham, K.M. (2013). The *Drosophila* BTB domain protein Jim Lovell has roles in multiple larval and adult behaviors. PLoS One *8*, e61270.

Boggs, R.T., Gregor, P., Idriss, S., Belote, J.M., and McKeown, M. (1987). Regulation of sexual differentiation in *Drosophila melanogaster* via alternative splicing of RNA from the transformer gene. Cell *50*, 739-747.

Boltz, K.A., Ellis, L.L., and Carney, G.E. (2007). *Drosophila melanogaster* p24 genes have developmental, tissue-specific, and sex-specific expression patterns and functions. Dev Dyn *236*, 544-555.

Bookout, A.L., and Mangelsdorf, D.J. (2003). Quantitative real-time PCR protocol for analysis of nuclear receptor signaling pathways. Nuclear Receptor Signaling *1*, e012.

Boulan, L., Martin, D., and Milan, M. (2013). bantam miRNA promotes systemic growth by connecting insulin signaling and ecdysone production. Curr Biol *23*, 473-478.

Brand, A.H., and Perrimon, N. (1993). Targeted gene expression as a means of altering cell fates and generating dominant phenotypes. Development *118*, 401-415.

Brennecke, J., Stark, A., Russell, R.B., and Cohen, S.M. (2005). Principles of microRNA-target recognition. PLoS Biol *3*, e85.

Burtis, K.C., and Baker, B.S. (1989). *Drosophila* doublesex gene controls somatic sexual differentiation by producing alternatively spliced mRNAs encoding related sex-specific polypeptides. Cell *56*, 997-1010.

Bushati, N., and Cohen, S.M. (2007). microRNA functions. Annu Rev Cell Dev Biol *23*, 175-205.

Carlson, S.D., Juang, J.L., Hilgers, S.L., and Garment, M.B. (2000). Blood barriers of the insect. Annu Rev Entomol *45*, 151-174.

Carney, G.E., Wade, A.A., Sapra, R., Goldstein, E.S., and Bender, M. (1997). DHR3, an ecdysone-inducible early-late gene encoding a *Drosophila* nuclear receptor, is required for embryogenesis. Proceedings of the National Academy of Sciences of the United States of America *94*, 12024-12029.

Caygill, E.E., and Johnston, L.A. (2008). Temporal regulation of metamorphic processes in *Drosophila* by the let-7 and miR-125 heterochronic microRNAs. Curr Biol *18*, 943-950.

Chang, P.L., Dunham, J.P., Nuzhdin, S.V., and Arbeitman, M.N. (2011). Somatic sex-specific transcriptome differences in *Drosophila* revealed by whole transcriptome sequencing. BMC Genomics *12*, 364.

Chawla, G., and Sokol, N.S. (2012). Hormonal activation of let-7-C microRNAs via EcR is required for adult *Drosophila melanogaster* morphology and function. Development *139*, 1788-1797.

Chen, B., Liu, H., Ren, J., and Guo, A. (2012). Mutation of *Drosophila* dopamine receptor DopR leads to male-male courtship behavior. Biochem Biophys Res Commun *423*, 557-563.

Chen, Y., and Stallings, R.L. (2007). Differential patterns of microRNA expression in neuroblastoma are correlated with prognosis, differentiation, and apoptosis. Cancer Res *67*, 976-983.

Christiansen, A.E., Keisman, E.L., Ahmad, S.M., and Baker, B.S. (2002). Sex comes in from the cold: the integration of sex and pattern. Trends Genet *18*, 510-516.

Cline, T.W., and Meyer, B.J. (1996). Vive la difference: males vs females in flies vs worms. Annu Rev Genet *30*, 637-702.

Clyne, J.D., and Miesenbock, G. (2008). Sex-specific control and tuning of the pattern generator for courtship song in *Drosophila*. Cell *133*, 354-363.

Dalton, J.E., Fear, J.M., Knott, S., Baker, B.S., McIntyre, L.M., and Arbeitman, M.N. (2013). Male-specific fruitless isoforms have different regulatory roles conferred by distinct zinc finger DNA binding domains. BMC Genomics *14*, 659.

Daneman, R., and Barres, B.A. (2005). The blood brain barrier: lessons from moody flies. Cell *123*, 9-12.

Dauwalder, B. (2008). Systems behavior: of male courtship, the nervous system and beyond in *Drosophila*. Curr Genomics *9*, 517-524.

Dauwalder, B. (2011). The roles of fruitless and doublesex in the control of male courtship. Int Rev Neurobiol *99*, 87-105.

Dauwalder, B., Tsujimoto, S., Moss, J., and Mattox, W. (2002). The *Drosophila* takeout gene is regulated by the somatic sex-determination pathway and affects male courtship behavior. Genes Dev *16*, 2879-2892.

Dean, T., Xu, R., Joiner, W., Sehgal, A., and Hoshi, T. (2011). *Drosophila* QVR/SSS modulates the activation and C-type inactivation kinetics of Shaker K(+) channels. J Neurosci *31*, 11387-11395.

Demir, E., and Dickson, B.J. (2005). fruitless splicing specifies male courtship behavior in *Drosophila*. Cell *121*, 785-794.

DeSalvo, M.K., Mayer, N., Mayer, F., and Bainton, R.J. (2011). Physiologic and anatomic characterization of the brain surface glia barrier of *Drosophila*. Glia *59*, 1322-1340.

Diler, A.S., Uzum, G., Akgun Dar, K., Aksu, U., Atukeren, P., and Ziylan, Y.Z. (2007). Sex differences in modulating blood brain barrier permeability by NO in pentylenetetrazol-induced epileptic seizures. Life Sci *80*, 1274-1281.

Doench, J.G., and Sharp, P.A. (2004). Specificity of microRNA target selection in translational repression. Genes Dev *18*, 504-511.

Dong, Y., and Benveniste, E.N. (2001). Immune function of astrocytes. Glia *36*, 180-190.

Du, T., and Zamore, P.D. (2005). microPrimer: the biogenesis and function of microRNA. Development *132*, 4645-4652.

Dubrovsky, E.B., Dubrovskaya, V.A., Bernardo, T., Otte, V., DiFilippo, R., and Bryan, H. (2011). The *Drosophila* FTZ-F1 nuclear receptor mediates juvenile hormone activation of E75A gene expression through an intracellular pathway. J Biol Chem *286*, 33689-33700.

Edwards, J.S., Swales, L.S., and Bate, M. (1993). The differentiation between neuroglia and connective tissue sheath in insect ganglia revisited: the neural lamella and perineurial sheath cells are absent in a mesodermless mutant of *Drosophila*. J Comp Neurol *333*, 301-308.

Ejima, A., and Griffith, L.C. (2008). Courtship initiation is stimulated by acoustic signals in *Drosophila melanogaster*. PLoS One *3*, e3246.

Ellis, L.L., and Carney, G.E. (2009). *Drosophila melanogaster* males respond differently

at the behavioural and genome-wide levels to *Drosophila melanogaster* and *Drosophila simulans* females. Journal of Evolutionary Biology *22*, 2183-2191.

Ellis, L.L., and Carney, G.E. (2010). Mating alters gene expression patterns in *Drosophila melanogaster* male heads. BMC Genomics *11*, 558.

Ellis, L.L., and Carney, G.E. (2011). Socially-responsive gene expression in male *Drosophila melanogaster* is influenced by the sex of the interacting partner. Genetics *187*, 157-169.

Esslinger, S.M., Schwalb, B., Helfer, S., Michalik, K.M., Witte, H., Maier, K.C., Martin, D., Michalke, B., Tresch, A., Cramer, P.*, et al.* (2013). *Drosophila* miR-277 controls branched-chain amino acid catabolism and affects lifespan. RNA Biol *10*, 1042-1056.

Eun, S.H., Stoiber, P.M., Wright, H.J., McMurdie, K.E., Choi, C.H., Gan, Q., Lim, C., and Chen, X. (2013). MicroRNAs downregulate bag of marbles to ensure proper terminal differentiation in the *Drosophila* male germline. Development *140*, 23-30.

Faivre-Sarrailh, C., Banerjee, S., Li, J., Hortsch, M., Laval, M., and Bhat, M.A. (2004). *Drosophila* contactin, a homolog of vertebrate contactin, is required for septate junction organization and paracellular barrier function. Development *131*, 4931-4942.

Ferveur, J.F. (2010). *Drosophila* female courtship and mating behaviors: sensory signals, genes, neural structures and evolution. Curr Opin Neurobiol *20*, 764-769.

Ferveur, J.F., and Greenspan, R.J. (1998). Courtship behavior of brain mosaics in *Drosophila*. J Neurogenet *12*, 205-226.

Ferveur, J.F., Stortkuhl, K.F., Stocker, R.F., and Greenspan, R.J. (1995). Genetic feminization of brain structures and changed sexual orientation in male *Drosophila*. Science *267*, 902-905.

Foley, N.H., Bray, I.M., Tivnan, A., Bryan, K., Murphy, D.M., Buckley, P.G., Ryan, J., O'Meara, A., O'Sullivan, M., and Stallings, R.L. (2010). MicroRNA-184 inhibits neuroblastoma cell survival through targeting the serine/threonine kinase AKT2. Mol Cancer *9*, 83.

Friedman, R.C., Farh, K.K., Burge, C.B., and Bartel, D.P. (2009). Most mammalian mRNAs are conserved targets of microRNAs. Genome Res *19*, 92-105.

Fujii, S., and Amrein, H. (2002). Genes expressed in the *Drosophila* head reveal a role for fat cells in sex-specific physiology. EMBO J *21*, 5353-5363.

Furuse, M., and Tsukita, S. (2006). Claudins in occluding junctions of humans and flies. Trends Cell Biol *16*, 181-188.

Gao, L., Hou, X., Wu, L., Zhang, F., Zhang, Q., Ye, X., Yang, Y., and Lin, X. (2013a). *Drosophila* miR-960 negatively regulates Hedgehog signaling by suppressing Smoothened, Costal-2 and Fused. Cell Signal *25*, 1301-1309.

Gao, L., Wu, L., Hou, X., Zhang, Q., Zhang, F., Ye, X., Yang, Y., and Lin, X. (2013b). *Drosophila* miR-932 modulates hedgehog signaling by targeting its co-receptor brother of ihog. Developmental Biology *377*, 166-176.

Garbuzov, A., and Tatar, M. (2010). Hormonal regulation of *Drosophila* microRNA let-7 and miR-125 that target innate immunity. Fly (Austin) *4*, 306-311.

Gehrke, S., Imai, Y., Sokol, N., and Lu, B. (2010). Pathogenic LRRK2 negatively regulates microRNA-mediated translational repression. Nature *466*, 637-641.

Genova, J.L., and Fehon, R.G. (2003). Neuroglian, Gliotactin, and the Na+/K+ ATPase are essential for septate junction function in *Drosophila*. The Journal of Cell Biology *161*, 979-989.

Gilbert, M., Smith, J., Roskams, A.J., and Auld, V.J. (2001). Neuroligin 3 is a vertebrate gliotactin expressed in the olfactory ensheathing glia, a growth-promoting class of macroglia. Glia *34*, 151-164.

Goldman, T.D., and Arbeitman, M.N. (2007). Genomic and functional studies of *Drosophila* sex hierarchy regulated gene expression in adult head and nervous system tissues. PLoS Genet *3*, e216.

Greenspan, R.J., and Ferveur, J.F. (2000). Courtship in *Drosophila*. Annu Rev Genet *34*, 205-232.

Grimson, A., Farh, K.K., Johnston, W.K., Garrett-Engele, P., Lim, L.P., and Bartel, D.P. (2007). MicroRNA targeting specificity in mammals: determinants beyond seed pairing. Mol Cell *27*, 91-105.

Hall, J.C. (1977). Portions of the central nervous system controlling reproductive behavior in *Drosophila melanogaster*. Behav Genet *7*, 291-312.

Hall, J.C. (1979). Control of male reproductive behavior by the central nervous system of *Drosophila*: dissection of a courtship pathway by genetic mosaics. Genetics *92*, 437-457.

Hall, J.C. (1994). The mating of a fly. Science *264*, 1702-1714.

Hammond, S.M., Bernstein, E., Beach, D., and Hannon, G.J. (2000). An RNA-directed nuclease mediates post-transcriptional gene silencing in *Drosophila* cells. Nature *404*, 293-296.

Heinrichs, V., Ryner, L.C., and Baker, B.S. (1998). Regulation of sex-specific selection of fruitless 5' splice sites by transformer and transformer-2. Mol Cell Biol *18*, 450-458.

Hermeking, H. (2010). The miR-34 family in cancer and apoptosis. Cell Death Differ *17*, 193-199.

Hilgers, V., Bushati, N., and Cohen, S.M. (2010). *Drosophila* microRNAs 263a/b confer robustness during development by protecting nascent sense organs from apoptosis. PLoS Biol *8*, e1000396.

Hoxha, V., Lama, C., Chang, P.L., Saurabh, S., Patel, N., Olate, N., and Dauwalder, B. (2013). Sex-specific signaling in the blood brain barrier is required for male courtship in *Drosophila*. PLoS Genet *9*, e1003217.

Huang, Y.C., Smith, L., Poulton, J., and Deng, W.M. (2013). The microRNA miR-7 regulates Tramtrack69 in a developmental switch in *Drosophila* follicle cells. Development *140*, 897-905.

Hutvagner, G., and Zamore, P.D. (2002). A microRNA in a multiple-turnover RNAi enzyme complex. Science *297*, 2056-2060.

Iovino, N., Pane, A., and Gaul, U. (2009). miR-184 has multiple roles in *Drosophila* female germline development. Dev Cell *17*, 123-133.

Ishimoto, H., Sakai, T., and Kitamoto, T. (2009). Ecdysone signaling regulates the formation of long-term courtship memory in adult *Drosophila melanogaster*. Proceedings of the National Academy of Sciences of the United States of America

106, 6381-6386.

Ito, H., Fujitani, K., Usui, K., Shimizu-Nishikawa, K., Tanaka, S., and Yamamoto, D. (1996). Sexual orientation in *Drosophila* is altered by the satori mutation in the sex-determination gene fruitless that encodes a zinc finger protein with a BTB domain. Proceedings of the National Academy of Sciences of the United States of America *93*, 9687-9692.

Ito, H., Sato, K., Koganezawa, M., Ote, M., Matsumoto, K., Hama, C., and Yamamoto, D. (2012). Fruitless recruits two antagonistic chromatin factors to establish single-neuron sexual dimorphism. Cell *149*, 1327-1338.

Jones-Rhoades, M.W., Bartel, D.P., and Bartel, B. (2006). MicroRNAS and their regulatory roles in plants. Annu Rev Plant Biol *57*, 19-53.

Kadener, S., Menet, J.S., Sugino, K., Horwich, M.D., Weissbein, U., Nawathean, P., Vagin, V.V., Zamore, P.D., Nelson, S.B., and Rosbash, M. (2009). A role for microRNAs in the *Drosophila* circadian clock. Genes Dev *23*, 2179-2191.

Khan, E. (2005). An examination of the blood brain barrier in health and disease. British Journal of Nursing *14*, 509-513.

Kim, W.J., Jan, L.Y., and Jan, Y.N. (2012). Contribution of visual and circadian neural circuits to memory for prolonged mating induced by rivals. Nature Neuroscience *15*, 876-883.

Kimura, K., Hachiya, T., Koganezawa, M., Tazawa, T., and Yamamoto, D. (2008). Fruitless and doublesex coordinate to generate male-specific neurons that can initiate courtship. Neuron *59*, 759-769.

Kloosterman, W.P., Wienholds, E., Ketting, R.F., and Plasterk, R.H. (2004). Substrate requirements for let-7 function in the developing zebrafish embryo. Nucleic Acids Res *32*, 6284-6291.

Koelle, M.R., Segraves, W.A., and Hogness, D.S. (1992). DHR3: a *Drosophila* steroid receptor homolog. Proceedings of the National Academy of Sciences of the United States of America *89*, 6167-6171.

Koh, K., Joiner, W.J., Wu, M.N., Yue, Z., Smith, C.J., and Sehgal, A. (2008). Identification of SLEEPLESS, a sleep-promoting factor. Science *321*, 372-376.

Kohatsu, S., Koganezawa, M., and Yamamoto, D. (2011). Female contact activates male-specific interneurons that trigger stereotypic courtship behavior in *Drosophila*. Neuron *69*, 498-508.

Kubli, E. (2003). Sex-peptides: seminal peptides of the *Drosophila* male. Cell Mol Life Sci *60*, 1689-1704.

Kucherenko, M.M., and Shcherbata, H.R. (2013). Steroids as external temporal codes act via microRNAs and cooperate with cytokines in differential neurogenesis. Fly (Austin) *7*, 173-183.

Kugler, J.M., Chen, Y.W., Weng, R., and Cohen, S.M. (2013). miR-989 is required for border cell migration in the *Drosophila* ovary. PLoS One *8*, e67075.

Kwon, C., Han, Z., Olson, E.N., and Srivastava, D. (2005). MicroRNA1 influences cardiac differentiation in *Drosophila* and regulates Notch signaling. Proceedings of the National Academy of Sciences of the United States of America *102*, 18986-18991.

Lacaille, F., Hiroi, M., Twele, R., Inoshita, T., Umemoto, D., Maniere, G., Marion-Poll, F., Ozaki, M., Francke, W., Cobb, M.*, et al.* (2007). An inhibitory sex pheromone tastes bitter for *Drosophila* males. PLoS One *2*, e661.

LaFerriere, H., Guarnieri, D.J., Sitaraman, D., Diegelmann, S., Heberlein, U., and Zars, T. (2008). Genetic dissociation of ethanol sensitivity and memory formation in *Drosophila melanogaster*. Genetics *178*, 1895-1902.

Lam, G., Hall, B.L., Bender, M., and Thummel, C.S. (1999). DHR3 is required for the prepupal-pupal transition and differentiation of adult structures during *Drosophila* metamorphosis. Developmental Biology *212*, 204-216.

Lazareva, A.A., Roman, G., Mattox, W., Hardin, P.E., and Dauwalder, B. (2007). A role for the adult fat body in *Drosophila* male courtship behavior. PLoS Genet *3*, e16.

Lee, G., Foss, M., Goodwin, S.F., Carlo, T., Taylor, B.J., and Hall, J.C. (2000). Spatial, temporal, and sexually dimorphic expression patterns of the fruitless gene in the *Drosophila* central nervous system. J Neurobiol *43*, 404-426.

Lee, R.C., Feinbaum, R.L., and Ambros, V. (1993). The *C. elegans* heterochronic gene lin-4 encodes small RNAs with antisense complementarity to lin-14. Cell *75*, 843-

854.

Lewis, B.P., Burge, C.B., and Bartel, D.P. (2005). Conserved seed pairing, often flanked by adenosines, indicates that thousands of human genes are microRNA targets. Cell *120*, 15-20.

Li, P., Peng, J., Hu, J., Xu, Z., Xie, W., and Yuan, L. (2011). Localized expression pattern of miR-184 in *Drosophila*. Mol Biol Rep *38*, 355-358.

Li, W., Cressy, M., Qin, H., Fulga, T., Van Vactor, D., and Dubnau, J. (2013). MicroRNA-276a functions in ellipsoid body and mushroom body neurons for naive and conditioned olfactory avoidance in *Drosophila*. J Neurosci *33*, 5821-5833.

Li, X., and Carthew, R.W. (2005). A microRNA mediates EGF receptor signaling and promotes photoreceptor differentiation in the *Drosophila* eye. Cell *123*, 1267-1277.

Li, X., Ding, L., Xu, Y., Wang, Y., and Ping, Q. (2009). Targeted delivery of doxorubicin using stealth liposomes modified with transferrin. International Journal of Pharmaceutics *373*, 116-123.

Li, Y., and Padgett, R.W. (2012). bantam is required for optic lobe development and glial cell proliferation. PLoS One *7*, e32910.

Li, Y., Wang, F., Lee, J.A., and Gao, F.B. (2006). MicroRNA-9a ensures the precise specification of sensory organ precursors in *Drosophila*. Genes Dev *20*, 2793-2805.

Lindquist, S. (1986). The heat-shock response. Annu Rev Biochem *55*, 1151-1191.

Lingel, A., Simon, B., Izaurralde, E., and Sattler, M. (2003). Structure and nucleic-acid binding of the *Drosophila* Argonaute 2 PAZ domain. Nature *426*, 465-469.

Lingel, A., Simon, B., Izaurralde, E., and Sattler, M. (2004). Nucleic acid 3'-end recognition by the Argonaute2 PAZ domain. Nat Struct Mol Biol *11*, 576-577.

Lisciotto, C.A., DeBold, J.F., and Miczek, K.A. (1990). Sexual differentiation and the effects of alcohol on aggressive behavior in mice. Pharmacol Biochem Behav *35*, 357-362.

Liu, G., Mao, J., Jiang, Z., Sun, T., Hu, Y., Jiang, Z., Zhang, C., Dong, J., Huang, Q., and

Lan, Q. (2013). Transferrin-modified Doxorubicin-loaded biodegradable nanoparticles exhibit enhanced efficacy in treating brain glioma-bearing rats. Cancer Biotherapy & Radiopharmaceuticals *28*, 691-696.

Liu, N., Abe, M., Sabin, L.R., Hendriks, G.J., Naqvi, A.S., Yu, Z., Cherry, S., and Bonini, N.M. (2011). The exoribonuclease Nibbler controls 3' end processing of microRNAs in *Drosophila*. Curr Biol *21*, 1888-1893.

Liu, N., Landreh, M., Cao, K., Abe, M., Hendriks, G.J., Kennerdell, J.R., Zhu, Y., Wang, L.S., and Bonini, N.M. (2012). The microRNA miR-34 modulates ageing and neurodegeneration in *Drosophila*. Nature *482*, 519-523.

Liu, S., Gao, S., Zhang, D., Yin, J., Xiang, Z., and Xia, Q. (2010). MicroRNAs show diverse and dynamic expression patterns in multiple tissues of *Bombyx mori.* BMC Genomics *11*, 85.

Liu, S., Zhang, L., Li, Q., Zhao, P., Duan, J., Cheng, D., Xiang, Z., and Xia, Q. (2009). MicroRNA expression profiling during the life cycle of the silkworm (*Bombyx mori*). BMC Genomics *10*, 455.

Loya, C.M., Lu, C.S., Van Vactor, D., and Fulga, T.A. (2009). Transgenic microRNA inhibition with spatiotemporal specificity in intact organisms. Nature Methods *6*, 897-903.

Lytle, J.R., Yario, T.A., and Steitz, J.A. (2007). Target mRNAs are repressed as efficiently by microRNA-binding sites in the 5' UTR as in the 3' UTR. Proceedings of the National Academy of Sciences of the United States of America *104*, 9667-9672.

Manoli, D.S., Foss, M., Villella, A., Taylor, B.J., Hall, J.C., and Baker, B.S. (2005). Male-specific fruitless specifies the neural substrates of *Drosophila* courtship behaviour. Nature *436*, 395-400.

Manoli, D.S., Meissner, G.W., and Baker, B.S. (2006). Blueprints for behavior: genetic specification of neural circuitry for innate behaviors. Trends Neurosci *29*, 444-451.

Marrone, A.K., Edeleva, E.V., Kucherenko, M.M., Hsiao, N.H., and Shcherbata, H.R. (2012). Dg-Dys-Syn1 signaling in *Drosophila* regulates the microRNA profile.

BMC Cell Biology *13*, 26.

Mayer, F., Mayer, N., Chinn, L., Pinsonneault, R.L., Kroetz, D., and Bainton, R.J. (2009). Evolutionary conservation of vertebrate blood brain barrier chemoprotective mechanisms in *Drosophila*. J Neurosci *29*, 3538-3550.

McGuire, S.E., Le, P.T., Osborn, A.J., Matsumoto, K., and Davis, R.L. (2003). Spatiotemporal rescue of memory dysfunction in *Drosophila*. Science *302*, 1765-1768.

McGuire, S.E., Mao, Z., and Davis, R.L. (2004a). Spatiotemporal gene expression targeting with the TARGET and gene-switch systems in *Drosophila*. Sci STKE *2004*, pl6.

McGuire, S.E., Roman, G., and Davis, R.L. (2004b). Gene expression systems in *Drosophila*: a synthesis of time and space. Trends Genet *20*, 384-391.

McRobert, S.P., and Tompkins, L. (1985). The effect of transformer, doublesex and intersex mutations on the sexual behavior of *Drosophila melanogaster*. Genetics *111*, 89-96.

Meissner, G.W., Manoli, D.S., Chavez, J.F., Knapp, J.M., Lin, T.L., Stevens, R.J., Mellert, D.J., Tran, D.H., and Baker, B.S. (2011). Functional dissection of the neural substrates for sexual behaviors in *Drosophila melanogaster*. Genetics *189*, 195-211.

Miyamoto, T., and Amrein, H. (2008). Suppression of male courtship by a *Drosophila* pheromone receptor. Nature Neuroscience *11*, 874-876.

Murchison, E.P., and Hannon, G.J. (2004). miRNAs on the move: miRNA biogenesis and the RNAi machinery. Curr Opin Cell Biol *16*, 223-229.

Nesler, K.R., Sand, R.I., Symmes, B.A., Pradhan, S.J., Boin, N.G., Laun, A.E., and Barbee, S.A. (2013). The miRNA pathway controls rapid changes in activity-dependent synaptic structure at the *Drosophila melanogaster* neuromuscular junction. PLoS One *8*, e68385.

Oztas, B. (1998). Sex and blood brain barrier. Pharmacological research : the official Journal of the Italian Pharmacological Society *37*, 165-167.

Oztas, B., Camurcu, S., and Kaya, M. (1992). Influence of sex on the blood brain barrier

permeability during bicuculline-induced seizures. Int J Neurosci *65*, 131-139.

Oztas, B., and Kaya, M. (1998). Influence of orchidectomy and ovariectomy on the blood brain barrier permeability during bicuculline-induced seizures. Horm Metab Res *30*, 500-503.

Pan, Y., Robinett, C.C., and Baker, B.S. (2011). Turning males on: activation of male courtship behavior in *Drosophila melanogaster*. PLoS One *6*, e21144.

Pancratov, R., Peng, F., Smibert, P., Yang, S., Jr., Olson, E.R., Guha-Gilford, C., Kapoor, A.J., Liang, F.X., Lai, E.C., Flaherty, M.S.*, et al.* (2013). The miR-310/13 cluster antagonizes beta-catenin function in the regulation of germ and somatic cell differentiation in the *Drosophila* testis. Development *140*, 2904-2916.

Parks, A.L., Cook, K.R., Belvin, M., Dompe, N.A., Fawcett, R., Huppert, K., Tan, L.R., Winter, C.G., Bogart, K.P., Deal, J.E.*, et al.* (2004). Systematic generation of high-resolution deletion coverage of the *Drosophila melanogaster* genome. Nat Genet *36*, 288-292.

Peng, C., Li, W.A., Fu, P., Chakraborty, T., Hussain, M., Guthikonda, M., Rafols, J.A., and Ding, Y. (2013). At low doses ethanol maintains blood brain barrier (BBB) integrity after hypoxia and reoxygenation: a brain slice study. Neurological Research *35*, 790-797.

Peters, L., and Meister, G. (2007). Argonaute proteins: mediators of RNA silencing. Mol Cell *26*, 611-623.

Poliak, S., and Peles, E. (2003). The local differentiation of myelinated axons at nodes of Ranvier. Nat Rev Neurosci *4*, 968-980.

Qian, L., Wythe, J.D., Liu, J., Cartry, J., Vogler, G., Mohapatra, B., Otway, R.T., Huang, Y., King, I.N., Maillet, M.*, et al.* (2011). Tinman/Nkx2-5 acts via miR-1 and upstream of Cdc42 to regulate heart function across species. The Journal of Cell Biology *193*, 1181-1196.

Rana, T.M. (2007). Illuminating the silence: understanding the structure and function of small RNAs. Nat Rev Mol Cell Biol *8*, 23-36.

Rezaval, C., Pavlou, H.J., Dornan, A.J., Chan, Y.B., Kravitz, E.A., and Goodwin, S.F. (2012). Neural circuitry underlying *Drosophila* female postmating behavioral

responses. Curr Biol *22*, 1155-1165.

Rideout, E.J., Billeter, J.C., and Goodwin, S.F. (2007). The sex-determination genes fruitless and doublesex specify a neural substrate required for courtship song. Curr Biol *17*, 1473-1478.

Rideout, E.J., Dornan, A.J., Neville, M.C., Eadie, S., and Goodwin, S.F. (2010). Control of sexual differentiation and behavior by the doublesex gene in *Drosophila melanogaster*. Nature Neuroscience *13*, 458-466.

Robinett, C.C., Vaughan, A.G., Knapp, J.M., and Baker, B.S. (2010). Sex and the single cell. II. There is a time and place for sex. PLoS Biol *8*, e1000365.

Roman, G. (2004). The genetics of *Drosophila* transgenics. Bioessays *26*, 1243-1253.

Ryner, L.C., Goodwin, S.F., Castrillon, D.H., Anand, A., Villella, A., Baker, B.S., Hall, J.C., Taylor, B.J., and Wasserman, S.A. (1996). Control of male sexual behavior and sexual orientation in *Drosophila* by the fruitless gene. Cell *87*, 1079-1089.

Saija, A., Princi, P., De Pasquale, R., and Costa, G. (1990). The bioflavonoid O-(beta-hydroxyethyl)-rutoside affects the cerebral metabolism and the permeability of the blood brain barrier in the rat. Pharmacological research : the Official Journal of the Italian Pharmacological Society *22 Suppl 1*, 69-70.

Sanders, L.E., and Arbeitman, M.N. (2008). Doublesex establishes sexual dimorphism in the *Drosophila* central nervous system in an isoform-dependent manner by directing cell number. Developmental Biology *320*, 378-390.

Sandoval, K.E., and Witt, K.A. (2008). Blood brain barrier tight junction permeability and ischemic stroke. Neurobiol Dis *32*, 200-219.

Sarov-Blat, L., So, W.V., Liu, L., and Rosbash, M. (2000). The *Drosophila* takeout gene is a novel molecular link between circadian rhythms and feeding behavior. Cell *101*, 647-656.

Schmidt, H., Rickert, C., Bossing, T., Vef, O., Urban, J., and Technau, G.M. (1997). The embryonic central nervous system lineages of *Drosophila melanogaster*. II. Neuroblast lineages derived from the dorsal part of the neuroectoderm. Developmental Biology *189*, 186-204.

Schwabe, T., Bainton, R.J., Fetter, R.D., Heberlein, U., and Gaul, U. (2005). GPCR

signaling is required for blood brain barrier formation in *Drosophila*. Cell *123*, 133-144.

Shen, J., Ford, D., Landis, G.N., and Tower, J. (2009). Identifying sexual differentiation genes that affect *Drosophila* life span. BMC Geriatr *9*, 56.

Sherman, D.L., and Brophy, P.J. (2005). Mechanisms of axon ensheathment and myelin growth. Nat Rev Neurosci *6*, 683-690.

Siegel, R.W., and Hall, J.C. (1979). Conditioned responses in courtship behavior of normal and mutant *Drosophila*. Proceedings of the National Academy of Sciences of the United States of America *76*, 3430-3434.

Silver, S.J., Hagen, J.W., Okamura, K., Perrimon, N., and Lai, E.C. (2007). Functional screening identifies miR-315 as a potent activator of wingless signaling. Proceedings of the National Academy of Sciences of the United States of America *104*, 18151-18156.

So, W.V., Sarov-Blat, L., Kotarski, C.K., McDonald, M.J., Allada, R., and Rosbash, M. (2000). takeout, a novel *Drosophila* gene under circadian clock transcriptional regulation. Mol Cell Biol *20*, 6935-6944.

Sokol, N.S., Xu, P., Jan, Y.N., and Ambros, V. (2008). *Drosophila* let-7 microRNA is required for remodeling of the neuromusculature during metamorphosis. Genes Dev *22*, 1591-1596.

Spieth, H.T. (1974). Courtship behavior in *Drosophila*. Annu Rev Entomol *19*, 385-405.

Stockinger, P., Kvitsiani, D., Rotkopf, S., Tirian, L., and Dickson, B.J. (2005). Neural circuitry that governs *Drosophila* male courtship behavior. Cell *121*, 795-807.

Stork, T., Engelen, D., Krudewig, A., Silies, M., Bainton, R.J., and Klambt, C. (2008). Organization and function of the blood brain barrier in *Drosophila*. J Neurosci *28*, 587-597.

Taylor, B.J., and Truman, J.W. (1992). Commitment of abdominal neuroblasts in *Drosophila* to a male or female fate is dependent on genes of the sex-determining hierarchy. Development *114*, 625-642.

Teleman, A.A., Maitra, S., and Cohen, S.M. (2006). *Drosophila* lacking microRNA miR-278 are defective in energy homeostasis. Genes Dev *20*, 417-422.

Tepass, U., and Hartenstein, V. (1994). The development of cellular junctions in the *Drosophila* embryo. Developmental Biology *161*, 563-596.

Tiklova, K., Senti, K.A., Wang, S., Graslund, A., and Samakovlis, C. (2010). Epithelial septate junction assembly relies on melanotransferrin iron binding and endocytosis in *Drosophila*. Nature Cell Biology *12*, 1071-1077.

Tivnan, A., Foley, N.H., Tracey, L., Davidoff, A.M., and Stallings, R.L. (2010). MicroRNA-184-mediated inhibition of tumour growth in an orthotopic murine model of neuroblastoma. Anticancer Res *30*, 4391-4395.

Tokusumi, T., Tokusumi, Y., Hopkins, D.W., Shoue, D.A., Corona, L., and Schulz, R.A. (2011). Germ line differentiation factor Bag of Marbles is a regulator of hematopoietic progenitor maintenance during *Drosophila* hematopoiesis. Development *138*, 3879-3884.

Tower, J. (2006). Sex-specific regulation of aging and apoptosis. Mech Ageing Dev *127*, 705-718.

Treherne, J.E. (1962). Transfer of substances between the blood and central nervous system in vertebrate and invertebrate animals. Nature *196*, 1181-1183.

Truscott, M., Islam, A.B., Lopez-Bigas, N., and Frolov, M.V. (2011). mir-11 limits the proapoptotic function of its host gene, dE2f1. Genes Dev *25*, 1820-1834.

Usui-Aoki, K., Ito, H., Ui-Tei, K., Takahashi, K., Lukacsovich, T., Awano, W., Nakata, H., Piao, Z.F., Nilsson, E.E., Tomida, J.*, et al.* (2000). Formation of the male-specific muscle in female *Drosophila* by ectopic fruitless expression. Nature Cell Biology *2*, 500-506.

Villella, A., and Hall, J.C. (1996). Courtship anomalies caused by doublesex mutations in *Drosophila melanogaster*. Genetics *143*, 331-344.

Vilmos, P., Bujna, A., Szuperak, M., Havelda, Z., Varallyay, E., Szabad, J., Kucerova, L., Somogyi, K., Kristo, I., Lukacsovich, T.*, et al.* (2013). Viability, longevity, and egg production of *Drosophila melanogaster* are regulated by the miR-282 microRNA. Genetics *195*, 469-480.

Vodala, S., Pescatore, S., Rodriguez, J., Buescher, M., Chen, Y.W., Weng, R., Cohen, S.M., and Rosbash, M. (2012). The oscillating miRNA 959-964 cluster impacts

Drosophila feeding time and other circadian outputs. Cell Metab *16*, 601-612.

von Philipsborn, A.C., Liu, T., Yu, J.Y., Masser, C., Bidaye, S.S., and Dickson, B.J. (2011). Neuronal control of *Drosophila* courtship song. Neuron *69*, 509-522.

Von Schilcher, F. (1976). The behavior of cacophony, a courtship song mutant in *Drosophila melanogaster*. Behav Biol *17*, 187-196.

Watanabe, K., Toba, G., Koganezawa, M., and Yamamoto, D. (2011). Gr39a, a highly diversified gustatory receptor in *Drosophila*, has a role in sexual behavior. Behav Genet *41*, 746-753.

Weng, R., Chin, J.S., Yew, J.Y., Bushati, N., and Cohen, S.M. (2013). controls male reproductive success in. Elife *2*, e00640.

Weng, R., and Cohen, S.M. (2012). *Drosophila* miR-124 regulates neuroblast proliferation through its target anachronism. Development *139*, 1427-1434.

Wienholds, E., Kloosterman, W.P., Miska, E., Alvarez-Saavedra, E., Berezikov, E., de Bruijn, E., Horvitz, H.R., Kauppinen, S., and Plasterk, R.H. (2005). MicroRNA expression in zebrafish embryonic development. Science *309*, 310-311.

Wilson, R.S., Arnold, S.E., Beck, T.L., Bienias, J.L., and Bennett, D.A. (2008). Change in depressive symptoms during the prodromal phase of Alzheimer disease. Arch Gen Psychiatry *65*, 439-445.

Wong, T.S., Liu, X.B., Wong, B.Y., Ng, R.W., Yuen, A.P., and Wei, W.I. (2008). Mature miR-184 as potential oncogenic microRNA of squamous cell carcinoma of tongue. Clin Cancer Res *14*, 2588-2592.

Wu, L.F., Gao, L., Hou, X.M., Zhang, Q.H., Li, S., Yang, Y.F., and Lin, X.H. (2012a). *Drosophila* miR-5 suppresses Hedgehog signaling by directly targeting Smoothened. FEBS Lett *586*, 4052-4060.

Wu, M.N., Joiner, W.J., Dean, T., Yue, Z., Smith, C.J., Chen, D., Hoshi, T., Sehgal, A., and Koh, K. (2010). SLEEPLESS, a Ly-6/neurotoxin family member, regulates the levels, localization and activity of Shaker. Nature Neuroscience *13*, 69-75.

Wu, V.M., Schulte, J., Hirschi, A., Tepass, U., and Beitel, G.J. (2004). Sinuous is a *Drosophila* claudin required for septate junction organization and epithelial tube size control. The Journal of Cell Biology *164*, 313-323.

Wu, Y.C., Chen, C.H., Mercer, A., and Sokol, N.S. (2012b). Let-7-complex microRNAs regulate the temporal identity of *Drosophila* mushroom body neurons via chinmo. Dev Cell *23*, 202-209.

Yager, J., Richards, S., Hekmat-Scafe, D.S., Hurd, D.D., Sundaresan, V., Caprette, D.R., Saxton, W.M., Carlson, J.R., and Stern, M. (2001). Control of *Drosophila* perineurial glial growth by interacting neurotransmitter-mediated signaling pathways. Proceedings of the National Academy of Sciences of the United States of America *98*, 10445-10450.

Yamamoto, D., Fujitani, K., Usui, K., Ito, H., and Nakano, Y. (1998). From behavior to development: genes for sexual behavior define the neuronal sexual switch in *Drosophila*. Mech Dev *73*, 135-146.

Yamamoto, D., and Koganezawa, M. (2013). Genes and circuits of courtship behaviour in *Drosophila* males. Nat Rev Neurosci *14*, 681-692.

Yan, K.S., Yan, S., Farooq, A., Han, A., Zeng, L., and Zhou, M.M. (2003). Structure and conserved RNA binding of the PAZ domain. Nature *426*, 468-474.

Yang, X., Schadt, E.E., Wang, S., Wang, H., Arnold, A.P., Ingram-Drake, L., Drake, T.A., and Lusis, A.J. (2006). Tissue-specific expression and regulation of sexually dimorphic genes in mice. Genome Res *16*, 995-1004.

Yu, J.Y., Kanai, M.I., Demir, E., Jefferis, G.S., and Dickson, B.J. (2010). Cellular organization of the neural circuit that drives *Drosophila* courtship behavior. Curr Biol *20*, 1602-1614.

Zeng, X., Asmaro, K., Ren, C., Gao, M., Peng, C., Ding, J.Y., Fredrickson, V., Ji, X., and Ding, Y. (2012). Acute ethanol treatment reduces blood brain barrier dysfunction following ischemia/reperfusion injury. Brain Research *1437*, 127-133.

Zhang, X., Luo, D., Pflugfelder, G.O., and Shen, J. (2013). Dpp signaling inhibits proliferation in the *Drosophila* wing by Omb-dependent regional control of bantam. Development *140*, 2917-2922.

Zhang, Y., and Lai, Z.C. (2013). Mob as tumor suppressor is regulated by bantam microRNA through a feedback loop for tissue growth control. Biochem Biophys Res Commun *439*, 438-442.

Zlokovic, B.V. (2008). The blood brain barrier in health and chronic neurodegenerative disorders. Neuron *57*, 178-201.